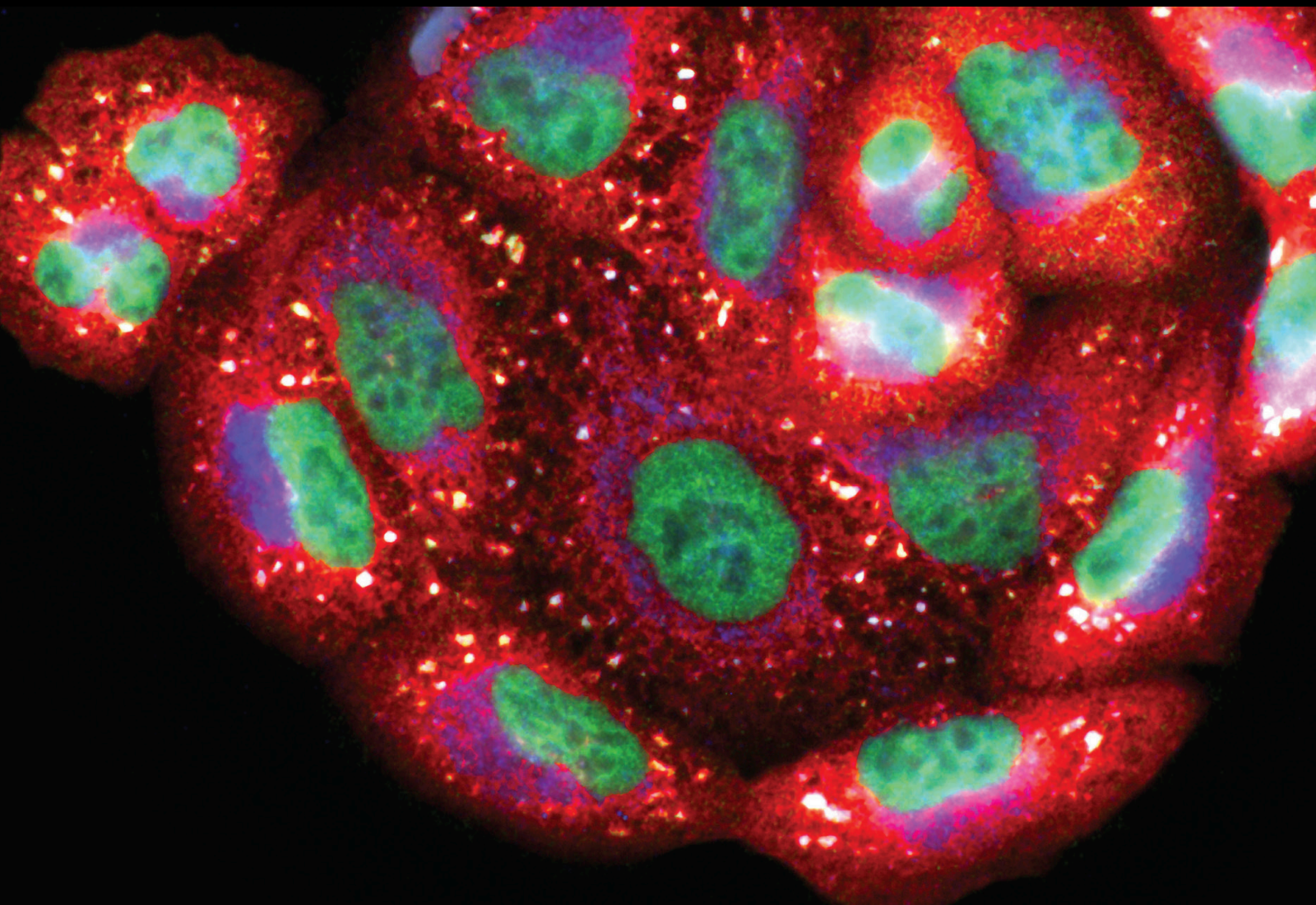


(In)Fertility and Oxidative Stress: New Insights into Novel Redox Mechanisms Controlling Fundamental Reproductive Processes

Lead Guest Editor: Elisabete Silva

Guest Editors: Henrique Almeida and José Pedro Castro





**(In)Fertility and Oxidative Stress: New Insights
into Novel Redox Mechanisms Controlling
Fundamental Reproductive Processes**

Oxidative Medicine and Cellular Longevity

**(In)Fertility and Oxidative Stress: New Insights
into Novel Redox Mechanisms Controlling
Fundamental Reproductive Processes**

Lead Guest Editor: Elisabete Silva

Guest Editors: Henrique Almeida and José Pedro Castro



Copyright © 2020 Hindawi Limited. All rights reserved.

This is a special issue published in "Oxidative Medicine and Cellular Longevity" All articles are open access articles distributed under the Creative Commons Attribution License, which permits unrestricted use, distribution, and reproduction in any medium, provided the original work is properly cited.

Chief Editor

Jeannette Vasquez-Vivar, USA

Editorial Board

Ivanov Alexander, Russia
Fabio Altieri, Italy
Fernanda Amicarelli, Italy
José P. Andrade, Portugal
Cristina Angeloni, Italy
Antonio Ayala, Spain
Elena Azzini, Italy
Peter Backx, Canada
Damian Bailey, United Kingdom
Sander Bekeschus, Germany
Ji C. Bihl, USA
Consuelo Borrás, Spain
Nady Braidy, Australia
Ralf Braun, Austria
Laura Bravo, Spain
Amadou Camara, USA
Gianluca Carnevale, Italy
Roberto Carnevale, Italy
Angel Catalá, Argentina
Giulio Ceolotto, Italy
Shao-Yu Chen, USA
Ferdinando Chiaradonna, Italy
Zhao Zhong Chong, USA
Alin Ciobica, Romania
Ana Cipak Gasparovic, Croatia
Giuseppe Cirillo, Italy
Maria R. Ciriolo, Italy
Massimo Collino, Italy
Graziamaria Corbi, Italy
Manuela Corte-Real, Portugal
Mark Crabtree, United Kingdom
Manuela Curcio, Italy
Andreas Daiber, Germany
Felipe Dal Pizzol, Brazil
Francesca Danesi, Italy
Domenico D'Arca, Italy
Sergio Davinelli, USA
Claudio De Lucia, Italy
Yolanda de Pablo, Sweden
Sonia de Pascual-Teresa, Spain
Cinzia Domenicotti, Italy
Joël R. Drevet, France
Grégory Durand, France
Javier Egea, Spain

Ersin Fadillioglu, Turkey
Ioannis G. Fatouros, Greece
Qingping Feng, Canada
Gianna Ferretti, Italy
Giuseppe Filomeni, Italy
Swaran J. S. Flora, India
Teresa I. Fortoul, Mexico
Rodrigo Franco, USA
Joaquin Gadea, Spain
Juan Gambini, Spain
José Luís García-Giménez, Spain
Gerardo García-Rivas, Mexico
Janusz Gebicki, Australia
Alexandros Georgakilas, Greece
Husam Ghanim, USA
Rajeshwary Ghosh, USA
Eloisa Gitto, Italy
Daniela Giustarini, Italy
Saeid Golbidi, Canada
Aldrin V. Gomes, USA
Tilman Grune, Germany
Nicoletta Guaragnella, Italy
Solomon Habtemariam, United Kingdom
Eva-Maria Hanschmann, Germany
Tim Hofer, Norway
John D. Horowitz, Australia
Silvana Hrelia, Italy
Stephan Immenschuh, Germany
Maria Isagulians, Latvia
Luigi Iuliano, Italy
FRANCO J. L, Brazil
Vladimir Jakovljevic, Serbia
Marianna Jung, USA
Peeter Karihtala, Finland
Eric E. Kelley, USA
Kum Kum Khanna, Australia
Neelam Khaper, Canada
Thomas Kietzmann, Finland
Demetrios Kouretas, Greece
Andrey V. Kozlov, Austria
Jean-Claude Lavoie, Canada
Simon Lees, Canada
Christopher Horst Lillig, Germany
Paloma B. Liton, USA

Ana Lloret, Spain
Lorenzo Loffredo, Italy
Daniel Lopez-Malo, Spain
Antonello Lorenzini, Italy
Nageswara Madamanchi, USA
Kenneth Maiese, USA
Marco Malaguti, Italy
Tullia Maraldi, Italy
Reiko Matsui, USA
Juan C. Mayo, Spain
Steven McAnulty, USA
Antonio Desmond McCarthy, Argentina
Bruno Meloni, Australia
Pedro Mena, Italy
V́ctor M. Mendoza-Núñez, Mexico
Maria U. Moreno, Spain
Trevor A. Mori, Australia
Ryuichi Morishita, Japan
Fabiana Morroni, Italy
Luciana Mosca, Italy
Ange Mouithys-Mickalad, Belgium
Iordanis Mourouzis, Greece
Danina Muntean, Romania
Colin Murdoch, United Kingdom
Pablo Muriel, Mexico
Ryoji Nagai, Japan
David Nieman, USA
Hassan Obied, Australia
Julio J. Ochoa, Spain
Pál Pacher, USA
Pasquale Pagliaro, Italy
Valentina Pallottini, Italy
Rosalba Parenti, Italy
Vassilis Paschalis, Greece
Visweswara Rao Pasupuleti, Malaysia
Daniela Pellegrino, Italy
Ilaria Peluso, Italy
Claudia Penna, Italy
Serafina Perrone, Italy
Tiziana Persichini, Italy
Shazib Pervaiz, Singapore
Vincent Pialoux, France
Ada Popolo, Italy
José L. Quiles, Spain
Walid Rachidi, France
Zsolt Radak, Hungary
Namakkal Soorappan Rajasekaran, USA

Sid D. Ray, USA
Hamid Reza Rezvani, France
Alessandra Ricelli, Italy
Paola Rizzo, Italy
Francisco J. Romero, Spain
Joan Roselló-Catafau, Spain
H. P. Vasantha Rupasinghe, Canada
Gabriele Saretzki, United Kingdom
Luciano Saso, Italy
Nadja Schroder, Brazil
Sebastiano Sciarretta, Italy
Ratanesh K. Seth, USA
Honglian Shi, USA
Cinzia Signorini, Italy
Mithun Sinha, USA
Carla Tatone, Italy
Frank Thévenod, Germany
Shane Thomas, Australia
Carlo G. Tocchetti, Italy
Angela Trovato Salinaro, Italy
Paolo Tucci, Italy
Rosa Tundis, Italy
Giuseppe Valacchi, Italy
Daniele Vergara, Italy
Victor M. Victor, Spain
László Virág, Hungary
Natalie Ward, Australia
Philip Wenzel, Germany
Georg T. Wondrak, USA
Michal Wozniak, Poland
Sho-ichi Yamagishi, Japan
Liang-Jun Yan, USA
Guillermo Zalba, Spain
Mario Zoratti, Italy

Contents

(In)Fertility and Oxidative Stress: New Insights into Novel Redox Mechanisms Controlling Fundamental Reproductive Processes

E. Silva , H. Almeida , and J. P. Castro

Editorial (2 pages), Article ID 4674896, Volume 2020 (2020)

Subchronic Exposure to Cadmium Causes Persistent Changes in the Reproductive System in Female Wistar Rats

Marzenna Nasiadek , Marian Danilewicz , Michał Klimczak, Joanna Stragierowicz, and Anna Kilanowicz

Research Article (17 pages), Article ID 6490820, Volume 2019 (2019)

Apocynin Dietary Supplementation Delays Mouse Ovarian Ageing

F. Timóteo-Ferreira, S. Mendes , N. A. Rocha, L. Matos , A. R. Rodrigues , H. Almeida , and E. Silva 

Research Article (11 pages), Article ID 5316984, Volume 2019 (2019)

Metformin Improves Fertility in Obese Males by Alleviating Oxidative Stress-Induced Blood-Testis Barrier Damage

Jifeng Ye, Dandan Luo, Xiaolin Xu, Mingqi Sun, Xiaohui Su, Zhenhua Tian, Meijie Zhang, Chunxiao Yu , and Qingbo Guan 

Research Article (17 pages), Article ID 9151067, Volume 2019 (2019)

New Insights into the Process of Placentation and the Role of Oxidative Uterine Microenvironment

Sara Mendes , Filipa Timóteo-Ferreira , Henrique Almeida , and Elisabete Silva 

Review Article (18 pages), Article ID 9174521, Volume 2019 (2019)

Testicular Toxicity of Water Pipe Smoke Exposure in Mice and the Effect of Treatment with Nootkatone Thereon

Badreldin H. Ali, Suhail Al-Salam , Sirin A. Adham, Khalid Al Balushi , Mohammed Al Za'abi, Sumaya Beegam, Priya Yuvaraju, Priyadarsini Manoj, and Abderrahim Nemmar 

Research Article (10 pages), Article ID 2416935, Volume 2019 (2019)

Editorial

(In)Fertility and Oxidative Stress: New Insights into Novel Redox Mechanisms Controlling Fundamental Reproductive Processes

E. Silva ^{1,2} **H. Almeida** ^{1,2} and **J. P. Castro**³

¹Ageing and Stress Group, Instituto de Biologia Molecular e Celular, Instituto de Investigação e Inovação em Saúde, Universidade do Porto, Portugal

²Unidade de Biologia Experimental, Departamento de Biomedicina, Faculdade de Medicina da Universidade do Porto, Portugal

³Brigham and Women's Hospital, Harvard Medical School, Boston, USA

Correspondence should be addressed to E. Silva; elisabete.silva@i3s.up.pt

Received 19 December 2019; Accepted 20 December 2019; Published 22 January 2020

Copyright © 2020 E. Silva et al. This is an open access article distributed under the Creative Commons Attribution License, which permits unrestricted use, distribution, and reproduction in any medium, provided the original work is properly cited.

Fertility is the capacity to conceive and produce offspring whereas infertility is considered the failure to do so after 12 months of regular, unprotected sexual intercourse. Currently, millions of people suffer from infertility and concerns therein increase worldwide, especially in developing countries where the majority of infertility diagnosis are established [1]. It is estimated to affect 1 in 6 couples with an almost equal contribution of male or female to the number of cases [2]. Underlying causes associate with modern lifestyle patterns or disorders that include increased maternal ageing, obesity and diabetes, anxiety, alcohol consumption, smoking, and exposure to pollutants, including those acting as endocrine disruptors.

Common to all of these conditions is the excessive production of reactive oxygen species (ROS) which may result in oxidative stress (OS) if the cellular antioxidant capacity is insufficient or ineffective to counteract ROS formation. OS is believed to contribute to infertility by interfering with fundamental processes involved in reproduction, including spermatogenesis, folliculogenesis, fertilization, implantation, and placentation [3–5]. At the subcellular level, excessive ROS production dysregulates cell signalling networks and promotes oxidation of DNA, lipids, and proteins, which can ultimately lead to cellular dysfunction by functionally altering subcellular structures such as the endoplasmic reticulum or the mitochondria, to name a few. Thus, studies focusing on causal connections between ROS, infertility, reproductive ageing, pregnancy-related pathologies, and cellular stress are of main interest.

The most significant contributor to infertility is maternal ageing, mainly because of the age-related decay in follicle number and oocyte quality. F. Timóteo-Ferreira et al. novel findings showed that specific antioxidant supplementation in mice is able to counteract age-related oxidative stress in the ovary, fibrosis, and inflammation, thus providing an effective role in delaying ovarian ageing. The uterus is also an important contributor because it must provide an adequate microenvironment for blastocyst implantation. M. Nasiadek et al. evaluated the effect of subchronic exposure to cadmium, an environmental toxicant and endocrine disruptor present in food and smoking tobacco, on rat female reproductive system. They showed persisting cadmium-mediated plasma and uterine estradiol concentration changes, oestrous cyclicity disorders, and increased lipid peroxidation in the uterus that is able to result in ovarian and uterine dysfunction leading to infertility. In fact, the possibility that an abnormal uterine microenvironment, already present before or at the time of implantation, jeopardizes fertility and increases the risk for the development of pregnancy-related complications was reviewed by S. Mendes et al. The review addressed mechanisms by which uterine factors regulate placentation, with a special focus on ROS physiological and pathophysiological role.

The possibility of improving male fertility by alleviating OS was also addressed in this special issue. The manuscript by J. Ye et al. provided new insights into the use of metformin to improve obesity-associated male infertility. Metformin beneficial effects were mediated by a reduction of ectopic

lipid accumulation in the testis, reduction of OS production, and mitigation of high-fat-diet-induced injury to the blood-testis barrier, all accompanied by male fertility improvement. An interesting article (B. H. Ali et al.) addressing water pipe smoke-induced testicular toxicity and the protective effect of nootkatone, a sesquiterpenoid isolated from plants with antioxidant and anti-inflammatory properties, is also included.

This special issue contributes with original articles that highlight and unravel mechanisms by which OS promotes infertility of both male or female origin and new antioxidant approaches that may improve fertility.

Conflicts of Interest

The editors declare that they have no conflicts of interest regarding the publication of the special issue.

Acknowledgments

The guest editors thank all the authors for having submitted their research to this special issue and all the reviewers for having provided their valuable contribution to improve the quality of this work. They also acknowledge the Portuguese Government and the European Union for providing Elisabete Silva financial support through the DL57/2016/CP1327/CT006 contract. Finally, they thank the editorial board and all the staff for the opportunity and support that made this special issue publication possible.

E. Silva
H. Almeida
J. P. Castro

References

- [1] M. C. Inhorn and P. Patrizio, "Infertility around the globe: new thinking on gender, reproductive technologies and global movements in the 21st century," *Human Reproduction Update*, vol. 21, no. 4, pp. 411–426, 2015.
- [2] A. Agarwal, A. Mulgund, A. Hamada, and M. R. Chyatte, "A unique view on male infertility around the globe," *Reproductive Biology and Endocrinology*, vol. 13, no. 1, 2015.
- [3] A. Agarwal, S. Gupta, and R. K. Sharma, "Role of oxidative stress in female reproduction," *Reproductive Biology and Endocrinology*, vol. 3, no. 1, p. 28, 2005.
- [4] A. Agarwal, N. Parekh, M. K. Panner Selvam et al., "Male oxidative stress infertility (MOSI): proposed terminology and clinical practice guidelines for management of idiopathic male infertility," *The World Journal of Men's Health*, vol. 37, no. 3, pp. 296–312, 2019.
- [5] S. S. Du Plessis, A. Agarwal, J. Halabi, and E. Tvrda, "Contemporary evidence on the physiological role of reactive oxygen species in human sperm function," *Journal of Assisted Reproduction and Genetics*, vol. 32, no. 4, pp. 509–520, 2015.

Research Article

Subchronic Exposure to Cadmium Causes Persistent Changes in the Reproductive System in Female Wistar Rats

Marzenna Nasiadek ¹, Marian Danilewicz ², Michał Klimczak,¹ Joanna Stragierowicz,¹ and Anna Kilanowicz¹

¹Department of Toxicology, Medical University of Lodz, Muszynskiego 1, 90-151 Lodz, Poland

²Department of Pathology, Medical University of Lodz, Pomorska 251, 92-213 Lodz, Poland

Correspondence should be addressed to Marzenna Nasiadek; marzenna.nasiadek@umed.lodz.pl

Received 25 April 2019; Revised 28 September 2019; Accepted 11 November 2019; Published 18 December 2019

Guest Editor: Henrique Almeida

Copyright © 2019 Marzenna Nasiadek et al. This is an open access article distributed under the Creative Commons Attribution License, which permits unrestricted use, distribution, and reproduction in any medium, provided the original work is properly cited.

Cadmium (Cd) is an environmental toxicant and endocrine disruptor in humans and animals, and recent studies have illustrated that the uterus is exceedingly sensitive to Cd toxicity. The aim of the study was to investigate the influence of subchronic (90 days) oral Cd exposure in daily doses of 0.09-4.5 mg/kg b.w. on the balance of sex hormones by estimating estradiol (E_2) and progesterone (P) concentrations in the uterus and plasma in comparison with the effects of 17β - E_2 . Additionally, the uterine weight, histopathological changes in the uterus and ovaries, the regularity of the estrous cycle, Cd bioaccumulation in uterine tissue, and selected biochemical parameters of oxidative stress were determined. A long period of observation (three and six months following the administration period) was used to assess whether the existing effects are reversible. The lowest dose of Cd caused effects similar to 17β - E_2 : an increase of E_2 concentration in the uterus, endometrial epithelium thickness, and disturbed estrous cycle with estrus phase prolongation. The obtained results suggest that Cd causes nonlinear response. Higher doses of Cd caused a significant decrease in E_2 concentration in the uterus and plasma, estrous cycle disturbances, endometrium atrophy, and structural damage in the ovaries. This dose additionally induces lipid peroxidation in the uterine tissues. It is noteworthy that a prolonged time of observation after terminating the exposure showed persistent changes in the concentration of E_2 in uterine tissue, as well as alterations in estrous cycle phases, and an increase in lipid peroxidation in the uterus. Moreover, significant positive correlations between the plasma E_2 concentration and endometrial epithelium thickness in all studied groups were found. In summary, subchronic oral Cd exposure of female rats may result in impaired fertility processes.

1. Introduction

Cadmium (Cd) is an important industrial and environmental pollutant. In addition, it should be taken into account that Cd pollution is global; hence, this metal has been placed 7th on the list of substances that pose a potential threat to human health due to their known or suspected toxicity [1]. Cd is used for the plating of steel, as a plastic stabilizer, as an electrode material in nickel-cadmium batteries, and as a material in semiconductors. Mining, smelting, and industrial use have resulted in the increased bioaccessibility of Cd in the environment, and anthropogenic sources are the most significant threat to human health [2]. Although Cd is used in a variety of manufactured products, for most people in the general

population the primary sources of exposure are food and smoking tobacco [2, 3]. Cigarette smoking contributes between two and four μg of Cd per pack. The European Food Safety Authority (EFSA) has estimated the average daily dietary exposure of Cd to be between 20.3 and 74.2 $\mu\text{g}/\text{day}$ per 70 kg person [4]. Specific groups at risk of consuming higher dietary Cd than is recognized as safe are children and vegetarians [5].

Women are thought to be at greater risk of increased Cd accumulation as the concentrations of Cd in the blood, tissue, and urine are higher than in males due to lower concentrations of iron [6–9]. In humans, Cd accumulates not only in the kidney and liver, but also in the reproductive organs [10–12]. To date, many *in vivo* studies indicate the toxic

effects of Cd on female reproductive organs, including the endocrine system, the effects which seem to depend not only on the dose but also on the route of Cd administration [13–24]. However, the mechanism of Cd reproductive toxicity has not yet been elucidated completely, and there are still controversies with regard to the estrogen-like effect of this metal. Cd is listed as a metalloestrogen because of its ability to bind to the cellular estrogen receptor (ER) and hence mimic the actions of estrogens [25]. Johnson et al. [26] reported that Cd exposure in ovariectomized rats produced uterine hyperplasia, increased growth of the mammary glands, and the induction of hormone-regulated genes. Ali et al. [27] suggest that Cd exposure induces a limited spectrum of estrogenic responses *in vivo* and that, in certain targets, the effects of Cd might not be mediated via classical ER signaling through estrogen response element-regulated genes. Because of disturbed steroid hormone secretion, it is also suggested that the direct effect of Cd on the ovaries or the indirect effect of Cd on the hypothalamus-pituitary-gonadal axis should not be excluded. It was proved in *in vivo* studies that Cd administration leads to histopathological alterations in the ovary (degeneration of the corpus luteum, damaged and less numerous oocytes, and degeneration of granulosa cells) and uterus (an increase in the luminal epithelial height and in the endometrial thickness) [24, 28–30]. In addition, subacute Cd administration led to Cd accumulation and the induction of oxidative stress in rat ovaries and uterus [29, 31]. The results of our previous work indicate that subacute (30-day) exposure to Cd leads to histopathological changes in the ovaries and in the uterus, as well as disturbances in the concentrations of circulating steroid hormones, suggesting an antiestrogenic effect, which was associated with abnormalities in the estrous cycle in female rats [24]. Despite that environmental exposure to Cd is lifelong, data on the subchronic or long-term effects of Cd on the uterus is still limited. Thus, the aim of the study was to investigate the subchronic effects of Cd on the female rat reproductive system—by estimating the balance of sex hormones based on estradiol (E_2) and progesterone (P) concentrations in the uterus and plasma in comparison with the effects of 17β - E_2 . Additionally, the uterine weight, histopathological changes of the uterus and ovaries, estrous cyclicity, Cd bioaccumulation in uterine tissue, and selected biochemical parameters of oxidative stress were determined. In order to discover whether the existing effects are reversible, we used a long period of observation in the exposed females, i.e., three and six months after the subchronic Cd administration period, after which the same parameters were determined.

2. Material and Methods

2.1. Animal Selection, Care, and Drug Treatment. Adult female Wistar rats (12 weeks old) were kept in polypropylene cages at a controlled temperature of $22 \pm 1^\circ\text{C}$ and relative humidity of 50–60% with free access to tap water and a diet low in phytoestrogen content (Ssniff R/M-H). The rats were allowed to acclimate for two weeks, during which the regularity of the estrous cycles was confirmed.

The regularly cycling rats were separated into three experimental groups (each $n = 56$), A, B, and C, which were then divided into seven subgroups (each $n = 8$). The experimental design and dose regiment is summarized in Figure 1. The four Cd subgroups (from each of the following groups: A, B, and C) received Cd orally by gavage for 90 days (CdCl_2 , Sigma-Aldrich, St. Louis MO, USA) at different daily doses of 0.09, 0.9, 1.8, and 4.5 mg/kg b.w., which corresponded to 1/1000, 1/100, 1/50, and 1/20 LD_{50} (88 mg/kg b.w.) [32], respectively. The three control subgroups (from each of the following groups: A, B, and C) were administered distilled water (pure control), peanut oil (oil control), and 17β - E_2 in a dose of 0.03 mg/kg b.w. (Sigma-Aldrich, St. Louis, MO, USA) dissolved in peanut oil (positive control). After 90 days of exposure, group A was sacrificed; however, groups B and C were subjected to three-month (90-day) and six-month (180-day) observation periods, respectively. The animals from the control subgroups received vehicle following the same protocol used for the rats exposed to Cd. The daily water intake and feeding habits of all the animals were carefully observed throughout the experimental schedule. During and following the treatment, all animals were observed carefully for mortality, body weight, and gross behavioral changes. All procedures conducted on the rats were approved by the Local Animal Ethical Committee of the Medical University of Lodz (LKE 46/LB/481/2009; 14/LB481/DLZ/2012).

2.1.1. Euthanasia, Tissue Collection, and Preservation. The female rats which were in the estrus stage were weighed and underwent euthanasia after 90 days of exposure (group A), and after 90 days (group B) or 180 days (group C) of observation following a 90-day exposure. Blood samples were collected from all rats by heart puncture under light carbon dioxide anesthesia into Vacutainer tubes for metal analysis (S-Monovette, Sarstedt). The ovaries and the uterus were dissected out and weighed. For histological examination, part of the uterus and all of the ovaries were fixed in 10% formalin.

For Cd analysis, whole blood (1 mL) was kept in acid-washed cryotubes at -80°C , while the remaining part of the blood was centrifuged at $3000 \times g$ (10 min, 4°C) to separate the plasma. Part of the uterus was stored at -80°C in cryotubes for Cd analysis. The plasma for hormone analysis and biochemical assays (sex hormones and total antioxidant status (TAS) concentrations) was stored at -20°C .

2.2. Cd Concentration Assessment. The whole blood and uterus Cd concentrations were measured using GFAAS (Hitachi Z-8270) with the Zeeman-type background correction, autosampler, and pyrocoated tube. Earlier, the whole blood and uterus samples were digested with ultrapure HNO_3 , using a microwave digestion system (MARSXpress, CEM Corporation, USA). To determine Cd concentrations, samples were prepared in duplicate. For each series of analyses, internal quality controls were used (analyses of reference samples: Seronorm Whole Blood Level 1 (Sero, Norway) and Bovine liver 1577b (National Institute of Standards and Technology)). The analytical quality control was in the range of reference values. The limit of detection (LOD) for Cd

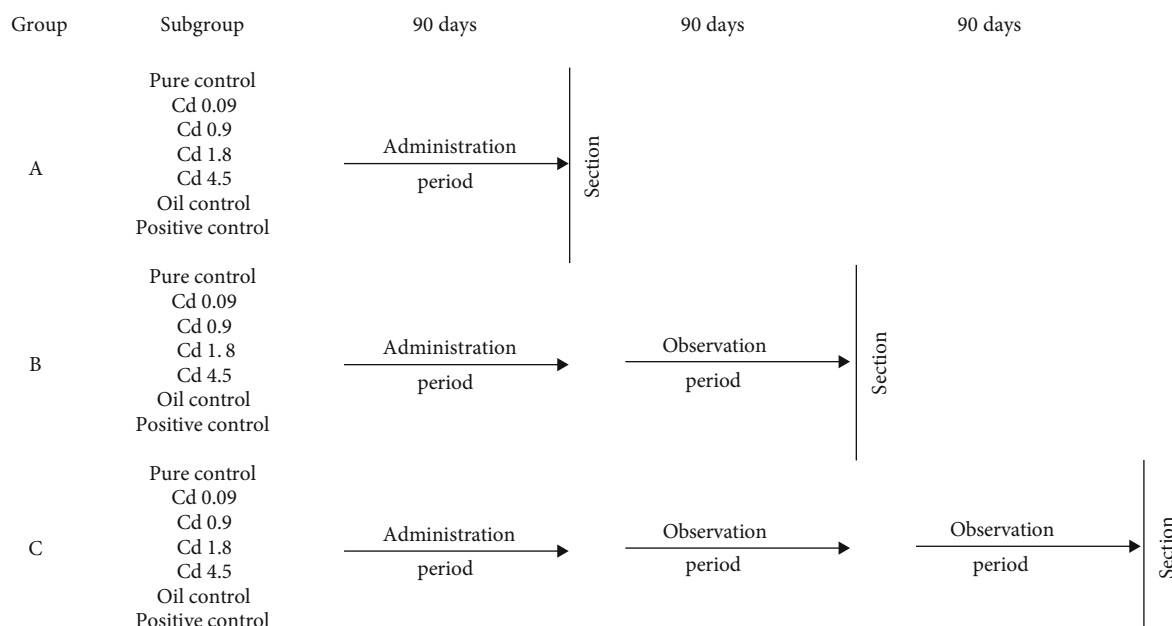


FIGURE 1: Experimental model.

determined by GFAAS was $0.2 \mu\text{g/L}$ or 0.2 ng/g wet tissue. Cd concentrations in whole blood and uterine tissue were expressed as $\mu\text{g/L}$ or $\mu\text{g/g}$ wet tissue.

2.3. Estrous Cycle Assessment. The estrous cycle was determined by cytological examination of vaginal smears obtained for two consecutive weeks prior to conducting the experiments and two weeks before section. The stages of rat estrous cycle were classified as proestrus, estrus, metaestrus, and diestrus according to the presence, absence or proportions of vaginal smears of three cell types: cornified cells (keratinized), epithelial cells, and leukocytes. The estrous cycle duration was calculated as the number of days between the estrus and proestrus stage [33, 34].

2.4. Histopathological Examinations. Part of the uterus and ovaries were fixed in 10% formalin for 24 h and then embedded in paraffin blocks, sliced into $5 \mu\text{m}$ sections, and stained with hematoxylin-eosin (H&E) for the histopathological evaluation. The sections were examined under a light microscope (Olympus BX51; Olympus, Tokyo, Japan).

2.5. Measuring Endometrial Epithelium Thickness. The thickness of the epithelial layer was evaluated using a computer image analysis system consisting of a PC equipped with a Pentagram graphic tablet, an Indeo Fast card (frame grabber, true-color, real-time) produced by Indeo (Taiwan), and a color TV camera from Panasonic (Japan) coupled with a Carl Zeiss microscope (Germany). This system was programmed (MultiScan 18.03 software, produced by Computer Scanning Systems, Poland) to calculate the distance (semiautomatic function). In each case, measurements were performed in high-power monitor fields and then the mean endometrial epithelium thickness was calculated.

2.6. Biochemical Analysis

2.6.1. Plasma Sex Hormone Concentration. The plasma E_2 and P concentrations were determined by an electrochemiluminescence method using a Roche Diagnostic kit on a Cobas 2601 analyzer (LOD: $E_2 = 5 \text{ pg/mL}$; $P = 0.03 \text{ ng/mL}$). The values reported are the sum of estradiol and estrone because chromatographic purification of the samples was not performed.

The concentrations of E_2 and P in the rat tissue were determined using an ELISA kit according to the manufacturer's instructions, respectively: rat (E_2) ELISA kit—catalog No. 201-11-0175, SRB (China), and (P) ELISA kit—catalog No. CSB-E07282r Cusabio Biotech Co., Ltd, (Japan). The sensitivities of the kits were $E_2 = 3.112 \text{ pg/mL}$ and $P = 0.25 \text{ ng/mL}$. The samples of uterus for hormone analysis were homogenized well to produce 10% homogenates in PBS and stored overnight at -20°C . For the assay of E_2 , the samples were centrifuged for 20 min at $2000\text{--}3000 \times g$. For the assay of P, after two freeze-thaw cycles were performed to break the cell membranes, the homogenate was centrifuged for 5 min at $5000 \times g$ at $2\text{--}8^\circ\text{C}$. The E_2 and P assays in the supernatant were carried out immediately.

2.6.2. Determination of Plasma TAS. The major antioxidant defences in plasma include ascorbate, protein thiols, bilirubin, urate, and α -tocopherol. Applying this method (TAS) allows to determine these major antioxidants in plasma. The plasma TAS was measured with a Ransel NX 2332 ready-made test (Randox Laboratories), according to the manufacturer's instructions. The TAS concentration was expressed as mM.

2.6.3. Determination of Catalase (CAT) Activity in Uterus. The uterus tissues were rapidly excised and homogenized in

an ice bath using phosphate-buffered saline (pH 7.4) with 0.01% digitonin using a Kika Labortechnik T-25 basic homogenizer. The homogenate was centrifuged at $10,000 \times g$ for 30 min at 4°C. CAT activity in the supernatant of the uterus homogenate was measured using a CAT 240 colorimetric assay kit for CAT activity (Applied Bioanalytical Labs) according to the manufacturer's instructions. CAT activity was expressed as U/mg protein. Protein concentrations in supernatants were determined according to Lowry et al. [35].

2.6.4. Determination of GSH in Uterus. The GSH concentration in the uterus (10% homogenate in phosphate-buffered saline pH 8.0) was determined according to Sedlak and Lindsay [36]. This method allows to assay nonprotein sulfhydryl compounds (NPSH), the sum of cellular glutathione and cysteine. Glutathione exists in thiol-reduced (GSH) and disulfide-oxidized (GSSG) forms. The GSH accounts for more than 90% of total NPSH [37], while the GSSG content is less than 1% of GSH [38]. The standard curve was obtained by using GSH, hence the results were expressed as GSH concentration ($\mu\text{mol/g}$ tissue).

2.6.5. Determination of MDA in Uterus. MDA concentrations, an indicator of free radical generation, which increases at the end of the lipid peroxidation, were estimated according to Uchiyama and Mihara [39]. The concentration of MDA was expressed as nmol/g tissue.

2.7. Statistical Analysis. All biochemical data were analyzed by STATISTICA software (StatSoft, Poland). We used the Kruskal-Wallis one-way analysis of variance followed by a pair-wise comparison of selected means with the Mann-Whitney *U*-test. We used Spearman's rank correlation (*r*) to assess univariate associations.

In the estrous cycle, the statistical analysis was comprised of the following: (1) the mean length of the estrous cycle in the controls and the Cd-exposed females, and (2) the frequency of each of the four cycle phases. The one-way analysis of variance following Dunnett's test was used in the case of variance homogeneity, and the Kruskal-Wallis analysis of variance was followed by the nonparametric test in the case of heterogeneity. Frequency data were analyzed with the Fisher's exact probability test. The statistical significance was set at $p \leq 0.05$.

3. Results

During the whole administration time (90 days) and observation periods (three or six months) no changes in animal behavior or appearance were noted; all rats survived until the termination of the study. There were also no significant changes in feed and water intake during the Cd administration or observation periods (data not shown). Moreover, integral toxicity parameters, such as body weight, selected organs' (liver, kidneys, and uterus) absolute and relative weights, and weight gain were unchanged in all groups (Supplementary Table S1 and S2).

3.1. Cd Concentration. Subchronic *per os* administration of Cd at the range of doses used in this study resulted in a significant dose-dependent increase in whole blood Cd concentration (Cd-B), as depicted in Figure 2. The mean Cd-B in rats from all pure control groups did not exceed $0.3 \mu\text{g/L}$. With the exception of the lowest Cd dose (0.09 mg/kg b.w.), significantly elevated Cd-B were maintained for both three and six months following the exposure. However, a decreasing trend in Cd-B could be observed in the postexposure period for all used doses (Figure 2). For the first three months of observation, the rate of Cd-B decrease was faster (about 10 times) than during the subsequent three months of observation (about twice). Only in the case of the lowest dose (0.09 mg/kg b.w.) did the Cd-B concentration decrease about three times after three months following the exposure period.

Like the whole blood, the concentration of Cd in the uterus was also dose-dependent (Figure 3). In the case of the uterus, the mean increase in Cd concentration, after 90 days' administration with Cd doses of 0.09, 0.9, 1.8, and 4.5 mg/kg b.w., was 15-, 80-, 320-, and 500-fold, respectively, compared to the control group. However, in contrast to Cd-B, all used doses caused a significant increase in Cd concentrations in this tissue, which was maintained at nearly the same concentration for up to six months after the end of the administration period. Moreover, in the examined females, a significant, strong correlation between the Cd-B and Cd concentrations in uterine tissues was observed after 90 days of exposure ($r = 0.98$; $p \leq 0.05$) and after three ($r = 0.92$; $p \leq 0.05$) and six months following termination of the exposure ($r = 0.96$; $p \leq 0.05$).

3.2. Concentrations of Sex Hormones. Concentrations of selected sex hormones (E_2 and P) and their ratio (P/E_2), both in the plasma and in the uterus tissue, are presented in Figures 4 and 5. The E_2 plasma concentration significantly decreased after administration of Cd in doses 0.9–4.5 mg/kg b.w. (Figure 4(a)), but this effect was not observed in the postexposure periods. In the case of the uterus, only the lowest dose (0.09 mg/kg b.w.) and the positive control caused a significant E_2 concentration increase in contrast to the other Cd doses, where the opposite trend was observed (Figure 5(a)). However, after 90 and 180 days of observation, in almost all animals exposed to Cd, a diminished concentration of E_2 was noted (Figure 5(a)). In the positive control group, the remarkably higher concentration of E_2 noted at the end of the exposure lasted up to six months in the plasma and up to three months in the uterus (Figures 4(a) and 5(a)).

The concentration of P in plasma seems to be unaffected by Cd administration (Figure 4(b)). In the uterus, only exposure to the lowest dose resulted in a significant increase in P concentration (Figure 5(b)). For a better illustration of the disturbed hormonal homeostasis, a P/E_2 ratio was calculated (Figures 4(c) and 5(c)). As shown in the results from Figure 4(c), significant disturbances in the calculated ratio of hormones' concentrations (P/E_2) in the plasma was observed only after 90 days of the exposure in the groups of rats administrated Cd at doses of 0.9–4.5 mg/kg b.w., which

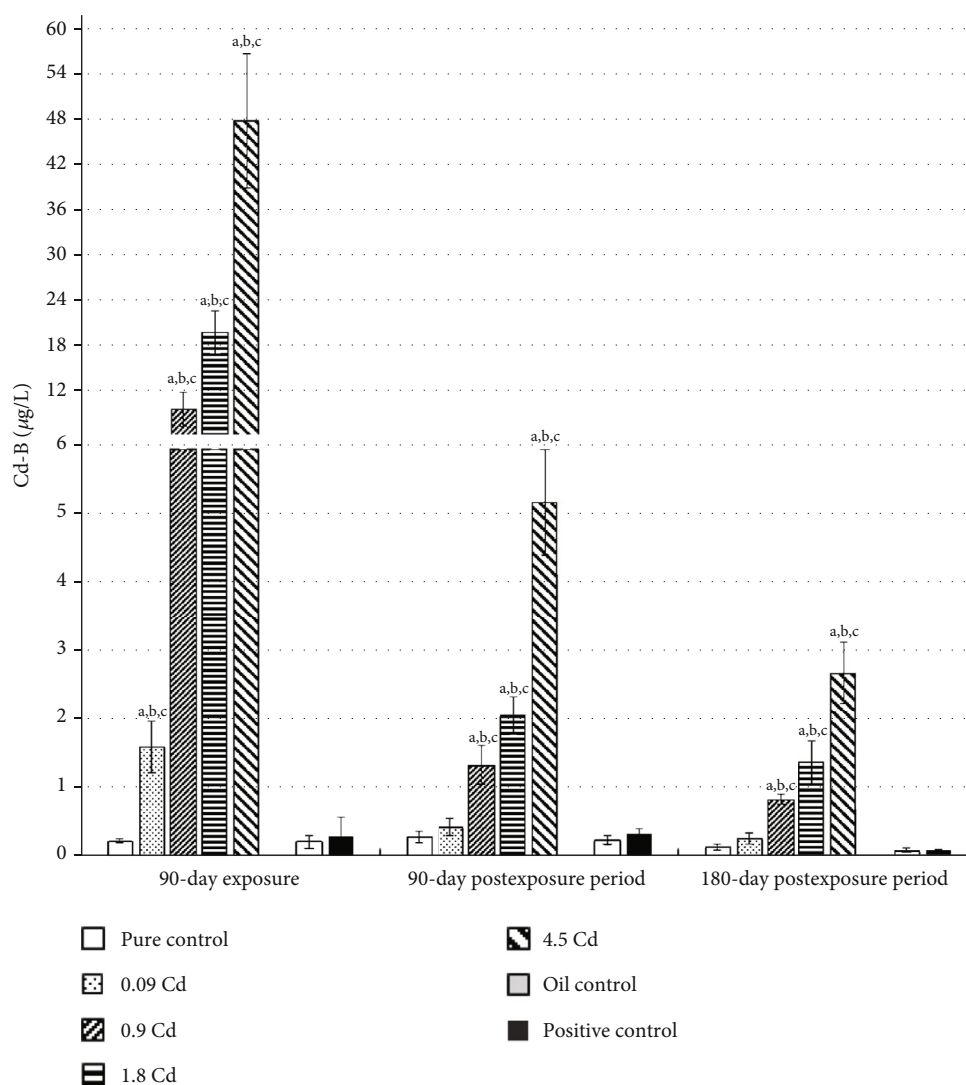


FIGURE 2: Cadmium concentrations in blood (Cd-B) following 90-day oral exposure to CdCl_2 or 17β -estradiol (positive control), at the 90-day and 180-day postexposure periods. $p \leq 0.05$ (a—vs. pure control group, b—vs. oil control, and c—vs. positive control).

mainly result from a decrease of E_2 concentration in the plasma of these females. However, in uterine tissue, significant changes were detected in the calculated ratio of P/ E_2 hormones in all assessed groups, which persisted until termination of the observation, with the exception of the group administered the lowest dose, in which the changes were not statistically significant (Figure 5(c)).

3.3. Estrous Cycle. The results of the estrous cycle analysis after exposure to Cd are presented in Table 1 and in Supplementary Figures S1–S3. For better readability of the observed disorders, which often occur in individual rats and sometimes there was no statistical significance in the group observed, in the figures, they are presented for each female rat individually. The highest number of both extended cycles and different phase lengths was recorded after 90 days of exposure in almost all groups administered Cd. The largest prolongation of the cycle length (5.6 ± 0.3 days) was noted in the positive control, which was caused by the

prolongation of the estrus phase at the expense of the diestrus and proestrus phases. In the groups of female rats exposed to Cd in doses of 0.09–1.8 mg/kg b.w., a statistically significant prolongation of the cycle was also noted in 37.5–50% of the rats; however, it was conditioned not only by the estrus phase (doses of 0.09 and 1.8 mg/kg b.w.) but also by the diestrus phase (dose of 0.9 mg/kg b.w.). After the rats were administered the highest dose of Cd (4.5 mg/kg b.w.), no significant increase in the duration of the cycle length was observed, but the individual phases, especially diestrus and proestrus, were significantly extended and shortened, respectively.

After both three and six months of postexposure observation, a significant prolongation of the cycle length among the exposed groups was maintained only at the lowest Cd dose (0.09 mg/kg b.w.) among 25% and 37.5% of the rats, respectively. However, the statistically significant prolongation of the estrus phase was only observed after 180 days of the postexposure period (Supplementary Figure S3).

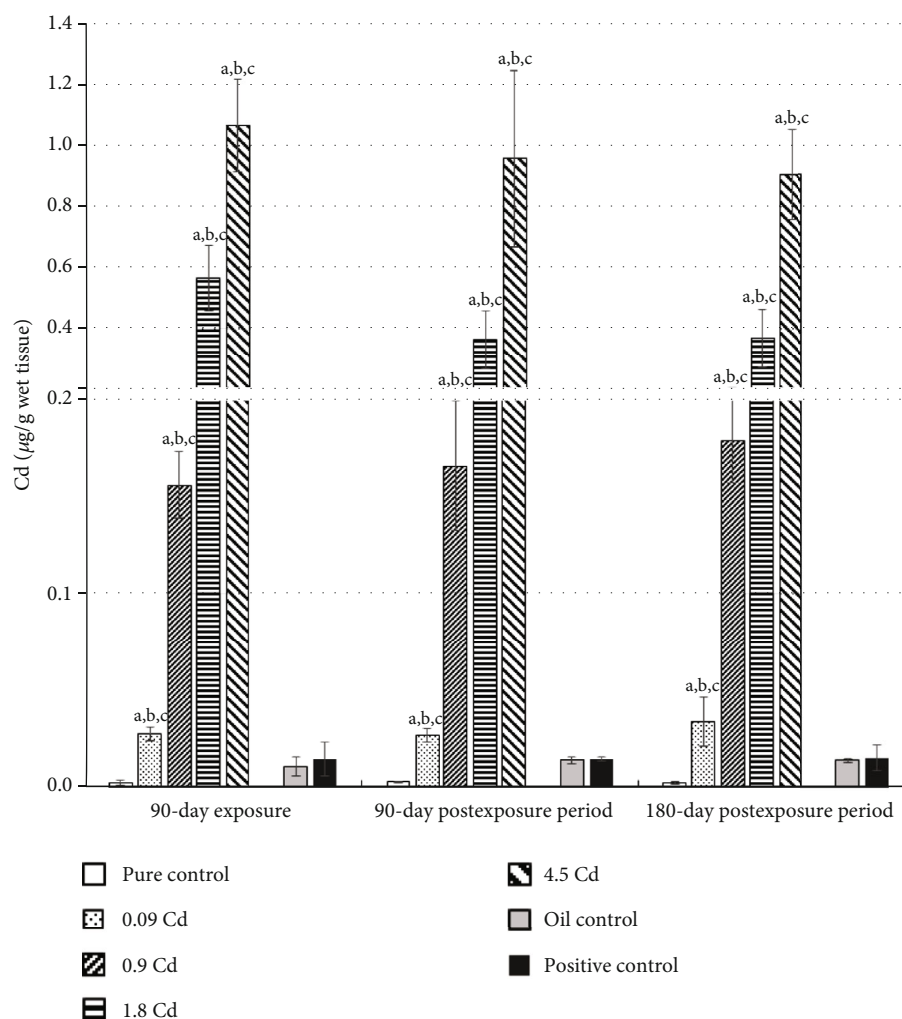


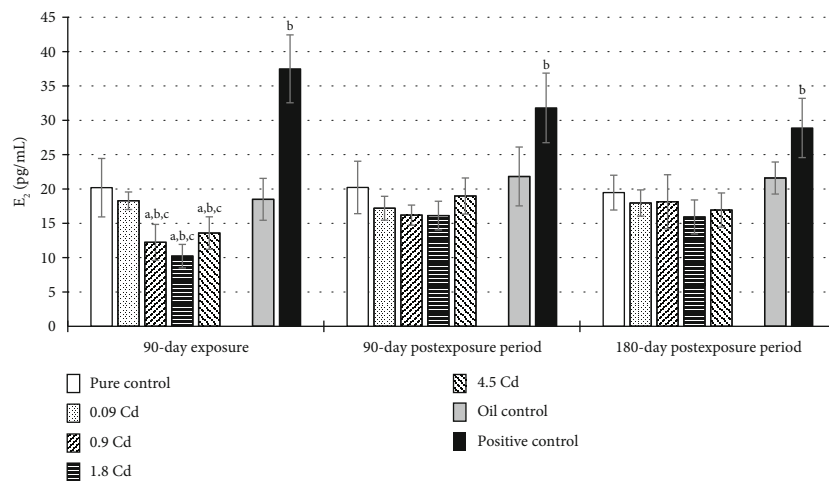
FIGURE 3: Cadmium concentrations in the uterus following 90-day oral exposure to CdCl_2 or 17β -estradiol (positive control), at the 90-day and 180-day postexposure periods. $p \leq 0.05$ (a—vs. pure control group, b—vs. oil control, and c—vs. positive control).

Administration of a higher dose (0.9 mg/kg b.w.) both after 90 and 180 days of observation led only to a statistically significant extension of the estrus phase; however, it did not lead to significant changes in the duration of the whole cycle length (Supplementary Figures S2 and S3). In the positive control, no changes were noted in the estrous cycle length after six months of observation (Table 1). Nevertheless, in individual females, estrus and diestrus phase prolongation and shortening of the proestrus phase, especially after six months was observed (Supplementary Figure S3).

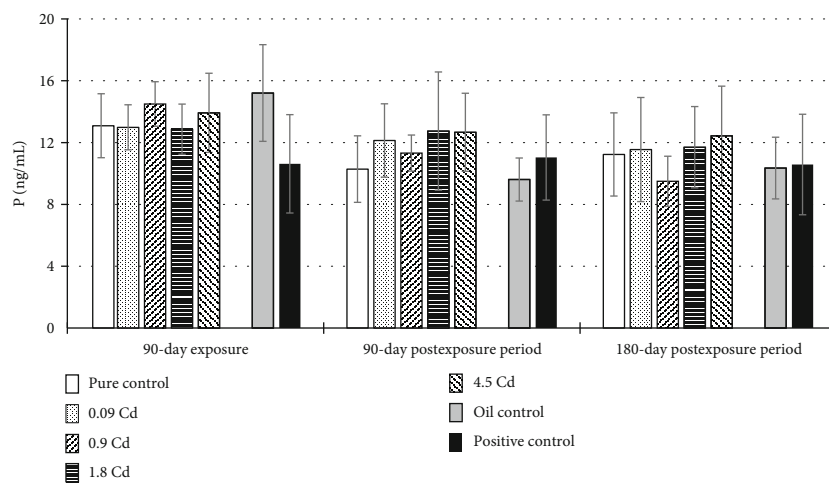
3.4. Endometrial Epithelium Thickness. Morphometric analysis during the estrus stage showed that Cd administered orally (0.09, 0.9, 1.8, and 4.5 mg/kg b.w.) for 90 days induced a significantly increased thickness of the epithelial layer only after the smallest dose when compared to the pure control group (Table 2). Similar endometrium changes with increased glands in the uterus in the group of females treated with 17β -E₂ were observed. These changes might suggest endometrial hyperplasia. Furthermore, the increase

in endometrial epithelium thickness (1.6-fold) was detected in comparison to the oil and pure control groups, which persisted for six months following the termination of exposure to 17β -E₂ (Table 2 and Figures 6(g) and (h)). In contrast, after the administration of higher doses of Cd, we observed a noticeable endometrium atrophy (a thin epithelial layer and not numerous glands), especially after a 180-day postexposure period, (Figures 6(c) and (d)) resulting from a decrease in E₂, both in the plasma and in uterine tissue, confirmed by a significant correlation coefficient between the concentration of E₂ in the plasma and endometrial epithelium thickness in all examined groups: $r = 0.51$ ($p \leq 0.05$) for the exposure period (group A), $r = 0.54$ ($p \leq 0.05$) after three months of observation (group B), and $r = 0.71$ ($p \leq 0.01$) for the six-month observation period (group C) (Figure 7).

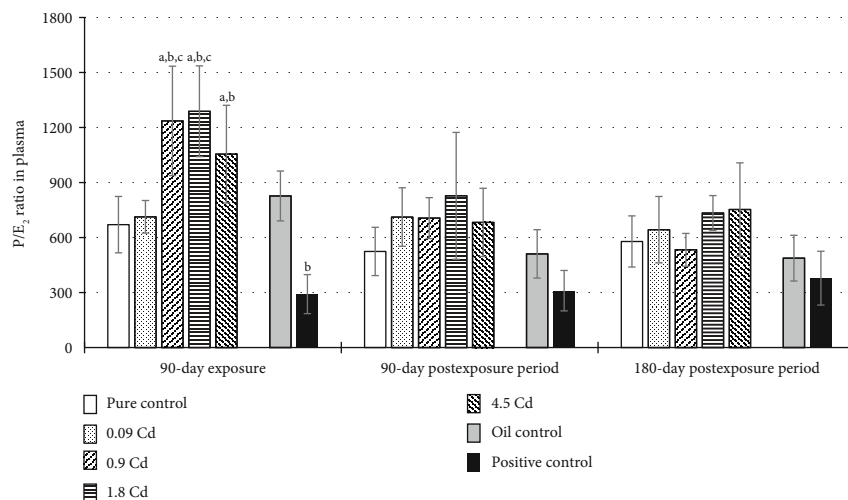
3.5. Ovary Histology. The control group demonstrated a normal basic structure of rat ovaries, usually containing a corpus luteum and all developmental stages of follicles (Figure 8(a)). The Cd-exposed group (4.5 mg/kg b.w.) showed histopathological alterations in the ovary: degeneration of the



(a)

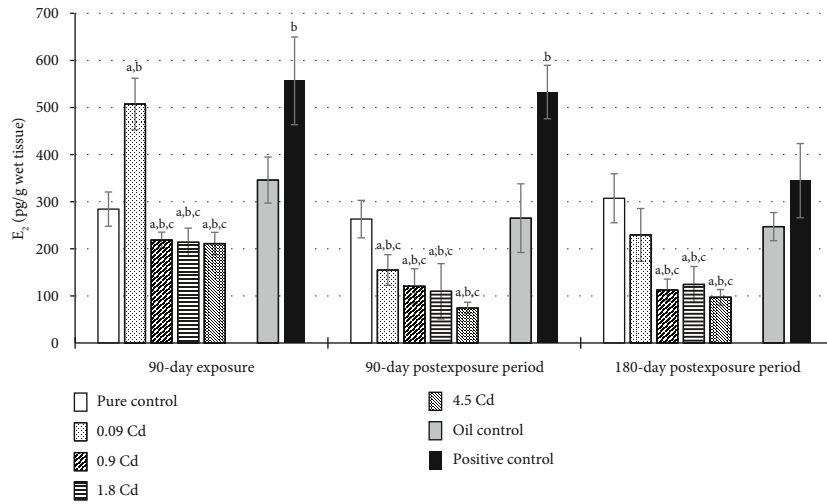


(b)

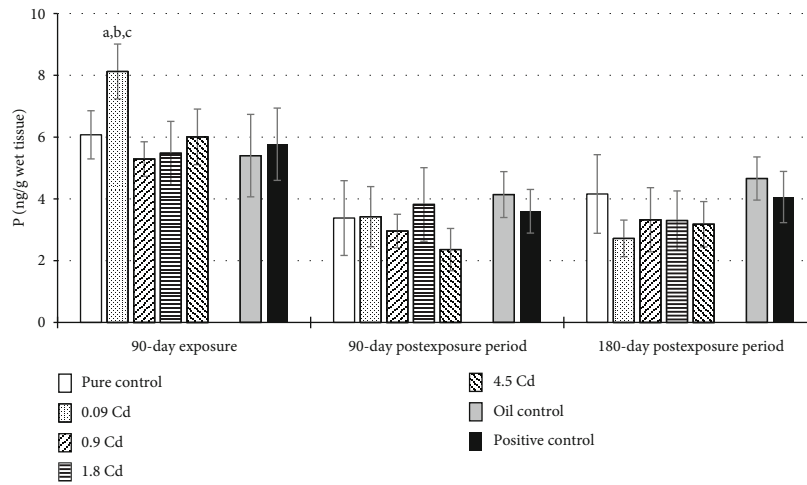


(c)

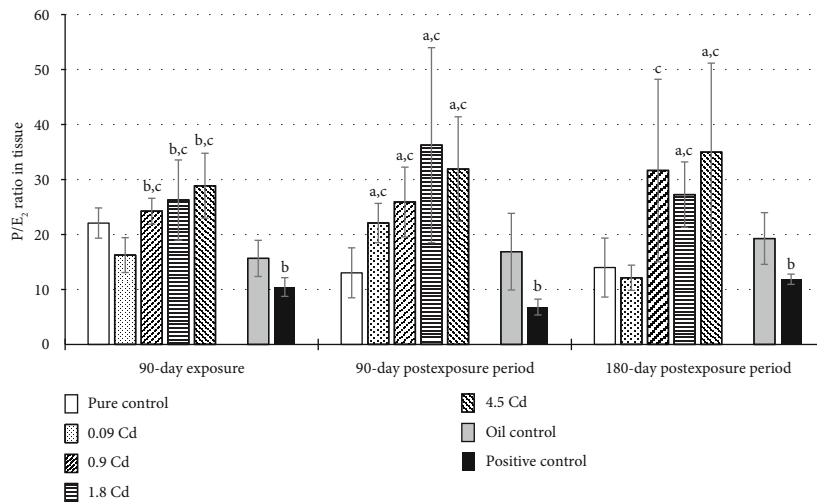
FIGURE 4: E₂ (a) and P (b) concentrations and the ratio of P/E₂ (c) in plasma following 90-day oral exposure to CdCl₂ or 17β-estradiol (positive control), at the 90-day and 180-day postexposure periods. *p* ≤ 0.05 (a—vs. pure control group, b—vs. oil control, and c—vs. positive control).



(a)



(b)



(c)

FIGURE 5: E₂ (a) and P (b) concentrations and the ratio of P/E₂ (c) in uterine tissue following 90-day oral exposure to CdCl₂ or 17β-estradiol (positive control), at the 90-day and 180-day postexposure periods. *p* ≤ 0.05 (a—vs. pure control group, b—vs. oil control, and c—vs. positive control).

TABLE 1: Cycle phases and all cycle lengths following oral, subchronic CdCl₂, or 17 β -estradiol (positive control) exposure and 90- and 180-day postexposure periods in comparison to controls.

Treatment	Dose (mg/kg b.w.)	Proestrus	Phase length (days)			Cycle length (days)	No. of extended cycles
			Estrus	Metaestrus	Diestrus		
Group A (90-day exposure)							
Pure control	0	1.8 \pm 0.1	2.8 \pm 0.2	2.6 \pm 0.1	4.7 \pm 0.2	4.3 \pm 0.1	0
Cd	0.09	1.2 \pm 0.1 ^a	4.6 \pm 1.0 ^a	1.9 \pm 0.3 ^a	4.6 \pm 0.7	5.4 \pm 0.8 ^a	4
Cd	0.9	1.8 \pm 0.2	2.9 \pm 0.2	2.2 \pm 0.2	5.1 \pm 0.2 ^a	4.7 \pm 0.2 ^a	3
Cd	1.8	1.8 \pm 0.2	3.4 \pm 0.2 ^a	2.3 \pm 0.2	4.4 \pm 0.2	4.9 \pm 0.3 ^a	3
Cd	4.5	1.4 \pm 0.1 ^a	2.8 \pm 0.2	2.6 \pm 0.1	5.2 \pm 0.2 ^a	4.5 \pm 0.3	4
Oil control	0	2.3 \pm 0.1	2.6 \pm 0.1	2.9 \pm 0.2	4.3 \pm 0.2	3.9 \pm 0.2	0
Positive control	0.03	1.4 \pm 0.1 ^a	4.6 \pm 0.4 ^a	2.3 \pm 0.2	3.7 \pm 0.3 ^a	5.6 \pm 0.3 ^a	5
Group B (90-day exposure and 90-day postexposure periods)							
Pure control	0	1.7 \pm 0.1	2.3 \pm 0.1	2.8 \pm 0.2	4.3 \pm 0.2	3.8 \pm 0.1	0
Cd	0.09	1.7 \pm 0.1	1.9 \pm 0.3 ^a	2.6 \pm 0.3	4.8 \pm 0.4	4.8 \pm 0.5 ^a	2
Cd	0.9	1.6 \pm 0.1	2.9 \pm 0.2 ^a	2.2 \pm 0.2 ^a	4.0 \pm 0.2	4.1 \pm 0.1	0
Cd	1.8	1.6 \pm 0.1	2.6 \pm 0.2	2.6 \pm 0.1	4.1 \pm 0.1	4.0 \pm 0.1	0
Cd	4.5	1.8 \pm 0.2	2.4 \pm 0.2	2.8 \pm 0.2	4.0 \pm 0.2	3.9 \pm 0.1	0
Oil control	0	1.6 \pm 0.1	2.3 \pm 0.2	2.9 \pm 0.2	4.1 \pm 0.2	4.0 \pm 0.1	0
Positive control	0.03	1.6 \pm 0.1	2.2 \pm 0.1	2.7 \pm 0.2	4.4 \pm 0.1	4.1 \pm 0.1	0
Group C (90-day exposure and 180-day postexposure periods)							
Pure control	0	1.6 \pm 0.1	2.8 \pm 0.1	3.1 \pm 0.3	4.4 \pm 0.1	4.1 \pm 0.1	0
Cd	0.09	1.5 \pm 0.3	4.9 \pm 0.9 ^a	2.7 \pm 0.3	2.9 \pm 0.4 ^a	5.3 \pm 0.9 ^a	3
Cd	0.9	1.6 \pm 0.2	4.1 \pm 0.6 ^a	2.8 \pm 0.2	3.5 \pm 0.3 ^a	4.3 \pm 0.3	1
Cd	1.8	1.6 \pm 0.1	2.8 \pm 0.1	3.4 \pm 0.1	4.2 \pm 0.1	4.0 \pm 0.1	0
Cd	4.5	1.8 \pm 0.1	2.8 \pm 0.1	3.6 \pm 0.3	3.9 \pm 0.3	4.2 \pm 0.1	0
Oil control	0	1.4 \pm 0.1	2.8 \pm 0.1	3.2 \pm 0.2	4.7 \pm 0.2	4.1 \pm 0.1	0
Positive control	0.03	1.4 \pm 0.1	2.9 \pm 0.1	3.3 \pm 0.2	4.1 \pm 0.2	4.3 \pm 0.2	1

All values are expressed as means \pm SEM ($n = 8$). ^aSignificantly different from pure control ($p \leq 0.05$).

TABLE 2: Endometrial epithelium thickness (μm) after subchronic oral exposure to CdCl₂ or 17 β -estradiol (E₂) exposure and 90- and 180-day postexposure periods in comparison to controls.

Groups	Endometrial epithelium thickness (μm)						
	Pure control	0.09 mgCd/kg	0.9 mgCd/kg	1.8 mgCd/kg	4.5 mgCd/kg	Oil control	Positive control
A—90-day exposure	19.2 \pm 2.2	27.0 \pm 3.1 ^{a,c}	21.7 \pm 3.6 ^c	20.1 \pm 3.1 ^c	24.5 \pm 6.3 ^c	21.9 \pm 3.3	36.4 \pm 2.5 ^b
B—90-day postexposure period	21.8 \pm 4.3	21.9 \pm 1.9 ^c	19.4 \pm 2.1 ^c	17.9 \pm 2.1 ^c	19.1 \pm 2.9 ^c	21.80 \pm 1.7	34.8 \pm 2.5 ^b
C—180-day postexposure period	21.7 \pm 1.7	19.6 \pm 1.3 ^c	18.9 \pm 2.5 ^c	17.1 \pm 1.7 ^{a,b,c}	16.5 \pm 1.6 ^{a,b,c}	22.5 \pm 2.1	33.8 \pm 4.1 ^b

All values are expressed as mean \pm SD. ^a $p \leq 0.05$, significantly different from pure control animals. ^b $p \leq 0.05$, significantly different from oil control. ^c $p \leq 0.05$, significantly different from positive control.

corpus luteum and damaged and less numerous oocytes (Figures 8(b) and 8(c)). In the positive control, no degenerative changes in the ovaries were reported (Figure 8(d)).

3.6. Oxidative Stress Parameters. Administration of Cd at the two highest doses (1.8 and 4.5 mg/kg b.w.) results in a significant rise of MDA concentration in the uterus (Table 3), but this effect persisted for the whole observation period following the exposure (up to six months) only after the highest dose (4.5 mg/kg b.w.). The same dose also

affects the activity of the uterine CAT causing a significant decrease (around 25% compared to the pure control), but only just after the administration period. On the other hand, no changes in the concentration of GSH in this tissue were observed throughout all studied doses and periods. In the case of TAS, only the administration of E₂ caused a remarkable increase of TAS in the plasma after the termination of exposure (Table 3). However, such effect was not noted in either observation periods or in the case of Cd exposure.

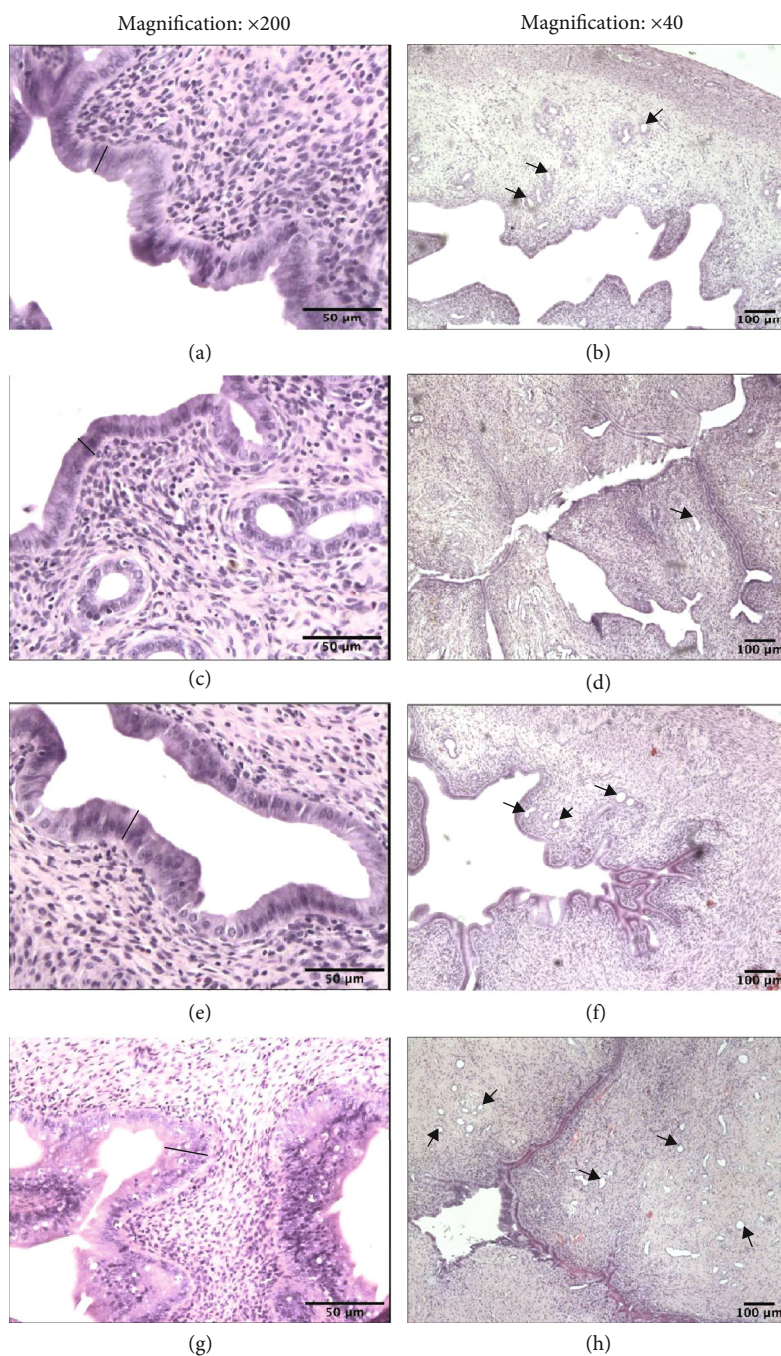


FIGURE 6: Effect of CdCl_2 on uterine histology. Photomicrographs of uterine sections stained with hematoxylin and eosin from rats after a 180-day postexposure period (magnification: $\times 200$ and $\times 40$). (a and b) Sections from the uteri of pure control rats. A thick epithelial layer is seen as well as many glands. (c) Sections from the uteri of the Cd group (4.5 mgCd/kg). The epithelial layer is thin and contains a small number of the cells. (d) Sections from the uteri of the Cd group (4.5 mgCd/kg). The epithelial layer is thin, and the glands are not numerous. (e and f) Sections from the uteri of oil control rats. The epithelial layer is similar to that of the pure control rats. (g) Sections from the uteri of the 17β -estradiol group (0.03 mg E_2 /kg). Notice the increased thickness of the epithelial layer. (h) Sections from the uteri of the 17β -estradiol group (0.03 mg E_2 /kg). Numerous uterine glands are seen. Black bars represent epithelial thickness; arrows—uterine gland.

4. Discussion

There is a growing fear that a lifetime exposure to xenobiotics, which disturb hormonal homeostasis, may cause permanent change in the functioning of the organism,

particularly in the reproductive system. Studies on the xenoestrogenicity of Cd conducted so far are ambiguous; some of them indicate its estrogenic activity [21, 25, 26, 40], while others show an antiestrogenic effect [21, 41, 42]. In the current study, to assess the estrogenic-like effect of Cd

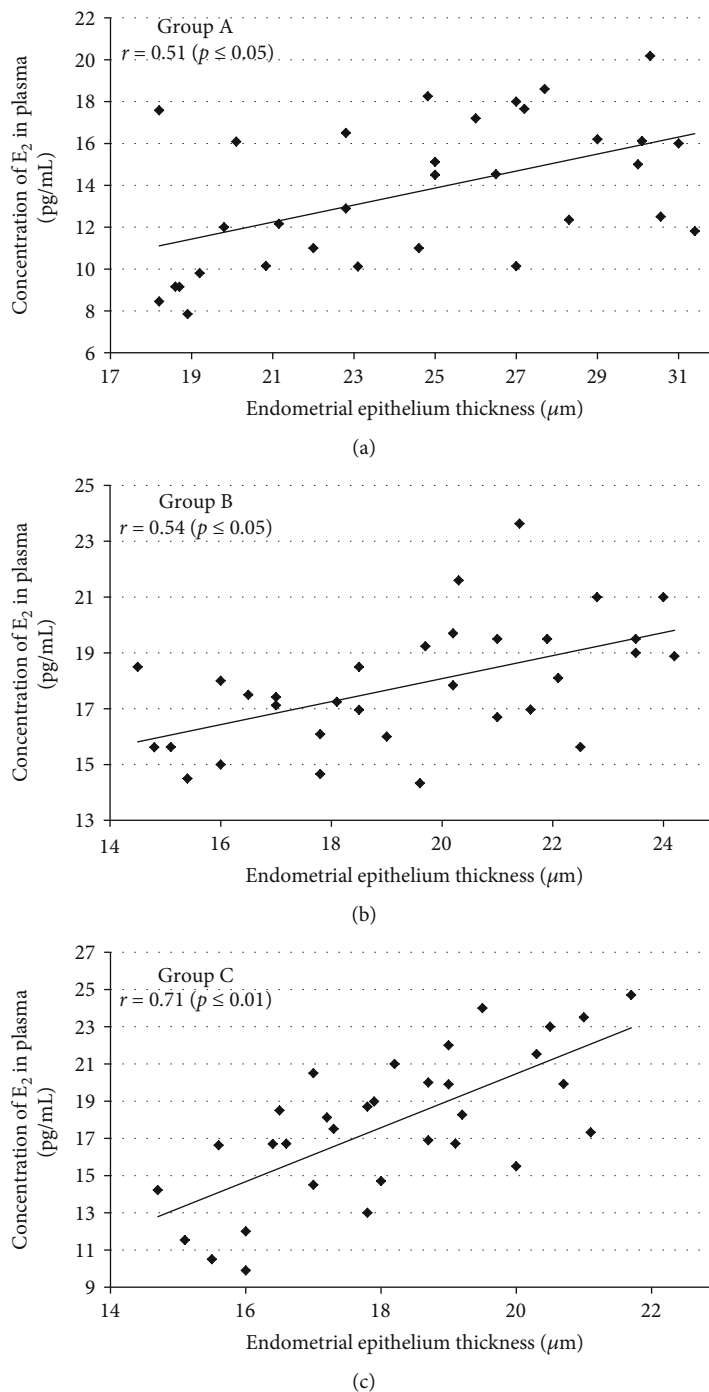


FIGURE 7: Association between plasma E₂ concentration and endometrial epithelium thickness in Cd-exposed rats from group A (90-day exposure) (a); group B (90-day exposure and 90-day postexposure periods) (b); and group C (90-day exposure and 180-day postexposure periods) (c).

in female rats, we applied a 90-day Cd exposure model with a long observation period (up to six months) of exposed animals compared to control groups, including a positive control. We used *per os* administration, because this route is consistent with the general population’s exposure to this metal. Average daily Cd intakes in European countries have been estimated between 0.00029 and 0.00106 mg/kg [4]. The lowest daily dose of Cd adopted in this study (0.09 mg/kg b.w.) was similar to a lower level of general population envi-

ronmental exposure [43, 44]. In our study, Cd-B in rats exposed to 0.09 mg/kg b.w. for 90 days were similar to those observed in smokers in the general population [2]. Cd-B in long-term Cd exposure is thought to be a good indicator of its internal dose and accumulation, not only in the kidney (the target organ) but also in other soft tissues, including the uterus [45, 46]. The results obtained both in this study and in our previous studies (30-day administration of Cd to female rats) confirm the relationship between Cd-B and

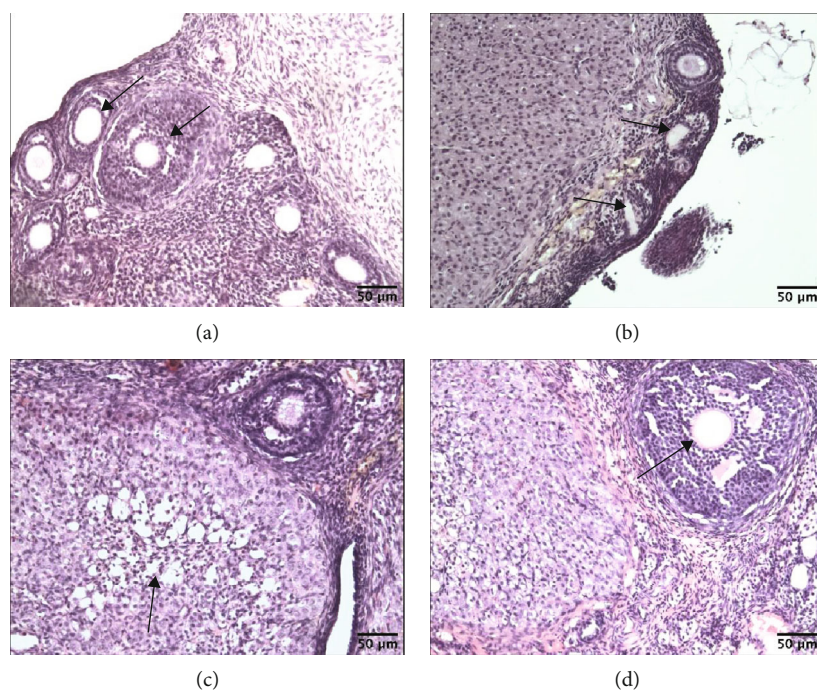


FIGURE 8: Effect of CdCl_2 on ovary histology. Photomicrographs of ovary sections stained with hematoxylin and eosin (magnification: $\times 100$) from rats after a 180-day postexposure period. (a) Sections from the ovaries of pure control rats. Notice numerous oocytes (arrows). (b) Sections from the ovaries of the Cd group (4.5 mg Cd/kg). The oocytes are scanty and two of them show degenerative changes (arrows). (c) Sections from the ovaries of the Cd group (4.5 mg Cd/kg). Arrow points—degenerative changes of corpus luteum. (d) Sections from the ovaries of the 17β -estradiol group (0.03 mg E_2 /kg). Corpus luteum and big follicle are seen (arrow—big follicle).

Cd uterus concentration [24]. After a 90-day administration of Cd, its concentration in the uterus increased in a dose-dependent manner and was about three times higher than that after a 30-day administration [24]. Moreover, Cd concentrations in the uterus six months after terminating the exposure were virtually at the same level as at the end of the administration period. Cd bioaccumulation in the uterine tissue was confirmed by numerous studies among smoking and nonsmoking women [11, 12, 46]. The health implications of Cd bioaccumulation in reproductive organs are still not well known.

Cd action as a metalloestrogen seems to depend not only on the level of exposure but also on its duration. While the administration of the lowest dose of Cd (0.09 mg/kg b.w.) caused estrogenic-like effects, in female rats which were administered higher doses, antiestrogenic effects were observed. The estrogenic effects of the lowest Cd dose were expressed by firstly, significantly higher E_2 concentrations in the uterine tissue which correlated with the endometrial epithelium thickness, and secondly, by the prolongation of the estrus stage in the estrous cycle, like in positive control receiving 17β - E_2 . An abnormal cycle was maintained for up to six months after the termination of the administration.

Uterus weight is one of the accepted endpoints useful in estrogenicity assessment of xenobiotics [47, 48]. Although changes in the endocrine profile or thickness of the epithelial endometrium may affect the weight of the uterus, in our study, the wet weight of the uterus was not significantly different compared to the pure control. Ali et al. [27] did not detect any changes in the wet weight of the uterus

either, but they did notice an increase in the uterine luminal epithelium in mice receiving Cd in doses of 50 and 500 $\mu\text{g}/\text{kg}$ b.w. Similarly, no changes in uterine weight due to Cd have been described in other studies [21, 49]; however, Johnson et al. [26] showed a significant increase in uterine weight in rats after a single *i.p.* injection of Cd at 5 $\mu\text{g}/\text{kg}$ b.w.

The mechanism of the estrogenic action of Cd in the uterus is thought to be associated with the ER. Stoica et al. [25] suggest that Cd ions can activate the ER by creating high-affinity interactions with the hormone receptor binding domain. Fechner et al. [50] revealed that Cd interacts with the ligand binding domain (LBD) of the $\text{ER}\alpha$ and affects the conformation of the receptor. However, the binding event, as well as the induced conformation change, greatly depends on the accessibility of the cysteine tails in the LBD. Kluxen et al. [51] showed that Cd exerts estrogen-like effects and modulates aryl hydrocarbon receptor (AhR) expression and that of AhR target genes. There are also studies indicating that Cd does not activate classical estrogen signaling in the uterus but interferes with its pathway [27].

The fact that the estrogen response induced by Cd is dose-dependent seems to be confirmed by *in vitro* studies. For instance, Denier et al. [52] demonstrated on yeast cells that Cd in low concentrations enhanced the estrogenic response due to the interaction of E_2 with ER. Importantly, in high concentrations, Cd was cytotoxic to yeast cells. The dose-dependent effect of Cd was also observed in our study. The administration of Cd at high doses (0.9–4.5 mg/kg b.w.) to female rats led to a decrease in E_2 concentration in both

TABLE 3: Oxidative stress biomarkers in rats after oral exposure to CdCl₂ or 17 β -estradiol (positive control) exposure and 90- and 180-day postexposure periods in comparison to controls.

Treatment	Doses (mg/kg b.w.)	TAS in plasma (mM)	GSH in uterus (μ mol/g)	CAT in uterus (U/mg protein)	MDA in uterus (nmol/g)
Group A (90-day exposure)					
Pure control	0	1.16 \pm 0.09	1.37 \pm 0.32	8.66 \pm 0.96	62.3 \pm 6.80
Cd	0.09	1.11 \pm 0.09	1.47 \pm 0.46	11.0 \pm 2.10	80.2 \pm 7.05
Cd	0.9	1.08 \pm 0.04	1.84 \pm 0.18	12.3 \pm 1.54	71.0 \pm 14.2
Cd	1.8	1.02 \pm 0.07	1.20 \pm 0.41	8.71 \pm 0.89	84.7 \pm 4.25 ^a
Cd	4.5	0.88 \pm 0.15	1.53 \pm 0.40	6.61 \pm 0.60 ^{a,b,c}	98.1 \pm 5.13 ^{a,b,c}
Oil control	0	0.95 \pm 0.11	1.80 \pm 0.10	8.99 \pm 1.68	61.8 \pm 3.52
Positive control	0.03	1.61 \pm 0.60 ^b	1.56 \pm 0.33	7.99 \pm 1.53	70.0 \pm 8.52
Group B (90-day exposure and 90-day postexposure periods)					
Pure control	0	1.04 \pm 0.09	1.46 \pm 0.31	9.02 \pm 1.60	65.2 \pm 11.30
Cd	0.09	1.01 \pm 0.06	1.24 \pm 0.21	9.88 \pm 1.82	74.5 \pm 10.92
Cd	0.9	1.00 \pm 0.03	1.14 \pm 0.19	11.0 \pm 1.54	74.8 \pm 14.64
Cd	1.8	0.96 \pm 0.07	1.32 \pm 0.20	7.89 \pm 1.15	72.9 \pm 9.07
Cd	4.5	0.93 \pm 0.08	1.29 \pm 0.05	7.25 \pm 1.61	94.6 \pm 19.50 ^a
Oil control	0	1.05 \pm 0.06	1.41 \pm 0.12	9.56 \pm 1.98	67.0 \pm 5.04
Positive control	0.03	1.18 \pm 0.06	1.61 \pm 0.54	10.2 \pm 1.63	68.9 \pm 9.02
Group C (90-day exposure and 180-day postexposure periods)					
Pure control	0	1.02 \pm 0.08	1.14 \pm 0.24	9.66 \pm 1.36	60.5 \pm 5.85
Cd	0.09	0.95 \pm 0.07	1.25 \pm 0.29	9.98 \pm 1.95	58.2 \pm 13.90
Cd	0.9	0.98 \pm 0.04	1.08 \pm 0.12	10.6 \pm 1.83	71.6 \pm 11.08
Cd	1.8	0.96 \pm 0.09	0.99 \pm 0.08	9.21 \pm 1.39	75.3 \pm 5.33
Cd	4.5	0.95 \pm 0.10	1.25 \pm 0.49	8.98 \pm 1.65	92.5 \pm 7.10 ^{a,b,c}
Oil control	0	1.02 \pm 0.06	1.21 \pm 0.24	10.0 \pm 0.91	64.9 \pm 6.93
Positive control	0.03	1.16 \pm 0.09	1.15 \pm 0.25	11.1 \pm 1.66	62.7 \pm 3.96

All values are expressed as mean \pm SD. ^a $p \leq 0.05$, significantly different from control pure animals. ^b $p \leq 0.05$, significantly different from oil control, ^c $p \leq 0.05$, significantly different from positive control.

plasma and uterine tissue. Although the effect of lowering E₂ concentrations in plasma by Cd exposure has been previously described [18, 19, 22], the same effect in the uterine tissue is, according to our knowledge, described here for the first time.

Disorders in E₂ secretion may have various causes, including, for example, ovary damage, which was observed in this study and was expressed as, among others, degeneration of the corpus luteum, damaged and less numerous oocytes, and degeneration of the granulosa cells. These effects are in agreement with the literature [20, 28–30]. Structural damage to the ovary and disturbed E₂ secretion noted after the highest Cd dose may contribute to the prolongation of the diestrus stage in the estrous cycle. Such observations are in line with our previous results from a 30-day experiment [24] and studies conducted by Samuel et al. [29]. Disorders in the cycle may be the first symptoms of reproductive aging [53]. This can be indirectly confirmed by decreased thickness of the epithelial endometrium observed in our study, which significantly correlated with a lowered concentration of E₂ in the plasma.

It is suggested that estradiol is a physiological antioxidant whose deficiency has been shown to be associated with oxidative stress [54]. Thus, the changes observed in the uterus of rats receiving high doses of Cd in this study may also be associated with the induction of oxidative stress in the reproductive organs and it cannot be ruled out that the induction of oxidative stress contributes to changes in hormonal balance. The mechanism of prooxidative Cd action is well known [55]. Although Cd is not a redox-active agent and is not able to directly generate ROS through the Fenton or Haber-Weiss reaction, it contributes to the occurrence of oxidative stress indirectly through weakening the antioxidative defence and increasing prooxidant concentrations, as well as causing mitochondria injury [56]. Numerous *in vitro* and *in vivo* studies confirmed that Cd disrupts the antioxidant defence by reducing the levels of antioxidants, which are important in the removal of ROS [55, 57]. Effects of ROS can be mitigated by antioxidants, both nonenzymatic and enzymatic, and key enzymatic antioxidants in cells are superoxide dismutase (SOD), catalase (CAT), and glutathione peroxidase

(GPx) [58, 59]. CAT plays a crucial role in scavenging peroxides such as H_2O_2 . Thus, its diminished activity may indicate cellular accumulation of this reactive oxygen species, which are capable of crossing cell membranes [58]. Although subacute (up to 30 days) administration of Cd leads to alterations in enzymatic antioxidant defence in rat uteri and ovaries [29, 31, 60–62], there is no data concerning subchronic Cd exposure. In the present subchronic study, decreased CAT activity and increased MDA concentration caused by the highest Cd dose seem to confirm disturbed redox balance in the uterus. Although other markers of oxidative stress were not determined, it could be assumed that the decrease of CAT activity may indicate an oxidative stress in this tissue.

It was reported that ROS may propagate the initial attack on lipid membranes to cause lipid peroxidation (LPO). MDA (malondialdehyde) is one of the numerous compounds formed during the process of LPO, which binds to, inter alia, proteins and DNA modifying its structure. Studies proved that these MDA adducts play a critical role in many cellular processes and may participate in secondary deleterious reactions that may cause profound changes in the biochemical properties of biomolecules, which may facilitate development of various pathological states [63]. The significantly increased MDA concentration in uterine tissue, which was observed in this study, remained up to six months after terminating the exposure. Thus, the histopathological changes in the uterus may be also the result of the indirect induction of lipid peroxidation by Cd.

Noteworthy, Cd could induce ROS production also nonenzymatically. Nonenzymatic antioxidants such as vitamins C and E, zinc and selenium, protein thiols (e.g., glutathione), bilirubin, and urate are often determined as total antioxidant status (TAS). In this study, the uterine concentration of GSH and plasma TAS in rats exposed to Cd did not differ significantly from that of control rats. Also, Mężyńska et al. [44, 64] did not observe a statistically significant difference in TAS concentrations analyzed in rat liver after a similar time (3 month) and level of Cd exposure (1 and 5 mg/kg b.w.). A significantly reduced hepatic TAS concentration was noticed only after ten months of Cd administration [44, 64]. Therefore, it has been suggested that the mechanism of oxidative stress induced by Cd may vary and depend on the time of exposure. Some studies indicate that chronic exposure to Cd probably induces ROS by overwhelming the antioxidant defence leading to increased lipid peroxidation [64, 65]. On the other hand, short-term exposure to Cd contributes to a significant depletion of glutathione and protein-bound sulfhydryl groups, which results in enhanced production of ROS [66, 67].

Unfortunately, it is very difficult to state whether Cd can affect reproduction in women through changes in sex hormones and/or through oxidative stress. So far, it has only been shown that Cd accumulates in women's uteri and it may also be responsible for impaired hormonal metabolism [10, 68–72]. Moreover, in several epidemiological studies, the relationship between dietary Cd exposure and incidence of hormone-related cancer, including in the endometrium and ovaries, has been observed [11, 73].

5. Conclusions

Our study indicates that Cd exhibits both estrogenic-like (in a low dose range) and antiestrogenic-like (in a high dose range) effects, which were connected with disturbed plasma and the uterine estradiol concentrations and estrous cyclicity disorders. These effects, as well as increased lipid peroxidation in the uterus and ovary, were observed for six months following termination of Cd exposure. In addition, Cd toxicity after the highest dose was also associated with structural damage of the uterus and ovaries. The obtained results indicate that women's long-term exposure to Cd may lead to reproductive system disorders, which might even result in infertility.

Data Availability

The data used to support the findings of this study are included within the article.

Conflicts of Interest

The authors declare that there is no conflict of interest regarding the publication of this paper.

Acknowledgments

This work was supported by the Polish National Science Centre (Grant No. N404 504938). The authors would like to thank Małgorzata Skrzypińska-Gawrysiak, Ph.D., and Krystyna Sitarek, Ph.D., for their helpful advice on various technical issues and Anna Jurek, M.A., for comments and suggestions during the preparation of the English version of this paper.

Supplementary Materials

The supplemental information provides additional data concerning organs and body weights of rats after oral exposure to $CdCl_2$ or 17β -estradiol (positive control) and 90 and 180-day postexposure periods in comparison to controls (Tables S1 and S2). Moreover, Figures S1, S2, and S3 depict the estrous cycle in single females after all periods of exposure to Cd or 17β -estradiol as well as in observation periods. (*Supplementary Materials*)

References

- [1] ATSDR, *Agency for Toxic Substances and Disease Registry, ATSDR's Substance Priority List*, 2017, <https://www.atsdr.cdc.gov/spl/index.html>.
- [2] G. F. Nordberg, A. Bernard, G. L. Diamond et al., "Risk assessment of effects of cadmium on human health (IUPAC Technical Report)," *Pure and Applied Chemistry*, vol. 90, no. 4, pp. 755–808, 2018.
- [3] L. Järup and A. Åkesson, "Current status of cadmium as an environmental health problem," *Toxicology and Applied Pharmacology*, vol. 238, no. 3, pp. 201–208, 2009.

- [4] EFSA, European Food Safety Authority, "Cadmium dietary exposure in the European population," *EFSA Journal*, vol. 10, no. 1, pp. 2551–2588, 2012.
- [5] EFSA, European Food Safety Authority, "Cadmium in food, scientific opinion of the panel on contaminants in the food chain," *The EFSA Journal*, vol. 980, pp. 1–139, 2009.
- [6] M. Vahter, M. Berglund, A. Åkesson, and C. Lidén, "Metals and women's health," *Environmental Research*, vol. 88, no. 3, pp. 145–155, 2002.
- [7] S. Satarug, J. R. Baker, P. E. B. Reilly, M. R. Moore, and D. J. Williams, "Cadmium levels in the lung, liver, kidney cortex, and urine samples from Australians without occupational exposure to metals," *Archives of Environmental Health: an International Journal*, vol. 57, no. 1, pp. 69–77, 2002.
- [8] S. Satarug and M. R. Moore, "Adverse health effects of chronic exposure to low-level cadmium in foodstuffs and cigarette smoke," *Environmental Health Perspectives*, vol. 112, no. 10, pp. 1099–1103, 2004.
- [9] M. Uetani, E. Kobayashi, Y. Suwazono, T. Kido, and K. Nogawa, "Cadmium exposure aggravates mortality more in women than in men," *International Journal of Environmental Health Research*, vol. 16, no. 4, pp. 273–279, 2006.
- [10] M. Nasiadek, T. Krawczyk, and A. Sapota, "Tissue levels of cadmium and trace elements in patients with myoma and uterine cancer," *Human and Experimental Toxicology*, vol. 24, no. 12, pp. 623–630, 2005.
- [11] A. Åkesson, B. Julin, and A. Wolk, "Long-term dietary cadmium intake and postmenopausal endometrial cancer incidence: a population-based prospective cohort study," *Cancer Research*, vol. 68, no. 15, pp. 6435–6441, 2008.
- [12] P. Rzymiski, P. Niedzielski, P. Rzymiski, K. Tomczyk, L. Kozak, and B. Poniedziałek, "Metal accumulation in the human uterus varies by pathology and smoking status," *Fertility and Sterility*, vol. 105, no. 6, pp. 1511–1518.e3, 2016.
- [13] K. Paksy, B. Varga, and P. Lázár, "Cadmium interferes with steroid biosynthesis in rat granulosa and luteal cells in vitro," *Biomaterials*, vol. 5, no. 4, pp. 245–250, 1992.
- [14] P. Massányi and V. Uhrin, "Histological changes in the uterus of rabbits after an administration of cadmium," *Journal of Environmental Science and Health. Part A: Environmental Science and Engineering and Toxicology*, vol. 32, no. 5, pp. 1459–1466, 1997.
- [15] M. P. Waalkes and S. Rehm, "Lack of carcinogenicity of cadmium chloride in female Syrian hamsters," *Toxicology*, vol. 126, no. 3, pp. 173–178, 1998.
- [16] M. Piasek and J. W. Laskey, "Effects of in vitro cadmium exposure on ovarian steroidogenesis in rats," *Journal of Applied Toxicology*, vol. 19, no. 3, pp. 211–217, 1999.
- [17] D. Tomislav, D. Vesna, T. Antun, C. Marijan, B. Ljiljana, and M. Darko, "The effect of cadmium salts on plasma hormone levels and histopathology of the ovaries in female rabbits," *Tieraerztliche Umschau*, vol. 57, no. 10, pp. 539–546, 2002.
- [18] X. Y. Han, Z. R. Xu, Y. Z. Wang, and W. L. Du, "Effects of cadmium on serum sex hormone levels in pigs," *Journal of Animal Physiology and Animal Nutrition*, vol. 90, no. 9–10, pp. 380–384, 2006.
- [19] W. Zhang and H. Jia, "Effect and mechanism of cadmium on the progesterone synthesis of ovaries," *Toxicology*, vol. 239, no. 3, pp. 204–212, 2007.
- [20] P. Massányi, N. Lukáč, V. Uhrin et al., "Female reproductive toxicology of cadmium," *Acta Biologica Hungarica*, vol. 58, no. 3, pp. 287–299, 2007.
- [21] N. Höfer, P. Diel, J. Wittsiepe, M. Wilhelm, and G. H. Degen, "Dose- and route-dependent hormonal activity of the metal-estrogen cadmium in the rat uterus," *Toxicology Letters*, vol. 191, no. 2–3, pp. 123–131, 2009.
- [22] A. W. Obianime and J. S. Aprioku, "Biochemical and hormonal effects of cadmium in female guinea pigs," *Journal of Toxicology and Environmental Health Sciences*, vol. 3, no. 2, pp. 39–43, 2011.
- [23] M. Monsefi and B. Fereydouni, "The effects of cadmium pollution on female rat reproductive system," *Journal of Infertility and Reproductive Biology*, vol. 1, no. 1, pp. 1–6, 2013.
- [24] M. Nasiadek, M. Danilewicz, K. Sitarek et al., "The effect of repeated cadmium oral exposure on the level of sex hormones, estrous cyclicity, and endometrium morphometry in female rats," *Environmental Science and Pollution Research International*, vol. 25, no. 28, pp. 28025–28038, 2018.
- [25] A. Stoica, B. S. Katzenellenbogen, and M. B. Martin, "Activation of estrogen receptor-alpha by the heavy metal cadmium," *Molecular Endocrinology*, vol. 14, no. 4, pp. 545–553, 2000.
- [26] M. D. Johnson, N. Kenney, A. Stoica et al., "Cadmium mimics the *in vivo* effects of estrogen in the uterus and mammary gland," *Natural Medicine*, vol. 9, no. 8, pp. 1081–1084, 2003.
- [27] I. Ali, P. E. Penttinen-Damdimopoulou, S. I. Mäkelä et al., "Estrogen-Like Effects of Cadmium *in Vivo* Do Not Appear to be Mediated via the Classical Estrogen Receptor Transcriptional Pathway," *Environmental Health Perspectives*, vol. 118, no. 10, pp. 1389–1394, 2010.
- [28] Y. Wang, X. Wang, Y. Wang et al., "Effect of cadmium on cellular ultrastructure in mouse ovary," *Ultrastructural Pathology*, vol. 39, no. 5, pp. 324–328, 2015.
- [29] J. B. Samuel, J. A. Stanley, R. A. Princess, P. Shanthi, and M. S. Sebastian, "Gestational cadmium exposure-induced ovotoxicity delays puberty through oxidative stress and impaired steroid hormone levels," *Journal of Medical Toxicology: Official Journal of the American College of Medical Toxicology*, vol. 7, no. 3, pp. 195–204, 2011.
- [30] P. Massányi, V. Uhrin, and M. Valent, "Correlation relationship between cadmium accumulation and histological structures of ovary and uterus in rabbits," *Journal of Environmental Science and Health. Part A: Environmental Science and Engineering and Toxicology*, vol. 32, no. 5, pp. 1621–1635, 1997.
- [31] M. Nasiadek, M. Skrzypińska-Gawrysiak, A. Daragó, E. Zwierzyńska, and A. Kilanowicz, "Involvement of oxidative stress in the mechanism of cadmium-induced toxicity on rat uterus," *Environmental Toxicology and Pharmacology*, vol. 38, no. 2, pp. 364–373, 2014.
- [32] A. J. Lehman, "Chemicals in foods: a report to the association of food and drug officials on current developments. Part II. Pesticides," *Association of Food and Drug Officials - Quarterly Bulletin*, vol. 15, pp. 122–125, 1951.
- [33] Organisation for Economic Co-operation and Development (OECD), "Guidance Document for Histologic Evaluation of Endocrine and Reproductive Tests in Rodents. Part 5: Preparation, Reading and Reporting of Vaginal Smears," *Series on testing and assessment*, 2009.

- [34] R. Fox and C. Laird, "Sexual cycles," in *Reproduction and Breeding Techniques for Laboratory Animals*, E. S. E. Hafez, Ed., pp. 107–122, Lee and Febiger, Philadelphia, 1970.
- [35] O. H. Lowry, N. J. Rosebrough, A. L. Farr, and R. J. Randall, "Protein measurement with the Folin phenol reagent," *The Journal of Biological Chemistry*, vol. 193, no. 1, pp. 265–275, 1951.
- [36] J. Sedlak and R. H. Lindsay, "Estimation of total, protein-bound, and nonprotein sulfhydryl groups in tissue with Ellman's reagent," *Analytical Biochemistry*, vol. 25, no. 1, pp. 192–205, 1968.
- [37] A. Meister, "Glutathione metabolism and its selective modification," *The Journal of Biological Chemistry*, vol. 263, no. 33, pp. 17205–17208, 1988.
- [38] S. C. Lu, "Regulation of glutathione synthesis," *Molecular Aspects of Medicine*, vol. 30, no. 1–2, pp. 42–59, 2009.
- [39] M. Uchiyama and M. Mihara, "Determination of malonaldehyde precursor in tissues by thiobarbituric acid test," *Analytical Biochemistry*, vol. 86, no. 1, pp. 271–278, 1978.
- [40] M. Brama, L. Gnassi, S. Basciani et al., "Cadmium induces mitogenic signaling in breast cancer cell by an ER α -dependent mechanism," *Molecular and Cellular Endocrinology*, vol. 264, no. 1–2, pp. 102–108, 2007.
- [41] E. Silva, M. J. Lopez-Espinosa, J. M. Molina-Molina, M. Fernández, N. Olea, and A. Kortenkamp, "Lack of activity of cadmium in in vitro estrogenicity assays," *Toxicology and Applied Pharmacology*, vol. 216, no. 1, pp. 20–28, 2006.
- [42] C. V. Rider, P. C. Hartig, M. C. Cardon, and V. S. Wilson, "Comparison of chemical binding to recombinant fathead minnow and human estrogen receptors alpha in whole cell and cell-free binding assays," *Environmental Toxicology and Chemistry*, vol. 28, no. 10, pp. 2175–2181, 2009.
- [43] D. Wang, H. Sun, Y. Wu et al., "Tubular and glomerular kidney effects in the Chinese general population with low environmental cadmium exposure," *Chemosphere*, vol. 147, pp. 3–8, 2016.
- [44] M. Mężyńska, M. Brzóska, J. Rogalska, and B. Piłat-Marcinkiewicz, "Extract from *Aronia melanocarpa* L. berries prevents cadmium-induced oxidative stress in the liver: a study in a rat model of low-level and moderate lifetime human exposure to this toxic metal," *Nutrients*, vol. 11, no. 1, p. 21, 2018.
- [45] G. Nordberg, T. Jin, A. Bernard et al., "Low bone density and renal dysfunction following environmental cadmium exposure in China," *AMBIO: A Journal of the Human Environment*, vol. 31, no. 6, pp. 478–481, 2002.
- [46] M. Nasiadek, E. Swiatkowska, A. Nowinska, T. Krawczyk, J. R. Wilczynski, and A. Sapota, "The effect of cadmium on steroid hormones and their receptors in women with uterine myomas," *Archives of Environmental Contamination and Toxicology*, vol. 60, no. 4, pp. 734–741, 2011.
- [47] OECD, *Organization for Economic Co-operation and Development, Guidelines for the Testing of Chemicals. Test no 440. Uterotrophic Bioassay in Rodents: A Short-Term Screening Test for Oestrogenic Properties*, ENV/EPOC, Paris OCD, 2007.
- [48] P. Diel, S. Schmidt, and G. Vollmer, "In vivo test systems for the quantitative and qualitative analysis of the biological activity of phytoestrogens," *Journal of Chromatography. B, Analytical Technologies in the Biomedical and Life Sciences*, vol. 777, no. 1–2, pp. 191–202, 2002.
- [49] W. Zhang, J. Yang, J. Wang et al., "Comparative studies on the increase of uterine weight and related mechanisms of cadmium and p-nonylphenol," *Toxicology*, vol. 241, no. 1–2, pp. 84–91, 2007.
- [50] P. Fechner, P. Damdimopoulou, and G. Gauglitz, "Biosensors paving the way to understanding the interaction between cadmium and the estrogen receptor alpha," *PLoS ONE*, vol. 6, no. 8, article e23048, 2011.
- [51] F. M. Kluxen, N. Höfer, G. Kretzschmar, G. H. Degen, and P. Diel, "Cadmium modulates expression of aryl hydrocarbon receptor-associated genes in rat uterus by interaction with the estrogen receptor," *Archives of Toxicology*, vol. 86, no. 4, pp. 591–601, 2012.
- [52] X. Denier, E. M. Hill, J. Rotchell, and C. Minier, "Estrogenic activity of cadmium, copper and zinc in the yeast estrogen screen," *Toxicology In Vitro*, vol. 23, no. 4, pp. 569–573, 2009.
- [53] J. M. Goldman, A. S. Murr, and R. L. Cooper, "The rodent estrous cycle: characterization of vaginal cytology and its utility in toxicological studies," *Birth Defects Research (Part B)*, vol. 80, no. 2, pp. 84–97, 2007.
- [54] T. Sugiyama, H. Minoura, N. Kawabe, M. Tanaka, and K. Nakashima, "Preferential expression of long form prolactin receptor mRNA in the rat brain during the oestrous cycle, pregnancy and lactation: hormones involved in its gene expression," *The Journal of Endocrinology*, vol. 141, no. 2, pp. 325–333, 1994.
- [55] M. Jurczuk, M. M. Brzóska, J. Moniuszko-Jakoniuk, M. Gałazyń-Sidorczuk, and E. Kulikowska-Karpińska, "Antioxidant enzymes activity and lipid peroxidation in liver and kidney of rats exposed to cadmium and ethanol," *Food and Chemical Toxicology*, vol. 42, no. 3, pp. 429–438, 2004.
- [56] J. Zhang, Y. Wang, L. Fu et al., "Subchronic cadmium exposure upregulates the mRNA level of genes associated to hepatic lipid metabolism in adult female CD1 mice," *Journal of Applied Toxicology*, vol. 38, no. 7, pp. 1026–1035, 2018.
- [57] S. Sarkar, P. Yadav, and D. Bhatnagar, "Lipid peroxidative damage on cadmium exposure and alterations in antioxidant system in rat erythrocytes: a study with relation to time," *Bio-metals*, vol. 11, no. 2, pp. 153–157, 1998.
- [58] L. He, T. He, S. Farrar, L. Ji, T. Liu, and X. Ma, "Antioxidants maintain cellular redox homeostasis by elimination of reactive oxygen species," *Cellular Physiology and Biochemistry*, vol. 44, no. 2, pp. 532–553, 2017.
- [59] S. Mendes, F. Timóteo-Ferreira, H. Almeida, and E. Silva, "New insights into the process of placentation and the role of oxidative uterine microenvironment," *Oxidative Medicine and Cellular Longevity*, vol. 2019, Article ID 9174521, 18 pages, 2019.
- [60] V. U. Nna, U. Z. Usman, E. O. Ofutet, and D. U. Owu, "Quercetin exerts preventive, ameliorative and prophylactic effects on cadmium chloride-induced oxidative stress in the uterus and ovaries of female Wistar rats," *Food and Chemical Toxicology*, vol. 102, pp. 143–155, 2017.
- [61] L. P. Nampoothiri, A. Agarwal, and S. Gupta, "Effect of co-exposure to lead and cadmium on antioxidant status in rat ovarian granulosa cells," *Archives of Toxicology*, vol. 81, no. 3, pp. 145–150, 2007.
- [62] D. Roopha and P. Latha, "Cadmium exposure-induced oxidative stress; delay in sexual maturation and impaired hormones in developing rat ovary," *Oxidants and Antioxidants in Medical Science*, vol. 2, no. 3, pp. 181–187, 2013.

- [63] A. Ayala, M. F. Muñoz, and S. Argüelles, "Lipid Peroxidation: Production, Metabolism, and Signaling Mechanisms of Malondialdehyde and 4-Hydroxy-2-Nonenal," *Oxidative Medicine and Cellular Longevity*, vol. 2014, Article ID 360438, 31 pages, 2014.
- [64] M. Mężyńska, M. Brzóska, J. Rogalska, and A. Galicka, "Extract from *Aronia melanocarpa* L. berries protects against cadmium-induced lipid peroxidation and oxidative damage to proteins and DNA in the liver: a study using a rat model of environmental human exposure to this xenobiotic," *Nutrients*, vol. 11, no. 4, p. 758, 2019.
- [65] M. Waisberg, P. Joseph, B. Hale, and D. Beyersmann, "Molecular and cellular mechanisms of cadmium carcinogenesis," *Toxicology*, vol. 192, no. 2–3, pp. 95–117, 2003.
- [66] F. Liu and K.-Y. Jan, "DNA damage in arsenite- and cadmium-treated bovine aortic endothelial cells," *Free Radical Biology and Medicine*, vol. 28, no. 1, pp. 55–63, 2000.
- [67] M. Andjelkovic, A. B. Djordjevic, E. Antonijevic et al., "Toxic effect of acute cadmium and lead exposure in rat blood, liver, and kidney," *International Journal of Environmental Research and Public Health*, vol. 16, no. 2, p. 274, 2019.
- [68] C. Nagata, Y. Nagao, C. Shibuya, Y. Kashiki, and H. Shimizu, "Urinary cadmium and serum levels of estrogens and androgens in postmenopausal Japanese women," *Cancer Epidemiology, Biomarkers & Prevention: A Publication of the American Association for Cancer Research, cosponsored by the American Society of Preventive Oncology*, vol. 14, no. 3, pp. 705–708, 2005.
- [69] C. M. Gallagher, B. S. Moonga, and J. S. Kovach, "Cadmium, follicle-stimulating hormone, and effects on bone in women age 42–60 years, NHANES III," *Environmental Research*, vol. 110, no. 1, pp. 105–111, 2010.
- [70] A. Z. Pollack, E. F. Schisterman, L. R. Goldman et al., "Cadmium, lead, and mercury in relation to reproductive hormones and anovulation in premenopausal women," *Environmental Health Perspectives*, vol. 119, no. 8, pp. 1156–1161, 2011.
- [71] L. W. Jackson, P. P. Howards, J. Wactawski-Wende, and E. F. Schisterman, "The association between cadmium, lead and mercury blood levels and reproductive hormones among healthy, premenopausal women," *Human Reproduction*, vol. 26, no. 10, pp. 2887–2895, 2011.
- [72] I. Ali, A. Engström, M. Vahter et al., "Associations between cadmium exposure and circulating levels of sex hormones in postmenopausal women," *Environmental Research*, vol. 134, pp. 265–269, 2014.
- [73] B. Julin, A. Wolk, and A. Åkesson, "Dietary cadmium exposure and risk of epithelial ovarian cancer in a prospective cohort of Swedish women," *British Journal of Cancer*, vol. 105, no. 3, pp. 441–444, 2011.

Research Article

Apocynin Dietary Supplementation Delays Mouse Ovarian Ageing

F. Timóteo-Ferreira^{1,2}, **S. Mendes**^{1,2}, **N. A. Rocha**², **L. Matos**^{1,2,3,4}, **A. R. Rodrigues**^{1,2},
H. Almeida^{1,2,5} and **E. Silva**^{1,2}

¹*Instituto de Biologia Molecular e Celular (IBMC) and Instituto de Inovação e Investigação em Saúde (I3S),
Universidade do Porto, Portugal*

²*Unit of Experimental Biology, Department of Biomedicine, Faculty of Medicine of Porto University, Portugal*

³*Faculty of Dental Medicine of Porto University, Portugal*

⁴*Faculty of Nutrition and Food Sciences of Porto University, Portugal*

⁵*Obstetrics-Gynecology, Hospital-CUF Porto, 4100 180 Porto, Portugal*

Correspondence should be addressed to E. Silva; elisabete.silva@i3s.up.pt

Received 26 April 2019; Accepted 10 September 2019; Published 20 October 2019

Academic Editor: Rosalba Parenti

Copyright © 2019 F. Timóteo-Ferreira et al. This is an open access article distributed under the Creative Commons Attribution License, which permits unrestricted use, distribution, and reproduction in any medium, provided the original work is properly cited.

Advanced maternal age is associated with higher infertility rates, pregnancy-associated complications, and progeny health issues. The ovary is considered the main responsible for these consequences due to a continuous decay in follicle number and oocyte quality. Intracellular imbalance between oxidant molecules and antioxidant mechanisms, in favour of the former, results in oxidative stress (OS) that is believed to contribute to ovarian ageing. This work is aimed at evaluating whether an age-related increase in ovarian OS, inflammation, and fibrosis may contribute to tissue dysfunction and whether specific antioxidant supplementation with a NADPH oxidase inhibitor (apocynin) could ameliorate them. Mice aged 8–12 weeks (reproductively young) or 38–42 weeks (reproductively aged) were employed. Aged mice were divided into two groups, with one receiving apocynin (5 mM) in the drinking water, for 7 weeks, upon which animals were sacrificed and their ovaries collected. Ovarian structure was similar at both ages, but the ovaries from reproductively aged mice exhibited lipofuscin deposition, enhanced fibrosis, and a significant age-related reduction in primordial and primary follicle number when compared to younger animals. Protein carbonylation and nitration, and markers of OS were significantly increased with age. Moreover, mRNA levels of inflammation markers, collagens, metalloproteinases (MMPs), and tissue inhibitor MMPs (TIMPs) were upregulated. Expression of the antifibrotic miRNA29c-3p was significantly reduced. Apocynin supplementation ameliorated most of the age-related observed changes, sometimes to values similar to those observed in young females. These findings indicate that there is an age-related increase in OS that plays an important role in enhancing inflammation and collagen deposition, contributing to a decline in female fertility. Apocynin supplementation suggests that the imbalance can be ameliorated and thus delay ovarian ageing harmful effects.

1. Introduction

During the last decades, developed and developing countries have experienced economic and educational changes that gave women the opportunity to reach higher professional and decision levels. As a consequence, childbearing has been postponed into a period of life when fertility success decreases and pregnancy-associated disorders increase significantly [1].

Human female fertility peaks in the early 20s and gradually declines until the mid-30s. Thereafter, reproductive

potential falls sharply, until it virtually ends at menopause around the age of 50 [2]. The ovary is believed to be the main fertility regulator due to the continuous age-related decay in follicle number and oocyte quality [3].

A theory for ovarian ageing holds that age-related disruption of redox homeostasis affects oocyte quality [4]. The continued generation of reactive oxygen species (ROS) together with an age-related decline in activity and expression of important follicle antioxidant enzymes results in an imbalance between ROS production and antioxidant defences. The condition leads to oxidative stress (OS) responsible for

protein, amino acid, lipid, and DNA damage that underlie ovarian ageing and fertility loss [5]. As a matter of fact, in follicular fluid of older women, the expression of important antioxidant enzymes, as catalase and specific glutathione S-transferases, is significantly lower when compared with younger women [6]. Similarly, superoxide dismutase 1, superoxide dismutase 2, and catalase gene expression in granulosa [7] and *cumulus oophorus* cells [8] are also downregulated during reproductive ageing. In this process, the use of specific antioxidant molecules has shown beneficial effects in delaying follicle depletion and fertility impairment [9–12].

Studies on ovarian ageing have expanded from the oocyte immediate surroundings to the ovarian stroma, mainly composed of an arrangement of extracellular matrix components (ECM) and fibroblasts and smooth muscle, endothelial, and immune cells. This microenvironment has an important impact on follicle development and oocyte quality. In fact, Briley et al. [13] verified ovarian microenvironment changes with age, specifically an increase in fibrosis and inflammation, and suggested its contributory role to the coincident decrease in oocyte quality. ROS are also believed to contribute to the synthesis and activation of various cytokines and growth factors, hence creating common feedforward and feedback mechanisms that promote tissue fibrosis [14].

Inflammation and ROS formation appear to be key factors in the pathogenesis of ovarian fibrosis [15], which reflects a disturbance of the synthesis and degradation of extracellular matrix (ECM) favouring excessive collagen deposition. Important regulators of ECM homeostasis are metalloproteinases (MMPs), a group of enzymes capable of degrading all types of ECM components [16], and tissue inhibitor metalloproteinases (TIMPs), both affected by ageing [17]. More recent studies have also identified specific microRNAs (miRNAs) as important mediators in fibrosis; they act either by regulating target genes involved in the process of ECM remodelling or by signalling pathways associated with it [18]. Reduction of ROS production by inhibiting NADPH oxidase (NOX) activity with apocynin has shown beneficial effects on renal [19, 20], cardiac [21], skeletal muscle [22], and pulmonary [23] fibrosis. Despite our previous results showing beneficial effects of apocynin supplementation on uterine ageing and fertility [24], its effect on ovarian redox imbalance, inflammation, and fibrosis during reproductive ageing is scarce.

In sum, an age-related low-grade inflammatory state may associate with ovarian collagen deposition and a progressive reduction in follicle number and oocyte quality. In this setting, it was hypothesized that an age-related increase in ovarian fibrosis and ROS underlies fertility reduction. To verify it, markers of oxidative stress, tissue fibrosis, and inflammation, along with the possibility to ameliorate those features by a specific antioxidant supplementation, were evaluated *in vivo*.

2. Material and Methods

2.1. Animal Handling and Ovarian Tissue Collection. All the experiments were performed according to the Portuguese law on animal welfare and according to the guidelines issued

by Federation of European Laboratory Animal Science Associations (FELASA). Female mice (C57BL/6J strain) obtained from Harlan were kept under controlled conditions (12 h light/dark cycle and room temperature at 22°C) and had free access to tap water and standard mouse chow. Young (8–12 weeks old) and reproductively aged (38–42 weeks old) female mice were employed. Reproductively aged mice were divided into two groups, with one receiving the antioxidant, apocynin, 5 mM, in drinking water 7 weeks prior to sacrifice. Water bottles were protected from light and changed twice a week. At the selected ages, female mice were anesthetized with isoflurane and euthanized by cervical dislocation, and the ovaries were excised. One ovary was immediately frozen in liquid nitrogen and subsequently kept at -80°C for molecular studies and the other was fixed overnight, in 4% paraformaldehyde, for structural studies.

2.2. Tissue Processing for Histological Techniques. Fixed ovaries were dehydrated with the aid of increasing concentrations of ethanol and diaphanized using benzol. Impregnation and inclusion were carried out in paraffin, and 5 µm thick sequential sections were mounted on poly-L-lysine-coated slides and dried overnight at 37°C. They were stored in plastic boxes to be used for all histological applications throughout this study.

2.3. Morphological Analysis of Ovarian Tissues. Ovarian sections for morphological examination were stained with hematoxylin & eosin (H&E) according to the following protocol. Slides were dewaxed twice with xylol and hydrated with decreasing concentrations of ethanol and water. Subsequently, slides were stained with Harris hematoxylin for 2 minutes and then stained with alcoholic eosin for 5 minutes. Finally, tissues were dehydrated with increasing concentrations of ethanol followed by two xylol passages. Slides were mounted in Entellan and air dried. Ovarian morphology was observed under light microscope equipped with a digital camera, and representative images at ovarian midsection were captured. Other ovarian sections were stained with Sudan Black 0.1% for lipofuscin examination. Slides were dewaxed and hydrated as previously described, stained with Sudan Black 0.1% for 20 minutes, dehydrated, and mounted.

2.4. Follicle Counting at Ovarian Midsection. H&E slides were used for follicle counting. The follicles were branded as primordial, primary, secondary, or antral, and *corpus luteum*. Follicles were classified as primordial or primary when oocytes were surrounded, respectively, by a single layer of squamous or cuboidal granulosa cells. Secondary follicles were identified by having more than one layer of granulosa cells with no visible antrum. Antral follicles are the ones that displayed small areas of follicular fluid (antrum) or a single large antral space. *Corpus luteum* were identified as intraovarian bund structures with morphologically homogeneous round cells, showing enhanced cytoplasm/nucleus ratio, when compared with granulosa cells, and deprived of oocyte. The number of follicles at ovarian midsection was obtained by calculating the mean counts of three ovarian midsections, representative of each animal, and a minimum of four animals per group was used.

2.5. Autofluorescence Lipofuscin Detection. Ovarian sections were dewaxed and hydrated as previously described. After washing in PBS, they were mounted in phosphate-buffered glycerol and observed under a fluorescence microscope (Carl Zeiss AxioImager Z1) equipped with a digital camera.

2.6. Fluorescent Immunohistochemistry. A fluorescent immunohistochemical technique was performed to detect protein carbonylation and nitration (markers of oxidative stress). Ovarian sections were dewaxed and hydrated as previously described. Slides were washed with phosphate-buffered saline (PBS) solution and permeabilized with 0.5% Triton™ X-100 in PBS for 5 minutes, followed by washing with PBS. For protein carbonylation assessment, an additional derivatization process was required before nonspecific signal blocking. The derivatization protocol was performed as previously published [25]. In brief, sections were incubated in 10 mM 2,4-dinitrophenylhydrazine (DNPH; Sigma-Aldrich) in 10% TFA for 10 minutes, the reaction stopped with 2 M Tris base pH 10, and slides were washed with PBS. Background staining was blocked with 2% bovine serum albumin (BSA) in PBS with 0.1% Tween 20 (PBS-T) for 1 hour at room temperature. Slides were then incubated with a rabbit polyclonal antibody recognizing DNP (1:250; Sigma-Aldrich) or a mouse monoclonal antibody recognizing nitrotyrosine (1:250; Santa Cruz Biotechnology) in PBS-T, overnight at 4°C. The following day, slides were washed in PBS-T, incubated with Alexa Fluor 488-conjugated anti-rabbit IgG secondary antibody (1:750; Molecular Probes) or in Alexa Fluor 568-conjugated anti-mouse IgG secondary antibody (1:750; Molecular Probes) in PBS-T for 1 hour at room temperature. Then, they were washed again, counterstained with 4',6-diamidino-2-phenyl-indole (DAPI), and mounted. Slides were examined, and images were recorded under a fluorescence microscope (Carl Zeiss AxioImager Z1) equipped with a digital camera. Signal extension was quantified using ImageJ software by identification of the threshold cut point, with blind intervention of three operators. A minimum of four animals per group was used, and a minimum of two representative sections of the midovary was examined.

2.7. Fibrosis Evaluation in Ovarian Tissue. Picrosirius red histochemical technique was performed for quantification of tissue fibrosis. Ovarian sections were dewaxed and hydrated as previously described. Then, slides were stained with sirius red solution for 90 minutes, rapidly passed through 0.5% acidified water, and subsequently dehydrated, with increasing concentrations of ethanol, followed by two xylol passages. Slides were mounted in Entellan for further visualization and analysis. This technique stains collagen in red and cytoplasm in yellow. Red staining (collagen) was quantified using the ImageJ software by identification of the threshold cut point, with blind intervention of three operators. A minimum of four animals per group was used, and a minimum of two sections of the midovary was examined.

2.8. Real-Time PCR. Ovarian RNA extraction and purification was performed with TripleXtractor direct RNA kit (GRiSP) following the manufacturer's instructions. Total

RNA was quantified by measuring the absorbance at 260 nm in a NanoDrop (Thermo Fisher Scientific), and RNA purity was evaluated by the ratio of absorbance at 260 and 280 nm. RNA samples were reverse transcribed to cDNA with the NZY First-Strand cDNA Synthesis kit (NZYTech). Real-time PCR was carried out using PowerUp SYBR Green Master Mix (Thermo Fisher Scientific) and specific primers (Table 1) in a StepOnePlus™ Real-Time PCR System (Applied Biosystems). Primers were designed using the online available specific mRNA sequences and Primer3 program. The derived sequences were submitted for a BLAST search to ensure exclusive alignment to the desired target genes. Amplification reactions were performed, in duplicate, according to conditions stated in Table 1. To check specificity, a dissociation curve was derived at the end of each run. Controls lacking reverse transcriptase were included to ensure no genomic DNA contamination during preparations. Results were normalized to 18S expression.

2.9. MicroRNA Quantification. Total RNA extraction was performed using the commercial Recover ALL™ Total Nucleic Acid Isolation Kit (Ambion), according to the manufacturer's instructions. In brief, for each sample, four paraffin-embedded ovaries were sectioned at 20 μm thickness. Each sample was dewaxed in 100% xylene, washed in 100% ethanol, and incubated with protease and digestion buffer for 2 hours at 50°C, followed by 15 minutes at 75°C. Nucleic acids were isolated and incubated with DNase mix for 30 min at room temperature. After a final purification, 7 μL of total RNA was reverse transcribed to cDNA using the MystiCq microRNA cDNA Synthesis Mix (Sigma-Aldrich Co.). In the process of cDNA synthesis, miRNAs were subjected to polyadenylation by poly(A) polymerase that catalysed the transfer of adenosine deoxynucleotides to the 3' end. ReadyScript Reverse Transcriptase and other necessary reagents for cDNA synthesis were subsequently added to convert the poly(A) tailed microRNAs into first-strand cDNA using an oligo-dT adapter primer. The unique sequence at the 5' end of the adapter primer allows amplification of microRNA cDNAs in real-time qPCR reactions using the MystiCq microRNA qPCR Universal Primer. Real-time PCR was carried out as previous described. Controls lacking reverse transcriptase were included to ensure no genomic DNA contamination during preparations, along with controls lacking poly(A) polymerase. Results were normalized to RNU1A (Qiagen) expression. Specific primers used were miR-21*_1; miR-29c_1; miR-215_1; and miR-212-3p_1 miScript Primer Assay (Qiagen), with annealing temperature of 55°C.

2.10. Statistical Analysis. Arithmetic means are given with standard error of the mean (SEM). Statistical analyses were performed with GraphPad Prism 6.01 using one-way analysis of variance (ANOVA), followed by the Tukey posttest. A $P < 0.05$ was considered statistically significant.

3. Results

3.1. Age-Related Alterations in Ovarian Morphology. To observe ovarian morphology, H&E-stained midorgan

TABLE 1: List of primers used in RT-PCR reactions.

Primers		Sequence	Annealing temperature	Fragment (bp)
Col1 α 1	Fwd	5'-GACGCATGGCCAAGAAGACA-3'	60°C	85
	Rev	5'-CTCGGGTTTCCACGCTCAC-3'		
Col3 α 1	Fwd	5'-AGCTTTGTGCAAAGTGAACC-3'	58°C	114
	Rev	5'-ATAGGACTGACCAAGGTGGC-3'		
Col5 α 1	Fwd	5'-CCTGGTTCAGTGAATTCAAGCG-3'	60°C	81
	Rev	5'-TCATTTGTACCACGCCACG-3'		
TGF- β 1	Fwd	5'-ATTCTGGCGTTACCTTGG-3'	60°C	120
	Rev	5'-AGCCCTGTATTCCGCTCCT-3'		
TNF- α	Fwd	5'-CCCTCACACTCAGATCATCTTCT-3'	60°C	61
	Rev	5'-GCTACGACGTGGGCTACAG-3'		
IL-1 β	Fwd	5'-TGACGGACCCAAAAGATGA-3'	60°C	87
	Rev	5'-TGCTGCGAGATTTGAAGCTG-3'		
CCL5	Fwd	5'-TGCCACGTCAAGGAGTATT-3'	60°C	84
	Rev	5'-ACTTGCGGTTCTTCGAG-3'		
MMP2	Fwd	5'-TGTCGCCCTAAAAACAGACA-3'	58°C	65
	Rev	5'-TGGGCAGCCATAGAAAGTG-3'		
MMP9	Fwd	5'-CCTGGAACACACGACATCT-3'	62°C	72
	Rev	5'-CACGCCAGAAGAATTTGCCAT-3'		
MMP12	Fwd	5'-GGGCTGCTCCCATGAATGAC-3'	56°C	85
	Rev	5'-GTCATTGGAATCTGTCTTTCCA-3'		
TIMP1	Fwd	5'-GGTGTGCACAGTGTTCCTGTTT-3'	60°C	72
	Rev	5'-TCCGTCCACAAACAGTGAGTGTC-3'		
TIMP2	Fwd	5'-GGATTCAAGTATGAGATCAAGC-3'	55°C	145
	Rev	5'-GCCTTCTCTGCAATTAGATAC-3'		
18S	Fwd	5'-CGCCGTAGAGGTGAAATTC-3'	60°C	67
	Rev	5'-CATTCTGGCAAATGCTTTCG-3'		

Fwd: forward; Rev: reverse; bp: base pairs.

sections (Figure 1(a)) revealed follicles in various stages of development, occupying most areas of the ovary, but predominantly in the periphery. Central areas were occupied by a heterogeneous stroma that included vessels, bundles of extracellular connective tissue, and respective cells.

A unique population of stroma cells was detected only in the ovaries of reproductively aged mice. They were large and multinucleated, with pale cytoplasm containing a yellow-brown pigment (Figure 1(a)), which displayed autofluorescence (Figure 1(b)). Fluorescence quenching by staining with Sudan Black indicated that these were deposits of lipofuscin (oxidized lipids and proteins) (Figure 1(b)). Ovarian stromal cells with the abovementioned characteristics were consistently observed in reproductively aged mice and correspond to multinucleated giant macrophages [13, 26]. Follicle number was evaluated and, as expected, in reproductively aged mice, a significant reduction was noticed. This was due to a

decrease in the number of primordial and primary follicles. Apocynin had no effect (Figure 1(c)).

3.2. Age and Antioxidant Supplementation Effect on Ovarian Oxidative Stress and Fibrosis. Tyrosine nitration and protein carbonylation were used to characterize ovarian oxidative stress (Figures 2 and 3). As shown in Figure 2, protein tyrosine nitration staining was found on the medullary stromal cells and partially colocalized with lipofuscin deposits. DNP immunoreactivity was observed in stromal cells, theca cells, oocytes, and corpus luteum (Figure 3). Reproductively aged females had increased expression of lipofuscin deposits (1.00 ± 0.41 vs. 8.53 ± 2.95), carbonylated (1.34 ± 0.09 vs. 3.17 ± 0.35), and nitrated proteins (1.00 ± 0.20 vs. 2.60 ± 0.26) (Figures 2(b) and 3(b)). The use of apocynin, that inhibits NOX-mediated superoxide production, resulted in a significant reduction in both carbonylated and nitrated

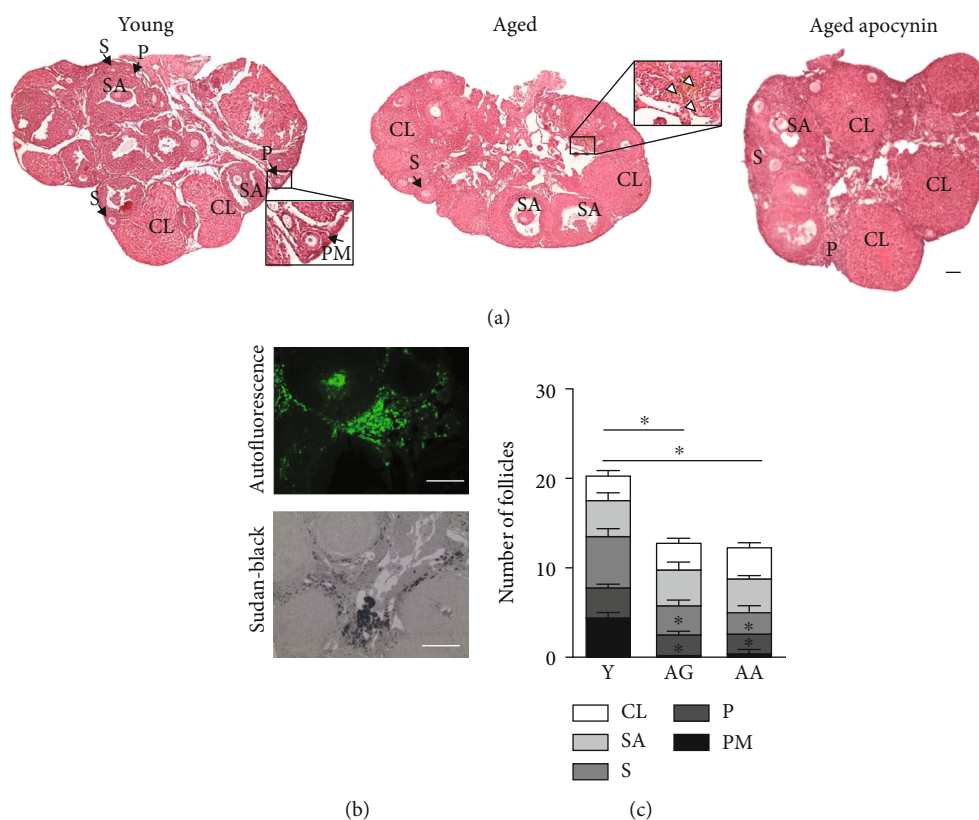


FIGURE 1: Ovarian structure and follicle number. (a) H&E-stained representative midovarian sections from young and aged mice. Note yellow-brown palely stained multinucleated cells, located in stroma of reproductively aged mice (white arrowheads). (b) Representative images of Sudan Black staining and autofluorescence in the ovaries of aged mice. Multinucleated cells stain intensely with Sudan Black and emit strong autofluorescence, indicating age-related deposition of oxidized proteins and lipids. Average quantification of autofluorescence area ($n = 4-5$ per group). (c) Follicle distribution at midovarian sections of young and reproductively aged mice ($n = 4$ per group), showing a significant decrease in primary and primordial follicle number of older animals. Y: young; AG: aged; AA: aged apocynin; PM: primordial follicles; P: primary follicles; S: secondary follicles; SA: secondary antral follicles; CL: corpus luteum. Bars = 100 μm . Data are presented as mean \pm SEM. * $P < 0.05$, compared with young female mice.

proteins, to levels similar to those observed in the younger group (Figures 2 and 3).

Oxidative stress appears to play a crucial role in the etiology of tissue fibrosis. Next, picosirius red (PSR) histochemical technique was used to evaluate ovary collagen fibril deposition. Slight PSR staining was observed around follicles, blood vessels, and epithelium of the ovarian surface (Figure 4(a)). However, a network-like, intense PSR staining, characteristic of fibrotic foci, was only seen on the ovarian stroma and increased significantly with age (1.00 ± 0.12 vs. 1.92 ± 0.09) (Figure 4). In contrast, reproductively aged females treated with apocynin exhibited significantly reduced PSR staining (1.43 ± 0.15) (Figure 4(b)).

3.3. Age and Treatment Effect on Inflammation Factors and Collagen Expression. As previously mentioned, synthesis and secretion of various growth factors and cytokines are interlinked with OS in feedforward and feedback cycle mechanisms that might contribute to fibrosis via enhanced inflammation. Reproductive ageing was accompanied by a significant increase in several cytokines [(CCL5 (1.00 ± 0.92 vs. 18.93 ± 5.96), TNF- α (1.00 ± 0.66 vs. 6.82 ± 1.73), IL-1 β (1.00 ± 0.40 vs. 15.55 ± 5.13)], including TGF- β 1

(1.00 ± 0.90 vs. 12.85 ± 3.81) that is considered the most important cytokine modulating fibrosis signalling (Figure 5). All those molecules also regulate specific miRNA expression involved in fibrosis. Interestingly, as shown in Figure 6, miRNA29c-3p, a “master fibromiRNA,” was found to be downregulated in the ovaries of reproductively aged females (1.00 ± 0.13 vs. 0.57 ± 0.06), unlike miRNA212-3p (1.00 ± 0.11 vs. 0.86 ± 0.13) and 21a-3p (1.00 ± 0.25 vs. 0.76 ± 0.14) that were not affected by ageing. Expression of miRNA 29c-3p was inversely correlated with collagen expression. Both collagen types Col1a1 (1.00 ± 0.88 vs. 11.48 ± 3.88) and Col5a1 (1.00 ± 0.91 vs. 10.51 ± 3.10) were significantly increased in aged females. Apocynin treatment normalized cytokine and collagen expression to levels similar to those observed in younger females (Figure 5).

3.4. MMP/TIMP Expression. MMPs regulate not only ECM degradation but also bioavailability and activity of cytokines, chemokines, and growth factors. MMP activity is, in turn, regulated by its specific TIMPs. During reproductive ageing expression of MMP9, TIMP1 and TIMP2 were significantly increased [(1.00 ± 0.95 vs. 16.80 ± 5.63), (1.00 ± 0.97 vs. 51.62 ± 16.61), and (1.00 ± 0.96 vs. 33.09)]

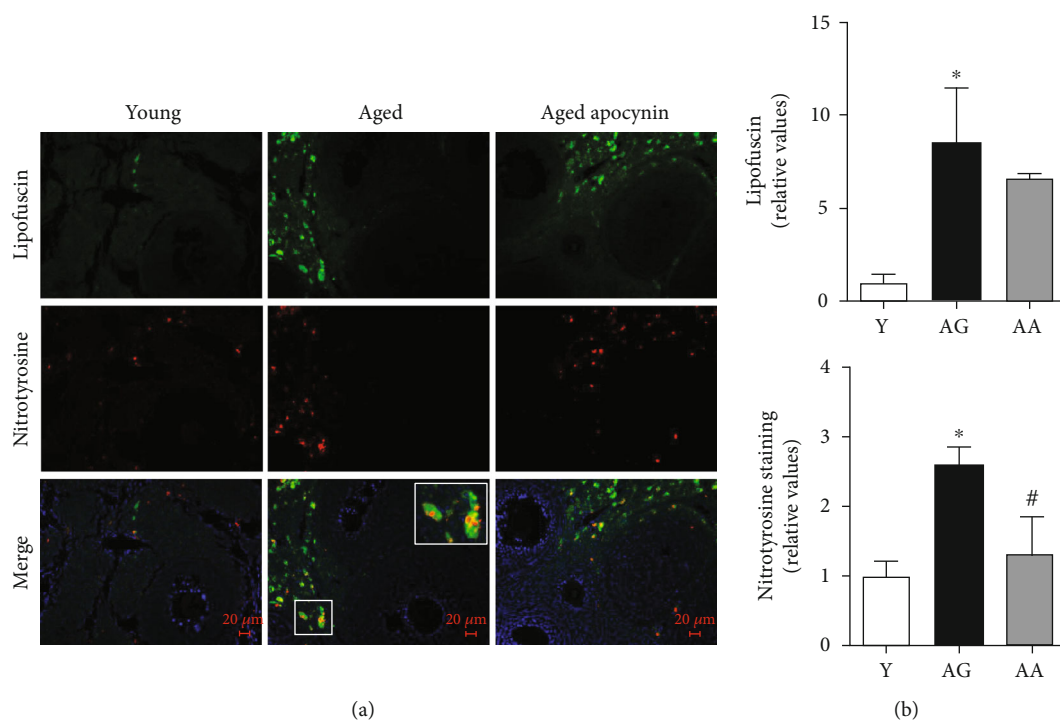


FIGURE 2: Protein nitration in the mouse ovaries evidenced by fluorescence immunohistochemistry, using a specific antibody. (a) Representative images of young, reproductively aged and apocynin-treated aged mice. Note tyrosine nitration staining and lipofuscin colocalization in the tissue. (b) Average quantification of lipofuscin and nitrated proteins stained area assuming young mice equals 1 ($n = 4-5$ per group). Y: young; AG: aged; AA: aged apocynin. Data are presented as mean \pm SEM. * $P < 0.05$, compared with young female mice; # $P < 0.05$, compared with reproductively aged female mice.

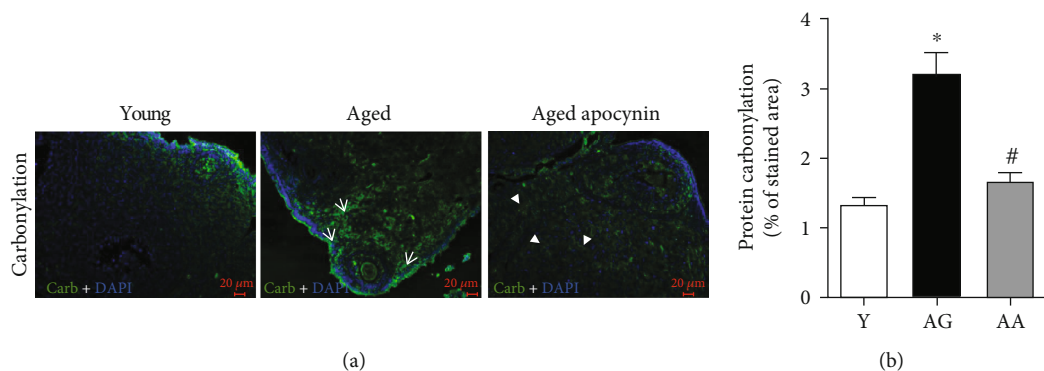


FIGURE 3: Protein carbonylation in the mouse ovaries evidenced by fluorescence immunohistochemistry, using a specific antibody for DNP. (a) Representative images of young, reproductively aged and apocynin-treated aged mice. Note the substantial carbonyl labeling increase in ovarian stroma cells (white arrows) and antioxidant-mediated amelioration (arrowheads). (b) Average quantification of stained area ($n = 4-5$ per group). Y: young; AG: aged; AA: aged apocynin. Data are presented as mean \pm SEM. * $P < 0.05$, compared with young female mice; # $P < 0.05$, compared with reproductively aged female mice.

± 10.88), respectively] (Figure 6). Once more, apocynin dietary supplementation reversed age-related observed changes (Figure 6).

4. Discussion

The present study revealed that, during reproductive ageing, the ovary undergoes morphological and molecular changes related with a disturbance of the redox homeostasis, shown by increased lipofuscin content, protein carbonylation and

nitration, and collagen deposition. Along with those changes, there was an age-related increase of inflammation and fibrosis, evidenced by higher relative expression of inflammation markers, MMPs, TIMPs, and a specific miRNA. Antioxidant supplementation with apocynin was capable of ameliorating features of the ovarian ageing process.

Over time, cells and tissues display structural changes that reflect age-related modifications in biomolecules and signalling pathways, eventually leading to tissue dysfunction [27]. Beyond time-related structural changes, the ovary is

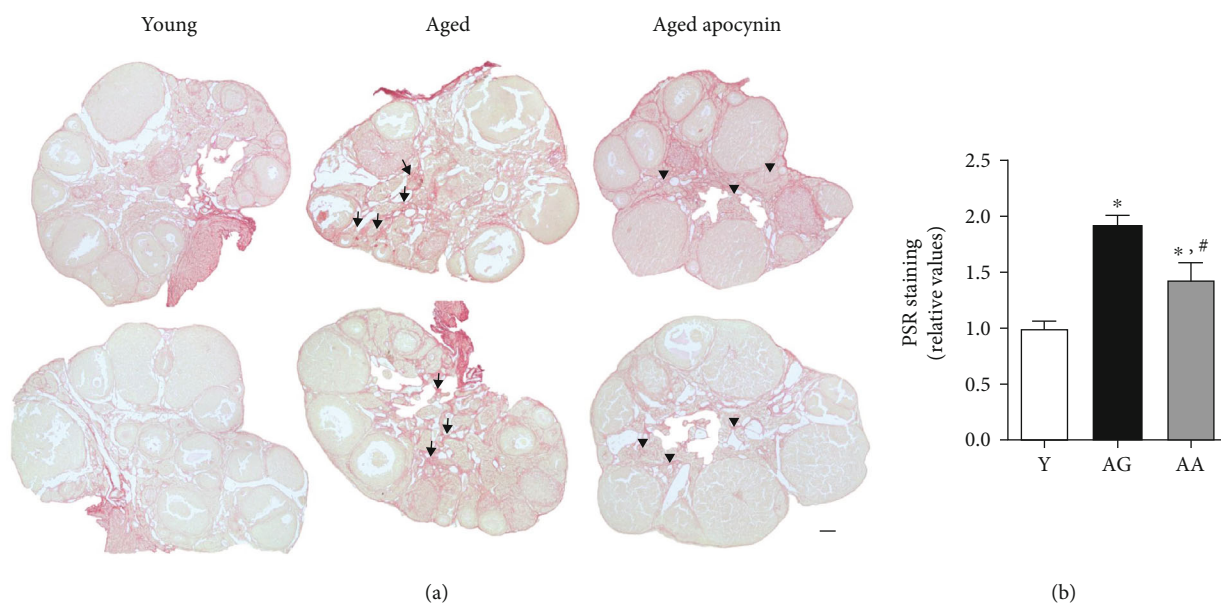


FIGURE 4: Fibrosis in mouse ovarian midsections stained by picosirius red. (a) Representative images of young, reproductively aged and apocynin-treated aged mice. Note increased deposition of collagen fibers in the stroma of reproductively aged mice (arrows) and antioxidant-mediated amelioration (arrowheads). (b) Relative quantification of stained area assuming young mice equals 1 ($n = 4$ per group). Y: young; AG: aged; AA: aged apocynin. Bar = $100\ \mu\text{m}$. Data are presented as mean \pm SEM. * $P < 0.05$, compared with young female mice; # $P < 0.05$, compared with reproductively aged female mice.

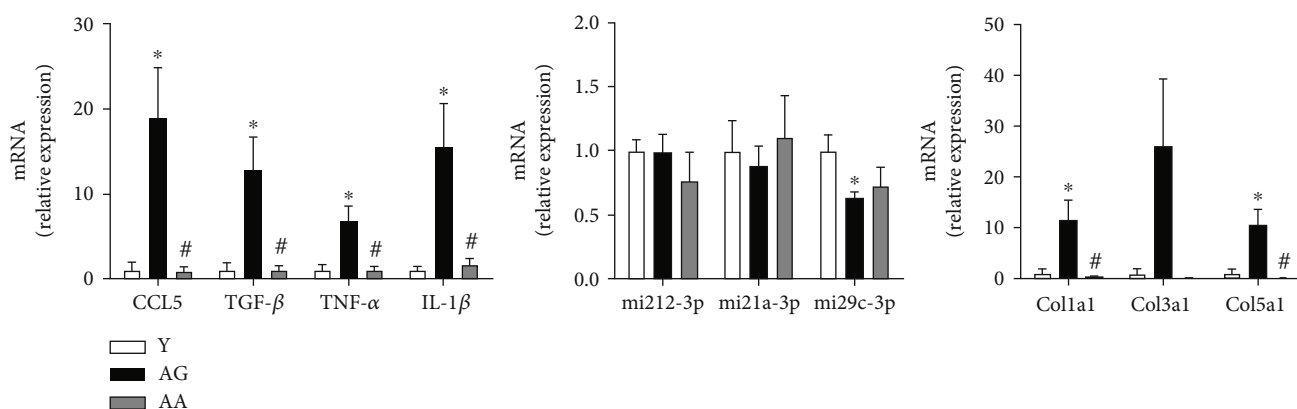


FIGURE 5: Expression of inflammation/fibrotic factors and extracellular matrix proteins. Relative mRNA and miRNA expression was calculated using the $2^{\Delta\text{CT}}$ ($\Delta\text{CT} = \text{CT}_{\text{reference RNA}} - \text{CT}_{\text{target}}$), and values were expressed as fold change over young group ($n = 4-7$ per group). Reproductive ageing is associated with an inflammatory and profibrotic ovarian microenvironment, increased levels of cytokines and collagens, and decreased level of the antifibrotic mi29c-3p RNA. Apocynin treatment reverts the expression of inflammation and fibrosis factors. Y: young; AG: aged; AA: aged apocynin. Data are presented as mean \pm SEM. * $P < 0.05$, compared with young female mice; # $P < 0.05$, compared with reproductively aged female mice.

distinctly affected by additional cyclic ones, tightly controlled by hormonal variations. The mild, albeit continued, inflammatory nature of such alterations subjects the ovary to recurrent OS, inflammatory cell invasion, and fibrosis, especially intensified during ageing, when a decrease in antioxidant defences deepens the cellular redox imbalance [6–8, 28, 29]. The regulatory mechanisms contributing to age-related ovarian changes are still poorly known. Previously, we demonstrated that dietary supplementation with apocynin enhanced pregnancy outcomes at a latter reproductive age by improving the observed age-related decrease in mouse litter size and restoring decidua layer thickness [24]. In this

work, apocynin was used to study its antioxidant properties in mitigating ovarian ageing effects.

Two features that distinguished young and reproductively aged ovaries were a unique population of multinucleated giant cells containing lipofuscin deposits and the number of follicles. In aged mice, a significant reduction in the number of primordial and primary follicles was observed, which agrees with the well-known time-related decline of the follicle resting pool [2, 30]. At this age, as expected, dietary supplementation with apocynin did not prevent the decline, because natural oocyte attrition had occurred. However, female fertility is not only dependent on the follicle pool

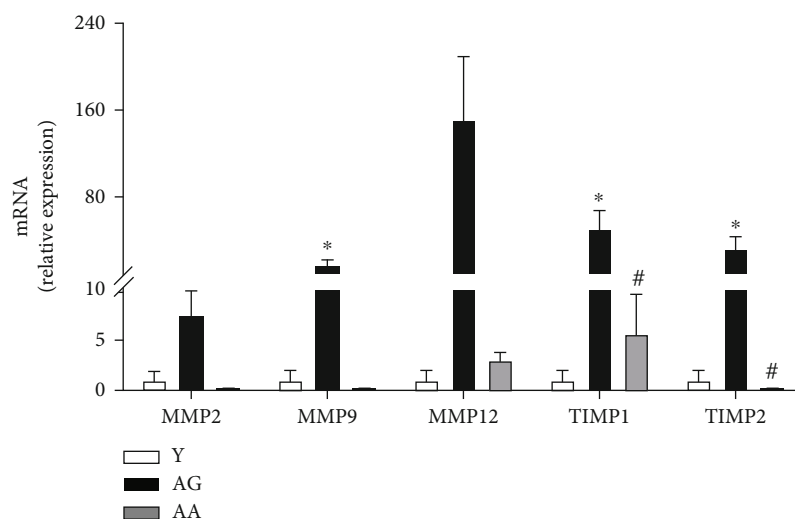


FIGURE 6: Expression of metalloproteinases and their tissue inhibitors. Relative mRNA expression was calculated using the $2^{-\Delta CT}$ ($\Delta CT = CT_{\text{reference RNA}} - CT_{\text{target}}$), and values were expressed as fold change over young group ($n = 4-7$ per group). Reproductive ageing is associated with increased metalloproteinases expression and their tissue inhibitors. Apocynin treatment normalizes RNA expression. Y: young; AG: aged; AA: aged apocynin. Data are presented as mean \pm SEM. * $P < 0.05$, compared with young female mice; # $P < 0.05$, compared with reproductively aged female mice.

but also on follicle and oocyte quality [31, 32], itself influenced by the ovarian oxidative microenvironment [13]. The ovarian stromal giant multinucleated cells present in reproductively aged mice were previously shown to be positive for a cell surface membrane protein—F4/80—highly expressed in macrophages [13, 20, 22]. Such observation supports the perception that they result from macrophage fusion. In the ovaries, macrophages are important contributors to the regulation of folliculogenesis and corpora lutea establishment and regression [33]. The unique presence of giant multinucleated cells in aged ovaries indicates that they associate closely to long-term effects on the tissue. Macrophage fusion is a hallmark of a low-grade chronic inflammatory condition, a recurrent oxidative challenge that potentiates phagocytic function for the disposal of cell debris [34, 35]. Such phagocytic cells are a source of factors that promote OS. Besides lipofuscin, itself a deposit of oxidized protein and lipid, our results suggest they also accumulate nitrated proteins. Probably, due to lipofuscin undegradable nature and inability to be removed from cells, apocynin treatment did not reduce its deposition, unlike protein carbonylation and nitration content.

The low-grade chronic inflammatory condition favours overproliferation of fibroblasts, excessive ECM deposition, and fibrosis [36]. In accordance with a previous study using two different strains of mice [13], the current study displays a significant age-related increase of fibrosis around follicles, blood vessels, and in the ovarian stroma. The observation that treatment with apocynin results in less ovarian fibrosis highlights the role of oxidative imbalance in its formation and suggests that NOX activity mediates local ROS production and susceptibility to fibrosis. NOX-derived ROS has, in fact, been associated with fibrosis in other organs such as the kidney [37], pancreas [38], and liver [39–41]. Moreover, as the inhibition prevents the enzyme cytoplasmic subunits

from binding transmembrane complexes necessary for NOX1 and NOX2 activation (but not NOX4), it supports the view that the beneficial effects observed in the current study were mediated by inhibition of those two isoforms. Future works with specific NOX4 inhibitors will be useful to investigate its role in ovarian fibrosis.

Inflammation has an important role in fibrosis establishment by promoting a set of interactions between profibrotic and antifibrotic cytokines [42]. In the present study, increased expression of genes involved in immune cell response and recruitment was noticed. In this setting, macrophages are the main innate immune cells that release cytokines and chemokines to the local environment, of which, most impressively, NOX-mediated ROS production is an important modulator [43–45]. We observed a significant age-related increase in CCL5, an important chemokine in macrophage recruitment; IL-1 β and TNF- α , proinflammatory cytokines involved in regulating endothelial cells in ECM production; and TGF- β 1, a multifunctional cytokine highly responsible for ECM homeostasis through several pathways. Equally to fibrosis, apocynin reduced their expression to young mouse levels demonstrating, once more, that ROS play a master role in fibrosis and inflammation associated with reproductive ageing.

TGF- β 1 involvement in ECM homeostasis includes the modulation of miRNAs that affect collagen deposition [46, 47]. Different types of miRNA with regulatory effects were recognized in mouse ovaries [48, 49]. In our study, the profibrotic miRNAs 21a-3p and 212-3p showed no differences with age. However, antifibrotic mi29c-3p, considered a “master fibrosis” regulator in several organs [47, 50–52], exhibited a significant reduction in the ovaries of reproductively aged females, which correlated with the significant increase in gene expression of Col1a1 and Col5a1. Surprisingly, apocynin attenuated, but not reverted, mi29c-3p

decrease. Further studies are needed for a better comprehension of the mechanisms involved.

In addition, age-associated changes in MMPs and TIMPs can further contribute to fibrosis, as they modulate the activation of macrophages and fibroblast originated proinflammatory cytokines, as TNF- α and TGF- β 1 [35]. Their roles in ECM remodelling as well as fibrosis establishment and progression are tissue specific. In reproductively aged ovaries, MMP9, TIMP1, and TIMP2 had a significant increase in gene expression. MMP9 is a gelatinase responsible for collagen degradation, including type I and V [53], that has been suggested to be directly regulated by TGF- β 1 [54] and to take part in its activation [55] by cleaving its latent form [56]. TIMP1 and TIMP2 have profibrotic roles by inhibiting MMP activity and contributing to ECM accumulation [16]. However, the efficiency of MMP inhibition differs with each TIMP. This could explain the observed significant increase of MMP9, despite the observed aged-related significant increase in TIMP, further emphasizing the important role and relationship with TGF- β 1. Our findings suggest that during reproductive ageing, the continued ROS-mediated inflammation disrupts ECM homeostatic processes inevitably ending in tissue fibrosis.

Overall, supplementation with apocynin ameliorated molecular and histological consequences of the ovarian ageing process. By diminishing ROS production, apocynin decreased tissue fibrosis, inflammation, and ECM deposition. This comes as a novel finding for the use of this antioxidant as, to our knowledge, no other work evaluated the capability of this compound in slowing down age-related ovarian reproductive ageing.

In summary, the present study provides evidence that structural features of ovarian ageing are consequence of local continued OS effects, with important negative impact on the ovarian stroma. Disruption of microenvironment, caused by a feedforward loop in which OS, inflammation, and ECM turnover dysregulation are important players, is believed to affect ovarian function and, ultimately, female fertility. Moreover, specific antioxidant supplementation can be seen as an important therapeutic way to ameliorate causes and effects of the ageing process induced by higher ROS production. Further investigation in this field, addressing apocynin effects on oocyte quality, may have major potential value to uncover fundamental biological mechanisms and devise therapeutic strategies.

Data Availability

The data used to support the findings of this study are available from the corresponding author upon request.

Conflicts of Interest

The authors declare that they have no conflicts of interest.

Acknowledgments

ES was funded by the Portuguese Government and the European Union through FCT/POPH/FSE under the fellowship

SFRH/BPD/72536/2010 and DL57/2016/CP1327/CT0006. ARR was funded by the Portuguese Government and the European Union through DL57/2016/CP1355/CT0009.

Supplementary Materials

Supplementary Figure 1: low amplification images of protein nitration and lipofuscin deposition in mouse ovaries. Supplementary Figure 2: low amplification images of protein carbonylation in mouse ovaries. (*Supplementary Materials*)

References

- [1] M. Mills, R. R. Rindfuss, P. McDonald, E. te Velde, and on behalf of the ESHRE Reproduction and Society Task Force, "Why do people postpone parenthood? Reasons and social policy incentives," *Human Reproduction Update*, vol. 17, no. 6, pp. 848–860, 2011.
- [2] F. J. Broekmans, M. R. Soules, and B. C. Fauser, "Ovarian aging: mechanisms and clinical consequences," *Endocrine Reviews*, vol. 30, no. 5, pp. 465–493, 2009.
- [3] E. R. te Velde and P. L. Pearson, "The variability of female reproductive ageing," *Human Reproduction Update*, vol. 8, no. 2, pp. 141–154, 2002.
- [4] J. J. Taún, "Aetiology of age-associated aneuploidy: a mechanism based on the 'free radical theory of ageing'," *Molecular Human Reproduction*, vol. 1, no. 4, pp. 163–165, 1995.
- [5] A. P. Wickens, "Ageing and the free radical theory," *Respiration Physiology*, vol. 128, no. 3, pp. 379–391, 2001.
- [6] M. C. Carbone, C. Tatone, S. Delle Monache et al., "Antioxidant enzymatic defences in human follicular fluid: characterization and age-dependent changes," *Molecular Human Reproduction*, vol. 9, no. 11, pp. 639–643, 2003.
- [7] C. Tatone, M. C. Carbone, S. Falone et al., "Age-dependent changes in the expression of superoxide dismutases and catalase are associated with ultrastructural modifications in human granulosa cells," *Molecular Human Reproduction*, vol. 12, no. 11, pp. 655–660, 2006.
- [8] L. Matos, D. Stevenson, F. Gomes, J. L. Silva-Carvalho, and H. Almeida, "Superoxide dismutase expression in human cumulus oophorus cells," *Molecular Human Reproduction*, vol. 15, no. 7, pp. 411–419, 2009.
- [9] J. Liu, M. Liu, X. Ye et al., "Delay in oocyte aging in mice by the antioxidant N-acetyl-L-cysteine (NAC)," *Human Reproduction*, vol. 27, no. 5, pp. 1411–1420, 2012.
- [10] M. Liu, Y. Yin, X. Ye et al., "Resveratrol protects against age-associated infertility in mice," *Human Reproduction*, vol. 28, no. 3, pp. 707–717, 2013.
- [11] X. M. Zhang, L. Li, J. J. Xu et al., "Rapamycin preserves the follicle pool reserve and prolongs the ovarian lifespan of female rats via modulating mTOR activation and sirtuin expression," *Gene*, vol. 523, no. 1, pp. 82–87, 2013.
- [12] J. J. Tarin, S. Perez-Albala, and A. Cano, "Oral antioxidants counteract the negative effects of female aging on oocyte quantity and quality in the mouse," *Molecular Reproduction & Development*, vol. 61, no. 3, pp. 385–397, 2002.
- [13] S. M. Briley, S. Jasti, J. M. McCracken et al., "Reproductive age-associated fibrosis in the stroma of the mammalian ovary," *Reproduction*, vol. 152, no. 3, pp. 245–260, 2016.
- [14] K. Richter, A. Konzack, T. Pihlajaniemi, R. Heljasvaara, and T. Kietzmann, "Redox-fibrosis: impact of TGF β 1 on ROS

- generators, mediators and functional consequences," *Redox Biology*, vol. 6, pp. 344–352, 2015.
- [15] K. Richter and T. Kietzmann, "Reactive oxygen species and fibrosis: further evidence of a significant liaison," *Cell and Tissue Research*, vol. 365, no. 3, pp. 591–605, 2016.
- [16] M. Giannandrea and W. C. Parks, "Diverse functions of matrix metalloproteinases during fibrosis," *Disease Models & Mechanisms*, vol. 7, no. 2, pp. 193–203, 2014.
- [17] S. Freitas-Rodríguez, A. R. Folgueras, and C. López-Otín, "The role of matrix metalloproteinases in aging: tissue remodeling and beyond," *Biochimica et Biophysica Acta (BBA) - Molecular Cell Research*, vol. 1864, no. 11, pp. 2015–2025, 2017, Part A.
- [18] C. Yang, S.-D. Zheng, H.-J. Wu, and S.-J. Chen, "Regulatory mechanisms of the molecular pathways in fibrosis induced by microRNAs," *Chinese Medical Journal*, vol. 129, no. 19, pp. 2365–2372, 2016.
- [19] X. Cheng, X. Zheng, Y. Song et al., "Apocynin attenuates renal fibrosis via inhibition of NOXs-ROS-ERK-myofibroblast accumulation in UUO rats," *Free Radical Research*, vol. 50, no. 8, pp. 840–852, 2016.
- [20] R. Xin, X. Sun, Z. Wang et al., "Apocynin inhibited NLRP3/XIAP signalling to alleviate renal fibrotic injury in rat diabetic nephropathy," *Biomedicine & Pharmacotherapy*, vol. 106, pp. 1325–1331, 2018.
- [21] Y. Q. Li, X. B. Li, S. J. Guo et al., "Apocynin attenuates oxidative stress and cardiac fibrosis in angiotensin II-induced cardiac diastolic dysfunction in mice," *Acta Pharmacologica Sinica*, vol. 34, no. 3, pp. 352–359, 2013.
- [22] C. Cabello-Verrugio, M. J. Acuna, M. G. Morales, A. Becerra, F. Simon, and E. Brandan, "Fibrotic response induced by angiotensin-II requires NAD(P)H oxidase-induced reactive oxygen species (ROS) in skeletal muscle cells," *Biochemical and Biophysical Research Communications*, vol. 410, no. 3, pp. 665–670, 2011.
- [23] T. Kilic, H. Parlakpınar, E. Taslidere et al., "Protective and therapeutic effect of apocynin on bleomycin-induced lung fibrosis in rats," *Inflammation*, vol. 38, no. 3, pp. 1166–1180, 2015.
- [24] E. Silva, A. I. Soares, F. Costa, J. P. Castro, L. Matos, and H. Almeida, "Antioxidant supplementation modulates age-related placental bed morphology and reproductive outcome in mice," *Biology of Reproduction*, vol. 93, no. 3, p. 56, 2015.
- [25] J. P. Castro, C. Ott, T. Jung, T. Grune, and H. Almeida, "Carbonylation of the cytoskeletal protein actin leads to aggregate formation," *Free Radical Biology & Medicine*, vol. 53, no. 4, pp. 916–925, 2012.
- [26] Y. Asano, "Age-related accumulation of non-heme ferric and ferrous iron in mouse ovarian stroma visualized by sensitive non-heme iron histochemistry," *The Journal of Histochemistry & Cytochemistry*, vol. 60, no. 3, pp. 229–242, 2012.
- [27] C. López-Otín, M. A. Blasco, L. Partridge, M. Serrano, and G. Kroemer, "The hallmarks of aging," *Cell*, vol. 153, no. 6, pp. 1194–1217, 2013.
- [28] J. Lim and U. Luderer, "Oxidative damage increases and antioxidant gene expression decreases with aging in the mouse ovary," *Biology of Reproduction*, vol. 84, no. 4, pp. 775–782, 2011.
- [29] S. Prasad, M. Tiwari, A. N. Pandey, T. G. Shrivastav, and S. K. Chaube, "Impact of stress on oocyte quality and reproductive outcome," *Journal of Biomedical Science*, vol. 23, no. 1, p. 36, 2016.
- [30] K. R. Hansen, N. S. Knowlton, A. C. Thyer, J. S. Charleston, M. R. Soules, and N. A. Klein, "A new model of reproductive aging: the decline in ovarian non-growing follicle number from birth to menopause," *Human Reproduction*, vol. 23, no. 3, pp. 699–708, 2008.
- [31] M. Herbert, D. Kalleas, D. Cooney, M. Lamb, and L. Lister, "Meiosis and maternal aging: insights from aneuploid oocytes and trisomy births," *Cold Spring Harbor Perspectives in Biology*, vol. 7, no. 4, article a017970, 2015.
- [32] D. Cimadomo, G. Fabozzi, A. Vaiarelli, N. Ubaldi, F. M. Ubaldi, and L. Rienzi, "Impact of maternal age on oocyte and embryo competence," *Frontiers in Endocrinology*, vol. 9, p. 327, 2018.
- [33] A. S. Care, K. R. Diener, M. J. Jasper, H. M. Brown, W. V. Ingman, and S. A. Robertson, "Macrophages regulate corpus luteum development during embryo implantation in mice," *The Journal of Clinical Investigation*, vol. 123, no. 8, pp. 3472–3487, 2013.
- [34] A. K. McNally and J. M. Anderson, "Macrophage fusion and multinucleated giant cells of inflammation," in *Cell Fusion in Health and Disease*, vol. 713 of *Advances in Experimental Medicine and Biology*, pp. 97–111, Springer, 2011.
- [35] T. A. Wynn and L. Barron, "Macrophages: master regulators of inflammation and fibrosis," *Seminars in Liver Disease*, vol. 30, no. 3, pp. 245–257, 2010.
- [36] F. Zhou, L.-B. Shi, and S.-Y. Zhang, "Ovarian fibrosis: a phenomenon of concern," *Chinese Medical Journal*, vol. 130, no. 3, pp. 365–371, 2017.
- [37] M. Sedeek, R. Nasrallah, R. M. Touyz, and R. L. Hebert, "NADPH oxidases, reactive oxygen species, and the kidney: friend and foe," *Journal of the American Society of Nephrology*, vol. 24, no. 10, pp. 1512–1518, 2013.
- [38] A. Masamune, T. Watanabe, K. Kikuta, K. Satoh, and T. Shimosegawa, "NADPH oxidase plays a crucial role in the activation of pancreatic stellate cells," *American Journal of Physiology Gastrointestinal and Liver Physiology*, vol. 294, no. 1, pp. G99–G108, 2008.
- [39] Y. H. Paik, K. Iwaisako, E. Seki et al., "The nicotinamide adenine dinucleotide phosphate oxidase (NOX) homologues NOX1 and NOX2/gp91^{phox} mediate hepatic fibrosis in mice," *Hepatology*, vol. 53, no. 5, pp. 1730–1741, 2011.
- [40] W. Cui, K. Matsuno, K. Iwata et al., "NOX1/nicotinamide adenine dinucleotide phosphate, reduced form (NADPH) oxidase promotes proliferation of stellate cells and aggravates liver fibrosis induced by bile duct ligation," *Hepatology*, vol. 54, no. 3, pp. 949–958, 2011.
- [41] S. De Minicis and D. A. Brenner, "NOX in liver fibrosis," *Archives of Biochemistry and Biophysics*, vol. 462, no. 2, pp. 266–272, 2007.
- [42] S. Van Linthout, K. Miteva, and C. Tschöpe, "Crosstalk between fibroblasts and inflammatory cells," *Cardiovascular Research*, vol. 102, no. 2, pp. 258–269, 2014.
- [43] W. Liu, Y. Peng, Y. Yin, Z. Zhou, W. Zhou, and Y. Dai, "The involvement of NADPH oxidase-mediated ROS in cytokine secretion from macrophages induced by Mycobacterium tuberculosis ESAT-6," *Inflammation*, vol. 37, no. 3, pp. 880–892, 2014.
- [44] T. Meng, J. Yu, Z. Lei et al., "Propofol reduces lipopolysaccharide-induced, NADPH oxidase (NOX₂) mediated TNF- α and IL-6 production in macrophages," *Clinical and Developmental Immunology*, vol. 2013, Article ID 325481, 9 pages, 2013.

- [45] M. Nagase, H. Kurihara, A. Aiba, M. J. Young, and T. Sakai, "Deletion of Rac1GTPase in the myeloid lineage protects against inflammation-mediated kidney injury in mice," *PLoS One*, vol. 11, no. 3, article e0150886, 2016.
- [46] S. O'Reilly, "MicroRNAs in fibrosis: opportunities and challenges," *Arthritis Research & Therapy*, vol. 18, no. 1, p. 11, 2016.
- [47] B. Wang, R. Komers, R. Carew et al., "Suppression of microRNA-29 expression by TGF- β 1 promotes collagen expression and renal fibrosis," *Journal of the American Society of Nephrology*, vol. 23, no. 2, pp. 252–265, 2012.
- [48] A. Schneider, S. J. Matkovich, B. Victoria et al., "Changes of ovarian microRNA profile in long-living Ames dwarf mice during aging," *PLoS One*, vol. 12, no. 1, article e0169213, 2017.
- [49] Y. Li, Y. Fang, Y. Liu, and X. Yang, "MicroRNAs in ovarian function and disorders," *Journal of Ovarian Research*, vol. 8, no. 1, 2015.
- [50] E. van Rooij, L. B. Sutherland, J. E. Thatcher et al., "Dysregulation of microRNAs after myocardial infarction reveals a role of miR-29 in cardiac fibrosis," *Proceedings of the National Academy of Sciences of the United States of America*, vol. 105, no. 35, pp. 13027–13032, 2008.
- [51] B. Maurer, J. Stanczyk, A. Jüngel et al., "MicroRNA-29, a key regulator of collagen expression in systemic sclerosis," *Arthritis & Rheumatism*, vol. 62, no. 6, pp. 1733–1743, 2010.
- [52] C. Roderburg, G. W. Urban, K. Bettermann et al., "Micro-RNA profiling reveals a role for miR-29 in human and murine liver fibrosis," *Hepatology*, vol. 53, no. 1, pp. 209–218, 2011.
- [53] M. Fanjul-Fernández, A. R. Folgueras, S. Cabrera, and C. López-Otín, "Matrix metalloproteinases: evolution, gene regulation and functional analysis in mouse models," *Biochimica et Biophysica Acta (BBA) - Molecular Cell Research*, vol. 1803, no. 1, pp. 3–19, 2010.
- [54] P. Serralheiro, E. Cairrão, C. J. Maia, M. João, C. M. C. Almeida, and I. Verde, "Effect of TGF-beta1 on MMP/TIMP and TGF-beta1 receptors in great saphenous veins and its significance on chronic venous insufficiency," *Phlebology: The Journal of Venous Disease*, vol. 32, no. 5, pp. 334–341, 2016.
- [55] T. Kobayashi, H. Kim, X. Liu et al., "Matrix metalloproteinase-9 activates TGF- β and stimulates fibroblast contraction of collagen gels," *American Journal of Physiology-Lung Cellular and Molecular Physiology*, vol. 306, no. 11, pp. L1006–L1015, 2014.
- [56] Q. Yu and I. Stamenkovic, "Cell surface-localized matrix metalloproteinase-9 proteolytically activates TGF-beta and promotes tumor invasion and angiogenesis," *Genes & Development*, vol. 14, no. 2, pp. 163–176, 2000.

Research Article

Metformin Improves Fertility in Obese Males by Alleviating Oxidative Stress-Induced Blood-Testis Barrier Damage

Jifeng Ye,^{1,2,3,4} Dandan Luo,^{1,2,3} Xiaolin Xu,^{1,2,3,5} Mingqi Sun,^{1,2,3} Xiaohui Su,^{1,2,3}
Zhenhua Tian,^{1,2,3} Meijie Zhang,^{1,2,3} Chunxiao Yu ,^{1,2,3} and Qingbo Guan ,^{1,2,3}

¹Department of Endocrinology and Metabolism, Shandong Provincial Hospital affiliated to Shandong University, Jinan, Shandong 250021, China

²Department of Endocrinology and Metabolism, Shandong Provincial Hospital affiliated to Shandong First Medical University, Jinan, Shandong 250021, China

³Department of Endocrinology and Metabolism, Shandong Provincial Key Laboratory of Endocrinology and Lipid Metabolism, Jinan, Shandong 250021, China

⁴Department of Endocrinology and Metabolism, The Second People's Hospital of Liaocheng, Shandong 252601, China

⁵Department of Rheumatology and Immunology, Dongying People's Hospital, Dongying, Shandong 257000, China

Correspondence should be addressed to Chunxiao Yu; yuchx08@163.com and Qingbo Guan; doctorguanqingbo@163.com

Received 4 February 2019; Revised 8 May 2019; Accepted 10 June 2019; Published 10 September 2019

Guest Editor: Elisabete Silva

Copyright © 2019 Jifeng Ye et al. This is an open access article distributed under the Creative Commons Attribution License, which permits unrestricted use, distribution, and reproduction in any medium, provided the original work is properly cited.

Background/Aims. Obesity, which is related to increased oxidative stress in various tissues, is a risk factor for male infertility. Metformin is reported to have an antioxidant effect; however, the precise role of metformin in obesity-induced male infertility remains unknown. The current study is aimed at exploring the effects of metformin and characterizing its underlying mechanism in the fertility of obese males. **Methods.** An obese male mouse model was generated by feeding mice with a high-fat diet; then, the mice were administered metformin in water for 8 weeks. Reproductive ability, metabolic parameters, and follicle-stimulating hormone (FSH) were assessed by cohabitation, enzymatic methods, and ELISA, respectively. Damage to the integrity of the blood-testis barrier (BTB), which ensures spermatogenesis, was assessed by transmission electron microscopy and immunofluorescence with a biotin tracer. Malondialdehyde (MDA), superoxide dismutase (SOD), and reactive oxygen species (ROS) were employed for the assessments of oxidative stress. BTB-related proteins were measured by immunoblotting. Nuclear factor κ B (NF- κ B) was assessed by immunofluorescence. **Results.** High-fat-diet-fed mice presented evident lipid metabolic disturbances, disrupted BTB integrity, and decreased reproductive function. Metformin alleviated the decrease in male fertility, decreased ectopic lipid deposition in the testis, and increased serum FSH levels. A further mechanistic analysis revealed that metformin ameliorated the high-fat-diet-induced injury to the BTB structure and permeability and restored the disordered BTB-related proteins, which might be associated with an improvement in oxidative stress and a recovery of NF- κ B activity in Sertoli cells (SCs). **Conclusion.** Metformin improves obese male fertility by alleviating oxidative stress-induced BTB damage. These findings provide new insights into the effect of metformin on various diseases and suggest future possibilities in the treatment of male infertility.

1. Introduction

Obesity is a complex metabolic disease that is determined by lifestyle factors, including environmental (food variety and intake, physical activity) and genetic factors. In recent decades, obesity has become a predominant health problem and has increased globally at an alarming rate [1]. Obesity

increases the risk for hypertension, diabetes, cardiovascular disease, and some cancers [2–6]. Furthermore, the negative impact of obesity on the male genital system is gradually being recognized. According to clinical investigations, overweight men or men with obesity show a decline in sperm quality, an increase in sperm DNA damage, and a decrease in embryo implantation rates compared with men with

normal body mass index (BMI) [7–10]. Additionally, animal experiments have shown that a high-fat diet can increase the male infertility rate and decrease sperm parameters [11–13]. Many previous studies involving mechanistic explorations have mainly focused on the effects of obesity or a high-fat diet on germ cells or Leydig cells. However, whether and how obesity damages Sertoli cells (SCs) or the blood-testis barrier (BTB) remains unclear.

SCs nurse developing germ cells and form the BTB between opposing SCs and adjacent Sertoli-germ cells [14–16]. The BTB is one of the tightest blood-tissue barriers, and it physically divides the seminiferous epithelium into the basal and apical compartments, in which different stages of germ cell development occur; these compartments are crucial to male fertility [17]. Several previous studies have demonstrated that various stimulators, such as high glucose [18], perfluorooctanesulfonate [19], cadmium [20, 21], amodiaquine [22], and bisphenol A [21], adversely affect male fertility via impairment of the BTB; however, whether obesity that is induced by a high-fat diet can provoke deleterious effects on the BTB has not been elucidated. The BTB comprises tight junctions (TJs), basal ectoplasmic specializations (basal ESs), gap junctions, and desmosomes. TJs, which coexist with basal ESs, are located between basal ESs and are reinforced by basal ESs [23]. The expression levels of TJ-related proteins (occludin and ZO-1) and basal ES-related proteins (N-cadherin and beta-catenin) are downregulated by exogenous stimulators, such as cadmium [20], perfluorooctanesulfonate [19], amodiaquine [22], and bisphenol A [24]. These studies indicate that TJs and basal ESs might be the molecular targets of exogenous stimulators.

Obesity can increase oxidative stress in the whole body [25], and an increase in testicular oxidative stress is a common feature in much of what underlies male infertility [26]. However, whether oxidative stress is involved in lipotoxicity-induced injury to SCs and the BTB is unclear. Metformin is a first-line hypoglycaemic agent. Beyond its glucose-lowering effects, metformin exhibits antioxidant properties in various tissues, an effect that is independent of its effect on insulin sensitivity, and acts to decrease lipid peroxidation [27, 28]. A recent clinical study has demonstrated for the first time that metformin improved semen quality in men with hyperinsulinaemia [29], but the underlying molecular mechanism is unclear. Moreover, a study in patients with polycystic ovarian syndrome (PCOS) has reported that metformin reduces angiogenesis through the nuclear factor κ B (NF- κ B) pathway [30]. However, whether metformin can improve the fertility of obese males and alleviate the damage of BTB in testis by inhibiting oxidative stress remains unknown.

In the present study, to determine the effect of metformin on fertility in obese males, an obese mouse model was induced with a high-fat diet, and metformin was administered. First, the effect of metformin on the reproductive ability of male mice was investigated. Alterations to the ultrastructure, BTB integrity, the expression of TJ proteins, and basal ES proteins were further assessed. In addition, the levels of oxidative stress and NF- κ B activity were measured to characterize the intracellular mechanism. This study

demonstrates a crucial role of metformin in obesity-induced male infertility.

2. Materials and Methods

2.1. Animals and Treatment. Seven-week-old C57BL/6 male mice and nine-week-old C57BL/6 female mice were obtained from the Vital River Corporation (Beijing, China) and housed in a temperature- and humidity-controlled room ($25 \pm 2^\circ\text{C}$ and $55 \pm 10\%$, respectively) on a 12-hour light/dark cycle with free access to water and food. All experimental procedures were approved by the ethics committee of Shandong Provincial Hospital affiliated with Shandong University, and the methods were performed according to the approved guidelines.

As shown in Figure S1, one week after feeding to adapt to the housing conditions, the male mice were randomly divided into two groups: the normal-diet group (N, $n = 20$) was fed a standard diet (Beijing Keao Xieli Feed Co. Ltd., China) in which 10% of the calories were from fat, and the high-fat-diet group (H, $n = 30$) was fed a high-fat diet (product #D12492, Research Diets Inc., New Brunswick, NJ, USA) in which 60% of the calories were from fat. Ten mice from each group were sacrificed at the end of the 8th week of feeding. The remaining mice in the N group were maintained on their standard diet (NN, $n = 10$), whereas the mice fed a high-fat diet ($n = 20$) were further subdivided into two subgroups. The first subgroup (HH, $n = 10$) was maintained on the high-fat diet, and the second subgroup (HH + MET, $n = 10$) was maintained on the high-fat diet with ~ 200 mg/kg body weight/day metformin (SFDA approval number H20023371, Sino-American Shanghai Squibb Pharmaceuticals Ltd., Shanghai, China) given in the drinking water [31]. The body weights of the mice were monitored at 5 pm every week during the entire feeding period (the adaptation week and the subsequent 8 or 16 weeks). All mice were sacrificed at the end of the 16th week of feeding.

2.2. Reproductive Ability Assay. To assess the reproductive ability of the male mice, at the 7th and 15th weeks after different feeding conditions, each male mouse was individually housed and mated with two female mice, which were randomly grouped by weight, for 5 consecutive days. On the second day, vaginal plugs were inspected to determine whether coitus had occurred. Female mice with vaginal plugs were moved into another cage and observed until the pups were born. The fertility of male mice was calculated according to the number of pregnant females. The number and weights of the pups were also statistically analyzed.

2.3. Blood Collection and Tissue Removal. At the 8th and 16th week, after being fasted for 8 h, all mice were anaesthetized by intraperitoneal injection with pentobarbital (40 mg/kg body weight) and sacrificed. Blood samples were obtained, and serum was extracted by centrifugation for the lipid profile and sex hormone analyses. For long-term storage, sera were kept at -80°C . Epididymal fat and testes were obtained immediately and weighed. The testis was fixed in modified

Davidson's fluid (MDF) [32] for morphological analysis and immunofluorescence, fixed in 2.5% glutaraldehyde and 1% osmium tetroxide for ultrastructure analysis, or stored in liquid nitrogen for assessments by Oil red O staining, determination of mRNA and protein expression, and oxidative stress-related testing.

2.4. Serum Lipid Profile and Sex Hormone Analysis. The serum levels of total cholesterol (TC), triglycerides (TG), high-density lipoprotein-cholesterol (HDL-c), low-density lipoprotein-cholesterol (LDL-c), and glucose (Glu) were determined using enzymatic methods with an Olympus AU5400 automatic biochemical analyzer (Olympus Co. Ltd., Japan). The follicle-stimulating hormone (FSH) level in the serum was measured using an ELISA kit (Abnova, Taiwan, China) according to the manufacturer's protocol for each assay.

2.5. Oil Red O Staining. To determine testicular lipid accumulation, frozen sections of the testis (10 μm) were fixed in 95% ethanol for 10 s, washed with distilled water for 10 s, stained with Oil red O (Changsha Guge Biotechnology Co. Ltd., China) for 10 min, washed again with distilled water for 10 s, and counterstained with haematoxylin for 30 s. Representative photomicrographs were captured using a microscope (Carl Zeiss, Germany).

2.6. Haematoxylin and Eosin (H&E) Staining Analysis. Testicular tissue samples were dehydrated in a graded series of ethanol solutions, embedded in paraffin, and coronally sectioned using a section cutter (Leica, USA) at a thickness of 4 μm . H&E staining was performed for morphological observation using a system incorporated in the Carl Zeiss microscope.

2.7. Testicular Transmission Electron Microscopy (TEM) Analysis. To characterize the changes in testis at the ultrastructural level, the testis was dehydrated in a progressive ethanol and acetone solution, embedded in Epon 812, sectioned using a LKB ultramicrotome (LKB Instruments Inc., Sweden), stained with uranyl acetate followed by lead citrate, observed with a JEM-1200EX Transmission Electron Microscope (JEOL, Japan), and photographed.

2.8. BTB Integrity Assay. The integrity of the BTB assessment was evaluated using a biotin tracer as described previously [19]. In short, the mice were anaesthetized, and the testes were exposed before sacrifice. The gaps below the testicular tunica albuginea were injected with 50 μl of EZ-Link Sulfo-NHS-LC-Biotin (10 mg/ml, freshly dissolved in physiological saline containing 1 mM CaCl_2 ; Pierce Biotechnology Inc., IL, USA). After 30 min, the animals were euthanized, and their testes were frozen in liquid nitrogen in preparation for cryosectioning (10 μm). The sections were fixed in 4% paraformaldehyde (PFA) for 20 min, washed with phosphate-buffered saline with 0.1% Tween20 (PBST) three times, blocked in 0.01 M phosphate buffer solution (PBS) containing 15% goat serum (Zhongshan Jinqiao Biotechnology Co. Ltd., China) and 1% bovine serum albumin (BSA, wt/vol) for 1 h, incubated with Alexa Fluor[®] 568-conjugated strepta-

vidin (Life Technologies Corp.-Invitrogen, CA, USA) and 4'-6-diamidino-2-phenylindole (DAPI, blue) (Invitrogen, UK) for 2 h at room temperature, and washed again with PBST five times (5 min per time). After mounting with antifade mounting medium P0128 (Beyotime Biotechnology, China), the sections were analyzed by fluorescence microscopy (Axio Imager A2, Carl Zeiss, Germany).

2.9. Immunoblotting Analysis. Frozen testes were lysed in RIPA buffer with a protease inhibitor cocktail, PMSF and sodium orthovanadate (Santa Cruz Biotechnology Inc., CA, USA), to extract the whole protein. The cytosol and nuclear protein were obtained using the Nuclear and Cytoplasmic Protein Extraction Kit (CW BIO, China) according to the manufacturer's instructions. The protein concentration was quantified using a BCA protein assay kit (Pierce Biotechnology Inc., IL, USA). A total of 120 μg whole protein or 60 μg nucleoprotein lysates was resolved by SDS-PAGE using 8% denaturing polyacrylamide gel, electrotransferred to a PVDF membrane (Millipore, America), and blotted with specific antibodies, namely, anti-ZO-1, anti-occludin, anti-N-cadherin, anti-beta-catenin, anti-nectin2, and anti-NF- κB /p65, with anti-beta-actin or anti-LaminB1 as a loading control for cytosolic proteins or nuclear proteins, respectively. The appropriate secondary antibodies conjugated to horseradish peroxidase (HRP) (Amersham, Little Chalfont Bucks, UK) were used at a 1 : 5000 dilution. The membranes were visualized using the HyGLO HRP detection kit (Denville, NJ, USA). The antibodies are shown in Table 1.

2.10. Isolation of RNA and Real-Time Polymerase Chain Reaction (PCR) Analysis. Total RNA was isolated from the tissues using an RNeasy Total RNA Isolation Kit (TaKaRa Bio Inc., Japan) and reverse-transcribed into cDNA (TaKaRa Bio Inc., Japan). Then, SYBR Green (DBI, Germany) quantitative PCR analysis reactions were performed using the Roche LightCycler 480 Detection System (Roche, Belgium). Each reaction comprised 10 μl of SYBR Green, 1 μl of cDNA, 1 μl of each primer pair (10 $\mu\text{mol}/\mu\text{l}$), and 8 μl of distilled water. The beta-actin gene was simultaneously detected as an endogenous reference. The relative gene expression levels were quantified using the $2^{-\Delta\Delta t}$ method, and the results are expressed as the fold change relative to the endogenous reference. The primer sequences are listed in Table 2.

2.11. Malondialdehyde (MDA), Superoxide Dismutase (SOD), and Reactive Oxygen Species (ROS) Measurements. Assay kits for MDA and SOD were provided by Beyotime Biotechnology (China), and an assay kit for ROS was provided by Nanjing Jiancheng Bioengineering Institute (China). The MDA content, SOD activity, and ROS levels were measured using the kits according to the manufacturer's instructions, and these measurements were normalized to total protein.

2.12. Immunofluorescence. The testicular tissues were fixed with MDF and embedded in paraffin blocks. The sections were deparaffinized, and antigen retrieval was performed with Tris-EDTA (pH = 9.0). After blocking with 10% normal goat or donkey serum (Zhongshan Jinqiao Biotechnology Co. Ltd., China) for 60 min at room temperature, the slides were

TABLE 1: Antibodies.

Antibody	Species	Dilution	Corporation	Catalogue number
ZO-1	Rabbit	1 : 50	Thermo Fisher Scientific	40-2200
Occludin	Rabbit	1 : 62.5	Thermo Fisher Scientific	71-1500
N-cadherin	Rabbit	1 : 500	Proteintech Group Inc.	13769-1-AP
beta-Catenin	Rabbit	1 : 1000	Proteintech Group Inc.	51067-2-AP
Nectin2	Rabbit	1 : 10000	Abcam	Ab135246
NF- κ B/p65	Rabbit	1 : 2500	Abcam	ab32536
beta-Actin	Rabbit	1 : 7500	Proteintech Group Inc.	60008-1
LaminB1	Mouse	1 : 7500	Proteintech Group Inc.	66095-1

TABLE 2: Primers for real-time PCR detection.

Gene	Species	Forward primer	Reverse primer
ZO-1	Mouse	GCCGCTAAGAGCACAGCAA	TCCCCACTCTGAAAATGAGGA
Occludin	Mouse	TTGAAAGTCCACCTCCTTACAGA	CCGGATAAAAAGAGTACGCTGG
N-cadherin	Mouse	AGCGCAGTCTTACCGAAGG	TCGCTGCTTTCATACTGAACTTT
beta-Catenin	Mouse	CCCAGTCCTTACGCAAGAG	CATCTAGCGTCTCAGGGAACA
Nectin2	Mouse	GCATCATTTGGAGGTATTATCGCT	GAGGGAGGTCCTTCCAGTTC
NF- κ B/p65	Mouse	CGGGATGGCTACTATGAGGC	CGTGAAAGGGGTTATTGTTGGT
beta-Actin	Mouse	GGCTGTATCCCCTCCATCG	CCAGTTGGTAACAATGCCATGT

incubated overnight at 4°C with ZO-1 (1 : 25) or NF- κ B/p65 (1 : 250) primary antibody. For the negative control, 0.01 mol/l PBS was added instead of the primary antibody. The tissues were then incubated with the Alexa Fluor® 488F (ab') 2 fragment of goat anti-rabbit IgG (H+L) (Thermo Fisher Scientific, USA) or with a donkey anti-Rabbit IgG (H+L) highly cross-absorbed secondary antibody, namely, Alexa Fluor® 555 (Thermo Fisher Scientific, USA) at a 1 : 1000 dilution at room temperature for 1 h. The nuclei were stained with DAPI, and the coverslips were sealed to the microscope slides using the mounting medium P0128. The specimens were imaged under a Carl Zeiss fluorescence microscope.

2.13. Statistical Analyses. Significant differences between the obtained values (mean \pm SD) were determined by an independent sample *t*-test or one-way analysis of variance (ANOVA) followed by the least significant difference (LSD) multiple comparison test. A *P* value of <0.05 was considered significant.

3. Results

3.1. High-Fat Diet Increases Body Weight, Induces Abnormalities in Glucose and Lipid Metabolism, and Downregulates Fertility in Male Mice. To evaluate the effect of a high-fat diet on the general characteristics and fertility of the mice, some mice were sacrificed after 8 weeks of feeding, and relevant parameters were examined. As shown in Figure 1(a), male C57BL/6 mice fed the high-fat diet gained significantly more body weight than the mice fed a normal

diet (47.25 ± 1.39 vs. 28.14 ± 2.25 , $P < 0.01$), which is consistent with the general pictures shown in Figure 1(b). Accompanied by weight gain, there was a significant increase of epididymal adipose in high-fat-diet mice (0.24 ± 0.10 vs. 1.37 ± 0.13 , $P < 0.01$, Figure 1(d)), although there was no change in testicular weight (Figure 1(c)). These findings demonstrated that an obese mouse model induced with a high-fat diet was successfully established.

Obesity is often accompanied by dyslipidaemia [33], which is defined as an increase of plasma TG and LDL-c or a decrease of plasma HDL-c [33, 34], or by hyperglycaemia [35]. Thus, the serum lipid profile and Glu in the obese mouse model were assessed. The results showed that the serum Glu levels and serum TC, HDL-c, and LDL-c in the high-fat-diet-fed mice increased significantly relative to those in the normal-diet-fed mice (Glu, 6.91 ± 1.38 vs. 12.13 ± 1.82 ; TC, 1.85 ± 0.13 vs. 3.08 ± 0.39 ; HDL-c, 1.65 ± 0.14 vs. 2.71 ± 0.38 ; LDL-c, 0.22 ± 0.04 vs. 0.41 ± 0.11 , $P < 0.01$), but there was no difference in serum TG (Figures 1(e) and 1(f)). These alterations are consistent with the results during the 16th week of feeding (Figures 2(e) and 2(f)). These results indicated that glucose and lipid metabolism was highly disrupted in the high-fat-diet-induced obese mouse model.

FSH regulates spermatogenesis and the function of SCs in mammals. To analyze whether the high-fat diet affects FSH, the level of serum FSH was measured. As shown in Figure 1(g), the serum FSH levels were lower in the high-fat-diet-fed mice than in the normal-diet-fed mice (5.39 ± 0.67 vs. 3.58 ± 1.43 , $P < 0.05$). These results indicated that FSH was abnormal in the high-fat-diet-induced obese mouse model.

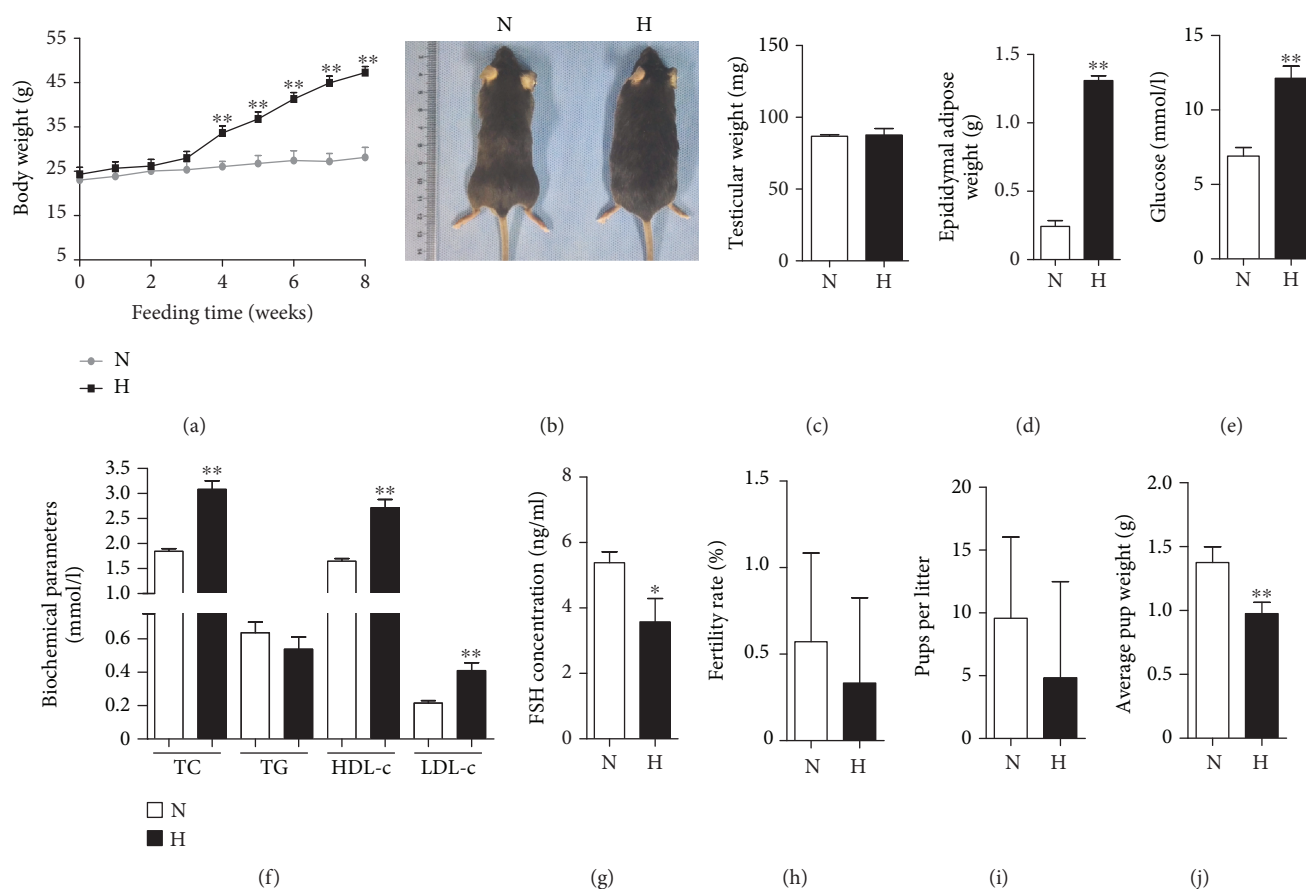


FIGURE 1: High-fat diet induces glycolipid metabolic abnormalities and damages the reproductive function of male mice. (a) Comparison of the time-dependent changes in body weight between the normal-diet-fed (N) and high-fat-diet-fed (H) groups during the 8 weeks of feeding. (b) Representative picture of normal-diet and high-fat-diet mice on the 8th week. Comparison of testicular weights (c) and epididymal adipose tissue (d) in the N and H groups on the 8th week. The serum glucose (e), biochemical parameters (f), and FSH levels (g) were assayed on the 8th week. $n = 10$ for each group. Comparison of fertility, including the fertility rate (h), number of pups per litter (i), and average pup weight (j) on the 8th week of feeding in the N and H groups. For the fertility assay, $n = 7$ males were included in each group. The results are presented as the mean \pm SD. * $P < 0.05$ and ** $P < 0.01$ vs. the corresponding N group.

To further assess the effect of the high-fat diet on the fertility of the male mice, the reproductive abilities of the male mice with different diets were assessed via cohabitation with female mice. No difference in the fertility rate or the number of pups per litter was observed between the high-fat-diet-fed mice and the normal-diet-fed mice (Figures 1(h) and 1(i)). The average pup weight of the offspring of the high-fat-diet-fed mice was significantly lower than that of the offspring of the normal-diet-fed mice (1.36 ± 0.12 vs. 0.98 ± 0.09 , $P < 0.01$, Figure 1(j)), suggesting that a high-fat diet might affect the offspring's size.

3.2. Metformin Ameliorates the Decrease in Male Fertility Caused by a High-Fat Diet Independently of the Regulation of Serum Glucose and Lipids. To investigate the effect of metformin on male fertility, the general characteristics, serum parameters, and fertility of mice were assessed after another 8 weeks of oral administration of metformin. As shown in Figures 2(a) and 2(b), the body weight of the oral metformin group did not decrease compared with that of the group fed the high-fat diet alone. Consistent with the body weight,

there were no differences in the testicular and epididymal adipose weights between the high-fat-diet group and the oral metformin group (Figures 2(c) and 2(d)). These results indicated that metformin did not ameliorate the weight gain or epididymal adipose accumulation caused by the high-fat diet during the additional 8 weeks of dosing. During the 16th week, serum Glu, TC, HDL-c, and LDL-c levels were increased significantly in the high-fat-diet-fed mice relative to those in the normal-diet-fed mice (Glu, 8.86 ± 0.63 vs. 13.52 ± 3.11 ; TC, 2.07 ± 0.33 vs. 4.57 ± 0.77 ; HDL-c, 1.79 ± 0.32 vs. 3.63 ± 1.05 ; LDL-c, 0.16 ± 0.03 vs. 0.47 ± 0.10 , $P < 0.01$), whereas these parameters did not differ between the high-fat-diet-fed mice and the oral metformin mice except HDL-c (a kind of "positive" cholesterol) [33, 36] (3.63 ± 1.05 vs. 4.30 ± 0.67 , $P < 0.05$, Figures 2(e) and 2(f)). These results indicated that metformin did not improve glucose and "adverse" serum lipid [33] metabolism at the present dosage and duration. However, compared with the serum FSH levels of the high-fat-diet-fed mice, those of the oral metformin mice were restored to normal levels (5.21 ± 0.86 vs. 6.60 ± 0.65 , $P < 0.05$) (Figure 2(g)). Intriguingly, although

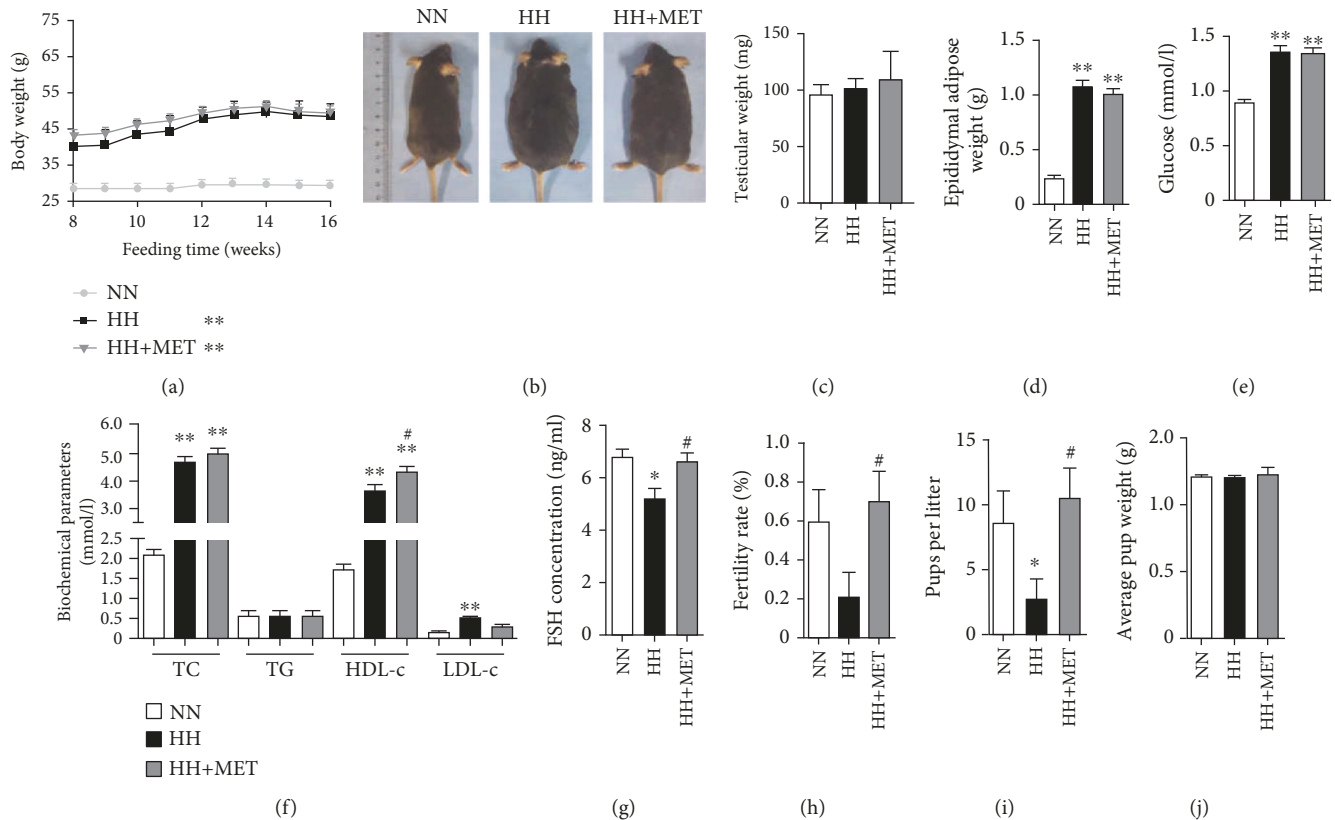


FIGURE 2: The effects of metformin on serum lipids, glucose, and FSH in high-fat-diet-induced obese male mice. (a) Comparison of the time-dependent changes in body weight among the NN, HH, and HH+MET groups during the 16 weeks of feeding. (b) Representative pictures of mice in each group on the 16th week. Comparison of testicular weights (c) and epididymal adipose tissue (d) of each group of mice on the 16th week. The serum glucose (e), serum lipid parameters (f), and FSH levels (g) were assessed on the 16th week of feeding. $n = 10$ for each group. Comparison of fertility, including the fertility rate (h), number of pups per litter (i), and average pup weight (j) on the 16th week of feeding. For the fertility assay, $n = 5$ males were included in each group. The results are presented as the mean \pm SD. * $P < 0.05$ and ** $P < 0.01$ vs. the corresponding NN group; # $P < 0.05$ vs. the corresponding HH group.

low-dosage metformin had no effect on high-fat-diet-induced dyslipidaemia or glucose, the reproductive ability assay showed that the fertility rate and number of pups per litter in the oral metformin group were significantly higher than those in the high-fat-diet group (fertility rate, 0.20 ± 0.42 vs. 0.70 ± 0.48 ; number of pups per litter, 2.60 ± 3.58 vs. 10.40 ± 4.67 , $P < 0.05$) and close to the normal level (Figures 2(h) and 2(i)). These results indicated that the decline in male fertility induced by a high-fat diet could be ameliorated through metformin treatment that independently regulated serum glucose and adverse lipids.

3.3. Metformin Improves High-Fat-Diet-Induced Testicular Lipid Deposition and Morphological Abnormalities. To determine the effect of the high-fat diet on lipid content in the testis, Oil red O staining was performed to visualize lipid deposition in the same cycle of the seminiferous epithelium. The testis sections of the high-fat-diet-fed mice exhibited abundant lipid content, mainly in the interstitial portion, and the lipid ectopic accumulation in seminiferous tubules was also increased. The testicular lipid deposition in seminiferous tubules of the oral metformin mice was clearly lower than that in the high-fat-diet-fed mice (0.49 ± 0.26

vs. 0.07 ± 0.01 , $P < 0.05$) (Figures 3(a) and 3(b)). These observations indicated that prior to the improvements in serum lipids and glucose, treatment with metformin alleviated ectopic lipid deposition in the testis.

To further assess the changes in the seminiferous tubules following exposure to a high-fat diet and oral metformin in mice, testicular morphology was analyzed by H&E staining. As shown in Figure 3(c), the seminiferous epithelia in the high-fat-diet group were severely disorganized, and cell adhesion between SCs and spermatogenic cells was disrupted and loosely arranged. After treatment with oral metformin, the spermatogenic epithelial morphology was improved, and the adhesion between cells was similar to that between cells in the normal-diet group. These findings demonstrated that metformin improved the high-fat-diet-induced disruption in the general structure of the seminiferous tubules.

3.4. Metformin Repairs the BTB Integrity Disruption Induced by a High-Fat Diet. The integrated BTB structure is one of the tightest blood-tissue barriers in the body, and it is crucial for maintaining cell adhesion between the opposing SCs and adjacent Sertoli-germ cells. To characterize the BTB

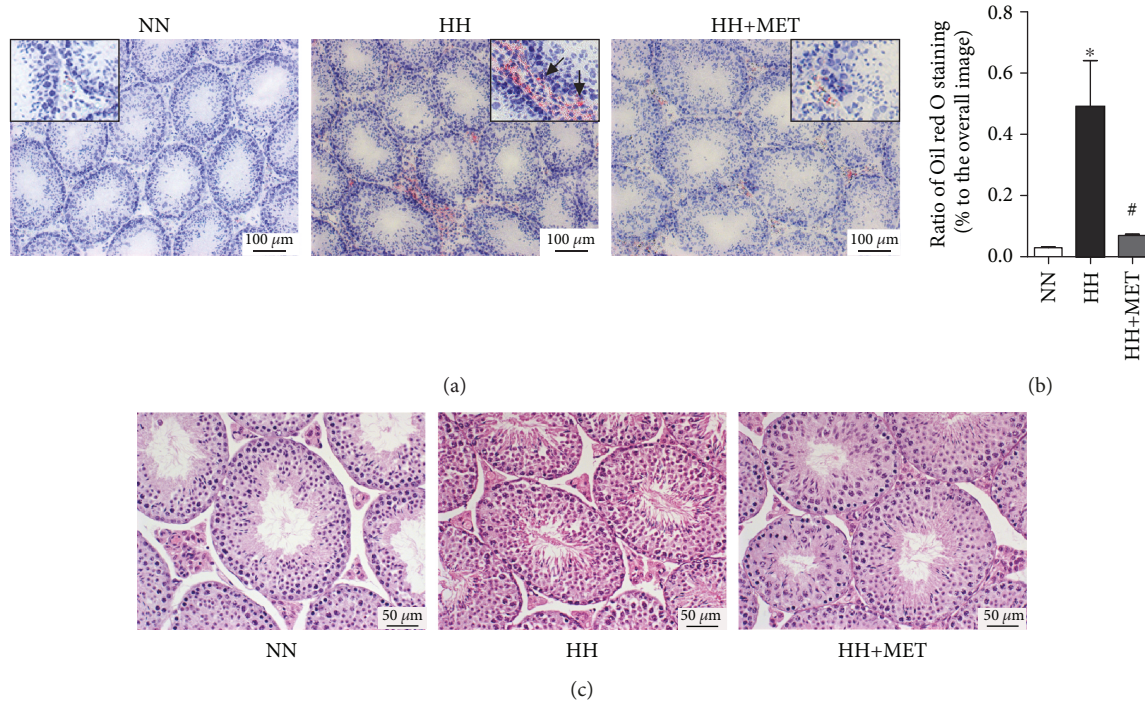


FIGURE 3: Metformin improves high-fat-diet-induced testicular lipid deposition and morphological abnormalities. (a) Oil red O-stained testicular sections on the 16th week of feeding. The boxed images are enlarged views of each section. The sections of seminiferous tubules are both in spermatogenic stage VIII. Scale bars = 100 μm . $n = 3$ for each group. (b) Ratio of Oil red O staining in seminiferous tubules (% to the overall image). The results are presented as the mean \pm SD. * $P < 0.05$ vs. the corresponding NN group; # $P < 0.05$ vs. the corresponding HH group. (c) H&E-stained testicular sections on the 16th week of feeding. $n = 3$ for each group. Scale bars = 100 μm . All of the above micrographs are representative of 3 independent experiments.

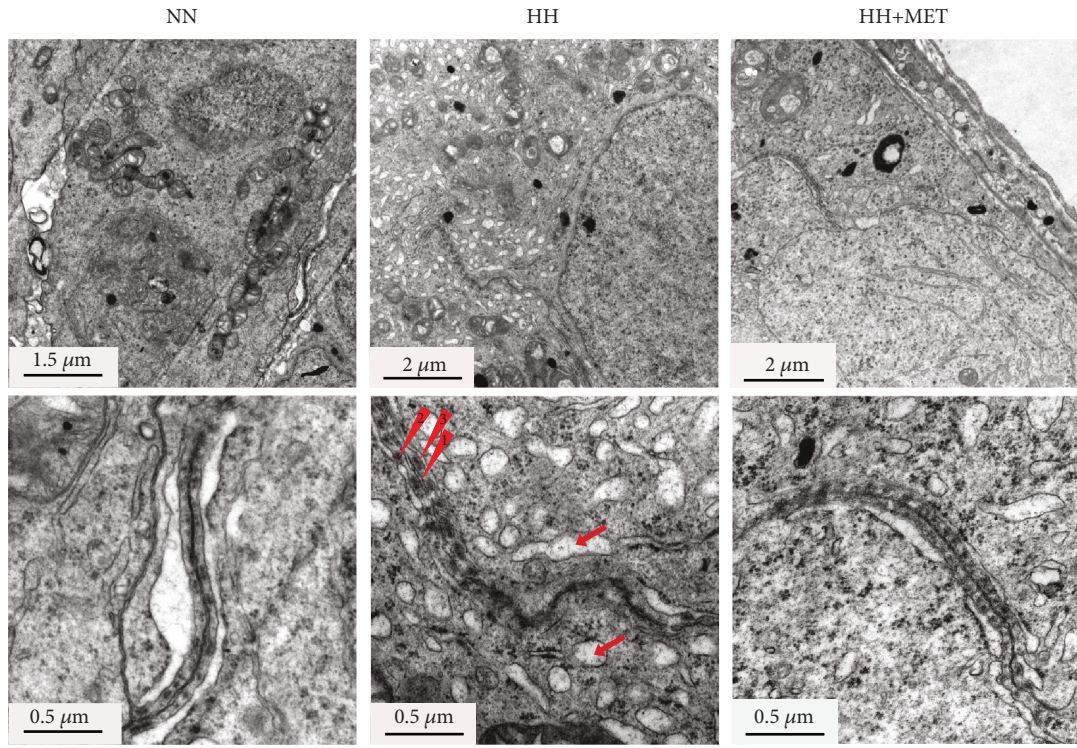
morphology at the ultrastructural level, a TEM analysis of the testis from each group of mice was performed. As depicted in Figure 4(a), the BTBs in the normal-diet-fed mice and oral metformin mice were lined with endoplasmic reticulum (ER) cisternae and clearly delimited, continuous, and tight. In contrast, the cell junctions adjoining SCs appeared discontinuous and dehiscent in the seminiferous tubules from the high-fat-diet-fed mice. These data showed that metformin repaired the injured integrity of the BTB, which was compromised severely by the high-fat diet. Furthermore, ER expansion and increased proteins alongside the BTB were found in the high-fat-diet-fed mice. The black particles beside the TJs, appearing as a net-like meshwork, represent polymers of interacting junctional transmembrane proteins [37]. These results indicated the possible existence of ER stress and the abnormal expression of BTB-related proteins.

Next, to further explore the effect of lipotoxicity on BTB integrity and the effect of metformin in the process, we analyzed BTB integrity with a biotin tracer (Figures 4(b) and 4(c)). In normal testes, junctions between the Sertoli-Sertoli and Sertoli-spermatid interfaces formed tight barriers that prevented large molecules from passing through. However, the BTB was opened after 16 weeks on the high-fat diet. Red fluorescent dye that was injected into the interstitium of the testes diffused into the BTB and appeared abundantly in the adluminal compartment. Additionally, only a small amount of red fluorescence appeared in the adluminal compartment of the HH+MET mice (2.20 ± 1.30 vs. $0.20 \pm$

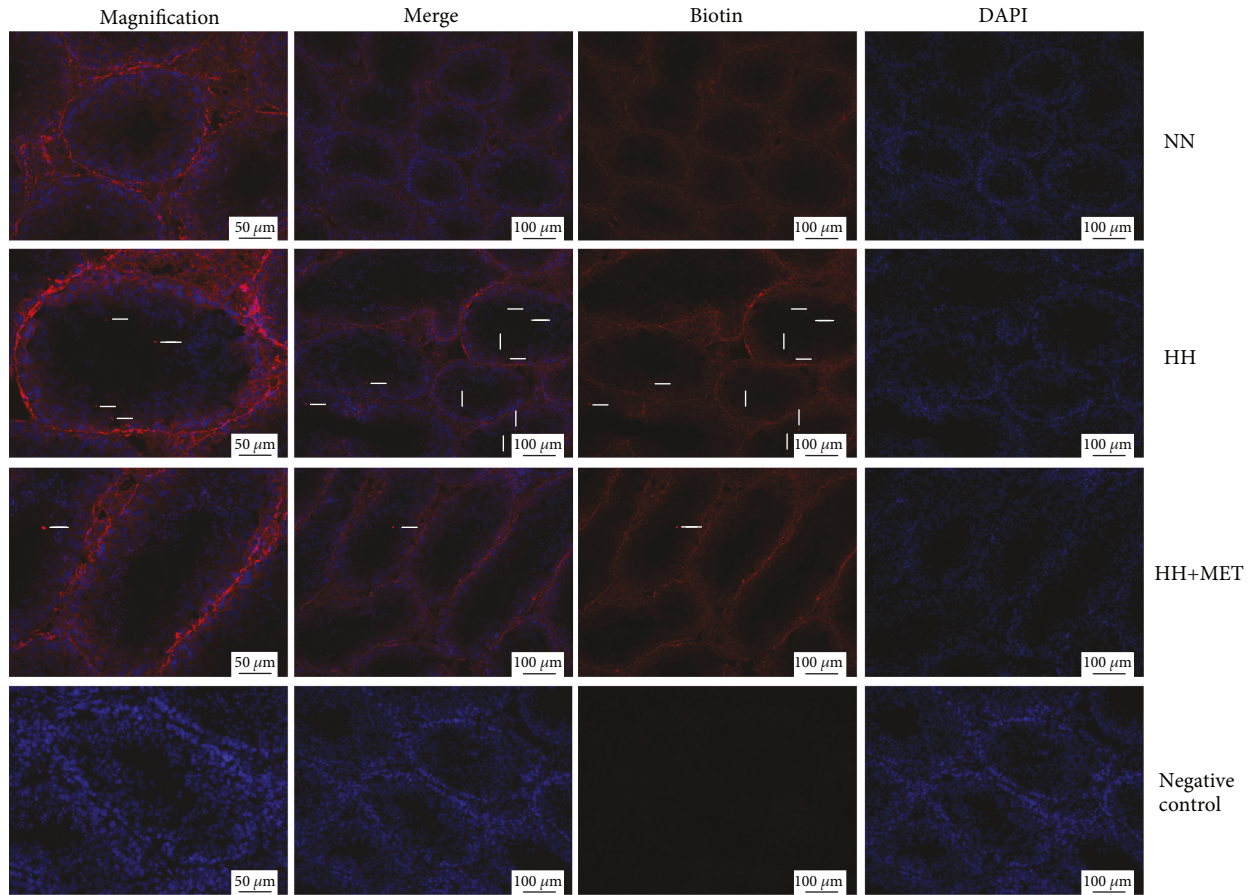
0.45 , $P < 0.01$) (Figure 4(b), HH vs. HH+MET). These results indicated that the integrity of the BTB in the testes of the high-fat-diet-fed mice was indeed disrupted and metformin essentially repaired this disruption.

3.5. Metformin Recovers the Disruption in Junction Protein Expression Induced by a High-Fat Diet. The integrity of the BTB is based on various junction proteins that form coexisting TJs and ectoplasmic specializations. To further verify the damage to the BTB induced by the high-fat diet and the protective effect of metformin, the mRNA and protein levels of BTB-related molecules were detected on the 16th week. Compared with the levels in the testis of the normal-diet group, although there was no significant change in the mRNA levels, TJ integral membrane proteins including ZO-1 and occludin were upregulated significantly in the testis of the high-fat-diet group (ZO-1, 1.11 ± 0.14 vs. 1.53 ± 0.31 , $P < 0.05$; occludin, 1.02 ± 0.13 vs. 1.43 ± 0.13 , $P < 0.05$). Metformin improved the abnormal protein expression of ZO-1 and occludin (ZO-1, 1.53 ± 0.31 vs. 0.88 ± 0.20 , $P < 0.01$; occludin, 1.43 ± 0.13 vs. 1.04 ± 0.30 , $P < 0.05$) (Figures 5(a)–5(c)). These results indicated that the modification of ZO-1 and occludin protein synthesis might be related to the protective effect of metformin on BTB damage induced by a high-fat diet.

In addition to the abnormalities in junction protein expression, the localization of the junction protein on the BTB affects the function of the BTB. To further verify the



(a)



(b)

FIGURE 4: Continued.

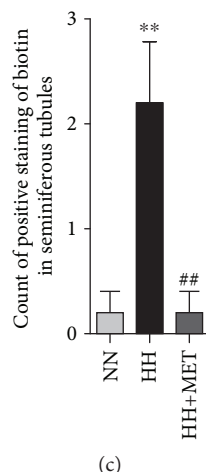


FIGURE 4: Metformin repairs the disruption of BTB integrity induced by a high-fat diet. (a) Transmission electron micrographs of the seminiferous epithelia of mice on the 16th week of feeding; the lower images are magnified views of each of the paired sections above. Red arrowhead 1 shows the cracked BTB between two adjacent Sertoli cells constituted by cellular tight junctions. Red arrowheads 2 and 3 indicate the increase in protein along both sides of the BTB. The red arrows represent expanded endoplasmic reticula. The corresponding scale bar is marked in the lower left corner of each image. $n = 3$ for each group. (b) On the 16th week of feeding, testes were injected with $50 \mu\text{l}$ of EZ-Link Sulfo-NHS-LC-Biotin (red), and cell nuclei were stained with DAPI (blue). In the sections of testes from NN mice, the red fluorescence of the biotin tracer was observed only in the interstitial spaces and basal compartment. In the HH + MET group, a small amount of red fluorescence was seen in the lumina of the seminiferous tubules (white arrow), whereas in the HH group mice, abundant red fluorescence was evident in the lumina of the seminiferous tubules (white arrows) beside the interstitial space and basal compartment. Scale bars = $50 \mu\text{m}$ for the magnified images, and scale bars = $100 \mu\text{m}$ for the other images. $n = 3$ for each group. All of the above micrographs are representative of 3 independent experiments. (c) Count of positive staining of biotin in seminiferous tubules. The results are presented as the mean \pm SD. ** $P < 0.01$ vs. the corresponding NN group; ## $P < 0.01$ vs. the corresponding HH group.

expression and localization of junction proteins on the BTB in testicular SCs, immunofluorescence of ZO-1 was performed. The high-fat diet increased ZO-1 accumulation on the BTB; metformin recovered the increase in ZO-1 on the BTB (Figure 5(d)), which was consistent with testicular ultrastructure and immunoblotting analyses of the testis. However, the localization of ZO-1 on the BTB was unaltered.

3.6. Metformin Suppresses the Oxidative Stress Level in the Testis via Inhibition of NF- κ B/p65 Activity in SC Nuclei. Obesity can increase oxidative stress in the whole body [25], and an increase in testicular oxidative stress is a common feature in much of what underlies male infertility [26]. Therefore, to evaluate whether metformin improves male mouse fertility by alleviating oxidative stress, testicular oxidative stress-related indexes were assessed in each group on the 16th week, and the indexes included MDA, an index of lipid peroxidation and one of the commonly used biomarkers of oxidative stress [38]; SOD, a type of scavenger of oxygen radicals [39] and a type of critical antioxidant enzyme that protects cells from oxidative stress [40]; and ROS, a kind of oxidative stress inducer species. As shown in Figure 6(a), although there was no difference in SOD activity, the fluorescence intensity of ROS was significantly higher in the testes of the high-fat-diet-fed mice than in those of the normal-diet-fed mice (705.3 ± 161.7 vs. 1357 ± 254.8 , $P < 0.05$). In the testes of the oral metformin mice, the fluorescence intensity of ROS

(1357 ± 254.8 vs. 716.1 ± 119.8 , $P < 0.05$) and concentration of MDA (4.81 ± 0.56 vs. 3.04 ± 0.49 , $P < 0.01$) significantly decreased to the normal level. These results indicated that metformin alleviated high-fat-diet-induced excess oxidative stress in the testes.

Oxidative stress leads to inflammation, a process that is most strongly influenced by the level of oxidative stress and mediated primarily by NF- κ B, which is a proinflammatory factor. To further verify whether NF- κ B was involved in the process, the protein in nuclei and mRNA expression levels of NF- κ B/p65 in the testis were assessed. Metformin treatment resulted in a significant decrease of the expression level of NF- κ B/p65 in the whole testis (1.09 ± 0.16 vs. 0.16 ± 0.08 and 1.17 ± 0.12 vs. 0.16 ± 0.08 , $P < 0.05$) (Figures 6(c) and 6(d)). However, high-fat diet and metformin did not affect NF- κ B/p65 mRNA expression in the whole testicular tissue (Figure 6(b)). NF- κ B is normally located in the cytoplasm, and activated NF- κ B localizes to the nucleus. To further represent the level of NF- κ B/p65 in SC nuclei, NF- κ B expression in SC nuclei was detected through an immunofluorescence method using cross-sections of deparaffinized testes. As shown in Figure 6(e), red fluorescence in the SC nuclei represents activated NF- κ B. The greatest abundance of activated NF- κ B in the SC nuclei existed in the high-fat-diet-fed mice, and the abundance in the oral metformin mice was similar to that in the normal-diet-fed mice. These results indicated that metformin reduced the expression of NF- κ B/p65 in the SC nuclei, which might be related to the

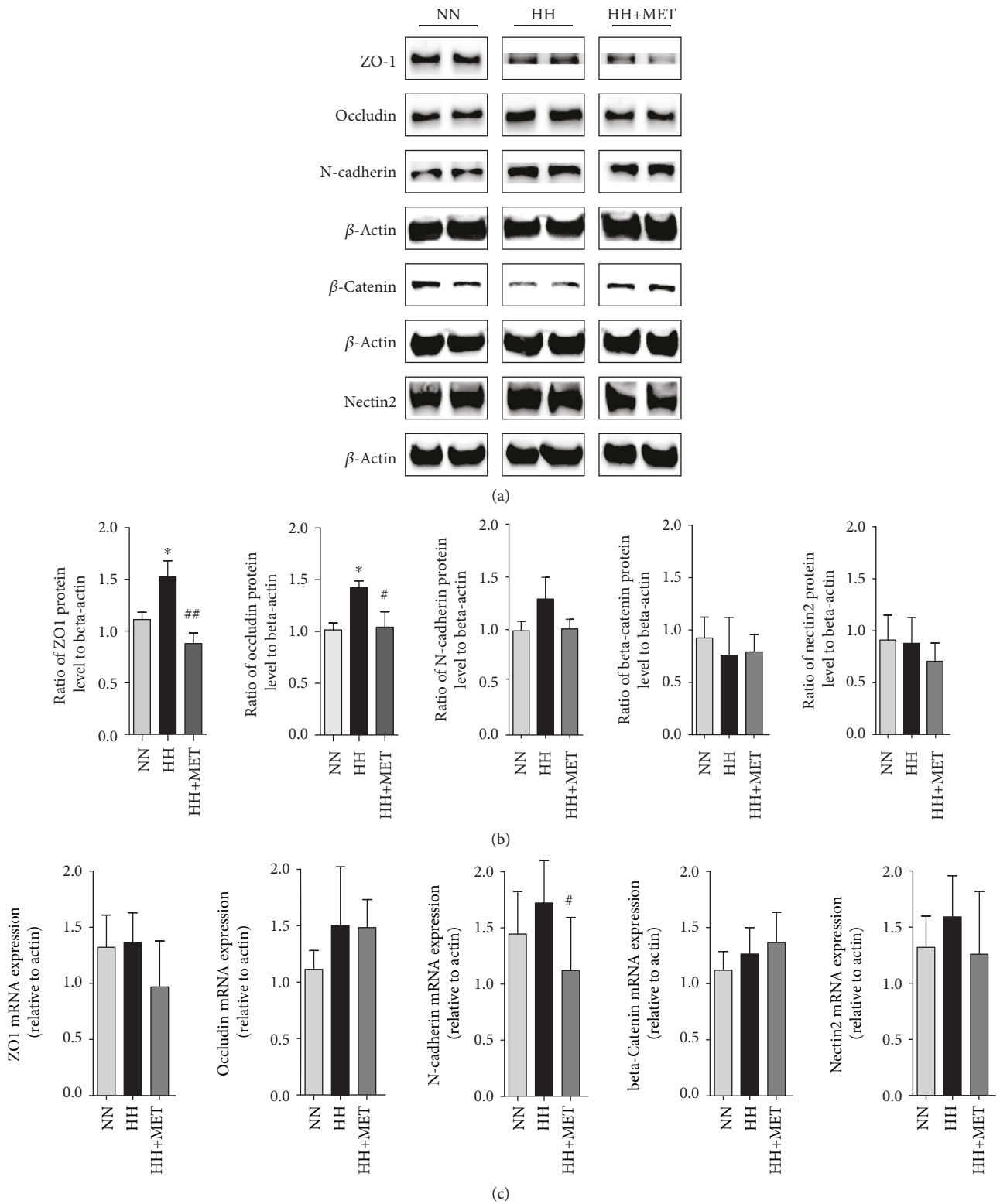


FIGURE 5: Continued.

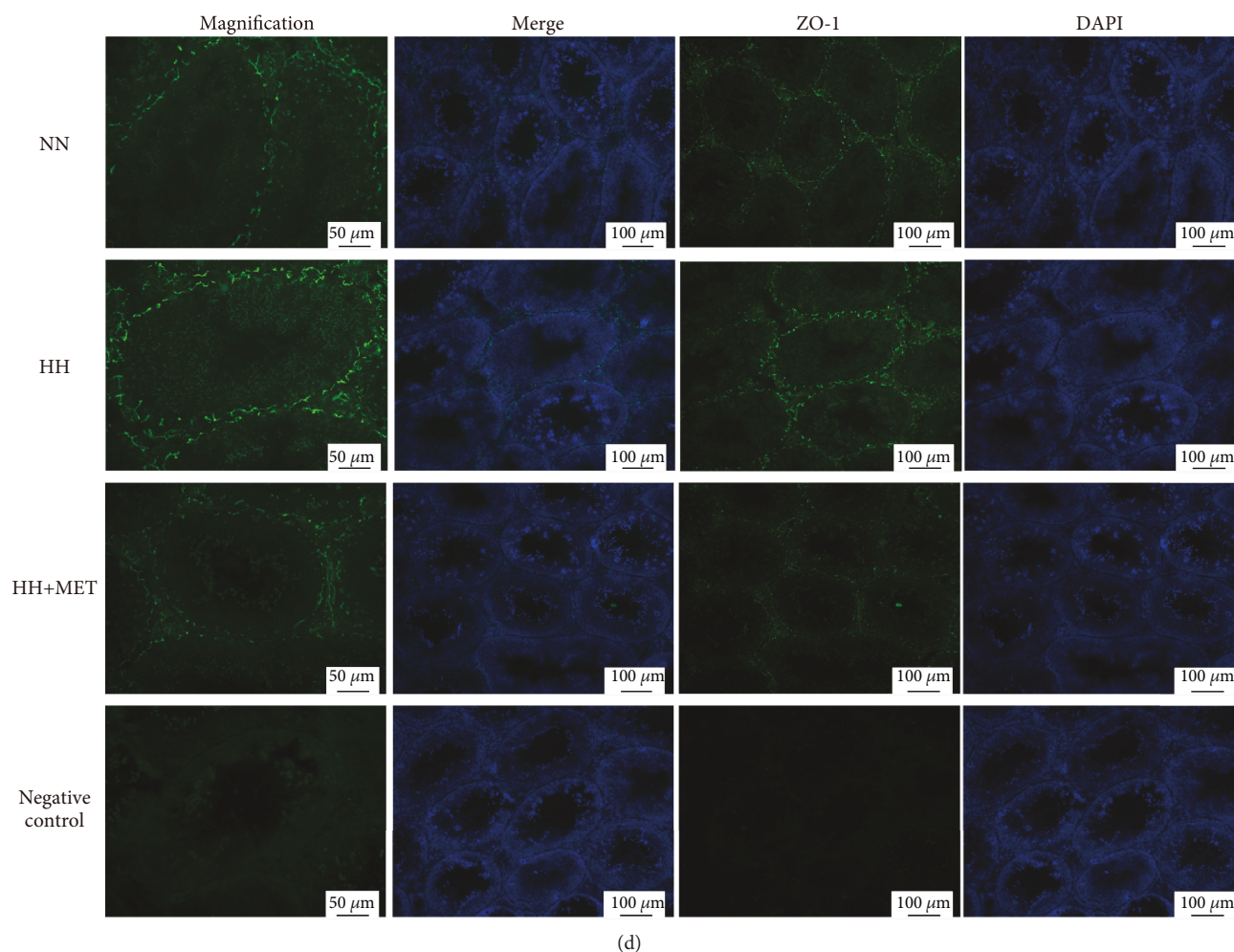


FIGURE 5: Metformin recovers the disordered junction protein expression induced by a high-fat diet. (a) The ZO-1, occludin, N-cadherin, β -catenin, and nectin2 bands in the immunoblotting analysis of the mouse testes. Testis lysates ($120 \mu\text{g}/\text{well}$) were loaded onto gels, electrotransferred onto membranes, and reacted with primary and secondary antibodies; beta-actin was used as the loading control. All gels were run under the same experimental conditions. The lower panel (b) is a densitometric histogram of the protein bands, and the results are expressed as the ratio of the corresponding protein to beta-actin. (c) The mRNA expression of ZO-1, occludin, N-cadherin, β -catenin, and nectin2 in mouse testes; gene expression was normalized to beta-actin. $*P < 0.05$ vs. the corresponding N group; $\#P < 0.05$ and $\#\#P < 0.01$ vs. the corresponding HH group. $n = 3$ for each group. (d) Immunofluorescence micrographs using cross-sections of testes. Green fluorescence represents ZO-1, and blue (DAPI dye) represents the nuclei. Scale bars = $50 \mu\text{m}$ for the magnified images, and scale bars = $100 \mu\text{m}$ for the other images. $n = 3$ for each group. All of the above panels are representative of 3 independent experiments.

reduction in excess oxidative stress in the testes induced by the high-fat diet.

4. Discussion

Obesity, which is associated with male infertility, has increased dramatically worldwide. Metformin, a commonly used hypoglycaemic agent, has been shown to play roles in nondiabetic diseases through antioxidant effects. However, whether metformin can improve the damage to male fertility caused by obesity remains unclear. In this study, by constructing a high-fat-diet-induced obese male mouse model and administering metformin in water, we demonstrated that metformin reduced the high level of oxidative stress in the testis of high-fat-diet-fed obese mice before improvements

in serum glucose and adverse lipids. In addition to the improvements in oxidative stress in the testis, the disrupted expression of junction proteins was ameliorated, the injured structure and integrity of the BTB were amended, and fertility was improved by metformin. These results suggested that metformin improved the reproductive function of obese male mice via an antioxidant effect independently of its regulation of serum glucose and lipids.

Metformin, a widely used medicine for the treatment of type 2 diabetes mellitus, has extensive protective effects on many organs and cells, such as the vessels, heart, brain, and ovaries [41–44]. Moreover, metformin can improve the reproductive function of obese females among patients with PCOS in clinical applications [45]. However, the role of metformin in the male gonads is controversial. An *in vitro* study

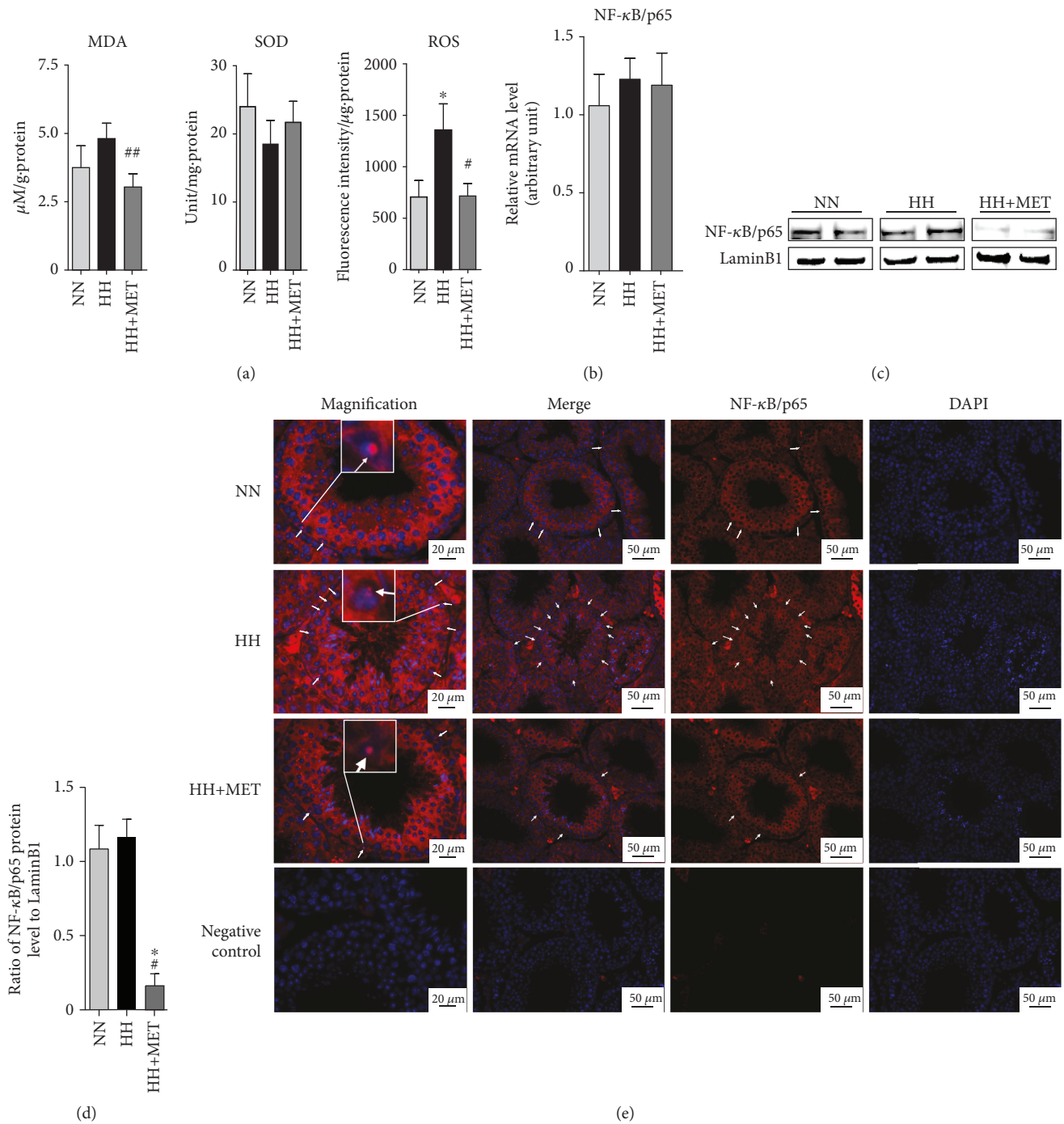


FIGURE 6: Metformin suppresses the oxidative stress level in the testis via inhibition of NF- $\kappa\text{B/p65}$ in SC nuclei. (a) The levels of MDA, SOD, and ROS in each group. All contents and enzyme activities were normalized to the total protein level, which was measured by means of the BCA method. $^*P < 0.05$ vs. the corresponding NN group; $^{\#}P < 0.05$ and $^{##}P < 0.01$ vs. the corresponding HH group. $n = 3$ for each group. (b) The mRNA expression of NF- $\kappa\text{B/p65}$ in mouse testes; gene expression was normalized to beta-actin. $n = 3$ for each group. (c) The NF- $\kappa\text{B/p65}$ bands in the immunoblotting analysis of the mouse testes. Testicular nucleoprotein lysates ($60 \mu\text{g}/\text{well}$) were loaded onto gels, electrotransferred onto membranes and reacted with primary and secondary antibodies; LaminB1 was used as the loading control. $n = 3$ for each group. (d) A densitometric histogram of the NF- $\kappa\text{B/p65}$ protein bands; the results are expressed as the ratio of the corresponding protein to LaminB1. $^*P < 0.05$ vs. the corresponding NN group; $^{##}P < 0.01$ vs. the corresponding HH group. (e) Immunofluorescence micrographs using cross-sections of deparaffinized testes. $n = 3$ for each group. Red fluorescence represents NF- $\kappa\text{B/p65}$, and blue fluorescence (DAPI dye) represents the nuclei. The white arrows represent the positively stained nuclei of Sertoli cells. A nucleus with the colocalization of DAPI and nuclear NF- κB was magnified in $20 \mu\text{m}$ images, which was framed in a white box. Scale bars = $20 \mu\text{m}$ for the magnified images, and scale bars = $50 \mu\text{m}$ for the other images. All of the above bands or micrographs are representative of 3 independent experiments.

has demonstrated that metformin played a beneficial role in energy metabolism in SCs [46]. Furthermore, metformin stimulates alanine production in SCs, inducing antioxidant activity and maintaining the NADH/NAD⁺ equilibrium. However, other studies have reported that metformin might disrupt normal testicular physiological processes, leading to spermatogenic failure [47]. These are indeed crucial results demonstrating the detrimental effects of metformin, which are apparently contradictory to the results presented here. Apart from the experimental methods used, the results of the previous study were obtained from healthy animals with apparently normal serum glucose and lipid metabolism. However, in our study, the effect of metformin was analyzed under hyperlipidaemic and hyperglycaemic conditions during adulthood in mice, which may explain the conflicting results when compared with other research.

The negative impact of obesity on the male genital system is gradually being recognized. Obesity-induced decreases in male fertility have been demonstrated in animal models and clinical investigations, and abnormalities in pituitary-gonadal axis hormones have been demonstrated in morbidly obese men [48, 49]. In our study, the high-fat diet resulted in decreased fertility in obese male mice, and further experiments demonstrated that the decreased fertility was accompanied by abnormalities in lipid metabolism and sex hormones. Apart from dyslipidaemia in obese male mice, ectopic lipid accumulation was abundant in the testicular interstitium, and some of the lipids penetrated the basement membrane and deposited ectopically in the basement compartment of the seminiferous tubules; the structure and integrity of the BTB were destroyed. This result demonstrates that lipotoxicity indeed injured the BTB, and the testis/seminiferous tubules were in a lipotoxic microenvironment. Of note, testicular lipid deposition did not increase testicular weight, which might be due to organ specificity of the testis or high-fat diet for a short period of time. In male peripheral gonads, lipid accumulation mainly deposited in the epididymis and surrounded testis, and a longer-term high-fat diet will be given in further study. Metformin played a substantial role in regulating lipid metabolism, and the 8-week treatment with metformin markedly reduced the ectopic lipid deposition in the testis; however, serum glucose and adverse lipids were not influenced significantly, which might be due to the lower dosage of metformin. Relative to the dose of metformin (200 mg/kg/d) used in this experiment, the dosage for humans suggested in the control of diabetes is 2000 mg/d (body weight = 70 kg); correspondingly, the dosage of metformin that might reduce serum glucose in male mice should be 260 mg/kg/d ($9.1 \times 2000 \text{ mg/d}/70 \text{ kg}$). To further verify this speculation, a higher dosage of metformin will be administered in further study. However, the data also suggest that metformin prioritizes the adjustment of lipid metabolism in the testicular tissue before regulating serum glucose and lipids. In addition to abnormalities in lipid metabolism, changes in gonadotropin levels were also analyzed; FSH, which decreased significantly in the high-fat-diet-fed mice, plays an important role in spermatogenesis via the FSH receptor (FSHR) [50]. With the decline in FSH, fertility decreased and the BTB was impaired in the high-fat-diet-

fed mice. Fertility and the integrity of BTB were recovered with the increase in FSH in the mice-administered metformin. These results indicate that a high-fat diet has a detrimental effect on pituitary gonadotropin FSH, which might also occur via lipotoxicity in the pituitary. Metformin, in addition to directly affecting the peripheral target gonad, can improve reproductive capacity by regulating the centre of the gonadal axis.

Previous studies on the mechanisms of male fertility have mainly focused on sperm parameters, Leydig cells, or reproductive hormones [9, 51–53]. The function of the SCs was overlooked. SCs provide nutrition and BTB support in spermatogenesis. Disrupting BTB integrity harms the reproductive system and results in reproductive dysfunction [19, 54]. As mentioned above, in the high-fat-diet-fed mice, abundant lipids were deposited ectopically in the testicular interstitium, and some lipids were deposited ectopically in the seminiferous tubules, indicating lipotoxicity in the testis or seminiferous tubules. In the high-fat-diet-fed mice, the expression of TJ-related proteins (ZO-1 and occludin) increased significantly, which were basically consistent with the previous studies [55]. Morgan et al. [55] found that the upregulation of ZO-1 and occludin was a compensation for BTB damage. Such changes might be an adaptive change because SCs increasingly synthesize tight-junction proteins and attempt to repair the dehiscent BTB. Disordered junction protein expression leads to injury to the structure and integrity of the BTB. TJ-associated proteins may be the targets of lipotoxicity, and this is consistent with previous studies of the effects of other exogenous stimulators on SC BTB, such as perfluorooctanesulfonate, cadmium, amodiaquine, and bisphenol A [19–22, 24]. In oral metformin mice, lipid accumulation in the testicular interstitium and seminiferous tubules decreased dramatically. In addition, with a concomitant decrease in ectopic lipid deposition, the disordered junction protein expression, damaged structure, and integrity of the BTB were ameliorated, and the decrease in fertility was resolved. These results indicate that metformin can directly regulate testicular lipid metabolism and hence reverse the injury to the BTB, improving decreased fertility.

Metformin has antioxidant properties. Previous studies have demonstrated that metformin can reduce ROS [56] and that, partly by reducing oxidative stress inducer species, metformin can confer health and lifespan benefits to laboratory mice and *C. elegans* [57, 58]. The high-fat-diet-fed mice exhibited decreased reproductive function together with increased ROS. Previous studies have demonstrated that hydrogen peroxide, the most abundant ROS in pathophysiology, can reduce the expression of occludin, a marker TJ protein and a principal target of redox processes, in cultured MDCK-II cells and that O₂⁻ can decrease occludin expression in cultured brain endothelial cells [59]. ROS also modulates the patterns of gene expression through functional alterations to transcription factors, such as NF- κ B [60]. NF- κ B activation is required in TNF- α -downregulated ZO-1 expression in the intestinal TJ barrier [61], and NF- κ B inhibitors (caffeic acid phenethyl ester) can recover the decreased expression of occludin and ZO-1 induced by methotrexate in the intestinal barrier [62]. In other words, NF- κ B is

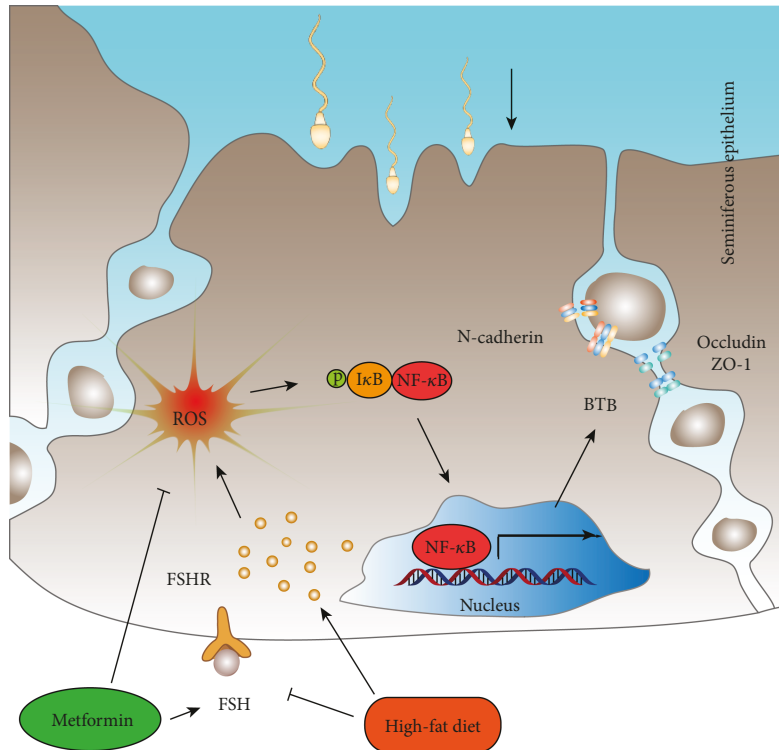


FIGURE 7: Model accounting for the mechanism of the metformin-mediated improvement of fertility in obese male mice. In mice on the high-fat diet, the ectopic deposition of adipose in the testis increases the level of oxidative stress, especially the level of ROS, activating NF- κ B in the cytoplasm, resulting in an increase in NF- κ B in the nuclei of SCs. The latter results in disordered junction protein expression, which leads to the destruction of BTB integrity and then the decline in spermatogenesis and male fertility. Metformin reduces lipid deposition in the testis, relieves oxidative stress in the testis, inhibits excessive activation of NF- κ B in SC nuclei, reverses the destruction of the BTB, and hence improves the reproductive function of male mice. In other words, metformin ameliorates the injury to the reproductive function of obese male mice via the ROS-NF- κ B pathway. In addition, FSH is decreased in high-fat-diet-fed male mice, and metformin increases the level of FSH in obese male mice, which might play a role in the process of the metformin-mediated improvement of fertility in obese male mice.

involved in the regulation of the expression of TJ-related proteins in other blood-tissue barriers and may regulate the expression of BTB-related proteins. Likewise, our data demonstrate that the level of ROS is significantly higher in high-fat-diet-fed mice than in normal-diet-fed mice and that NF- κ B is activated abundantly in high-fat-diet-fed mice compared with normal-diet-fed mice. Thus, the activated ROS-NF- κ B signalling pathway might be a contributor to high-fat-diet-induced BTB damage. Inhibition of NF- κ B signalling represents a viable strategy for disease therapy [63]. The levels of ROS and the abundance of activated NF- κ B/p65 in SC nuclei were significantly lower in the mice administered metformin than in the high-fat-diet-fed mice. This indicates that treatment with metformin reduces ROS levels, inhibits the activity of NF- κ B in SC nuclei, likely ameliorates lipotoxicity-induced disruption of BTB-associated proteins, and further repairs the structure and integrity of the BTB, upregulating the decrease in the fertility of obese male mice. All of these observations point towards crosstalk between an ROS-NF- κ B mediator and the intervening role of metformin in determining BTB function in a testicular fat ectopic accumulation microenvironment. The studies performed by Bonnefont-Rousselot et al. [64] and Esteghamati et al. [65] demonstrated that metformin

has a remarkable effect on oxidative stress. Our study further demonstrated that metformin inhibits the activity of NF- κ B in the SC nuclei of obese male mice and hence exerts a beneficial effect on the BTB.

5. Conclusion

In summary, the results of this study confirm that a high-fat diet causes abnormalities in glucose and lipid metabolism and serum FSH, increases oxidative stress, and disrupts BTB integrity in the testis, harming the reproductive system. Treatment with metformin decreases ectopic lipid accumulation in the testis, reduces the levels of oxidative stress, ameliorates the high-fat-diet-induced injury to the BTB, and improves fertility in obese male mice. The ROS-NF- κ B pathway may be a mechanism of metformin in this protective process (a diagram is shown in Figure 7). However, the mechanism of metformin is highly complex, and further studies are needed, including an examination of the mechanism underlying the effects of metformin on pituitary gonadotropin FSH and NF- κ B signalling. These results are important evidence of the beneficial effects of metformin on infertility in obese males and provide an effective treatment option for male infertility in obese men. Clinical trials will

be analyzed to further confirm the beneficial effects of metformin on the fertility of obese men.

Abbreviations

FSH:	Follicle-stimulating hormone
BTB:	Blood-testis barrier
MDA:	Malondialdehyde
SOD:	Superoxide dismutase
ROS:	Reactive oxygen species
NF- κ B:	Nuclear factor κ B
SCs:	Sertoli cells
BMI:	Body mass index
TJs:	Tight junctions
Basal ESs:	Basal ectoplasmic specializations
PCOS:	Polycystic ovarian syndrome
MDF:	Modified Davidson's fluid
TC:	Total cholesterol
TG:	Triglycerides
HDL-c:	High-density lipoprotein-cholesterol
LDL-c:	Low-density lipoprotein-cholesterol
Glu:	Glucose
H&E:	Haematoxylin and eosin
TEM:	Testicular transmission electron microscopy
PFA:	Paraformaldehyde
PBST:	Phosphate-buffered saline with 0.1% Tween20
PBS:	Phosphate buffer solution
BSA:	Bovine serum albumin
DAPI:	4'-6-Diamidino-2-phenylindole
HRP:	Horseradish peroxidase
PCR:	Polymerase chain reaction
ER:	Endoplasmic reticulum
FSHR:	FSH receptor

Data Availability

The data used to support the findings of this study are included within the article.

Conflicts of Interest

The authors have no conflicts of interest to declare.

Authors' Contributions

The work presented here was conducted in collaboration with all authors. Jifeng Ye performed the experiments and wrote the main manuscript. Mingqi Sun and Dandan Luo prepared the animals. Xiaolin Xu and Xiaohui Su detected the serum parameters. Zhenhua Tian and Meijie Zhang assisted in sorting out information. Chunxiao Yu designed the experiments and wrote the main manuscript. Qingbo Guan designed the experiments. All authors reviewed the manuscript.

Acknowledgments

This work was supported by grants from the National Natural Science Foundation (81770860, 81471078, and 81641030) and the Key Research and Development Plan of Shandong Province (2016GSF201007).

Supplementary Materials

Figure S1: the flowchart of the animal experiments. One week after feeding to adapt to the housing conditions, the male mice were randomly divided into two groups: the normal-diet group (N, $n = 20$) was fed a standard diet, and the high-fat-diet group (H, $n = 30$) was fed a high-fat diet. Ten mice from each group were sacrificed at the end of the 8th week of feeding. The remaining mice in the N group were maintained on their standard diet (NN, $n = 10$), whereas the mice fed a high-fat diet ($n = 20$) were further subdivided into two subgroups. The first subgroup (HH, $n = 10$) was maintained on the high-fat diet, and the second subgroup (HH + MET, $n = 10$) was maintained on the high-fat diet with ~ 200 mg/kg body weight/day metformin given in the drinking water. (*Supplementary Materials*)

References

- [1] World Health Organization, "Obesity and overweight," 2017, Fact sheet no. 311 <http://www.who.int/mediacentre/factsheets/fs311/en/>.
- [2] R. de Mutsert, Q. Sun, W. C. Willett, F. B. Hu, and R. M. van Dam, "Overweight in early adulthood, adult weight change, and risk of type 2 diabetes, cardiovascular diseases, and certain cancers in men: a cohort study," *American Journal of Epidemiology*, vol. 179, no. 11, pp. 1353–1365, 2014.
- [3] I. Ponce-Garcia, M. Simarro-Rueda, J. A. Carbayo-Herencia et al., "Prognostic value of obesity on both overall mortality and cardiovascular disease in the general population," *PLoS One*, vol. 10, no. 5, article e0127369, 2015.
- [4] T. J. Kim, H. Y. Shin, Y. Chang et al., "Metabolically healthy obesity and the risk for subclinical atherosclerosis," *Atherosclerosis*, vol. 262, pp. 191–197, 2017.
- [5] E. M. Cespedes Feliciano, C. H. Kroenke, J. A. Meyerhardt et al., "Metabolic dysfunction, obesity, and survival among patients with early-stage colorectal cancer," *Journal of Clinical Oncology*, vol. 34, no. 30, pp. 3664–3671, 2016.
- [6] J. M. Genkinger, C. M. Kitahara, L. Bernstein et al., "Central adiposity, obesity during early adulthood, and pancreatic cancer mortality in a pooled analysis of cohort studies," *Annals of Oncology*, vol. 26, no. 11, pp. 2257–2266, 2015.
- [7] C. Dupont, C. Faure, N. Sermondade et al., "Obesity leads to higher risk of sperm DNA damage in infertile patients," *Asian Journal of Andrology*, vol. 15, no. 5, pp. 622–625, 2013.
- [8] N. Sermondade, C. Faure, L. Fezeu et al., "BMI in relation to sperm count: an updated systematic review and collaborative meta-analysis," *Human Reproduction Update*, vol. 19, no. 3, pp. 221–231, 2013.
- [9] J. Samavat, I. Natali, S. Degl'Innocenti et al., "Acrosome reaction is impaired in spermatozoa of obese men: a preliminary study," *Fertility and Sterility*, vol. 102, no. 5, pp. 1274–1281.e2, 2014.
- [10] A. Soubry, L. Guo, Z. Huang et al., "Obesity-related DNA methylation at imprinted genes in human sperm: results from the TIEGER study," *Clinical Epigenetics*, vol. 8, no. 1, p. 51, 2016.
- [11] H. W. Bakos, M. Mitchell, B. P. Setchell, and M. Lane, "The effect of paternal diet-induced obesity on sperm function and fertilization in a mouse model," *International Journal of Andrology*, vol. 34, 5, part 1, pp. 402–410, 2011.

- [12] C. D. B. Fernandez, F. F. Bellentani, G. S. A. Fernandes et al., "Diet-induced obesity in rats leads to a decrease in sperm motility," *Reproductive Biology and Endocrinology*, vol. 9, no. 1, p. 32, 2011.
- [13] N. O. Palmer, H. W. Bakos, J. A. Owens, B. P. Setchell, and M. Lane, "Diet and exercise in an obese mouse fed a high-fat diet improve metabolic health and reverse perturbed sperm function," *American Journal of Physiology-Endocrinology and Metabolism*, vol. 302, no. 7, pp. E768–E780, 2012.
- [14] W. Y. Liu, Z. B. Wang, L. C. Zhang, X. Wei, and L. Li, "Tight junction in blood-brain barrier: an overview of structure, regulation, and regulator substances," *CNS Neuroscience & Therapeutics*, vol. 18, no. 8, pp. 609–615, 2012.
- [15] D. Günzel and A. S. L. Yu, "Claudins and the modulation of tight junction permeability," *Physiological Reviews*, vol. 93, no. 2, pp. 525–569, 2013.
- [16] E. A. Runkle and D. Mu, "Tight junction proteins: from barrier to tumorigenesis," *Cancer Letters*, vol. 337, no. 1, pp. 41–48, 2013.
- [17] P. T. K. Saunders, "Germ cell-somatic cell interactions during spermatogenesis," *Reproduction Supplement*, vol. 61, pp. 91–101, 2003.
- [18] M. G. Alves, A. D. Martins, J. E. Cavaco, S. Socorro, and P. F. Oliveira, "Diabetes, insulin-mediated glucose metabolism and Sertoli/blood-testis barrier function," *Tissue Barriers*, vol. 1, no. 2, article e23992, 2013.
- [19] Y. Lu, B. Luo, J. Li, and J. Dai, "Perfluorooctanoic acid disrupts the blood-testis barrier and activates the TNF α /p38 MAPK signaling pathway in vivo and in vitro," *Archives of Toxicology*, vol. 90, no. 4, pp. 971–983, 2016.
- [20] C. de Angelis, M. Galdiero, C. Pivonello et al., "The environment and male reproduction: the effect of cadmium exposure on reproductive function and its implication in fertility," *Reproductive Toxicology*, vol. 73, pp. 105–127, 2017.
- [21] D. D. Mruk and C. Y. Cheng, "Environmental contaminants: is male reproductive health at risk?," *Spermatogenesis*, vol. 1, no. 4, pp. 283–290, 2011.
- [22] Y. R. Niu, B. Wei, B. Chen et al., "Amodiaquine-induced reproductive toxicity in adult male rats," *Molecular Reproduction and Development*, vol. 83, no. 2, pp. 174–182, 2016.
- [23] C. Y. Cheng and D. D. Mruk, "The blood-testis barrier and its implications for male contraception," *Pharmacological Reviews*, vol. 64, no. 1, pp. 16–64, 2012.
- [24] A. T. A. G. de Freitas, M. A. Ribeiro, C. F. Pinho, A. R. Peixoto, R. F. Domeniconi, and W. R. Scarano, "Regulatory and junctional proteins of the blood-testis barrier in human Sertoli cells are modified by monobutyl phthalate (MBP) and bisphenol A (BPA) exposure," *Toxicology In Vitro*, vol. 34, pp. 1–7, 2016.
- [25] A. Munoz and M. Costa, "Nutritionally mediated oxidative stress and inflammation," *Oxidative Medicine and Cellular Longevity*, vol. 2013, Article ID 610950, 11 pages, 2013.
- [26] T. T. Turner and J. J. Lysiak, "Oxidative stress: a common factor in testicular dysfunction," *Journal of Andrology*, vol. 29, no. 5, pp. 488–498, 2008.
- [27] P. Faure, E. Rossini, N. Wiernsperger, M. J. Richard, A. Favier, and S. Halimi, "An insulin sensitizer improves the free radical defense system potential and insulin sensitivity in high fructose-fed rats," *Diabetes*, vol. 48, no. 2, pp. 353–357, 1999.
- [28] G. Kanigür-Sultuybek, M. Güven, İ. Onaran, V. Tezcan, A. Cenani, and H. Hatemi, "The effect of metformin on insulin receptors and lipid peroxidation in alloxan and streptozotocin induced diabetes," *Journal of Basic and Clinical Physiology and Pharmacology*, vol. 6, no. 3-4, pp. 271–280, 1995.
- [29] E. Bosman, A. D. Esterhuizen, F. A. Rodrigues, P. J. Becker, and W. A. Hoffmann, "Effect of metformin therapy and dietary supplements on semen parameters in hyperinsulinaemic males," *Andrologia*, vol. 47, no. 9, pp. 974–979, 2015.
- [30] B. K. Tan, R. Adya, J. Chen et al., "Metformin decreases angiogenesis via NF- κ B and Erk1/2/Erk5 pathways by increasing the antiangiogenic thrombospondin-1," *Cardiovascular Research*, vol. 83, no. 3, pp. 566–574, 2009.
- [31] Y. Wu, F. Wang, M. Fu, C. Wang, M. J. Quon, and P. Yang, "Cellular stress, excessive apoptosis, and the effect of metformin in a mouse model of type 2 diabetic embryopathy," *Diabetes*, vol. 64, no. 7, pp. 2526–2536, 2015.
- [32] J. R. Latendresse, A. R. Warbritton, H. Jonassen, and D. M. Creasy, "Fixation of testes and eyes using a modified Davidson's fluid: comparison with Bouin's fluid and conventional Davidson's fluid," *Toxicologic Pathology*, vol. 30, no. 4, pp. 524–533, 2002.
- [33] B. K. Kit, M. D. Carroll, D. A. Lacher, P. D. Sorlie, J. M. DeJesus, and C. Ogden, "Trends in serum lipids among US youths aged 6 to 19 years, 1988–2010," *JAMA*, vol. 308, no. 6, pp. 591–600, 2012.
- [34] T. J. Anderson, G. B. J. Mancini, J. Genest Jr., J. Grégoire, E. M. Lonn, and R. A. Hegele, "The new dyslipidemia guidelines: what is the debate?," *The Canadian Journal of Cardiology*, vol. 31, no. 5, pp. 605–612, 2015.
- [35] S. C. Bain, M. Feher, D. Russell-Jones, and K. Khunti, "Management of type 2 diabetes: the current situation and key opportunities to improve care in the UK," *Diabetes, Obesity & Metabolism*, vol. 18, no. 12, pp. 1157–1166, 2016.
- [36] F. Yuan, H. Dong, K. Fang, J. Gong, and F. Lu, "Effects of green tea on lipid metabolism in overweight or obese people: a meta-analysis of randomized controlled trials," *Molecular Nutrition & Food Research*, vol. 62, no. 1, 2018.
- [37] S. Aijaz, M. S. Balda, and K. Matter, "Tight junctions: molecular architecture and function," *International Review of Cytology*, vol. 248, pp. 261–298, 2006.
- [38] D. Tsikas, S. Rothmann, J. Y. Schneider et al., "Development, validation and biomedical applications of stable-isotope dilution GC-MS and GC-MS/MS techniques for circulating malondialdehyde (MDA) after pentafluorobenzyl bromide derivatization: MDA as a biomarker of oxidative stress and its relation to 15(S)-8-iso-prostaglandin F $_{2\alpha}$ and nitric oxide (\cdot NO)," *Journal of Chromatography B*, vol. 1019, pp. 95–111, 2016.
- [39] W. Droge, "Free radicals in the physiological control of cell function," *Physiological Reviews*, vol. 82, no. 1, pp. 47–95, 2002.
- [40] V. N. Reddy, E. Kasahara, M. Hiraoka, L. R. Lin, and Y. S. Ho, "Effects of variation in superoxide dismutases (SOD) on oxidative stress and apoptosis in lens epithelium," *Experimental Eye Research*, vol. 79, no. 6, pp. 859–868, 2004.
- [41] C. M. Sena, P. Matafome, T. Louro, E. Nunes, R. Fernandes, and R. M. Seica, "Metformin restores endothelial function in aorta of diabetic rats," *British Journal of Pharmacology*, vol. 163, no. 2, pp. 424–437, 2011.
- [42] H. Sasaki, H. Asanuma, M. Fujita et al., "Metformin prevents progression of heart failure in dogs: role of AMP-activated protein kinase," *Circulation*, vol. 119, no. 19, pp. 2568–2577, 2009.

- [43] R. R. Zhao, X. C. Xu, F. Xu et al., "Metformin protects against seizures, learning and memory impairments and oxidative damage induced by pentylentetrazole-induced kindling in mice," *Biochemical and Biophysical Research Communications*, vol. 448, no. 4, pp. 414–417, 2014.
- [44] H. Sova, U. Puistola, L. Morin-Papunen, and P. Karihtala, "Metformin decreases serum 8-hydroxy-2'-deoxyguanosine levels in polycystic ovary syndrome," *Fertility and Sterility*, vol. 99, no. 2, pp. 593–598, 2013.
- [45] J. M. Lord, I. H. K. Flight, and R. J. Norman, "Metformin in polycystic ovary syndrome: systematic review and meta-analysis," *BMJ*, vol. 327, no. 7421, p. 951, 2003.
- [46] M. G. Alves, A. D. Martins, C. V. Vaz et al., "Metformin and male reproduction: effects on Sertoli cell metabolism," *British Journal of Pharmacology*, vol. 171, no. 4, pp. 1033–1042, 2014.
- [47] O. Adaramoye, O. Akanni, O. Adesanoye, O. Labo-Popoola, and O. Olaremi, "Evaluation of toxic effects of metformin hydrochloride and glibenclamide on some organs of male rats," *Nigerian Journal of Physiological Sciences*, vol. 27, no. 2, pp. 137–144, 2012.
- [48] G. W. Strain, B. Zumoff, J. Kream et al., "Mild hypogonadotropic hypogonadism in obese men," *Metabolism*, vol. 31, no. 9, pp. 871–875, 1982.
- [49] S. Pellitero, I. Olaizola, A. Alastrue et al., "Hypogonadotropic hypogonadism in morbidly obese males is reversed after bariatric surgery," *Obesity Surgery*, vol. 22, no. 12, pp. 1835–1842, 2012.
- [50] H. Krishnamurthy, N. Danilovich, C. R. Morales, and M. R. Sairam, "Qualitative and quantitative decline in spermatogenesis of the follicle-stimulating hormone receptor knockout (FORKO) mouse," *Biology of Reproduction*, vol. 62, no. 5, pp. 1146–1159, 2000.
- [51] D. Guo, W. Wu, Q. Tang et al., "The impact of BMI on sperm parameters and the metabolite changes of seminal plasma concomitantly," *Oncotarget*, vol. 8, no. 30, pp. 48619–48634, 2017.
- [52] S. S. du Plessis, S. Cabler, D. A. McAlister, E. Sabanegh, and A. Agarwal, "The effect of obesity on sperm disorders and male infertility," *Nature Reviews Urology*, vol. 7, no. 3, pp. 153–161, 2010.
- [53] J. Zhao, L. Zhai, Z. Liu, S. Wu, and L. Xu, "Leptin level and oxidative stress contribute to obesity-induced low testosterone in murine testicular tissue," *Oxidative Medicine and Cellular Longevity*, vol. 2014, Article ID 190945, 14 pages, 2014.
- [54] Y. Fan, Y. Liu, K. Xue et al., "Diet-induced obesity in male C57BL/6 mice decreases fertility as a consequence of disrupted blood-testis barrier," *PLoS One*, vol. 10, no. 4, article e0120775, 2015.
- [55] D. H. Morgan, O. Ghribi, L. Hui, J. D. Geiger, and X. Chen, "Cholesterol-enriched diet disrupts the blood-testis barrier in rabbits," *American Journal of Physiology-Endocrinology and Metabolism*, vol. 307, no. 12, pp. E1125–E1130, 2014.
- [56] C. Algire, O. Moiseeva, X. Deschenes-Simard et al., "Metformin reduces endogenous reactive oxygen species and associated DNA damage," *Cancer Prevention Research*, vol. 5, no. 4, pp. 536–543, 2012.
- [57] A. Martin-Montalvo, E. M. Mercken, S. J. Mitchell et al., "Metformin improves healthspan and lifespan in mice," *Nature Communications*, vol. 4, no. 1, article 2192, 2013.
- [58] B. Onken and M. Driscoll, "Metformin induces a dietary restriction-like state and the oxidative stress response to extend *C. elegans* healthspan via AMPK, LKB1, and SKN-1," *PLoS One*, vol. 5, no. 1, article e8758, 2010.
- [59] I. E. Blasig, C. Bellmann, J. Cording et al., "Occludin protein family: oxidative stress and reducing conditions," *Antioxidants & Redox Signaling*, vol. 15, no. 5, pp. 1195–1219, 2011.
- [60] R. van den Berg, G. R. M. M. Haenen, H. van den Berg, and A. Bast, "Transcription factor NF- κ B as a potential biomarker for oxidative stress," *The British Journal of Nutrition*, vol. 86, Supplement 1, pp. S121–S127, 2001.
- [61] T. Y. Ma, G. K. Iwamoto, N. T. Hoa et al., "TNF- α -induced increase in intestinal epithelial tight junction permeability requires NF- κ B activation," *American Journal of Physiology-Gastrointestinal and Liver Physiology*, vol. 286, no. 3, pp. G367–G376, 2004.
- [62] S. Beutheu Youmba, L. Belmonte, L. Galas et al., "Methotrexate modulates tight junctions through NF- κ B, MEK, and JNK pathways," *Journal of Pediatric Gastroenterology and Nutrition*, vol. 54, no. 4, pp. 463–470, 2012.
- [63] T. D. Gilmore and M. R. Garbati, "Inhibition of NF- κ B signaling as a strategy in disease therapy," *Current Topics in Microbiology and Immunology*, vol. 349, pp. 245–263, 2011.
- [64] D. Bonnefont-Rousselot, B. Raji, S. Walrand et al., "An intracellular modulation of free radical production could contribute to the beneficial effects of metformin towards oxidative stress," *Metabolism*, vol. 52, no. 5, pp. 586–589, 2003.
- [65] A. Esteghamati, D. Eskandari, H. Mirmiranpour et al., "Effects of metformin on markers of oxidative stress and antioxidant reserve in patients with newly diagnosed type 2 diabetes: a randomized clinical trial," *Clinical Nutrition*, vol. 32, no. 2, pp. 179–185, 2013.

Review Article

New Insights into the Process of Placentation and the Role of Oxidative Uterine Microenvironment

Sara Mendes ^{1,2}, Filipa Timóteo-Ferreira ^{1,2}, Henrique Almeida ^{1,2,3}
and Elisabete Silva ^{1,2}

¹Ageing and Stress Group, IBMC (Instituto de Biologia Molecular e Celular), I3S (Instituto de Investigação e Inovação em Saúde), Universidade do Porto, Rua Alfredo Allen 208, 4200-135 Porto, Portugal

²Unidade de Biologia Experimental, Departamento de Biomedicina, Faculdade de Medicina, Universidade do Porto, Alameda Professor Hernâni Monteiro, 4200-319 Porto, Portugal

³Ginecologia-Obstetrícia, Hospital-CUF Porto, Estrada da Circunvalação 14341, 4100 180 Porto, Portugal

Correspondence should be addressed to Elisabete Silva; elisabete.silva@i3s.up.pt

Received 22 February 2019; Accepted 28 May 2019; Published 25 June 2019

Academic Editor: José L. Quiles

Copyright © 2019 Sara Mendes et al. This is an open access article distributed under the Creative Commons Attribution License, which permits unrestricted use, distribution, and reproduction in any medium, provided the original work is properly cited.

For a successful pregnancy to occur, a predecidualized receptive endometrium must be invaded by placental differentiated cells (extravillous trophoblast cells (EVTs)) and, at the same time, continue decidualization. EVT invasion is aimed at anchoring the placenta to the maternal uterus and ensuring local blood supply increase necessary to provide normal placental and foetal development. The first is achieved by migrating through the maternal endometrium and deeper into the myometrium, while the second by transforming uterine spiral arteries into large vessels. This process is a tightly regulated battle comprising interests of both the mother and the foetus. Invading EVTs are required to perform a scope of functions: move, adhere, proliferate, differentiate, interact, and digest the extracellular matrix (ECM); tolerate hypoxia; transform the maternal spiral arteries; and die by apoptosis. All these functions are modulated by their surrounding microenvironment: oxygen, soluble factors (e.g., cytokines, growth factors, and hormones), ECM proteins, and reactive oxygen species. A deeper comprehension of oxidative uterine microenvironment contribution to trophoblast function will be addressed in this review.

1. Introduction

Successful pregnancy depends on sequential and discrete events that include fertilization, implantation, decidualization, placentation, and birth. Placentation is the process of formation and development of the placenta and the associated modifications in maternal tissue. Its continued interaction character, involving two distinct genomes, suggests the presence of a fine-tuned regulation. In human placenta development, three structural regions are considered: the foetal placenta, with separated foetal and maternal blood, where physiological exchange of nutrients and waste products occurs; the basal plate, which borders the maternal surface and is crossed by maternal vessels; and the placental bed formed by maternal uterine tissue, comprising the modified endometrium (decidua) and is traversed by 100-150 mater-

nal spiral arteries that supply nutrients and oxygen (O₂) to the placenta and the foetus [1].

For a healthy pregnancy to proceed, a good anchoring of placental features and the transformation of maternal spiral arteries (SA) into flaccid capacitance vessels, that will ensure adequate blood supply to the foetus, are necessary. In normal pregnancy, such changes require important extravillous trophoblast cell (EVT) movement from the placental villi across the decidua and deep into the adjacent myometrium. In addition, appropriate invasion of maternal SA and their resulting remodelling underlies functional circulatory change establishment [2]. In contrast, deficient EVT invasion has been associated with insufficient SA remodelling, altered uteroplacental hemodynamics, overall placenta bed dysfunction, and the establishment of serious pregnancy complications [3]. In fact, an early defective development of the placental bed, and

consequent altered placentation, appears to contribute to late pregnancy complications such as preeclampsia, placental abruption, and intrauterine growth restriction (IUGR) [1, 2].

EVT invasion regulation and the molecular mechanisms underlying SA remodelling are the result of a complex network involving soluble factors and different cell types residing in the maternal placental bed. Emerging work indicates that an abnormal placentation is consequent to aberrant uterine microenvironment, already present before or at the time of blastocyst implantation [4–7]. This review will address uterine regulators of EVT dynamics with a special focus on reactive oxygen species (ROS) physiological and pathophysiological roles.

2. Pre(decidualization)

In many species, uterine changes aiming to create a suitable microenvironment for embryo implantation and development occur only after implantation. In humans, early changes may be recognized after ovulation and are designated predecidualization [8]. In the uterine stroma adjacent to SA, and in response to rising progesterone levels, fibroblast-like mesenchymal cells differentiate into an epithelioid structure. In addition, they accumulate cytoplasmic glycogen and lipids and secrete new products as components of extracellular matrix (ECM), protease inhibitors, cytokines, hormones, and other peptides. If implantation takes place, they will provide nutrition to the developing conceptus [9].

Progesterone-dependent differentiation of stroma cells is crucial for epithelium receptiveness and trophoblast-endometrium interactions. In fact, trophoblast spheroid attachment and growth in a coculture of endometrial epithelial cells and primary stromal cells were increased when stromal cells had been collected during the window of implantation time, not before [10].

Predecidualization also plays an important role in uterine natural killer (uNK) cell influx. In humans, they are recruited during predecidualization, and their increase peaks during the first trimester and diminishes thereafter, due to apoptosis. When compared with circulating NK cells, uNK cells have distinct features and functions. They are less cytotoxic and produce signalling molecules such as cytokines (e.g., tumour necrosis factor alpha (TNF- α) and interleukin- (IL-) 10 and 1 β), growth factors (e.g., tissue growth factor beta (TGF- β) and placental growth factor (PlGF)), angiogenic factors (e.g., vascular endothelial growth factor (VEGF)), and matrix metalloproteinases (MMPs) [11]. Moreover, they contribute to decidual angiogenesis regulation and SA remodelling and control EVT invasion [12].

3. Implantation and Early Placentation

Upon fertilization, the ovum travels in the fallopian tube where following several mitotic divisions, it reaches the morula stage (a compact mass of 12–16 cells). Continuing to divide, while receiving nutrients from the uterine environment, it attains approximately 100 cells that surround a fluid-filled cavity, where conceptus-derived secretions concentrate, characterizing the blastocyst stage [13]. During this

stage, asymmetric cell divisions give rise to two distinct populations: the outer blastocyst encircling trophoblast cells, which will originate both the placenta and the extraembryonic membranes, and the totipotent inner cell mass, which will develop into the embryo [14]. Between the 5th and the 6th day post fertilization, the blastocyst contacts with the uterine wall (apposition), attaches to the epithelium, and invades the receptive decidua to implant [15, 16] (Figure 1).

After implantation, trophoblasts that face directly the maternal tissue differentiate and fuse to form the syncytiotrophoblast, whereas those remaining behind, untouched by maternal tissue, do not fuse and are denominated cytotrophoblasts [17, 18] (Figure 1). They act as a rapidly dividing stem cell pool that feeds and fuses with the multinucleated syncytiotrophoblast and promotes its continuous growth. Soon, it will surround most of the blastocyst and, with an invasive phenotype, will penetrate deep into the uterine cavity lining. Within the syncytium, fluid-filled spaces coalesce and rearrange into lacunae, which are the primitive intervillous spaces in the placenta, where the maternal blood will circulate [19, 20].

While invasion evolves, columns of the syncytiotrophoblast masses establish a network around the lacunae to form trabeculae, very important for the remaining development of the villous tree. Subsequently, cytotrophoblast cells proliferate and invade through the trabeculae, until they reach their tips and contact with the decidua. Following their lateral spreading from the tips, they form a coating between the syncytiotrophoblast mantle and the maternal endometrium [21]. Therefore, at this stage, the blastocyst exhibits three different layers of trophoblastic covering: (1) the primary/early chorionic plate, which faces the embryo; (2) the lacunar system and trabeculae, which develops into the intervillous space and villous tree, respectively; and (3) the cytotrophoblastic shell or primitive basal plate, which contacts directly with the endometrium [21].

The cells from the cytotrophoblastic shell possess a distinct phenotype, as they exhibit a round outline structure and large amounts of glycogen. Those localized at the tips of villi differentiate into EVTs, leave the shell, and migrate across the endometrium, initiating the process of EVT invasion [22]. A batch of EVTs is responsible for SA remodelling: they disrupt the vascular smooth cell layer and replace the endothelium, converting muscular wall arteries into wide bore low-resistance vessels ensuring a local increase in blood supply, necessary to fulfil placenta requirements [23]. At the same time, these cells accumulate and plug the lumen of the transformed SA, obstructing blood cell circulation. Nevertheless, there is a plasma leak which results in a physiological gradient of O₂ between the mother and the foetus, with extreme importance for organogenesis [2]. In a phenomenon named deep placentation, EVTs further invade the decidua and reach as far as the inner third of the myometrium.

4. Modulators of EVT Function and Associated Signalling Pathways

Extravillous trophoblasts are not isolated elements as they are surrounded by decidual cells, vascular features, ECM

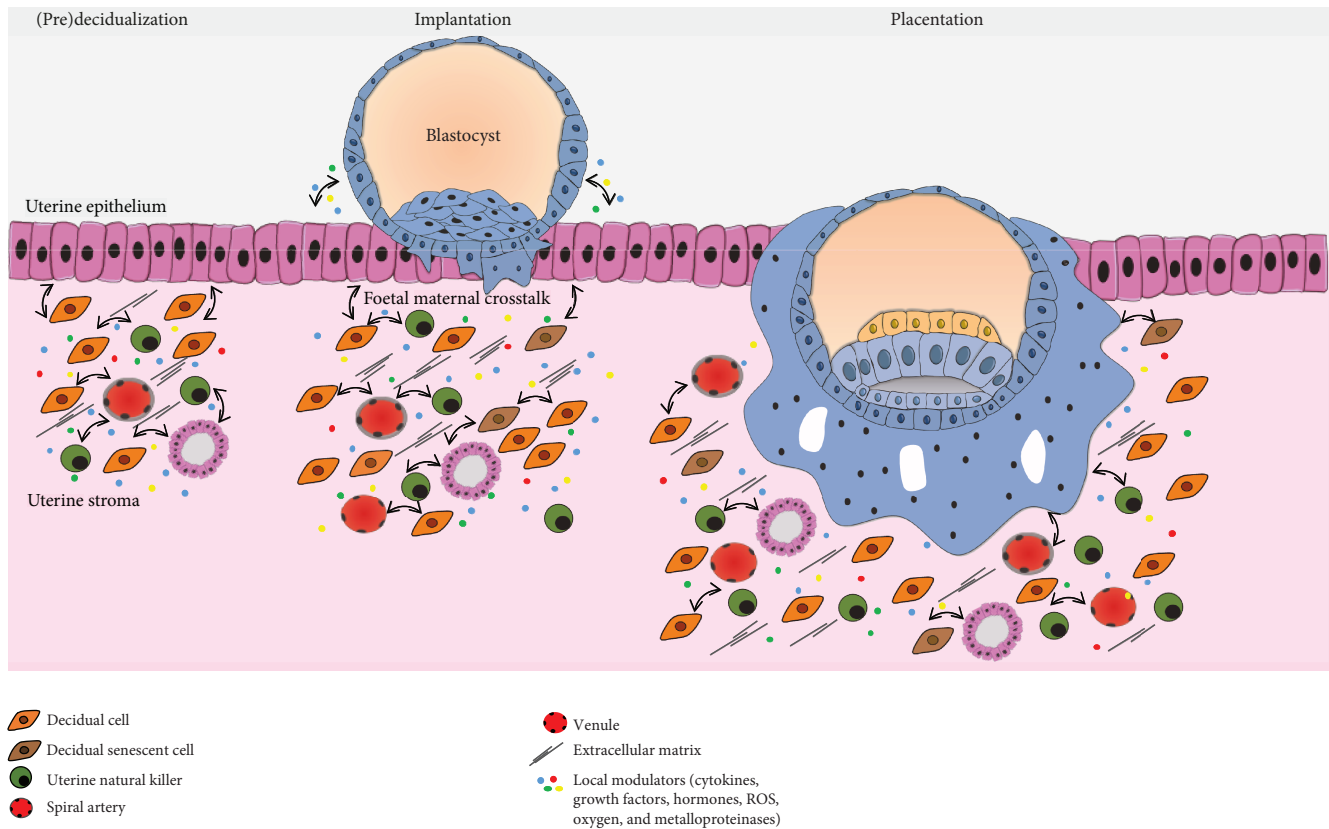


FIGURE 1: Human placenta development. Blastocyst implantation is mediated by the crosstalk between the blastocyst and the receiving endometrium. Early differentiated syncytiotrophoblast, displaying an invasive phenotype, allows the blastocyst to implant inside the endometrial stroma. Cytokines, growth factors, hormones, oxygen, extracellular matrix, and ROS all modulate trophoblast cell invasion of maternal decidua and myometrium and their capacity to transform spiral arteries. Many growth factors and cytokines, such as EGF, TGF- β , and TNF- α , secreted by the decidua and uNK cells act in a paracrine manner to regulate trophoblast function. These factors may also be secreted by the trophoblast cells and act in an autocrine manner to promote invasion.

proteins, uNK cells, and soluble factors, which together constitute the uterine microenvironment (Figure 2). This microenvironment must be suitable for an effective implantation that is the pillar for a successful pregnancy.

4.1. Oxygen. Low O_2 levels are essential for correct placental development. In fact, during the first trimester of pregnancy, when SA are plugged by EVT, there is an abrupt decrease in O_2 concentration from the decidua to the developing placenta [24, 25]. This gradient is essential for cell column basement-residing cytotrophoblast cells to proliferate, reach the tips of the columns, and differentiate into invading extravillous trophoblasts. It thus appears that dividing cytotrophoblasts are pushed forward, towards maternal tissue and higher O_2 levels, where they lose proliferative capacity, acquire an invasive phenotype, and start invading the maternal tissue [26]. Low O_2 levels also induce the expression and stability of transcription factors, such as hypoxia-inducible factor-1 (HIF-1), which promotes expression of genes that encode proteins involved in cell metabolism, essential for trophoblast proliferation and differentiation [27].

4.2. Adhesion Molecules and Receptors. The transition from proliferating cytotrophoblast cells to invasive EVT is also

dependent on specific cell receptors and cell adhesion molecule (CAM) alterations. It starts with trophoblast cell detachment from the basal membrane and culminates with de novo adhesion to uterine ECM, enabling EVT to further migrate and invade the myometrium and SA. A variety of molecules with a role in adhesion, motility, and migratory capacity are present in the EVT and include integrins, selectins, cadherins, kisspeptins, and ephrins [28, 29]. Integrins are the major family of CAM with a key importance in the above-mentioned processes. Their expression differs among trophoblast populations and modulates the binding to the ECM. In addition, locally produced cytokines can influence CAM expression, particularly TGF- β [30]. EVT integrins bind to ECM proteins and other decidual molecules and activate cellular pathways controlling trophoblast functions [31].

4.3. Extracellular Matrix. The decidual ECM is a 3-dimensional tissue structure where trophoblast lineages are embedded. This matrix is composed of a variety of proteins including collagen, fibronectin, laminin, vitronectin, trophin, and tascin [32]. ECM modulate EVT functions and, at the same time, EVT degrades and induce ECM remodelling to enable migration [33–35].

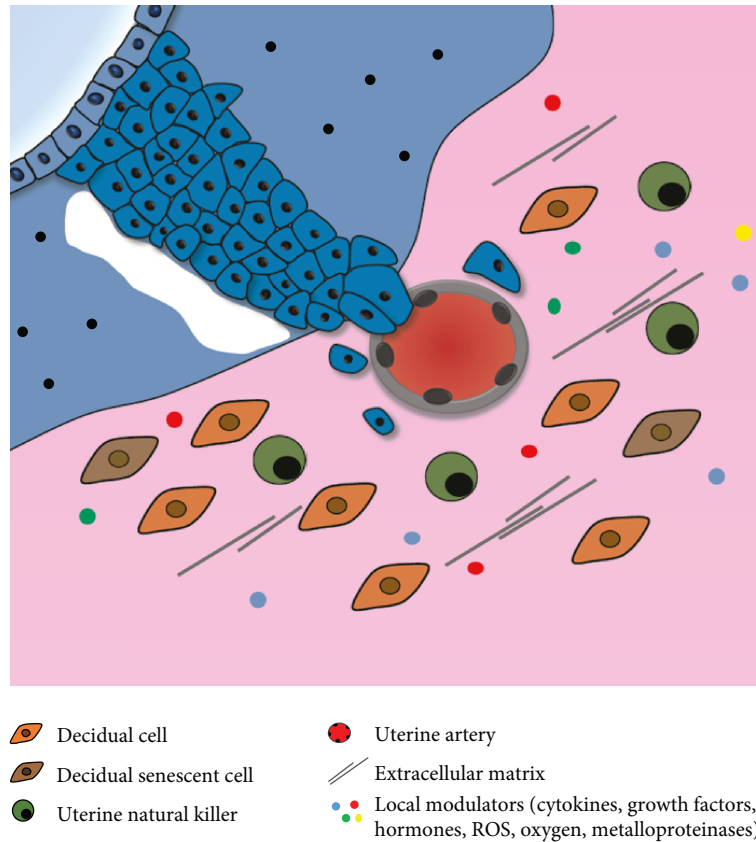


FIGURE 2: Extravillous trophoblast invasion and spiral artery remodelling. Within the syncytium, lacunae (the primitive intervillous space) are formed and proliferative cytotrophoblast cells emanate until they contact the endometrium (anchoring villi). At the tips of the villi, cytotrophoblasts differentiate into invasive trophoblast cells that will leave the villi and migrate through the stroma until they reach maternal spiral arteries or the deep myometrium. Interstitial extravillous trophoblasts that reach spiral arteries disrupt the vascular smooth muscle cell layer and replace it by fibrinoid material, while endovascular trophoblasts destroy their lumen and occupy their endometrium, converting them into low-resistance vessels.

TABLE 1: Classification of matrix metalloproteinases.

MMP classification		Enzyme substrates		Cell type/tissue secretion	References
Collagenases	Collagenase-1	MMP-1	Collagen types I, II, III, VII, and X	EVTs, decidua, and uNK	[39–42]
	Collagenase-2	MMP-8	Collagen types I and III	EVTs, decidua	[39, 43, 44]
	Collagenase-3	MMP-13	Collagen type I	EVTs, decidua	[39, 44–46]
Gelatinases	Gelatinase A	MMP-2	Collagen types I, III, IV, V, VII, and X; gelatin; fibronectin; and elastin	EVTs, decidua, and uNK	[39, 42, 44, 47–52]
	Gelatinase B	MMP-9	Collagen types I, III, IV, and V and gelatin	EVTs, decidua, and uNK	[39, 42, 44, 47–50, 52]
Stromelysins	Stromelysin-1	MMP-3	Collagen types III, IV, IX, and X; gelatin; laminin; fibronectin; and elastin	EVTs, decidua	[39, 44, 50, 53]
	Stromelysin-2	MMP-10	Collagen types II, IV, and V; fibronectin; and gelatin	EVTs, decidua, and uNK	[39, 44, 50, 54]
	Stromelysin-3	MMP-11	Collagen type IV	EVTs, decidua, and uNK	[39, 44]
	Matrilysin	MMP-7	Fibronectin and gelatin	EVTs, decidua, and uNK	[39, 41, 42, 44, 45]
	Matrilysin-2	MMP-26	Fibronectin and gelatin	EVTs, decidua	[39, 55, 56]
	Metalloelastase	MMP-12	Elastin and fibronectin	EVTs, decidua, and uNK	[39, 44, 57, 58]

ECM proteins are degraded by proteases, cathepsins, and MMPs [36]. MMPs belong to the family of zinc-dependent endopeptidases, with diverse members that degrade distinct units of the ECM (Table 1) [37, 38].

Regulation of MMP expression can be done at different levels: transcriptional (e.g., cytokines and growth factors), during secretion, by extracellular activation (e.g., plasmin-activated MMP-3), by inhibition (e.g., tissue inhibitors of metalloproteinases (TIMPs)), or by degradation [59, 60]. TIMPs are a family of extracellular proteins (TIMP-1, TIMP-2, TIMP-3, and TIMP-4), which act as specific protease inhibitors, binding to the catalytic MMP domain and counteracting MMP activity [61].

Cell-matrix or cell-cell contact mediates both MMPs and TIMPs production [62]. To invade, EVT must bind to ECM components, degrade them, and subsequently move through the tissue matrix. Cell surface adhesion molecules are essential for cell adhesion and constitutively express proteinases for ECM degradation [63]. Both EVT adhesion molecules and MMP secretion are dependent on ECM composition [36] and their phenotypic features. EVTs show an early predominant expression of MMP-2 that changes to MMP-9 later on during trophoblast invasion, to cope with decidual ECM alterations [64–67]. Overall, decidual cells, when in contact with EVTs, also express MMPs assisting in ECM degradation and further enhancing trophoblast invasion [67], but they also antagonize MMP activity by producing TIMPs and consequently blocking trophoblast invasion [68].

Decidual cells balance MMPs and TIMP secretion, control EVT migration, and prevent an exacerbate invasion [69] in a tight regulation and following a strict balance [70]. Thus, in order to achieve a correct placentation, uterine microarchitecture remodelling is necessary and requires a fine-tuned regulatory process operated by multiple players, of which only a limited number is currently known.

4.4. Soluble Factors—Cytokines and Growth Factors. Both timing and extension of EVT invasion are partly regulated by a plethora of paracrine and autocrine factors expressed by different cells comprising the decidua and EVTs themselves. Moreover, expression of these factors shows a considerable structural overlap, with several mediators being expressed by the decidua, uNK, and trophoblast cells [71]. In a decidualized endometrium, the cytokine/chemokine secretion is unique and, with the exception of leukaemia inhibitory factor (LIF), the expression of these soluble factors is increased when compared with nondecidualized stromal cells (Table 2).

Due to such alteration, it is conceivable that the decidual secretome has a role in controlling trophoblast invasion [73]. In a simplified way, soluble mediators can be divided in two groups: pro- and anti-invasive. Proinvasive paracrine factors, which have been shown to increase *in vitro* cell migration, invasion, and adhesion, comprise IL-1, IL-6, IL-8, IL-15, LIF, insulin-like growth factor-binding protein 1 (IGFBP-1), epidermal growth factor (EGF), interferon gamma-induced protein 10 (IP-10), RANTES (regulated on activation, normal T cell expressed and secreted), and chemokines CX3CL1 and CCL14. Anti-invasive factors

TABLE 2: Molecules secreted in response to decidualization.

Soluble factors	Reference
EGF ↑	[72]
IL-1 β ↑	[73]
IL-6 ↑	[73]
IL-8 ↑	[73]
IL-10 ↑	[74]
IL-11 ↑	[75, 76]
IL-15 ↑	[76]
IGFBP-1 ↑	[75, 76]
IP-10 ↑	[73]
LIF ↓	[77]
RANTES ↑	[73]
TGF- β ↑	[72]
TNF- α ↑	[72]
VEGF ↑	[72]

include IL-10, IL-12, TNF- α , TGF- β , interferon gamma (IFN- γ), chemokine CXCL12, VEGF, and endocrine gland-derived VEGF (EG-VEGF) (Table 3).

Apart from the decidua, other tissues are producers of trophoblast regulators. Leptin, produced in the adipose tissue and in trophoblasts, can enhance EVT invasion capacity by an effective increase in MMP-14 expression [134–136]. In a placental bed, paracrine factors bind to the EVT cognate receptors and trigger signalling cascades that regulate gene expression and enzymatic activity, which induce a shift in MMPs, ILs, and growth factor secretion. This variation further regulates, in a feedforward fashion, a plethora of soluble factors that also control invasion.

4.5. Signalling Pathways. Several signalling pathways are responsible for controlling migration and invasion of EVTs including mitogen-activated protein kinase (MAPK), phosphoinositide 3-kinase (PI3K)/protein kinase B (Akt), Janus kinase (JAK)/signal transducer and activator of transcription proteins (STATs), wingless (Wnt), and focal adhesion kinase (FAK) pathways. However, endometrium-derived soluble factors predominantly activate MAPK, JAK/STAT, and TGF- β -mediated signalling pathways.

One of the most important pathways of MAPK signalling is extracellular signal-regulated kinase (ERK) 1/2. It participates in essential functions as cell proliferation, differentiation, and survival [137]. This pathway can be activated by mitogens, phorbol esters, growth factors, and ROS [137, 138]. In pregnancy, ERK1/2 is important for placental development [139], trophoblast differentiation, and decidual invasion [138, 140]. Endothelin and prostaglandins activate ERK1/2 and promote EVT migration, while inhibition of this pathway reduces it [140]. The p38 MAPK pathway is also an important MAPK signalling pathway; it is activated by cytokines [141], among other agents, and is necessary in the control of apoptosis, inflammation, cell cycle regulation, senescence, and oncogenesis [141, 142]. In particular, the p38 α isoform plays a vital role in placental embryonic

TABLE 3: Soluble factors secretion and its effect on invasion.

Soluble factor	Secreted by	Effects on trophoblast invasion	References	
CCL14	Decidua	Increase migration by promoting CAM expression alterations (α -catenin and integrin β 5); increase invasion by increasing MMP-12 expression	[64, 78]	
CX3CL1		[78]		
EGF	Decidua and mesenchymal villi	Increase invasion by increasing MMP-9 and TIMP-1 expression	[65, 79–82]	
HGF	Decidua, placental stromal cells, and uNK	Increase invasion by upregulating of H2.0-like homeobox gene	[83, 84]	
IGFBP-1	Decidua	Increase invasion by increasing gelatinolytic activity	[31, 85–87]	
IL-1 β	Cytotrophoblasts, decidua, macrophages, and uNK	Increase invasion by increasing MMP-2, MMP-9, and urokinase plasminogen activator expression	[78, 88–95]	
Proinvasive	IL-6	Cytotrophoblasts and uNK	Increase invasion by increasing MMP-2 and MMP-9 expression	[91, 96–101]
	IL-8	Cytotrophoblasts, decidua, macrophages, and uNK	Increase invasion by increasing MMP-2, MMP-9, uPA, and plasminogen activator inhibitor (PAI) type 1 and 2 expression	[102, 103]
	IL-15	Decidual cells	Increase invasion by increasing MMP-1 expression	[76, 104, 105]
	IP-10	Endometrial stromal cells, uterine glandular cells, and uNK	Increase migration by increasing integrin expression (α 5 and β 3)	[106–108]
	LIF	Decidual stromal cells and uNK	Increase adhesion through changes in integrin expression; increase invasion by decreasing TIMP-1 expression	[109–115]
	RANTES	Uterine stromal cells	Increase adhesion and migration by increasing cytolytic activity and integrin expression (β 1)	[116–118]
	IL-11	Cytotrophoblasts, uNK, and decidua	Involvement in EVT function less understood; inhibiting invasion in HTR-8/SVneo and increasing in JEG-3	[119–121]
Anti-invasive	CXCL14	Decidual stromal cells	Decrease invasion by gelatinase activity suppression	[64]
	IL-10	Macrophages and uNK	Decrease invasion by downregulating MMP-2 and MMP-9 expression	[122]
	INF- γ	Cytotrophoblasts, decidua, and uNK	Decrease invasion by decreasing insulin-like growth factor receptor-II	[123–127]
	Kisspeptin-10	Cytotrophoblasts and decidua	Decrease invasion by binding to g protein-coupled receptor kisspeptin-1 receptor increasing Ca ²⁺ intracellular levels	[123–127]
	TGF- β	Cytotrophoblasts, decidua, and uNK	Decrease invasion by increasing of TIMP-1 and TIMP-2 and plasminogen activator inhibitor type 1 and 2 expression; increases adhesion by upregulating the expression of CAM (ezrin and e-cadherin)	[62, 79, 85, 123–125, 128–130]
	TNF- α	Cytotrophoblasts, decidua, macrophages, and uNK	Decrease invasion by upregulation plasminogen activator inhibitor type 1 expression	[123, 125, 130–132]
	VEGF	Decidua, macrophages, and uNK	Decrease invasion by inhibiting urokinase plasminogen activator expression	[133]

development and placental angiogenesis [143]. ERK1/2 inhibition in parallel with p38 MAPK decreases trophoblast differentiation [138]. Activation of the MAPK pathway in combination with the PI3K/Akt pathway promotes EVT (HTR-8/SVneo immortalized cell line) invasion and migration via MMP enhancement [144].

JAK/STAT3 signalling is indispensable for regulation of EVT proliferation and invasion capacity in response to cytokines and growth factors [145, 146]. Again, an interdependence between MAPK and JAK-STAT signalling pathways

was found to be involved in EGF-mediated HTR-8/SVneo cell invasion [146].

TGF- β signals through Smad-dependent (canonical) and Smad-independent (ERK, JNK, p38, and Rho GTPases) (noncanonical) pathways. Recent studies with JEG trophoblast cells demonstrate that activation of Smad3 promotes cell invasion by upregulation of MMP2 and MMP9 [147]. These findings contrast with previous reports where TGF- β decreased EVT invasion in HTR-8/SVneo cells, by inducing Snail-mediated downregulation of vascular endothelial-

cadherin [147]. TGF- β plays a role in multiple signalling networks in the cell, and depending on the second messengers involved, divergent responses can be attained.

ROS are important secondary messengers and play a role in the modulation of protein kinase activity. When a redox imbalance occurs, ROS can impair the EVT signalling network. Modification of essential amino acid residues by ROS, which consequently alter the protein structure and its function, is one of the plausible mechanisms of ROS actions [148].

5. Oxidative Stress and Placentation

5.1. Reactive Oxygen Species, Oxidative Stress, and Placentation. The ROS family comprises free radicals (i.e., species with at least one unpaired electron) and nonradical oxidants (i.e., oxidants with their electronic ground state complete). These species reactivity, half-lives, and diffusion capacities are variable. Hydroxyl radical ($\cdot\text{OH}$) is the most unstable and upon formation reacts rapidly with biomolecules in the vicinity [149]. In contrast, hydrogen peroxide (H_2O_2) is capable of crossing cell membranes and exerts its effects beyond the cell limits [150, 151].

Under physiological conditions, superoxide anion ($\text{O}_2^{\cdot-}$) is the most frequently generated radical. Its main source is the inner mitochondrial membrane during the respiratory chain, particularly the complexes I and III, by inevitable leakage of electrons to O_2 [152, 153]. $\text{O}_2^{\cdot-}$ can also be formed following electron leakage in a shorter electron transport chain at the endoplasmic reticulum (ER) and during the membrane-bound nicotinamide adenine dinucleotide phosphate oxidase (NOX) activity, which transfers one electron from NADPH to O_2 [154].

To cope with the continued ROS production, cells have developed antioxidant mechanisms that prevent their accumulation and deleterious actions. Antioxidants, enzymatic or nonenzymatic, can mitigate ROS effects by delaying oxidation or preventing it from happening. In cells, key enzymatic antioxidants are superoxide dismutase (SOD), catalase (CAT), and glutathione peroxidase (GPx) [155], whereas important nonenzymatic antioxidants comprise vitamins C (ascorbic acid) and E (tocopherol), zinc and selenium, glutathione, plant polyphenols, and carotenoids (carotene and β -carotene) [156]. Other molecules with moderate antioxidant properties may also be relevant because of their abundance, as is serum albumin [157].

ROS are normal products of cell metabolism with physiological roles in the organisms. They regulate signalling pathways through changes in the activity of structural proteins, transcription factors, membrane receptors, ion channels, and protein kinases/phosphatases [158]. However, when ROS levels rise, and antioxidant defences cannot neutralize them, the redox homeostasis is disrupted, and a new state referred as oxidative stress (OS) arises. OS leads to an impairment of redox signalling and causes molecular damage to biomolecules [159, 160]. OS condition is graded; while minor or moderated changes provoke an adaptive response and homeostasis restoration, higher ones result in violent perturbations that lead to pathological insults, damage beyond repair, and even cell death [159] (Figure 3).

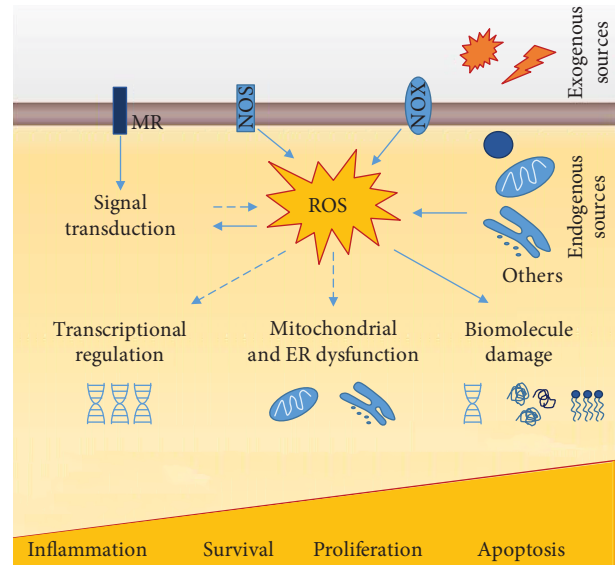


FIGURE 3: ROS sources and downstream cellular effects. Endogenous sources of ROS include mitochondrial metabolic reactions, NADPH oxidase activity, and microsomal cytochrome P450 detoxification pathways; exogenous sources comprehend ultraviolet radiation, X-rays and gamma-rays, ultrasounds, pesticides, herbicides, and xenobiotics. ROS are normal products of cell metabolism with physiological roles in the organisms. They regulate signalling pathways through changes in the activity of structural proteins, transcription factors, membrane receptors, ion channels, and protein kinases/phosphatases. However, when ROS levels rise, and antioxidant defence cannot neutralize them, the redox homeostasis is disrupted, and a new state referred to as oxidative stress (OS) arises. OS leads to impairment of redox signalling and induces damage to biomolecules. OS has a graded response with minor or moderated changes provoking an adaptive response and homeostasis restoration and violent perturbations leading to pathological insults, damage beyond repair, and even cell death. MR: membrane receptor; NOS: nitric oxide synthase; NOX: NADPH oxidase. Filled arrows indicate a direct action, while dashed arrows indicate indirect or simplified mechanisms.

5.1.1. ROS in the Endometrium Cycle. ROS are believed to be implicated in the regulation of the endometrial cycle (Figure 4) [161]. NOX-derived $\text{O}_2^{\cdot-}$ has been shown to activate the nuclear factor kappa-light-chain-enhancer of activated B cells (NF- κB) and regulate angiogenesis [162, 163], thus resulting in a determinant role in the endometrial cycle. Variations in SOD, GPx, and lipid peroxides in response to oestrogen and progesterone levels have also been reported [164, 165]. In a late secretory phase, steroid hormone fall reduces SOD activity and, consequently, increases ROS effects [166, 167]. ROS-mediated activation of NF- κB signalling cascade promotes prostaglandin secretion, vasoconstriction, and, ultimately, the endometrial shedding [168–171], at the end of the secretory phase. The exacerbated uterine ROS level and NF- κB activation may result in signalling pathway disruption and in a broad spectrum of uterine-related infertility disorders, as endometriosis [172]. In recurrent pregnancy loss (RPL), increased activity of antioxidant enzymes and decreased markers of OS in endometrial secretions before implantation associated positively with a successful

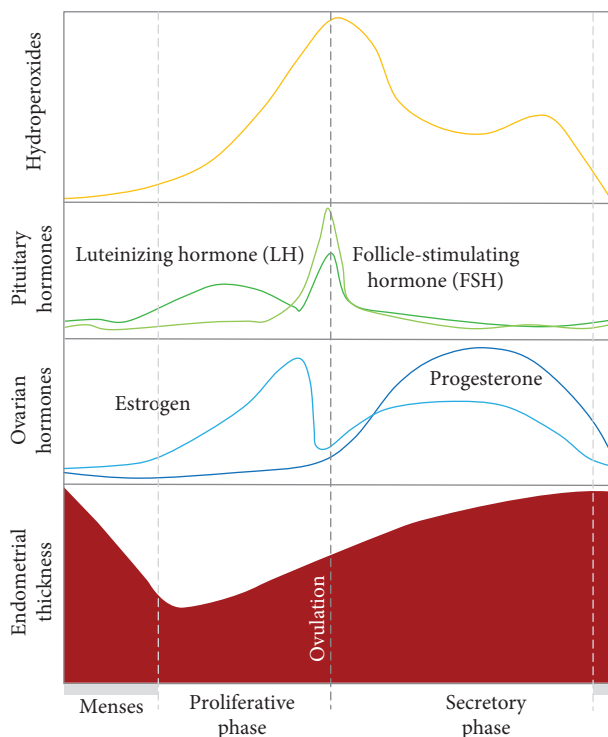


FIGURE 4: Diagrammatic representation of the different phases of the menstrual cycle, oxidative stress (OS) changes, and fluctuations in ovarian and pituitary hormones. Plasmatic OS marker (hydroperoxides) maximum levels are seen near ovarian and pituitary hormone peaks [161].

IVF outcome [173]. Moreover, endometrial alterations in progesterone-induced SGK1 (a serine-threonine protein kinase homologous to AKT) were also related to RPL due to impairment in OS defences [174].

5.1.2. ROS and Decidualization. Recent findings suggest that decidual stromal cells evolved from ancestor stromal cell fibroblasts, whose phenotype acquisition is modulated by redox signalling, ER stress, and cellular senescence [175]. In this context, resveratrol, a molecule with antioxidant and anti-inflammatory properties, inhibits decidualization in mice by repression of decidualization markers and abrogation of cellular senescence [176], whereas decidual cell ER sensitive to stressful conditions results in a decrement of decidual functioning [177, 178] and viability [179]. In short, during decidualization, redox-sensitive transcription factors and kinases are activated, making plausible the intervention of ROS and their regulators in this process [180–182] and extending it into placentation. In pregnancy, progesterone stimulates uterine stromal decidualization and decidual SOD expression [183, 184]. In addition, GPx3 is highly expressed in mice decidua, favouring its involvement in uterine transformation and implantation, a point further supported by the reduced pregnancy rates upon GPx3 inhibition [165].

5.1.3. ROS and Regulation of Trophoblast Function. EVT are also adversely regulated by OS because of their interference

with fundamental cellular pathways, reduction of MMP expression, upregulation of proinflammatory cytokine secretion, and induction of mitochondrial dysfunction [185–192]. These consequences disrupt EVT crosstalk within the uterine microenvironment and impair fundamental biological processes as differentiation, proliferation, migration, and vascular remodelling (Table 4). The use of specific antioxidant molecules may have beneficial effects on EVT functions [186, 188, 189].

5.1.4. The Ageing Uterus. In the aged uterus, indirect evidence supports the occurrence of cellular senescence, which is thought to affect decidual transformation [195] and promote preterm births [196, 197]. In addition, reproductively aged mice show age-related increase in uterine NOX and protein carbonylation content, contributing to abnormal decidualization and reduced fertility. NOX inhibition, but not enhanced H_2O_2 conversion using a SOD mimetic, restores local redox balance, repairs maternal-foetal interactions, and increases fertility [6]. In line with these results are the recent findings of Banerjee and coworkers reporting that low H_2O_2 levels increase EVT invasion, while high levels induce apoptosis [191, 194]. Interestingly, an age-related decrease in adrenal synthesis of dehydroepiandrosterone (DHEA) is believed to grant increased antioxidant capacity to decidualized cells and improve endometrial receptivity [198–200].

On a wider view, either by disturbing uterine decidual or embryo-derived cell functioning, important aspects of modern life style such as obesity, increased maternal age, alcohol consumption, and exposure to substances may act as endocrine disruptors and affect implantation and placentation through OS induction [6, 7, 185, 190, 193, 201].

Therefore, it is now recognized that, at the time of implantation, OS-related alterations in uterine microenvironment lead to a relevant disturbance at the foetus/maternal interface that impairs trophoblast invasion and spiral artery remodelling and stand at the root of major pregnancy-related complications of vascular origin, such as preeclampsia and IUGR.

5.2. AGEs, RAGEs, ROS, and Placentation. Glycation is a nonenzymatic reaction (not to be confused with the enzymatic reaction glycosylation), between reducing sugars (e.g., glucose, fructose, or galactose) and amino groups of proteins, lipids, or nucleic acids. Advanced glycation end-products (AGEs) are the result of a series of glycation reactions [202]. The formation of AGEs was first described by Maillard in the beginning of the 20th century; however, the chemical reactions were only described later in the setting of food research [202]. Briefly, in the classic Maillard reaction, electrophilic carbonyl groups of reducing sugars interact with free amino acid residues (especially arginine or lysine) and form unstable Schiff bases that reverse when glucose levels drop. Further rearrangements result in the formation of the more stable, but still reversible, “Amadori products,” which can react with peptides or protein amino acids, this time irreversibly, leading to the formation of AGEs [203, 204]. The Maillard reaction is not the unique pathway for AGE

TABLE 4: ROS-mediated regulation of trophoblast function.

Agent	Molecular effects	EVT functions	Reference
Decanoic acid	Disrupts mitochondrial function ↑ ROS generation ↓ Akt and ERK1/2 pathways	↓ proliferation ↓ invasion	[185]
Trichloroethylene	Disrupts mitochondrial function ↑ ROS generation ↑ proinflammatory cytokine production	—	[190]
Benzo(a)pyren-7,8-dihydrodiol-9,10-epoxide	Disrupts mitochondrial function ↑ ROS generation ↓ SOD activity Induces apoptosis	↓ invasion	[193]
Higher H ₂ O ₂ concentrations	Induces apoptosis	↓ invasion	[194]
Lower H ₂ O ₂ concentrations	↑ STAT 1 and 3 pathways ↑ MMP-9/TIMP-1 ratio	↑ invasion	[191]
Selenium (under hypoxic conditions)	↓ mitochondrial stress	↑ proliferation ↑ migration	[186]
Edaravone (under hypoxic conditions)	↓ ROS production	↑ proliferation ↑ migration	[187]
Flavonoids (under hypoxia/reoxygenation)	↓ ROS production	↑ invasion	[189]

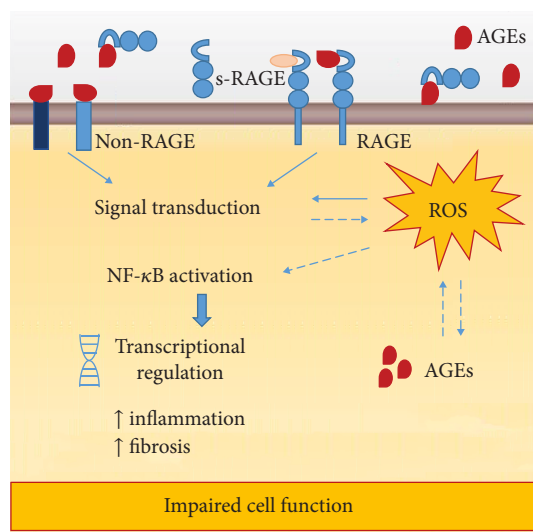


FIGURE 5: Advanced glycation end-product (AGE) pathological effects. Most of AGE effects are dependent on the interaction AGE/RAGE (receptor of AGE) and the activation of transduction pathways. However, AGEs can bind non-RAGE proteins, and interestingly, RAGE can be activated by other ligands. AGE interactions with membrane receptors trigger various ROS-mediated signalling pathways that converge on NF- κ B activation and transcriptional regulation of genes, which impairs cell function. The proteolytic cleavage of extracellular RAGE originates circulating peptides referred as soluble RAGE (sRAGE). It is believed that sRAGEs act as decoy receptors, which scavenge circulating AGEs, preventing them from binding functional membrane RAGE and inducing cellular responses.

formation because other reactions involving the formation of carbonyl-containing reactive compounds end up as AGEs [205, 206]. As such, it is not surprising that AGEs

are a quite complex, heterogeneous group of compounds, formed either exogenously (e.g., dietary AGEs) and endogenously, by different mechanisms and precursors. ROS, O₂, and transition metals are catalysers of AGE synthesis [207] and AGE interactions with membrane receptors that trigger various ROS-mediated signalling pathways, such as ERK1/2-MAPK, PI3K-Akt, and p38-SAPK-JNK [208, 209] (Figure 5).

Very little is known about AGE physiological role, and few researches have addressed this issue. Cerami hypothesized that AGEs were protein residues that acted as signals, targeting them to degradation, and that age-related AGE accumulation resulted from loss of efficiency of the removal system [210]. Other authors have explored methylglyoxal, an AGE precursor, as an antimicrobial and anticarcinogenic agent [211].

A handful of papers have also explored AGEs as preconditioners, preparing cells to exacerbated OS, and thus contributing to a future improvement in antioxidant/inflammation response [212–215]. Up to date, nothing is known about a putative antioxidant or antifibrotic effect of dietary AGEs on obstetric-related disorders, although there is a possibility that is worth exploring.

An increase in AGE levels accompanies the ageing process itself and is also a significant contributor and a major risk factor to the development of several age-associated disorders. Higher levels of circulating AGEs or AGE receptor (RAGE) activation have been found in diabetes, hypertension [216], systemic lupus erythematosus [217], rheumatoid arthritis [218], Alzheimer disease [219], and neoplasia [220, 221]. Interestingly, elevated circulation AGEs have also been found in pregnancy-associated complications such as severe preeclampsia [222] and gestational diabetes mellitus (GDM) [223] where it has been positively correlated with proinflammatory markers [224]. In animal models,

treatment with soluble RAGE, RAGE inhibitors, and antioxidant molecules ameliorates placental complications [225].

5.2.1. AGEs, ROS, and Regulation of Trophoblast Function. *In vitro* experiments with trophoblasts isolated from first trimester chorionic villi showed that AGE administration increased apoptosis, proinflammatory cytokine production, and monocyte migration. Activation of the NF- κ B pathway was crucial to the observed AGE-mediated cell responses, since an inhibitor of this pathway displayed beneficial effects [226]. In accordance, AGEs were found to be upstream molecules that trigger ROS production, activate soluble fms-like tyrosine kinase-1 (sFlt-1), VEGF, and PlGF [227], increase cytokine production in immortalized trophoblast cell lines isolated from first trimester villi (HTR-8/SVneo and Sw.71 cells), and enhance monocyte migration [228, 229]. This inflammatory environment conditions placenta development. Anti-RAGE immunoglobulin or antioxidant treatment also proved effective in reverting AGE-mediated cell effects [227]. Recently, work from Antoniotti et al. showed that uterine AGE levels found in obese women impair uterine transformation and trophoblast function [7].

Overall, data obtained from both *in vivo* and *in vitro* experiments demonstrated that AGEs alter trophoblast function through ROS increase and activation of the NF- κ B pathway [227, 229–231], supporting the view that an age-related imbalance in uterine oxidative microenvironment, present even before pregnancy, conditions implantation.

6. Concluding Remarks and Future Perspectives

Placenta central function is to supply an adequate amount of blood to properly nourish the foetus. To achieve this purpose, a receptive endometrium is permeated by extravillous trophoblast cells that invade it as deep as the muscular layer. This invasion anchors the placenta to the maternal uterus and guarantees local blood supply through a surprising structural and functional change in maternal spiral arteries: by way of the replacement of their walls by embryo-derived cells, their resistance properties are converted into capacitance features. Such a process requires coordination and cooperation between maternal and foetal tissues.

Similar to key roles played by ROS in processes as oocyte maturation and fertilization, ROS involvement continues in decidualization, implantation, modulation of trophoblast proliferation and differentiation, and embryo development.

A balance between oxidant and antioxidant molecules is vital for a successful ending. The placenta is a growing organ that must evade the adverse effects of homeostasis loss and adapt to reinstall homeostasis. However, when local redox status is significantly disturbed, and severe OS is established, molecular and cellular damage ensues. In the decidualized uterus, those events alter protein function and structure and signalling pathways, disrupt ECM and cytokine production, and hamper the microenvironment at the maternal-foetal interface.

More researchers are convinced that alterations in the foetal-maternal microenvironment before pregnancy, whether by ROS or AGEs, are the culprits and the etiopathogenic

roots of pregnancy-related complications of vascular origin. Clearly, we have much to learn, by unravelling ROS-mediated molecular mechanisms dysregulated at the uterus.

Conflicts of Interest

The authors declare that there is no conflict of interest regarding the publication of this paper.

References

- [1] F. Lyall, "The human placental bed revisited," *Placenta*, vol. 23, no. 8-9, pp. 555–562, 2002.
- [2] F. Lyall, "Priming and remodelling of human placental bed spiral arteries during pregnancy—a review," *Placenta*, vol. 26, pp. S31–S36, 2005.
- [3] C. W. G. Redman and I. L. Sargent, "Placental stress and pre-eclampsia: a revised view," *Placenta*, vol. 30, pp. 38–42, 2009.
- [4] E. R. Norwitz, "Defective implantation and placentation: laying the blueprint for pregnancy complications," *Reproductive Biomedicine Online*, vol. 13, no. 4, pp. 591–599, 2006.
- [5] S. Lu, H. Peng, H. Zhang et al., "Excessive intrauterine fluid cause aberrant implantation and pregnancy outcome in mice," *PLoS One*, vol. 8, no. 10, article e78446, 2013.
- [6] E. Silva, A. I. Soares, F. Costa, J. P. Castro, L. Matos, and H. Almeida, "Antioxidant supplementation modulates age-related placental bed morphology and reproductive outcome in mice," *Biology of Reproduction*, vol. 93, no. 3, p. 56, 2015.
- [7] G. S. Antoniotti, M. Coughlan, L. A. Salamonsen, and J. Evans, "Obesity associated advanced glycation end products within the human uterine cavity adversely impact endometrial function and embryo implantation competence," *Human Reproduction*, vol. 33, no. 4, pp. 654–665, 2018.
- [8] B. Gellersen and J. J. Brosens, "Cyclic decidualization of the human endometrium in reproductive health and failure," *Endocrine Reviews*, vol. 35, no. 6, pp. 851–905, 2014.
- [9] K. Vinketova, M. Mourdjeva, and T. Oreshkova, "Human decidual stromal cells as a component of the implantation niche and a modulator of maternal immunity," *Journal of Pregnancy*, vol. 2016, Article ID 8689436, 17 pages, 2016.
- [10] A. Evron, S. Goldman, and E. Shalev, "Effect of primary human endometrial stromal cells on epithelial cell receptivity and protein expression is dependent on menstrual cycle stage," *Human Reproduction*, vol. 26, no. 1, pp. 176–190, 2010.
- [11] L. M. Gaynor and F. Colucci, "Uterine natural killer cells: functional distinctions and influence on pregnancy in humans and mice," *Frontiers in Immunology*, vol. 8, p. 467, 2017.
- [12] J. C. Cheng, H. M. Chang, and P. C. K. Leung, "TGF- β 1 inhibits human trophoblast cell invasion by upregulating connective tissue growth factor expression," *Endocrinology*, vol. 158, no. 10, pp. 3620–3628, 2017.
- [13] J. L. Maitre, "Mechanics of blastocyst morphogenesis," *Biology of the Cell*, vol. 109, no. 9, pp. 323–338, 2017.
- [14] J. Aplin, "Maternal influences on placental development," *Seminars in Cell & Developmental Biology*, vol. 11, no. 2, pp. 115–125, 2000.
- [15] H. Matsumoto, "Molecular and cellular events during blastocyst implantation in the receptive uterus: clues from mouse

- models," *The Journal of Reproduction and Development*, vol. 63, no. 5, pp. 445–454, 2017.
- [16] B. C. Paria, Y. M. Huet-Hudson, and S. K. Dey, "Blastocyst's state of activity determines the "Window" of implantation in the receptive mouse uterus," *Proceedings of the National Academy of Sciences of the United States of America*, vol. 90, no. 21, pp. 10159–10162, 1993.
- [17] P. Bischof and I. Irminger-Finger, "The human cytotrophoblastic cell, a mononuclear chameleon," *The International Journal of Biochemistry & Cell Biology*, vol. 37, no. 1, pp. 1–16, 2005.
- [18] S. Handwerger, "New insights into the regulation of human cytotrophoblast cell differentiation," *Molecular and Cellular Endocrinology*, vol. 323, no. 1, pp. 94–104, 2010.
- [19] A. J. G. Pötgens, U. Schmitz, P. Bose, A. Versmold, P. Kaufmann, and H. G. Frank, "Mechanisms of syncytial fusion: a review," *Placenta*, vol. 23, pp. S107–S113, 2002.
- [20] J. D. Boyd and W. J. Hamilton, *The Human Placenta*, Cambridge [England]: Heffer, 1970.
- [21] K. Benirschke and P. Kaufman, *Pathology of the Human Placenta*, Springer, 2000.
- [22] D. N. Modi, G. Godbole, P. Suman, and S. K. Gupta, "Endometrial biology during trophoblast invasion," *Frontiers in Bioscience (Scholar Edition)*, vol. 4, pp. 1151–1171, 2012.
- [23] E. W. Dempsey, "The development of capillaries in the villi of early human placentas," *The American Journal of Anatomy*, vol. 134, no. 2, pp. 221–237, 1972.
- [24] E. Jauniaux, A. L. Watson, J. Hempstock, Y. P. Bao, J. N. Skepper, and G. J. Burton, "Onset of maternal arterial blood flow and placental oxidative stress. A possible factor in human early pregnancy failure," *The American Journal of Pathology*, vol. 157, no. 6, pp. 2111–2122, 2000.
- [25] I. Caniggia, J. Winter, S. J. Lye, and M. Post, "Oxygen and placental development during the first trimester: implications for the pathophysiology of pre-eclampsia," *Placenta*, vol. 21, pp. S25–S30, 2000.
- [26] P. Kaufmann, S. Black, and B. Huppertz, "Endovascular trophoblast invasion: implications for the pathogenesis of intrauterine growth retardation and preeclampsia," *Biology of Reproduction*, vol. 69, no. 1, pp. 1–7, 2003.
- [27] I. Caniggia, H. Mostachfi, J. Winter et al., "Hypoxia-inducible factor-1 mediates the biological effects of oxygen on human trophoblast differentiation through TGF β_3 ," *The Journal of Clinical Investigation*, vol. 105, no. 5, pp. 577–587, 2000.
- [28] L. K. Harris, C. J. P. Jones, and J. D. Aplin, "Adhesion molecules in human trophoblast - a review. II. Extravillous trophoblast," *Placenta*, vol. 30, no. 4, pp. 299–304, 2009.
- [29] J. D. Aplin, C. J. P. Jones, and L. K. Harris, "Adhesion molecules in human trophoblast - a review. I. Villous trophoblast," *Placenta*, vol. 30, no. 4, pp. 293–298, 2009.
- [30] D. Male, J. Rahman, A. Linke, W. Zhao, and W. Hickey, "An interferon-inducible molecule on brain endothelium which controls lymphocyte adhesion mediated by integrins," *Immunology*, vol. 84, no. 3, pp. 453–460, 1995.
- [31] L. M. Gleeson, C. Chakraborty, T. McKinnon, and P. K. Lala, "Insulin-like growth factor-binding protein 1 stimulates human trophoblast migration by signaling through $\alpha 5\beta 1$ integrin via mitogen-activated protein kinase pathway," *The Journal of Clinical Endocrinology and Metabolism*, vol. 86, no. 6, pp. 2484–2493, 2001.
- [32] J. S. Krussel, P. Bielfeld, M. L. Polan, and C. Simon, "Regulation of embryonic implantation," *European Journal of Obstetrics, Gynecology, and Reproductive Biology*, vol. 110, pp. S2–S9, 2003.
- [33] P. Xu, Y. Wang, Y. Piao et al., "Effects of matrix proteins on the expression of matrix metalloproteinase-2, -9, and -14 and tissue inhibitors of metalloproteinases in human cytotrophoblast cells during the first trimester," *Biology of Reproduction*, vol. 65, no. 1, pp. 240–246, 2001.
- [34] E. Staun-Ram and E. Shalev, "Human trophoblast function during the implantation process," *Reproductive Biology and Endocrinology*, vol. 3, no. 1, p. 56, 2005.
- [35] P. Lu, K. Takai, V. M. Weaver, and Z. Werb, "Extracellular matrix degradation and remodeling in development and disease," *Cold Spring Harbor Perspectives in Biology*, vol. 3, no. 12, 2011.
- [36] P. Bischof, A. Meisser, and A. Campana, "Biochemistry and molecular biology of trophoblast invasion," *Annals of the New York Academy of Sciences*, vol. 943, no. 1, pp. 157–162, 2001.
- [37] M. Cohen, A. Meisser, and P. Bischof, "Metalloproteinases and human placental invasiveness," *Placenta*, vol. 27, no. 8, pp. 783–793, 2006.
- [38] M. Seiki, "Membrane-type matrix metalloproteinases," *APMIS*, vol. 107, no. 1–6, pp. 137–143, 1999.
- [39] J. Anacker, S. E. Segerer, C. Hagemann et al., "Human decidua and invasive trophoblasts are rich sources of nearly all human matrix metalloproteinases," *Molecular Human Reproduction*, vol. 17, no. 10, pp. 637–652, 2011.
- [40] C. L. Deng, S. T. Ling, X. Q. Liu, Y. J. Zhao, and Y. F. Lv, "Decreased expression of matrix metalloproteinase-1 in the maternal umbilical serum, trophoblasts and decidua leads to preeclampsia," *Experimental and Therapeutic Medicine*, vol. 9, no. 3, pp. 992–998, 2015.
- [41] W. Li, N. Cui, M. Q. Mazzuca, K. M. Mata, and R. A. Khalil, "Increased vascular and uteroplacental matrix metalloproteinase-1 and -7 levels and collagen type I deposition in hypertension in pregnancy: role of TNF- α ," *American Journal of Physiology. Heart and Circulatory Physiology*, vol. 313, no. 3, pp. H491–h507, 2017.
- [42] Z. Ren, N. Cui, M. Zhu, and R. A. Khalil, "Placental growth factor reverses decreased vascular and uteroplacental MMP-2 and MMP-9 and increased MMP-1 and MMP-7 and collagen types I and IV in hypertensive pregnancy," *American Journal of Physiology. Heart and Circulatory Physiology*, vol. 315, no. 1, pp. H33–H47, 2018.
- [43] L. Rahkonen, E. M. Rutanen, M. Nuutila, S. Sainio, T. Sorsa, and J. Paavonen, "Matrix metalloproteinase-8 in cervical fluid in early and mid pregnancy: relation to spontaneous preterm delivery," *Prenatal Diagnosis*, vol. 30, no. 11, pp. 1079–1085, 2010.
- [44] T. T.-T. N. Nguyen, O. Shynlova, and S. J. Lye, "Matrix metalloproteinase expression in the rat myometrium during pregnancy, term labor, and postpartum," *Biology of Reproduction*, vol. 95, no. 1, p. 24, 2016.
- [45] K. Wolf, P. Sandner, A. Kurtz, and W. Moll, "Messenger ribonucleic acid levels of collagenase (MMP-13) and matrilysin (MMP-7) in virgin, pregnant, and postpartum uterus and cervix of rat," *Endocrinology*, vol. 137, no. 12, pp. 5429–5434, 1996.
- [46] S. J. Fortunato, B. LaFleur, and R. Menon, "Collagenase-3 (MMP-13) in fetal membranes and amniotic fluid during

- pregnancy," *American Journal of Reproductive Immunology*, vol. 49, no. 2, pp. 120–125, 2003.
- [47] R. Nissi, A. Talvensaari-Mattila, V. Kotila, M. Niinimäki, I. Järvelä, and T. Turpeenniemi-Hujanen, "Circulating matrix metalloproteinase MMP-9 and MMP-2/TIMP-2 complex are associated with spontaneous early pregnancy failure," *Reproductive Biology and Endocrinology*, vol. 11, no. 1, p. 2, 2013.
- [48] J. Chen and R. A. Khalil, "Matrix metalloproteinases in normal pregnancy and preeclampsia," *Progress in Molecular Biology and Translational Science*, vol. 148, pp. 87–165, 2017.
- [49] S. C. Riley, R. Leask, T. Chard, N. C. Wathen, A. A. Calder, and D. C. Howe, "Secretion of matrix metalloproteinase-2, matrix metalloproteinase-9 and tissue inhibitor of metalloproteinases into the intrauterine compartments during early pregnancy," *Molecular Human Reproduction*, vol. 5, no. 4, pp. 376–381, 1999.
- [50] A. Lombardi, S. Makieva, S. F. Rinaldi, F. Arcuri, F. Petraglia, and J. E. Norman, "Expression of matrix metalloproteinases in the mouse uterus and human myometrium during pregnancy, labor, and preterm labor," *Reproductive Sciences*, vol. 25, no. 6, pp. 938–949, 2017.
- [51] C. Guo and L. Piacentini, "Type I collagen-induced MMP-2 activation coincides with up-regulation of membrane type 1-matrix metalloproteinase and TIMP-2 in cardiac fibroblasts," *The Journal of Biological Chemistry*, vol. 278, no. 47, pp. 46699–46708, 2003.
- [52] H. F. Bigg, A. D. Rowan, M. D. Barker, and T. E. Cawston, "Activity of matrix metalloproteinase-9 against native collagen types I and III," *The FEBS Journal*, vol. 274, no. 5, pp. 1246–1255, 2007.
- [53] M. O'Brien, D. O'Shaughnessy, E. Ahamide, J. J. Morrison, and T. J. Smith, "Differential expression of the metalloproteinase MMP3 and the alpha5 integrin subunit in human myometrium at labour," *Molecular Human Reproduction*, vol. 13, no. 9, pp. 655–661, 2007.
- [54] N. Lagzouli, B. Sayer, S. Ashton, J. Cartwright, and G. Whitley, "Trophoblasts stimulate the release of MMP10 by endothelial cells," *Placenta*, vol. 45, p. 77, 2016.
- [55] Q. Li, H. Wang, Y. Zhao, H. Lin, Q. A. Sang, and C. Zhu, "Identification and specific expression of matrix metalloproteinase-26 in rhesus monkey endometrium during early pregnancy," *Molecular Human Reproduction*, vol. 8, no. 10, pp. 934–940, 2002.
- [56] K. Isaka, H. Nishi, H. Nakai et al., "Matrix metalloproteinase-26 is expressed in human endometrium but not in endometrial carcinoma," *Cancer*, vol. 97, no. 1, pp. 79–89, 2003.
- [57] U. Hiden, E. Glitzner, M. Ivanisevic et al., "MT1-MMP expression in first-trimester placental tissue is upregulated in type 1 diabetes as a result of elevated insulin and tumor necrosis factor- α levels," *Diabetes*, vol. 57, no. 1, pp. 150–157, 2007.
- [58] L. K. Harris, S. D. Smith, R. J. Keogh et al., "Trophoblast and vascular smooth muscle cell-derived MMP-12 mediates elastolysis during uterine spiral artery remodeling," *The American Journal of Pathology*, vol. 177, no. 4, pp. 2103–2115, 2010.
- [59] A. H. Baker, D. R. Edwards, and G. Murphy, "Metalloproteinase inhibitors: biological actions and therapeutic opportunities," *Journal of Cell Science*, vol. 115, no. 19, pp. 3719–3727, 2002.
- [60] C. Yan and D. D. Boyd, "Regulation of matrix metalloproteinase gene expression," *Journal of Cellular Physiology*, vol. 211, no. 1, pp. 19–26, 2007.
- [61] G. Murphy, "Tissue inhibitors of metalloproteinases," *Genome Biology*, vol. 12, no. 11, p. 233, 2011.
- [62] P. Bischoff, A. Meisser, and A. Campana, "Paracrine and autocrine regulators of trophoblast invasion—a review," *Placenta*, vol. 21, pp. S55–S60, 2000.
- [63] B. Huppertz, S. Kertschanska, A. Y. Demir, H. G. Frank, and P. Kaufmann, "Immunohistochemistry of matrix metalloproteinases (MMP), their substrates, and their inhibitors (TIMP) during trophoblast invasion in the human placenta," *Cell and Tissue Research*, vol. 291, no. 1, pp. 133–148, 1998.
- [64] N. J. Hannan and L. A. Salamonsen, "CX3CL1 and CCL14 regulate extracellular matrix and adhesion molecules in the trophoblast: potential roles in human embryo implantation," *Biology of Reproduction*, vol. 79, no. 1, pp. 58–65, 2008.
- [65] E. Staun-Ram, S. Goldman, D. Gabarin, and E. Shalev, "Expression and importance of matrix metalloproteinase 2 and 9 (MMP-2 and -9) in human trophoblast invasion," *Reproductive Biology and Endocrinology*, vol. 2, no. 1, p. 59, 2004.
- [66] K. Isaka, S. Usuda, H. Ito et al., "Expression and activity of matrix metalloproteinase 2 and 9 in human trophoblasts," *Placenta*, vol. 24, no. 1, pp. 53–64, 2003.
- [67] M. Iwahashi, Y. Muragaki, A. Ooshima, M. Yamoto, and R. Nakano, "Alterations in distribution and composition of the extracellular matrix during decidualization of the human endometrium," *Journal of Reproduction and Fertility*, vol. 108, no. 1, pp. 147–155, 1996.
- [68] S. Espino Y Sosa, A. Flores-Pliego, A. Espejel-Nuñez et al., "New insights into the role of matrix metalloproteinases in preeclampsia," *International Journal of Molecular Sciences*, vol. 18, no. 7, p. 1448, 2017.
- [69] E. Staun-Ram, S. Goldman, and E. Shalev, "p53 mediates epidermal growth factor (EGF) induction of MMP-2 transcription and trophoblast invasion," *Placenta*, vol. 30, no. 12, pp. 1029–1036, 2009.
- [70] Y. Seval, G. Akkoyunlu, R. Demir, and M. Asar, "Distribution patterns of matrix metalloproteinase (MMP)-2 and -9 and their inhibitors (TIMP-1 and TIMP-2) in the human decidua during early pregnancy," *Acta Histochemica*, vol. 106, no. 5, pp. 353–362, 2004.
- [71] M. Knofler and J. Pollheimer, "IFPA award in Placentology lecture: molecular regulation of human trophoblast invasion," *Placenta*, vol. 33, pp. S55–S62, 2012.
- [72] R. M. Popovici, L.-C. Kao, and L. C. Giudice, "Discovery of new inducible genes in in vitro decidualized human endometrial stromal cells using microarray technology," *Endocrinology*, vol. 141, no. 9, pp. 3510–3515, 2000.
- [73] S. Sharma, G. Godbole, and D. Modi, "Decidual control of trophoblast invasion," *American Journal of Reproductive Immunology*, vol. 75, no. 3, pp. 341–350, 2016.
- [74] P. Viganò, E. Somigliana, S. Mangioni, M. Vignali, M. Vignali, and A. M. Di Blasio, "Expression of interleukin-10 and Its receptor is up-regulated in early pregnant versus cycling human endometrium," *The Journal of Clinical Endocrinology & Metabolism*, vol. 87, no. 12, pp. 5730–5736, 2002.

- [75] N. Karpovich, P. Klemmt, J. H. Hwang et al., "The production of interleukin-11 and decidualization are compromised in endometrial stromal cells derived from patients with infertility," *The Journal of Clinical Endocrinology & Metabolism*, vol. 90, no. 3, pp. 1607–1612, 2005.
- [76] G. Godbole and D. Modi, "Regulation of decidualization, interleukin-11 and interleukin-15 by homeobox a 10 in endometrial stromal cells," *Journal of Reproductive Immunology*, vol. 85, no. 2, pp. 130–139, 2010.
- [77] L. L. Shuya, E. M. Menkhorst, J. Yap, P. Li, N. Lane, and E. Dimitriadis, "Leukemia inhibitory factor enhances endometrial stromal cell decidualization in humans and mice," *PLoS One*, vol. 6, no. 9, article e25288, 2011.
- [78] J. Hanna, D. Goldman-Wohl, Y. Hamani et al., "Decidual NK cells regulate key developmental processes at the human fetal-maternal interface," *Nature Medicine*, vol. 12, no. 9, pp. 1065–1074, 2006.
- [79] J. J. Lysiak, I. H. Connelly, N. K. S. Khoo, W. Stetler-Stevenson, and P. K. Lala, "Role of transforming growth factor- α (TGF α) and epidermal growth factor (EGF) on proliferation and invasion by first trimester human trophoblast," *Placenta*, vol. 15, pp. 455–467, 1994.
- [80] G. E. Hofmann, R. T. Scott Jr., P. A. Bergh, and L. Deligdisch, "Immunohistochemical localization of epidermal growth factor in human endometrium, decidua, and placenta," *The Journal of Clinical Endocrinology & Metabolism*, vol. 73, no. 4, pp. 882–887, 1991.
- [81] E. Y. Anteby, C. Greenfield, S. Natanson-Yaron et al., "Vascular endothelial growth factor, epidermal growth factor and fibroblast growth factor-4 and -10 stimulate trophoblast plasminogen activator system and metalloproteinase-9," *Molecular Human Reproduction*, vol. 10, no. 4, pp. 229–235, 2004.
- [82] Q. Qiu, M. Yang, B. K. Tsang, and A. Gruslin, "EGF-induced trophoblast secretion of MMP-9 and TIMP-1 involves activation of both PI3K and MAPK signalling pathways," *Reproduction*, vol. 128, no. 3, pp. 355–363, 2004.
- [83] J. E. Cartwright, D. P. Holden, and G. S. J. Whitley, "Hepatocyte growth factor regulates human trophoblast motility and invasion: a role for nitric oxide," *British Journal of Pharmacology*, vol. 128, no. 1, pp. 181–189, 1999.
- [84] S. Saito, S. Sakakura, M. Enomoto, M. Ichijo, K. Matsumoto, and T. Nakamura, "Hepatocyte growth factor promotes the growth of cytotrophoblasts by the paracrine mechanism," *Journal of Biochemistry*, vol. 117, no. 3, pp. 671–676, 1995.
- [85] J. A. Irving and P. K. Lala, "Functional role of cell surface integrins on human trophoblast cell migration: regulation by TGF- β , IGF-II, and IGFBP-1," *Experimental Cell Research*, vol. 217, no. 2, pp. 419–427, 1995.
- [86] V. K. Han, N. Bassett, J. Walton, and J. R. Challis, "The expression of insulin-like growth factor (IGF) and IGF-binding protein (IGFBP) genes in the human placenta and membranes: evidence for IGF-IGFBP interactions at the fetomaternal interface," *The Journal of Clinical Endocrinology and Metabolism*, vol. 81, no. 7, pp. 2680–2693, 1996.
- [87] T. McKinnon, C. Chakraborty, L. M. Gleeson, P. Chidiac, and P. K. Lala, "Stimulation of human extravillous trophoblast migration by IGF-II is mediated by IGF type 2 receptor involving inhibitory G protein(s) and phosphorylation of MAPK," *The Journal of Clinical Endocrinology and Metabolism*, vol. 86, no. 8, pp. 3665–3674, 2001.
- [88] P. Bischof and A. Campana, "Molecular mediators of implantation," *Best Practice & Research Clinical Obstetrics & Gynaecology*, vol. 14, no. 5, pp. 801–814, 2000.
- [89] P. Viganò, S. Mangioni, F. Pompei, and I. Chiodo, "Maternal-conceptus cross talk - a review," *Placenta*, vol. 24, pp. S56–S61, 2003.
- [90] A. Meisser, D. Chardonens, A. Campana, and P. Bischof, "Effects of tumour necrosis factor- α , interleukin-1 α , macrophage colony stimulating factor and transforming growth factor β on trophoblastic matrix metalloproteinases," *Molecular Human Reproduction*, vol. 5, no. 3, pp. 252–260, 1999.
- [91] A. Meisser, P. Cameo, D. Islami, A. Campana, and P. Bischof, "Effects of interleukin-6 (IL-6) on cytotrophoblastic cells," *Molecular Human Reproduction*, vol. 5, no. 11, pp. 1055–1058, 1999.
- [92] C. L. Librach, S. L. Feigenbaum, K. E. Bass et al., "Interleukin-1 β regulates human cytotrophoblast metalloproteinase activity and invasion in vitro," *The Journal of Biological Chemistry*, vol. 269, no. 25, pp. 17125–17131, 1994.
- [93] C. Simon, A. Frances, G. Piquette, M. Hendrickson, A. Milki, and M. L. Polan, "Interleukin-1 system in the maternotrophoblast unit in human implantation: immunohistochemical evidence for autocrine/paracrine function," *The Journal of Clinical Endocrinology and Metabolism*, vol. 78, no. 4, pp. 847–854, 1994.
- [94] N. Prutsch, V. Fock, P. Haslinger et al., "The role of interleukin-1 β in human trophoblast motility," *Placenta*, vol. 33, no. 9, pp. 696–703, 2012.
- [95] H. Husslein, S. Haider, G. Meinhardt, J. Prast, S. Sonderegger, and M. Knofler, "Expression, regulation and functional characterization of matrix metalloproteinase-3 of human trophoblast," *Placenta*, vol. 30, no. 3, pp. 284–291, 2009.
- [96] E. Jauniaux, B. Gulbis, L. Schandene, J. Collette, and J. Hustin, "Distribution of interleukin-6 in maternal and embryonic tissues during the first trimester," *Molecular Human Reproduction*, vol. 2, no. 4, pp. 239–243, 1996.
- [97] C. Das, V. S. Kumar, S. Gupta, and S. Kumar, "Network of cytokines, integrins and hormones in human trophoblast cells," *Journal of Reproductive Immunology*, vol. 53, no. 1–2, pp. 257–268, 2002.
- [98] S. Tabibzadeh, Q. F. Kong, A. Babaknia, and L. T. May, "Progressive rise in the expression of interleukin-6 in human endometrium during menstrual cycle is initiated during the implantation window," *Human Reproduction*, vol. 10, no. 10, pp. 2793–2799, 1995.
- [99] D. T. Vandermolen and Y. Gu, "Human endometrial interleukin-6 (IL-6): in vivo messenger ribonucleic acid expression, in vitro protein production, and stimulation thereof by IL-1 beta," *Fertility and Sterility*, vol. 66, no. 5, pp. 741–747, 1996.
- [100] P. Bischof, A. Meisser, and A. Campana, "Involvement of Trophoblast in Embryo Implantation: Regulation by Paracrine factors," *Journal of Reproductive Immunology*, vol. 39, no. 1–2, pp. 167–177, 1998.
- [101] M. Jovanovic and L. Vicovac, "Interleukin-6 stimulates cell migration, invasion and integrin expression in HTR-8/SVneo cell line," *Placenta*, vol. 30, no. 4, pp. 320–328, 2009.
- [102] L. G. de Oliveira, G. E. Lash, C. Murray-Dunning et al., "Role of interleukin 8 in uterine natural killer cell regulation of extravillous trophoblast cell invasion," *Placenta*, vol. 31, no. 7, pp. 595–601, 2010.

- [103] M. Jovanovic, I. Stefanoska, L. Radojicic, and L. Vicovac, "Interleukin-8 (CXCL8) stimulates trophoblast cell migration and invasion by increasing levels of matrix metalloproteinase (MMP)2 and MMP9 and integrins $\alpha 5$ and $\beta 1$," *Reproduction*, vol. 139, no. 4, pp. 789–798, 2010.
- [104] B. Toth, T. Haufe, C. Scholz et al., "Placental interleukin-15 expression in recurrent miscarriage," *American Journal of Reproductive Immunology*, vol. 64, no. 6, pp. 402–410, 2010.
- [105] M. Zygmunt, D. Hahn, N. Kiesenbauer, K. Munstedt, and U. Lang, "Invasion of cytotrophoblastic (JEG-3) cells is up-regulated by interleukin-15 in vitro," *American Journal of Reproductive Immunology*, vol. 40, no. 5, pp. 326–331, 1998.
- [106] F. Dominguez, S. Martinez, A. Quinonero et al., "CXCL10 and IL-6 induce chemotaxis in human trophoblast cell lines," *Molecular Human Reproduction*, vol. 14, no. 7, pp. 423–430, 2008.
- [107] H. Y. Sela, D. S. Goldman-Wohl, R. Haimov-Kochman et al., "Human trophoblast apposition is regulated by interferon γ -induced protein 10 (IP-10) during early implantation," *Placenta*, vol. 34, no. 3, pp. 222–230, 2013.
- [108] K. Nagaoka, H. Nojima, F. Watanabe et al., "Regulation of blastocyst migration, apposition, and initial adhesion by a chemokine, interferon gamma-inducible protein 10 kDa (IP-10), during early gestation," *The Journal of Biological Chemistry*, vol. 278, no. 31, pp. 29048–29056, 2003.
- [109] E. B. Cullinan, S. J. Abbondanzo, P. S. Anderson, J. W. Pollard, B. A. Lessey, and C. L. Stewart, "Leukemia inhibitory factor (LIF) and LIF receptor expression in human endometrium suggests a potential autocrine/paracrine function in regulating embryo implantation," *Proceedings of the National Academy of Sciences of the United States of America*, vol. 93, no. 7, pp. 3115–3120, 1996.
- [110] Z. Kondera-Anasz, J. Sikora, and A. Mielczarek-Palacz, "Leukemia inhibitory factor: an important regulator of endometrial function," *American Journal of Reproductive Immunology*, vol. 52, no. 2, pp. 97–105, 2004.
- [111] H. Bhatt, L. J. Brunet, and C. L. Stewart, "Uterine expression of leukemia inhibitory factor coincides with the onset of blastocyst implantation," *Proceedings of the National Academy of Sciences of the United States of America*, vol. 88, no. 24, pp. 11408–11412, 1991.
- [112] A. M. Sharkey, A. King, D. E. Clark et al., "Localization of leukemia inhibitory factor and its receptor in human placenta throughout pregnancy," *Biology of Reproduction*, vol. 60, no. 2, pp. 355–364, 1999.
- [113] P. Bischof, L. Haenggeli, and A. Campana, "Effect of leukemia inhibitory factor on human cytotrophoblast differentiation along the invasive pathway," *American Journal of Reproductive Immunology*, vol. 34, no. 4, pp. 225–230, 1995.
- [114] A. Tapia, L. A. Salamonsen, U. Manuelpillai, and E. Dimitriadis, "Leukemia inhibitory factor promotes human first trimester extravillous trophoblast adhesion to extracellular matrix and secretion of tissue inhibitor of metalloproteinases-1 and -2," *Human Reproduction*, vol. 23, no. 8, pp. 1724–1732, 2008.
- [115] P. Suman and S. K. Gupta, "STAT3 and ERK1/2 cross-talk in leukaemia inhibitory factor mediated trophoblastic JEG-3 cell invasion and expression of mucin 1 and Fos," *American Journal of Reproductive Immunology*, vol. 72, no. 1, pp. 65–74, 2014.
- [116] U. A. Kayisli, N. G. Mahutte, and A. Arici, "Uterine chemokines in reproductive physiology and pathology," *American Journal of Reproductive Immunology*, vol. 47, no. 4, pp. 213–221, 2002.
- [117] H. Fujiwara, T. Higuchi, Y. Sato et al., "Regulation of human extravillous trophoblast function by membrane-bound peptidases," *Biochimica et Biophysica Acta*, vol. 1751, no. 1, pp. 26–32, 2005.
- [118] T. L. Thirkill, K. Lowe, H. Vedagiri, T. N. Blankenship, A. I. Barakat, and G. C. Douglas, "Macaque trophoblast migration is regulated by RANTES," *Experimental Cell Research*, vol. 305, no. 2, pp. 355–364, 2005.
- [119] E. Dimitriadis, L. A. Salamonsen, and L. Robb, "Expression of interleukin-11 during the human menstrual cycle: coincidence with stromal cell decidualization and relationship to leukaemia inhibitory factor and prolactin," *Molecular Human Reproduction*, vol. 6, no. 10, pp. 907–914, 2000.
- [120] P. Paiva, L. A. Salamonsen, U. Manuelpillai et al., "Interleukin-11 promotes migration, but not proliferation, of human trophoblast cells, implying a role in placentation," *Endocrinology*, vol. 148, no. 11, pp. 5566–5572, 2007.
- [121] P. Suman, G. Godbole, R. Thakur et al., "AP-1 transcription factors, mucin-type molecules and MMPs regulate the IL-11 mediated invasiveness of JEG-3 and HTR-8/SVneo trophoblastic cells," *PLoS One*, vol. 7, no. 1, article e29745, 2012.
- [122] I. Roth and S. J. Fisher, "IL-10 is an autocrine inhibitor of human placental cytotrophoblast MMP-9 production and invasion," *Developmental Biology*, vol. 205, no. 1, pp. 194–204, 1999.
- [123] S. Bauer, J. Pollheimer, J. Hartmann, P. Husslein, J. D. Aplin, and M. Knofler, "Tumor necrosis factor- α inhibits trophoblast migration through elevation of plasminogen activator inhibitor-1 in first-trimester villous explant cultures," *The Journal of Clinical Endocrinology and Metabolism*, vol. 89, no. 2, pp. 812–822, 2004.
- [124] M. Bilban, N. Ghaffari-Tabrizi, E. Hintermann et al., "Kisspeptin-10, a KiSS-1/metastin-derived decapeptide, is a physiological invasion inhibitor of primary human trophoblasts," *Journal of Cell Science*, vol. 117, no. 8, pp. 1319–1328, 2004.
- [125] P. K. Lala and C. H. Graham, "Mechanisms of trophoblast invasiveness and their control: the role of proteases and protease inhibitors," *Cancer Metastasis Reviews*, vol. 9, no. 4, pp. 369–379, 1990.
- [126] G. E. Lash, H. A. Otun, B. A. Innes et al., "Interferon- γ inhibits extravillous trophoblast cell invasion by a mechanism that involves both changes in apoptosis and protease levels," *The FASEB Journal*, vol. 20, no. 14, pp. 2512–2518, 2006.
- [127] J. Pollheimer, P. Husslein, and M. Knofler, "Invasive trophoblasts generate regulatory collagen XVIII cleavage products," *Placenta*, vol. 26, pp. S42–S45, 2005.
- [128] C. H. Graham, I. Connelly, J. R. MacDougall, R. S. Kerbel, W. G. Stetler-Stevenson, and P. K. Lala, "Resistance of malignant trophoblast cells to both the anti-proliferative and anti-invasive effects of transforming growth factor- β ," *Experimental Cell Research*, vol. 214, no. 1, pp. 93–99, 1994.
- [129] G. E. Lash, H. A. Otun, B. A. Innes, J. N. Bulmer, R. F. Searle, and S. C. Robson, "Inhibition of trophoblast cell invasion by TGF β 1, 2, and 3 is associated with a decrease in active proteases1," *Biology of Reproduction*, vol. 73, no. 2, pp. 374–381, 2005.

- [130] S. Saito, K. Nishikawa, T. Morii et al., "Cytokine production by CD16-CD56^{bright} natural killer cells in the human early pregnancy decidua," *International Immunology*, vol. 5, no. 5, pp. 559–563, 1993.
- [131] S. Haider and M. Knofler, "Human tumour necrosis factor: physiological and pathological roles in placenta and endometrium," *Placenta*, vol. 30, no. 2, pp. 111–123, 2009.
- [132] L. Nadeem, S. Munir, G. Fu et al., "Nodal signals through activin receptor-like kinase 7 to inhibit trophoblast migration and invasion: implication in the pathogenesis of preeclampsia," *The American Journal of Pathology*, vol. 178, no. 3, pp. 1177–1189, 2011.
- [133] A. Athanassiades, G. S. Hamilton, and P. K. Lala, "Vascular endothelial growth factor stimulates proliferation but not migration or invasiveness in human extravillous trophoblast1," *Biology of Reproduction*, vol. 59, no. 3, pp. 643–654, 1998.
- [134] H. Liu, Y. Wu, F. Qiao, and X. Gong, "Effect of leptin on cytotrophoblast proliferation and invasion," *Journal of Huazhong University of Science and Technology. Medical Sciences*, vol. 29, no. 5, pp. 631–636, 2009.
- [135] R. R. Gonzalez, L. Devoto, A. Campana, and P. Bischof, "Effects of leptin, interleukin-1alpha, interleukin-6, and transforming growth factor- β on markers of trophoblast invasive phenotype: integrins and metalloproteinases," *Endocrine*, vol. 15, no. 2, pp. 157–164, 2001.
- [136] M. Castellucci, R. de Matteis, A. Meisser et al., "Leptin modulates extracellular matrix molecules and metalloproteinases: possible implications for trophoblast invasion," *Molecular Human Reproduction*, vol. 6, no. 10, pp. 951–958, 2000.
- [137] M. R. Junttila, S. P. Li, and J. Westermark, "Phosphatase-mediated crosstalk between MAPK signaling pathways in the regulation of cell survival," *The FASEB Journal*, vol. 22, no. 4, pp. 954–965, 2008.
- [138] G. Daoud, M. Amyot, E. Rassart, A. Masse, L. Simoneau, and J. Lafond, "ERK1/2 and p38 regulate trophoblasts differentiation in human term placenta," *The Journal of Physiology*, vol. 566, no. 2, pp. 409–423, 2005.
- [139] M. Aouadi, B. Binetruy, L. Caron, Y. Le Marchand-Brustel, and F. Bost, "Role of MAPKs in development and differentiation: lessons from knockout mice," *Biochimie*, vol. 88, no. 9, pp. 1091–1098, 2006.
- [140] K. C. Moon, J. S. Park, E. R. Norwitz et al., "Expression of extracellular signal-regulated kinase1/2 and p38 mitogen-activated protein kinase in the invasive trophoblasts at the human placental bed," *Placenta*, vol. 29, no. 5, pp. 391–395, 2008.
- [141] L. R. Coulthard, D. E. White, D. L. Jones, M. F. McDermott, and S. A. Burchill, "p38^{MAPK}: stress responses from molecular mechanisms to therapeutics," *Trends in Molecular Medicine*, vol. 15, no. 8, pp. 369–379, 2009.
- [142] K. Ono and J. Han, "The p38 signal transduction pathway: activation and function," *Cellular Signalling*, vol. 12, no. 1, pp. 1–13, 2000.
- [143] J. S. Mudgett, J. Ding, L. Guh-Siesel et al., "Essential role for p38 α mitogen-activated protein kinase in placental angiogenesis," *Proceedings of the National Academy of Sciences of the United States of America*, vol. 97, no. 19, pp. 10454–10459, 2000.
- [144] Y. Zhang, F. Jin, X. C. Li et al., "The YY1-HOTAIR-MMP2 signaling axis controls trophoblast invasion at the maternal-fetal interface," *Molecular Therapy*, vol. 25, no. 10, pp. 2394–2403, 2017.
- [145] F. L. Pereira de Sousa, W. Chaiwangyen, D. M. Morales-Prieto et al., "Involvement of STAT1 in proliferation and invasiveness of trophoblastic cells," *Reproductive Biology*, vol. 17, no. 3, pp. 218–224, 2017.
- [146] A. Malik, R. Pal, and S. K. Gupta, "Interdependence of JAK-STAT and MAPK signaling pathways during EGF-mediated HTR-8/SVneo cell invasion," *PLoS One*, vol. 12, no. 5, article e0178269, 2017.
- [147] Z. Huang, S. Li, W. Fan, and Q. Ma, "Transforming growth factor β 1 promotes invasion of human JEG-3 trophoblast cells via TGF- β /Smad3 signaling pathway," *Oncotarget*, vol. 8, no. 20, pp. 33560–33570, 2017.
- [148] Y. Son, Y. K. Cheong, N. H. Kim, H. T. Chung, D. G. Kang, and H. O. Pae, "Mitogen-activated protein kinases and reactive oxygen species: how can ROS activate MAPK pathways," *Journal of Signal Transduction*, vol. 2011, Article ID 792639, 6 pages, 2011.
- [149] B. Halliwell and C. E. Cross, "Oxygen-derived species: their relation to human disease and environmental stress," *Environmental Health Perspectives*, vol. 102, pp. 5–12, 1994.
- [150] J. P. Kehrer, "The Haber-Weiss reaction and mechanisms of toxicity," *Toxicology*, vol. 149, no. 1, pp. 43–50, 2000.
- [151] J. P. Castro, T. Jung, T. Grune, and H. Almeida, "Actin carbonylation: from cell dysfunction to organism disorder," *Journal of Proteomics*, vol. 92, pp. 171–180, 2013.
- [152] G. J. Burton and E. Jauniaux, "Oxidative stress," *Best Practice & Research. Clinical Obstetrics & Gynaecology*, vol. 25, no. 3, pp. 287–299, 2011.
- [153] E. Cadenas and K. J. A. Davies, "Mitochondrial free radical generation, oxidative stress, and aging," *Free Radical Biology & Medicine*, vol. 29, no. 3-4, pp. 222–230, 2000.
- [154] B. P. Tu and J. S. Weissman, "Oxidative protein folding in eukaryotes: mechanisms and consequences," *The Journal of Cell Biology*, vol. 164, no. 3, pp. 341–346, 2004.
- [155] L. He, T. He, S. Farrar, L. Ji, T. Liu, and X. Ma, "Antioxidants maintain cellular redox homeostasis by elimination of reactive oxygen species," *Cellular Physiology and Biochemistry*, vol. 44, no. 2, pp. 532–553, 2017.
- [156] I. Mirończuk-Chodakowska, A. M. Witkowska, and M. E. Zujko, "Endogenous non-enzymatic antioxidants in the human body," *Advances in Medical Sciences*, vol. 63, no. 1, pp. 68–78, 2018.
- [157] M. Roche, P. Rondeau, N. R. Singh, E. Tarnus, and E. Bourdon, "The antioxidant properties of serum albumin," *FEBS Letters*, vol. 582, no. 13, pp. 1783–1787, 2008.
- [158] J. Zhang, X. Wang, V. Vikash et al., "ROS and ROS-mediated cellular signaling," *Oxidative Medicine and Cellular Longevity*, vol. 2016, Article ID 4350965, 18 pages, 2016.
- [159] H. Sies, C. Berndt, and D. P. Jones, "Oxidative stress," *Annual Review of Biochemistry*, vol. 86, no. 1, pp. 715–748, 2017.
- [160] H. Sies, "Oxidative stress: a concept in redox biology and medicine," *Redox Biology*, vol. 4, pp. 180–183, 2015.
- [161] U. Cornelli, G. Belcaro, M. R. Cesarone, and A. Finco, "Analysis of oxidative stress during the menstrual cycle," *Reproductive Biology and Endocrinology*, vol. 11, no. 1, p. 74, 2013.
- [162] K. Bedard and K. H. Krause, "The NOX family of ROS-generating NADPH oxidases: physiology and pathophysiology," *Physiological Reviews*, vol. 87, no. 1, pp. 245–313, 2007.

- [163] J. M. Davis and R. L. Auten, "Maturation of the antioxidant system and the effects on preterm birth," *Seminars in Fetal & Neonatal Medicine*, vol. 15, no. 4, pp. 191–195, 2010.
- [164] K. Strehlow, S. Rotter, S. Wassmann et al., "Modulation of antioxidant enzyme expression and function by estrogen," *Circulation Research*, vol. 93, no. 2, pp. 170–177, 2003.
- [165] X. Xu, J.-Y. Leng, F. Gao et al., "Differential expression and anti-oxidant function of glutathione peroxidase 3 in mouse uterus during decidualization," *FEBS Letters*, vol. 588, no. 9, pp. 1580–1589, 2014.
- [166] N. Sugino, S. Takiguchi, S. Kashida, A. Karube, Y. Nakamura, and H. Kato, "Superoxide dismutase expression in the human corpus luteum during the menstrual cycle and in early pregnancy," *Molecular Human Reproduction*, vol. 6, no. 1, pp. 19–25, 2000.
- [167] K. H. Al-Gubory, C. Garrel, P. Faure, and N. Sugino, "Roles of antioxidant enzymes in corpus luteum rescue from reactive oxygen species-induced oxidative stress," *Reproductive Biomedicine Online*, vol. 25, no. 6, pp. 551–560, 2012.
- [168] S. Preuthippan, S. H. Chen, J. L. Tilly, K. Kugu, R. R. Lareu, and A. M. Dharmarajan, "Inhibition of nitric oxide synthesis potentiates apoptosis in the rabbit corpus luteum," *Reproductive Biomedicine Online*, vol. 9, no. 3, pp. 264–270, 2004.
- [169] Y. Takagi, T. Nikaido, T. Toki et al., "Levels of oxidative stress and redox-related molecules in the placenta in preeclampsia and fetal growth restriction," *Virchows Archiv*, vol. 444, no. 1, pp. 49–55, 2004.
- [170] A. Agarwal, S. Gupta, L. Sekhon, and R. Shah, "Redox considerations in female reproductive function and assisted reproduction: from molecular mechanisms to health implications," *Antioxidants & Redox Signaling*, vol. 10, no. 8, pp. 1375–1404, 2008.
- [171] G. Serviddio, G. Loverro, M. Vicino et al., "Modulation of endometrial redox balance during the menstrual cycle: relation with sex hormones," *The Journal of Clinical Endocrinology and Metabolism*, vol. 87, no. 6, pp. 2843–2848, 2002.
- [172] J. Mier-Cabrera, L. Jimenez-Zamudio, E. Garcia-Latorre, O. Cruz-Orozco, and C. Hernandez-Guerrero, "Quantitative and qualitative peritoneal immune profiles, T-cell apoptosis and oxidative stress-associated characteristics in women with minimal and mild endometriosis," *BJOG*, vol. 118, no. 1, pp. 6–16, 2011.
- [173] M. E. Rahiminejad, A. Moaddab, M. Ganji et al., "Oxidative stress biomarkers in endometrial secretions: a comparison between successful and unsuccessful in vitro fertilization cycles," *Journal of Reproductive Immunology*, vol. 116, pp. 70–75, 2016.
- [174] M. S. Salker, M. Christian, J. H. Steel et al., "Deregulation of the serum- and glucocorticoid-inducible kinase SGK1 in the endometrium causes reproductive failure," *Nature Medicine*, vol. 17, no. 11, pp. 1509–1513, 2011.
- [175] E. M. Erkenbrack, J. D. Maziarz, O. W. Griffith et al., "The mammalian decidual cell evolved from a cellular stress response," *PLoS Biology*, vol. 16, no. 8, article e2005594, 2018.
- [176] A. Ochiai, K. Kuroda, R. Ozaki et al., "Resveratrol inhibits decidualization by accelerating downregulation of the CRABP2-RAR pathway in differentiating human endometrial stromal cells," *Cell Death & Disease*, vol. 10, no. 4, p. 276, 2019.
- [177] Y. Yang, X. Pei, Y. Jin, Y. Wang, and C. Zhang, "The roles of endoplasmic reticulum stress response in female mammalian reproduction," *Cell and Tissue Research*, vol. 363, no. 3, pp. 589–597, 2016.
- [178] X. W. Gu, J. Q. Yan, H. T. Dou et al., "Endoplasmic reticulum stress in mouse decidua during early pregnancy," *Molecular and Cellular Endocrinology*, vol. 434, pp. 48–56, 2016.
- [179] H. J. Gao, Y. M. Zhu, W. H. He et al., "Endoplasmic reticulum stress induced by oxidative stress in decidual cells: a possible mechanism of early pregnancy loss," *Molecular Biology Reports*, vol. 39, no. 9, pp. 9179–9186, 2012.
- [180] M. Christian, Y. Pohnke, R. Kempf, B. Gellersen, and J. J. Brosens, "Functional association of PR and CCAAT/enhancer-binding protein beta isoforms: promoter-dependent cooperation between PR-B and liver-enriched inhibitory protein, or liver-enriched activatory protein and PR-A in human endometrial stromal cells," *Molecular Endocrinology*, vol. 16, no. 1, pp. 141–154, 2002.
- [181] M. Christian, X. Zhang, T. Schneider-Merck et al., "Cyclic AMP-induced forkhead transcription factor, FKHR, cooperates with CCAAT/enhancer-binding protein beta in differentiating human endometrial stromal cells," *The Journal of Biological Chemistry*, vol. 277, no. 23, pp. 20825–20832, 2002.
- [182] M. Takano, Z. Lu, T. Goto et al., "Transcriptional cross talk between the forkhead transcription factor forkhead box O1A and the progesterone receptor coordinates cell cycle regulation and differentiation in human endometrial stromal cells," *Molecular Endocrinology*, vol. 21, no. 10, pp. 2334–2349, 2007.
- [183] N. Sugino, K. Shimamura, S. Takiguchi et al., "Changes in activity of superoxide dismutase in the human endometrium throughout the menstrual cycle and in early pregnancy," *Human Reproduction*, vol. 11, no. 5, pp. 1073–1078, 1996.
- [184] N. Sugino, S. Kashida, S. Takiguchi, Y. Nakamura, and H. Kato, "Induction of superoxide dismutase by decidualization in human endometrial stromal cells," *Molecular Human Reproduction*, vol. 6, no. 2, pp. 178–184, 2000.
- [185] C. Yang, W. Lim, F. W. Bazer, and G. Song, "Decanoic acid suppresses proliferation and invasiveness of human trophoblast cells by disrupting mitochondrial function," *Toxicology and Applied Pharmacology*, vol. 339, pp. 121–132, 2018.
- [186] J. Y. Na, J. Seok, S. Park, J. S. Kim, and G. J. Kim, "Effects of selenium on the survival and invasion of trophoblasts," *Clinical and Experimental Reproductive Medicine*, vol. 45, no. 1, pp. 10–16, 2018.
- [187] Y. Zheng, Y. Zhao, Q. Luo et al., "Edaravone protects against cobalt chloride-induced dysfunctions in apoptosis and invasion in trophoblast cells," *Molecular Reproduction and Development*, vol. 83, no. 7, pp. 576–587, 2016.
- [188] J. Kim, K. S. Lee, J. H. Kim et al., "Aspirin prevents TNF- α -induced endothelial cell dysfunction by regulating the NF- κ B-dependent miR-155/eNOS pathway: role of a miR-155/eNOS axis in preeclampsia," *Free Radical Biology & Medicine*, vol. 104, pp. 185–198, 2017.
- [189] V. J. Ebeboni, J. M. Dickenson, and S. D. Sivasubramaniam, "Antioxidative effects of flavonoids and their metabolites against hypoxia/reoxygenation-induced oxidative stress in a human first trimester trophoblast cell line," *Food Chemistry*, vol. 272, pp. 117–125, 2019.
- [190] I. Hassan, A. M. Kumar, H. R. Park, L. H. Lash, and R. Loch-Caruso, "Reactive oxygen stimulation of interleukin-6 release in the human trophoblast cell line HTR-8/SVneo by the trichlorethylene metabolite S-(1,2-dichloro)-l-cysteine," *Biology of Reproduction*, vol. 95, no. 3, p. 66, 2016.

- [191] P. Banerjee, A. Malik, S. S. Malhotra, and S. K. Gupta, "Role of STAT signaling and autocrine action of chemokines during H₂O₂ induced HTR-8/SVneo trophoblastic cells invasion," *Journal of Cellular Physiology*, vol. 234, no. 2, pp. 1380–1397, 2019.
- [192] B. Zhuang, X. Luo, H. Rao et al., "Oxidative stress-induced C/EBP β inhibits β -catenin signaling molecule involving in the pathology of preeclampsia," *Placenta*, vol. 36, no. 8, pp. 839–846, 2015.
- [193] W. Wang, R. Wang, Q. Zhang, G. Mor, and H. Zhang, "Benzo(a)pyren-7,8-dihydrodiol-9,10-epoxide induces human trophoblast swan 71 cell dysfunctions due to cell apoptosis through disorder of mitochondrial fission/fusion," *Environmental Pollution*, vol. 233, pp. 820–832, 2018.
- [194] M. Murata, K. Fukushima, T. Takao, H. Seki, S. Takeda, and N. Wake, "Oxidative stress produced by xanthine oxidase induces apoptosis in human extravillous trophoblast cells," *The Journal of Reproduction and Development*, vol. 59, no. 1, pp. 7–13, 2013.
- [195] M. C. Velarde and R. Menon, "Positive and negative effects of cellular senescence during female reproductive aging and pregnancy," *The Journal of Endocrinology*, vol. 230, no. 2, pp. R59–R76, 2016.
- [196] Y. Hirota, J. Cha, M. Yoshie, T. Daikoku, and S. K. Dey, "Heightened uterine mammalian target of rapamycin complex 1 (mTORC1) signaling provokes preterm birth in mice," *Proceedings of the National Academy of Sciences of the United States of America*, vol. 108, no. 44, pp. 18073–18078, 2011.
- [197] K. E. Burnum, Y. Hirota, E. S. Baker et al., "Uterine deletion of Trp53 compromises antioxidant responses in the mouse decidua," *Endocrinology*, vol. 153, no. 9, pp. 4568–4579, 2012.
- [198] D. A. Gibson, I. Simitsidellis, O. Kelepouri, H. O. D. Critchley, and P. T. K. Saunders, "Dehydroepiandrosterone enhances decidualization in women of advanced reproductive age," *Fertility and Sterility*, vol. 109, no. 4, pp. 728–734.e2, 2018.
- [199] A. Qin, J. Qin, Y. Jin et al., "DHEA improves the antioxidant capacity of endometrial stromal cells and improves endometrium receptivity via androgen receptor," *European Journal of Obstetrics, Gynecology, and Reproductive Biology*, vol. 198, pp. 120–126, 2016.
- [200] Ö. Çelik, M. Acet, A. İmren et al., "DHEA supplementation improves endometrial HOXA-10 mRNA expression in poor responders," *Journal of the Turkish-German Gynecological Association*, vol. 18, no. 4, pp. 160–166, 2017.
- [201] T. A. Coll, G. Chaufan, L. G. Pérez-Tito, M. R. Ventureira, M. d. C. Ríos de Molina, and E. Cebral, "Cellular and molecular oxidative stress-related effects in uterine myometrial and trophoblast-decidual tissues after perigestational alcohol intake up to early mouse organogenesis," *Molecular and Cellular Biochemistry*, vol. 440, no. 1–2, pp. 89–104, 2018.
- [202] J. E. Hodge, "Dehydrated foods, chemistry of browning reactions in model systems," *Journal of Agricultural and Food Chemistry*, vol. 1, no. 15, pp. 928–943, 1953.
- [203] N. Ahmed, "Advanced glycation endproducts—role in pathology of diabetic complications," *Diabetes Research and Clinical Practice*, vol. 67, no. 1, pp. 3–21, 2005.
- [204] R. G. Paul and A. J. Bailey, "Glycation of collagen: the basis of Its central role in the late complications of ageing and diabetes," *The International Journal of Biochemistry & Cell Biology*, vol. 28, no. 12, pp. 1297–1310, 1996.
- [205] S. Del Turco and G. Basta, "An update on advanced glycation endproducts and atherosclerosis," *BioFactors*, vol. 38, no. 4, pp. 266–274, 2012.
- [206] J. Uribarri and K. R. Tuttle, "Advanced glycation end products and nephrotoxicity of high-protein diets," *Clinical Journal of the American Society of Nephrology*, vol. 1, no. 6, pp. 1293–1299, 2006.
- [207] S. R. Thorpe and J. W. Baynes, "Maillard reaction products in tissue proteins: new products and new perspectives," *Amino Acids*, vol. 25, no. 3–4, pp. 275–281, 2003.
- [208] C. Ott, K. Jacobs, E. Haucke, A. Navarrete Santos, T. Grune, and A. Simm, "Role of advanced glycation end products in cellular signaling," *Redox Biology*, vol. 2, pp. 411–429, 2014.
- [209] J. Xie, J. D. Mendez, V. Mendez-Valenzuela, and M. M. Aguilar-Hernandez, "Cellular signalling of the receptor for advanced glycation end products (RAGE)," *Cellular Signalling*, vol. 25, no. 11, pp. 2185–2197, 2013.
- [210] A. Cerami, "Aging of Proteins and Nucleic Acids: What Is the Role of Glucose?," *Trends in Biochemical Sciences*, vol. 11, no. 8, pp. 311–314, 1986.
- [211] J. Uribarri, M. D. del Castillo, M. P. de la Maza et al., "Dietary advanced glycation end products and their role in health and disease," *Advances in Nutrition*, vol. 6, no. 4, pp. 461–473, 2015.
- [212] S. Ruhs, N. Nass, B. Bartling et al., "Preconditioning with Maillard reaction products improves antioxidant defence leading to increased stress tolerance in cardiac cells," *Experimental Gerontology*, vol. 45, no. 10, pp. 752–762, 2010.
- [213] B. Leuner, S. Ruhs, H. J. Brömme et al., "RAGE-dependent activation of gene expression of superoxide dismutase and vanins by AGE-rich extracts in mice cardiac tissue and murine cardiac fibroblasts," *Food & Function*, vol. 3, no. 10, pp. 1091–1098, 2012.
- [214] A. Simm, S. Ruhs, N. Nass et al., "Physiological and Pathophysiological Importance of Advanced Glycation End-products," *Free Radical Biology and Medicine*, vol. 65, pp. S11, 2013.
- [215] S. Ruhs, N. Nass, V. Somoza et al., "Maillard reaction products enriched food extract reduce the expression of myofibroblast phenotype markers," *Molecular Nutrition & Food Research*, vol. 51, no. 4, pp. 488–495, 2007.
- [216] M. Baumann, "Role of advanced glycation end products in hypertension and cardiovascular risk: human studies," *Journal of the American Society of Hypertension*, vol. 6, no. 6, pp. 427–435, 2012.
- [217] K. de Leeuw, R. Graaff, R. de Vries et al., "Accumulation of advanced glycation endproducts in patients with systemic lupus erythematosus," *Rheumatology*, vol. 46, no. 10, pp. 1551–1556, 2007.
- [218] L. De Groot, M. D. Posthumus, C. G. M. Kallenberg, and M. Bijl, "Risk factors and early detection of atherosclerosis in rheumatoid arthritis," *European Journal of Clinical Investigation*, vol. 40, no. 9, pp. 835–842, 2010.
- [219] V. Srikanth, A. Maczurek, T. Phan et al., "Advanced glycation endproducts and their receptor RAGE in Alzheimer's disease," *Neurobiology of Aging*, vol. 32, no. 5, pp. 763–777, 2011.

- [220] A. Taguchi, D. C. Blood, G. del Toro et al., "Blockade of RAGE-amphoterin signalling suppresses tumour growth and metastases," *Nature*, vol. 405, no. 6784, pp. 354–360, 2000.
- [221] A. Rojas, H. Figueroa, and E. Morales, "Fueling inflammation at tumor microenvironment: the role of multiligand/rage axis," *Carcinogenesis*, vol. 31, no. 3, pp. 334–341, 2010.
- [222] E. A. Oliver, C. S. Buhimschi, A. T. Dulay et al., "Activation of the receptor for advanced glycation end products system in women with severe preeclampsia," *The Journal of Clinical Endocrinology and Metabolism*, vol. 96, no. 3, pp. 689–698, 2011.
- [223] I. U. Jiménez, E. Díaz-Díaz, J. S. Castro et al., "Circulating concentrations of advanced glycation end products, Its association with the development of diabetes mellitus," *Archives of Medical Research*, vol. 48, no. 4, pp. 360–369, 2017.
- [224] S. Li and H. Yang, "Relationship between advanced glycation end products and gestational diabetes mellitus," *The Journal of Maternal-Fetal & Neonatal Medicine*, vol. 32, no. 17, pp. 2783–2789, 2018.
- [225] X. Tang, Q. Qin, X. Xie, and P. He, "Protective effect of sRAGE on fetal development in pregnant rats with gestational diabetes mellitus," *Cell Biochemistry and Biophysics*, vol. 71, no. 2, pp. 549–556, 2015.
- [226] H. Konishi, M. Nakatsuka, C. Chekir et al., "Advanced glycation end products induce secretion of chemokines and apoptosis in human first trimester trophoblasts," *Human Reproduction*, vol. 19, no. 9, pp. 2156–2162, 2004.
- [227] Q. T. Huang, M. Zhang, M. Zhong et al., "Advanced glycation end products as an upstream molecule triggers ROS-induced sFlt-1 production in extravillous trophoblasts: a novel bridge between oxidative stress and preeclampsia," *Placenta*, vol. 34, no. 12, pp. 1177–1182, 2013.
- [228] K. Shirasuna, K. Seno, A. Ohtsu et al., "AGEs and HMGB1 increase inflammatory cytokine production from human placental cells, resulting in an enhancement of monocyte migration," *American Journal of Reproductive Immunology*, vol. 75, no. 5, pp. 557–568, 2016.
- [229] K. Seno, S. Sase, A. Ozeki et al., "Advanced glycation end products regulate interleukin-1 β production in human placenta," *The Journal of Reproduction and Development*, vol. 63, no. 4, pp. 401–408, 2017.
- [230] M. Lappas, M. Permezel, and G. E. Rice, "Advanced glycation endproducts mediate pro-inflammatory actions in human gestational tissues via nuclear factor- κ B and extracellular signal-regulated kinase 1/2," *The Journal of Endocrinology*, vol. 193, no. 2, pp. 269–277, 2007.
- [231] L. Jiang, J. Yan, and L. Wu, "Study of the relationship between AGEs and oxidative stress damage to trophoblast cell mitochondria," *Ginekologia Polska*, vol. 88, no. 7, pp. 372–378, 2017.

Research Article

Testicular Toxicity of Water Pipe Smoke Exposure in Mice and the Effect of Treatment with Nootkatone Thereon

Badreldin H. Ali,¹ Suhail Al-Salam ,² Sirin A. Adham,³ Khalid Al Balushi ,¹ Mohammed Al Za'abi,¹ Sumaya Beegam,⁴ Priya Yuvaraju,⁴ Priyadarsini Manoj,¹ and Abderrahim Nemmar ⁴

¹Department of Pharmacology and Clinical Pharmacy, College of Medicine and Health Sciences, Sultan Qaboos University, Muscat, Oman

²Department of Pathology, College of Medicine and Health Sciences, UAE University, Al Ain, UAE

³Department of Biology, College of Science, Sultan Qaboos University, Muscat, Oman

⁴Department of Physiology, College of Medicine and Health Sciences, UAE University, Al Ain, UAE

Correspondence should be addressed to Abderrahim Nemmar; anemmar@uaeu.ac.ae

Received 6 February 2019; Accepted 2 June 2019; Published 25 June 2019

Guest Editor: Henrique Almeida

Copyright © 2019 Badreldin H. Ali et al. This is an open access article distributed under the Creative Commons Attribution License, which permits unrestricted use, distribution, and reproduction in any medium, provided the original work is properly cited.

There is a worldwide increase in the popularity of water pipe (shisha) tobacco smoking including in Europe and North America. However, little is known about the effects of water pipe smoke (WPS) exposure on male reproductivity. We have recently demonstrated that WPS exposure in mice induces testicular toxicity including inflammation and oxidative stress. Nootkatone, a sesquiterpenoid found in grapefruit, has antioxidant and anti-inflammatory effects. However, the possible protective effect of nootkatone on WPS-induced testicular toxicity has not been reported before. Here, we tested the effects of treatment of mice with nootkatone on WPS-induced testicular toxicity. Mice were exposed to normal air or WPS (30 minutes/day, for 30 days). Nootkatone (90 mg/kg) was given orally to mice by gavage, 1 h before WPS or air exposure. Nootkatone treatment significantly ameliorated the WPS-induced increase in plasma levels of inhibin, uric acid, and lactate dehydrogenase activity. Nootkatone also significantly mitigated the decrease in testosterone, androgen-binding protein, and estradiol concentrations in the plasma induced by WPS. In testicular homogenates, WPS exposure caused a decrease in the total nitric oxide level and an increase in the proinflammatory cytokine interleukin-1 β level and oxidative stress markers including malondialdehyde, cytochrome C, and 8-Oxo-2'-deoxyguanosine. All the latter effects were significantly alleviated by nootkatone treatment. Moreover, in testicular homogenate, nootkatone inhibited the expression of nuclear factor-kappaB induced by WPS. Likewise, histological examination of mouse testes showed that nootkatone treatment ameliorated the deterioration of spermatogenesis induced by WPS exposure. We conclude that nootkatone ameliorated the WPS-induced testicular inflammation and oxidative stress and hormonal and spermatogenesis alterations.

1. Introduction

Tobacco consumption is an established major public health problem that results in substantial morbidity and mortality [1, 2]. Water pipe smoking (WPS) (also termed *huqqa*, *sheesha*, *nargilah*, *hubble-bubble*, and *qalyan*), an ancient and common method of tobacco consumption in Asia and North Africa [3, 4], is regaining widespread global popularity, especially among the young population in Western countries [5, 6]. It involves passage of air that

is heated by charcoal across tobacco flavored by or sweetened with either fruit or molasses sugar, which makes the smoke more aromatic than cigarette smoke. Contrary to common belief, the smoke produced from the heated tobacco in WPS is equally or even more toxic than cigarette smoke [7, 8]. WPS has been proven to be more genotoxic than cigarette smoking [9].

Nootkatone (C₁₅H₂₂O) is a sesquiterpenoid isolated from some plants such as grapefruit and rhizomes of *Cyperus rotundus* and has been reported before to significantly

mitigate DNA damage in mice exposed to diesel exhaust particles, and thrombogenicity and systemic and cardiac oxidative stresses, by mechanisms which may include heme oxygenase-1 and nuclear factor erythroid-derived 2-like 2 activation [10]. It has also been shown to possess anti-inflammatory and antioxidant actions in lung tissues of mice [11].

We have previously reported that subacute and chronic WPS exposure exerts deleterious effects on the testes of mice [12, 13]. These adverse effects included reductions in the plasma concentrations of some reproductive hormones and increased oxidative stress and inflammation biomarkers in plasma and testes. As nootkatone is reported to counteract the latter two actions [10, 11], it was of interest to investigate if treatment of WPS-exposed mice with this agent would ameliorate the testicular toxicity of WPS.

2. Materials and Methods

2.1. Animals and WPS Exposure. This research was reviewed and sanctioned by the Institutional Review Board of the College of Medicine and Health Sciences (UAEU), and experiments were conducted according to the protocols approved by the Institutional Animal Care and Research Advisory Committee.

Thirty-two male BALB/c mice (Taconic Farms Inc., Germantown, NY, USA) were housed in a conventional animal house at controlled temperature (at 26°C) and humidity of 60% and maintained on a 12-hour light-dark cycle (lights on at 6:00 am). Mice were randomly placed, eight each, in a plastic cage and were given *ad libitum* supply of water and a standard pellet diet. The animals were left to acclimatize for a week and then were randomly divided into four equal groups: air-exposed (control), WPS-exposed, nootkatone-treated (90 mg/kg, by oral gavage), and exposed to WPS and treated with nootkatone (90 mg/kg, by oral gavage) groups. The treatments were given for 30 min daily for 30 consecutive days. This dose was selected from previous research conducted in our laboratory on nootkatone [10].

Mice were positioned in soft restraints and connected to the exposure tower [13]. The animals were exposed to either WPS or air through their noses using a nose-only exposure system connected to a water pipe (inExpose System, SCIREQ, Canada). The details of the exposure were reported in a previous publication (e.g., [14]). Mice were exposed to a commercial product of apple-flavored tobacco (Al Fakher Tobacco Trading, Ajman, UAE). Tobacco was lit with an instant light charcoal disk (Star, 3.5 cm diameter and 1 cm width). As is the case for human use, the smoke from the water pipe first passes through the water before it is drawn into the exposure tower. The exposure regimen is controlled by a computerized system (inExpose System, SCIREQ, Canada). A computer-controlled puff was generated every minute, leading to a two-second puff duration of WPS exposure followed by 58 s of fresh air. The duration of each exposure session was 30 min/day.

Following the last exposure session to WPS or air, mice in the four groups were immediately placed in metabolic cages

TABLE 1: Effect of treatment with nootkatone on the urine cotinine level in mice daily exposed to water pipe smoke for 30 days.

Group	Cotinine (ng/mL)
AE	0.66 ± 0.14
WPS	1.92 ± 0.21 ^a
NK	0.78 ± 0.12
WPS + NK	1.31 ± 0.10 ^{a,b,c}

The values in the table are mean ± SEM ($n = 7$). Nootkatone (90 mg/kg/day) was given to the mice by oral gavage for 30 days. AE: air exposure; WPS: water pipe smoke; NK: nootkatone. Different superscripts indicate significance as follows ($P < 0.05$ was considered significant): a denotes significance of the control group vs. different groups, b denotes significance of the WPS group vs. the WPS + NK-treated group, and c denotes significance of the NK group vs. the WPS + NK-treated group.

and urine of each mouse was collected over a 24 h period and the volume was measured. Immediately after urine collection, mice were anesthetized with sodium pentobarbital (45 mg/kg, i.p.) and blood was collected from the inferior vena cava in tubes with the anticoagulant ethylenediaminetetraacetic acid (EDTA) (4%). The collected blood was spun at 4°C for 15 min at $900 \times g$, and the plasma obtained was stored at -80°C to await analysis.

Mice were then sacrificed with an overdose of anesthesia. The testes from all animals were collected and rinsed with ice-cold PBS (pH 7.4) and weighed. The left and half of the right testis were immediately frozen at -80°C pending biochemical and molecular analyses. The other half of the right testis was used for histologic al studies.

2.2. Biochemical Tests in Plasma. Androgen-binding protein (ABP) and inhibin concentrations in plasma were measured by ELISA kits purchased from BioSource company (San Diego, CA, USA) and CUSABIO (Hubei, Wuhan, China), respectively. Plasma uric acid was measured using an autoanalyzer BS-120 (Mindray, Shenzhen, China). Lactate dehydrogenase (LDH) activity was measured using a kit from Abcam (Cambridge, UK).

2.3. Urine Cotinine Analysis. The concentration of cotinine, the nicotine metabolite in urine, was measured by an ELISA kit from Creative Diagnostics (Shirley, NY, USA).

2.4. Assessment of Testicular Oxidant/Antioxidant Status. The testes were dissected out, and the right testis from each mouse was thoroughly washed with ice-cold normal saline, weighed, and minced. Part of the testis was homogenized (10% *w/v*) in cold potassium phosphate buffer (pH 7.4, 0.05 M), and the homogenate was centrifuged at 1500 g for 10 min at 4°C. Thereafter, a colorimetric kit from BioVision (Milpitas, CA, USA) was used for the estimation of lipid peroxidation as malondialdehyde (MDA) concentration in the testicular supernatant. Total nitric oxide (NO) and nitrite/nitrate in the testicular supernatant were measured using a kit from R&D Systems (Minneapolis, MN, USA). Testicular protein was estimated using the BCA Protein Quantitation Kit from BioVision (Milpitas, CA, USA).

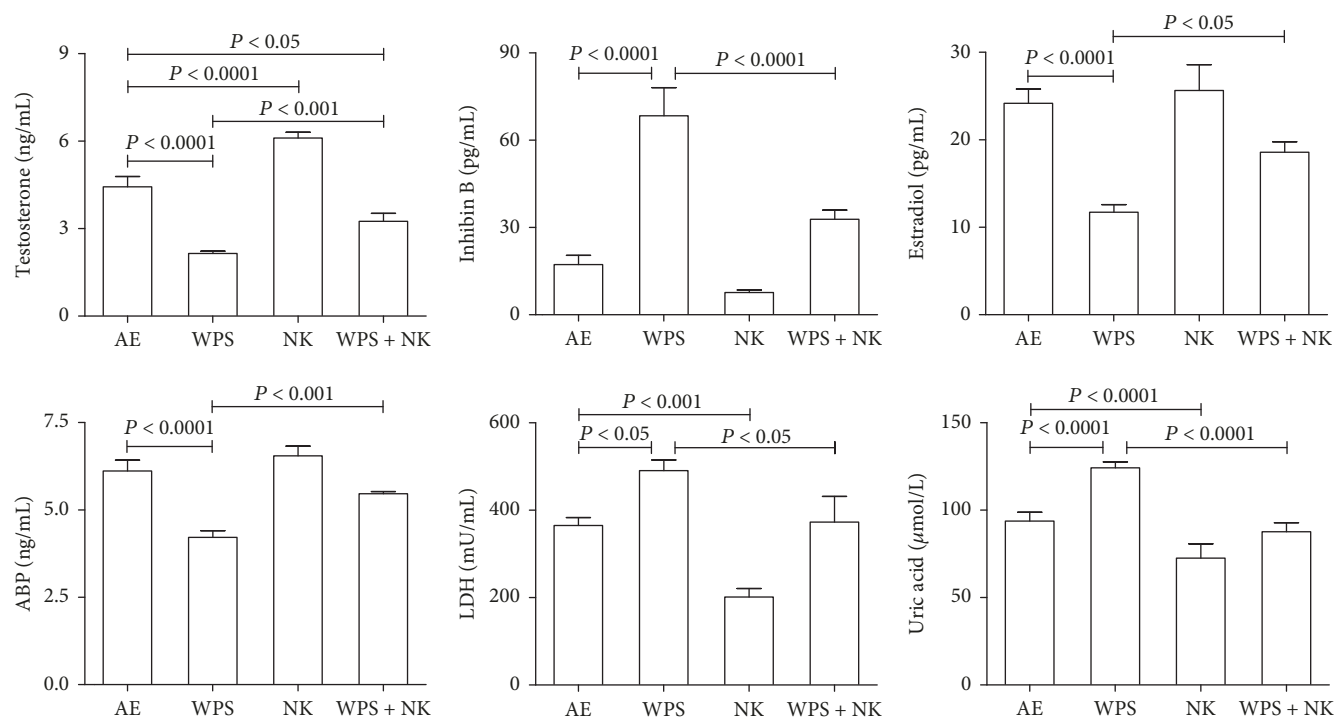


FIGURE 1: The plasma concentrations of testosterone, inhibin B, estradiol, androgen-binding protein (ABP), lactate dehydrogenase (LDH), and uric acid in mice exposed to normal air (AE) or water pipe smoking (WPS) (30 min/day) with or without treatment with nootkatone (NK) (90 mg/kg/day). Each vertical column with a bar represents the mean \pm SEM (from 8 mice in each group). P less than 0.05 was considered significant.

Part of the testicular homogenate was centrifuged at 9391 g for 30 min at 4°C. Cytosolic fraction (supernatant) obtained was used to measure cytochrome C using an R&D Systems ELISA kit (Minneapolis, MN, USA). The remaining supernatant was centrifuged at 10000 g for 20 min at 4°C. The supernatant obtained was further centrifuged at 12000 g for 20 min at 4°C to obtain the postmitochondrial supernatant, which was used for the estimation of interleukin-1beta (IL-1 β) and 8-hydroxy-2'-deoxyguanosine (8-OHdG) using ELISA kits purchased from Thermo Fisher Scientific (Waltham, MA, USA) and BioVision (Milpitas, CA, USA), respectively.

2.5. Histopathological Assessment. A piece of the testis was taken from randomly selected five controls and six WPS-exposed animals, five nootkatone-treated animals, and six mice treated with either NK or nootkatone + WPS and placed first in Bouin's fluid for an hour, then transferred to 10% formalin, and processed as described before [13]. Four μ m sections were prepared from paraffin blocks and stained with hematoxylin and eosin.

The stained sections were assessed in a blinded fashion by a pathologist using an Olympus microscope (EX41, Tokyo, Japan). Spermatogenesis was evaluated using Johnsen's mean testicular biopsy score (MTBS) criteria [15]. A score of 1–10 was given to each tubule according to germ cell maturation (1, neither germ cells nor Sertoli cells are present; 2, Sertoli cells without germ cells; 3, only spermatogonia; 4, only a few spermatocytes; 5, many spermatocytes; 6, only a few early spermatids; 7, no spermatozoa but many spermatids are present; 8, only a few spermatozoa are present; 9, many spermatozoa are present but spermatogenesis is disorganized; and 10, complete spermatogenesis and perfect tubules). For these evaluations, MTBS was calculated in 100 tubules of each testes using an Olympus E41 Microscope.

2.6. Western Blotting Technique. Testis protein expression for NF- κ B was estimated using Western blotting technique. Briefly, testis tissues collected from the mice were immediately snap frozen with liquid nitrogen and stored at -80°C . Later, the tissues were weighed, rinsed with saline, and homogenized with lysis buffer (Cell Signaling Technology, USA). Protease and phosphatase inhibitors (Sigma, Berlin, Germany) were added to the protein lysate samples. The homogenates were centrifuged for 20 min at 4°C. Protein estimation was done in the supernatants collected using a Pierce bicinchoninic acid (BCA) protein assay kit (Thermo Fisher, Waltham, MA, USA). Protein lysate samples were all adjusted to have 100 μ g of total protein per sample and were electrophoretically separated using 12% sodium dodecyl sulfate polyacrylamide gel electrophoresis (SDS-PAGE) and then transferred onto polyvinylidene difluoride membranes (Bio-Rad, Hercules, CA, USA). The immunoblots were then blocked with 5% nonfat milk and subsequently probed with either the NF- κ B p65 (ab ab16502) or the GAPDH (ab8245) (Abcam, UK) at a 1 : 1000 dilution, incubated at 4°C as a normalizing internal control overnight.

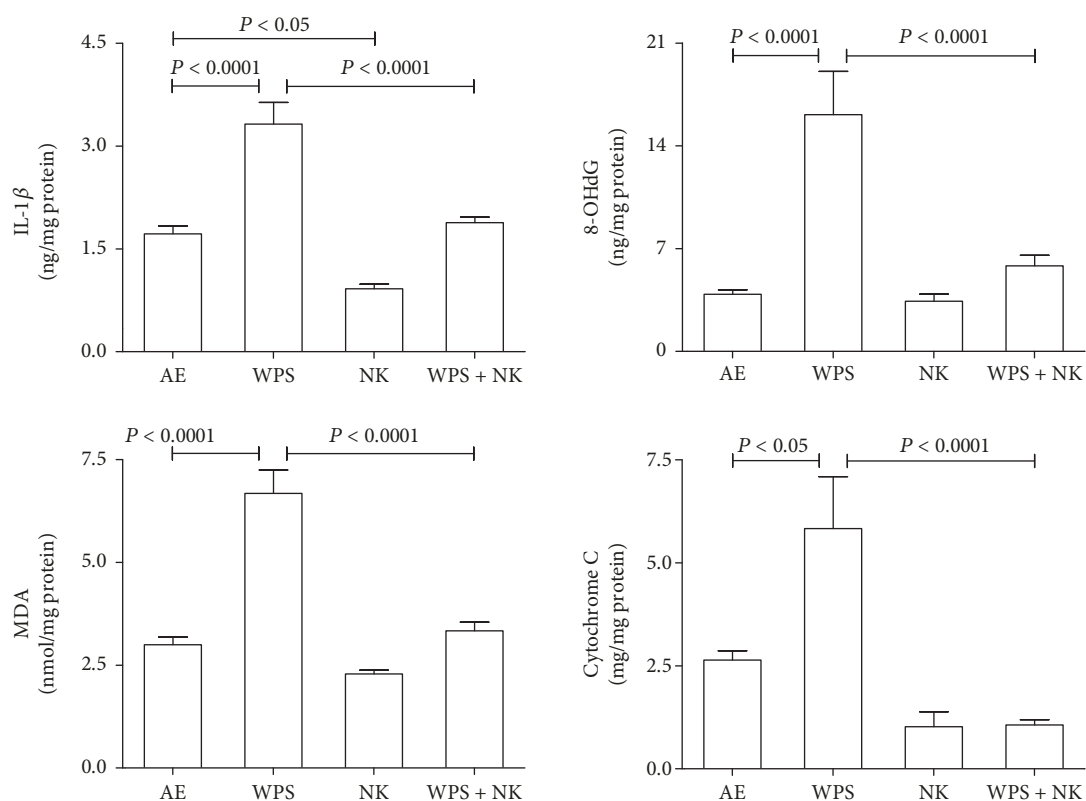


FIGURE 2: The testicular homogenate concentrations of interleukin-1 β (IL-1 β), 8-Oxo-2'-deoxyguanosine (8-OHdG), malondialdehyde (MDA), and cytochrome C in mice exposed to normal air (AE) or water pipe smoking (WPS) (30 min/day) with or without treatment with nootkatone (NK) (90 mg/kg/day). Each vertical column with a bar represents the mean \pm SEM (from 8 mice in each group). P less than 0.05 was considered significant.

The blots were then washed three times for 5 minutes and incubated with goat anti-rabbit IgG horseradish peroxidase-conjugated secondary antibody at 1:5000 dilutions (Abcam, Cambridge, UK) for 2 h at room temperature and developed using the clarity Western ECL Substrate (Bio-Rad, Hercules, CA, USA). The densitometric analysis of the protein bands was performed using the Image Lab™ software (Bio-Rad, USA).

2.7. Immunofluorescence. Mouse testes were embedded in paraffin blocks, and sections 3 mm thick were placed on positively charged slides. The slides were deparaffinized and dehydrated, and antigen retrieval was done in 200 mM EDTA solution at pH 9 for 30 minutes at 90°C. The activity of endogenous peroxidases was blocked by adding 2% hydrogen peroxide for 15 min. The slides were washed twice in phosphate buffer saline (PBS) (Sigma, Germany) and then in PBS + 0.05% Triton X-100 for 5 min each. The slides were incubated with a blocking solution of 5% normal goat serum for 30 min at room temperature and then incubated overnight at 4°C with anti-8-hydroxy-2'-deoxyguanosine antibody (ab48508) diluted in antibody diluent (Dako, USA). After washing 3 times with 1 \times PBS (Sigma, Germany), the slides were incubated with (1:500) secondary antibody (anti-rabbit conjugated to Alexa Fluor® 488 fluorescent dye) (Cell Signaling, USA) for 1 hour. DAPI (Cell Signaling Technology), the nuclear stain (1250), was added for 3 min.

Finally, slides were mounted by fluorescent mounting media (Dako, USA) and visualized under the fluorescent microscope (Nikon H600L), with digital a camera (DS-Ri2) and the imaging software NIS-Elements version 4.40.

2.8. Drugs, Chemicals, and Kits. Nootkatone was brought from Sigma-Aldrich (St. Louis, MI, USA). All the other chemicals used were of the highest grade available. The sources of each kit used were mentioned above.

2.9. Statistical Analysis. Values obtained are reported as mean \pm standard error of the mean (SEM). Statistical significance was assessed by one-way analysis of variance (ANOVA) followed by Bonferroni's multiple comparison tests using GraphPad Prism software, version 5.03. To ascertain if parameters were normally distributed, the KD normality test was applied and $P < 0.05$ was considered significant.

3. Results

3.1. Body and Testicular Weight. WPS exposure, with or without nootkatone, did not significantly affect the body weight of treated mice or their absolute testis weights. WPS exposure, however, slightly increased the relative testis weight, an effect that was significantly mitigated by nootkatone concomitant treatment.

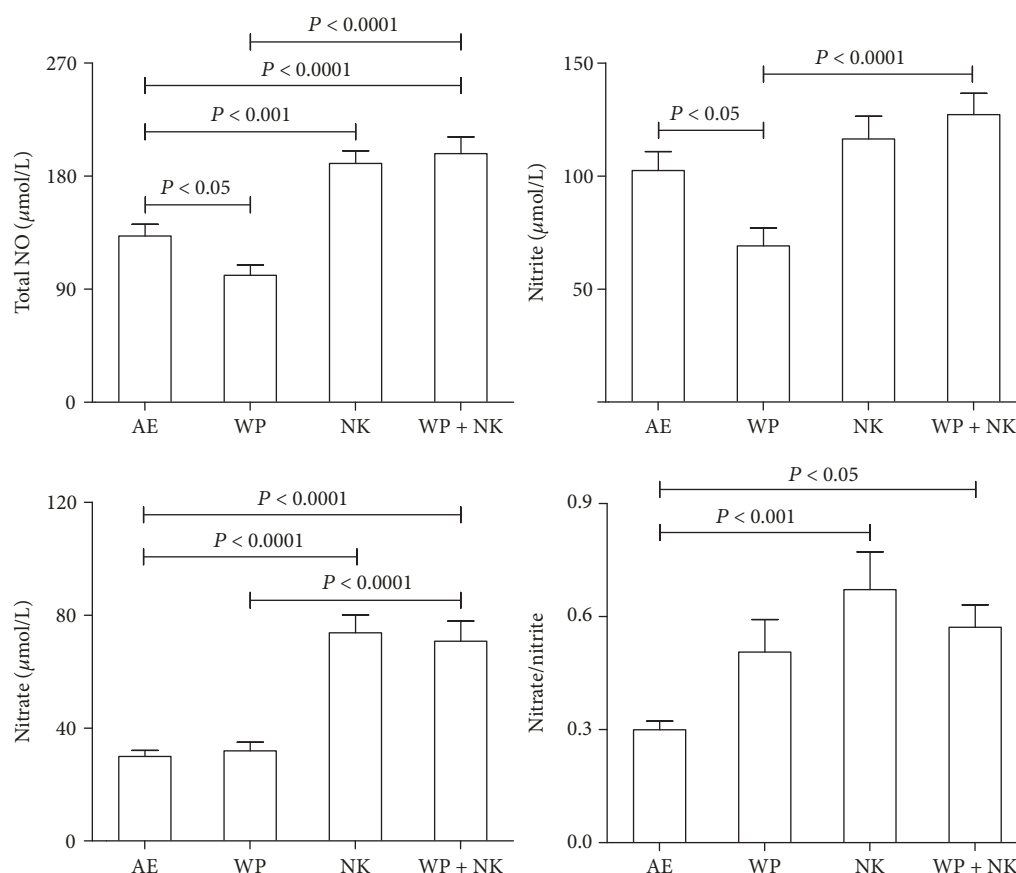


FIGURE 3: The concentrations of nitrite, nitrate, total nitric oxide, and nitrite/nitrate in testicular homogenates of mice exposed to normal air (AE) or water pipe smoking (WPS) (30 min/day) with or without treatment with nootkatone (NK) (90 mg/kg/day). Each vertical column with a bar represents the mean \pm SEM (from 7 mice in each group). P less than 0.05 was considered significant.

3.2. Urinary Cotinine Concentration. Table 1 depicts the concentration of the nicotine metabolite, cotinine, in urine of controls, WPS-exposed, nootkatone-treated, and WPS-exposed + nootkatone-treated mice. The cotinine urinary level in WPS-exposed mice was 191% higher than that in control mice. Coadministration of WPS and nootkatone reduced the level to 98.5%.

3.3. Plasma Analytes. As shown in Figure 1, WPS exposure significantly increased the concentrations of inhibin and uric acid, as well as the activity of LDH. The exposure also significantly decreased the plasma concentrations of testosterone, androgen-binding protein, and estradiol ($P < 0.0001$). Nootkatone treatment significantly ameliorated the WPS-induced increase in plasma levels of inhibin, uric acid, and lactate dehydrogenase activity. Nootkatone also significantly mitigated the decrease in testosterone, androgen-binding protein, and estradiol concentrations in the plasma induced by WPS.

3.4. Assessment of Testicular Inflammatory and Oxidative Stress Status. As shown in Figure 2, WPS exposure significantly increased the concentrations of IL-1 β , 8-OHdG, MDA, and cytochrome C when compared to the controls ($P < 0.05$ – $P < 0.0001$). Nootkatone treatment alone significantly reduced the inflammatory cytokine ($P < 0.05$) when

compared to the control and did not affect the other testicular analytes measured. Simultaneous exposure to WPS and nootkatone treatment significantly mitigated the increase in the four measured analytes induced by WPS exposure ($P < 0.05$ – $P < 0.0001$).

3.5. Assessment of Testicular Nitrosative Stress Status. These results are shown in Figure 3. WPS exposure significantly reduced total NO and nitrite levels ($P < 0.05$ – $P < 0.001$) but did not significantly affect nitrate levels, when compared to the controls. WPS exposure raised the ratio of nitrate to nitrite insignificantly. Concomitant exposure to WPS and nootkatone treatment significantly mitigated the decrease in the total NO and nitrite analytes induced by WPS exposure ($P < 0.05$ – $P < 0.0001$).

3.6. WPS and the Proinflammatory Marker NF- κ B p65. Western blot analysis shown in Figure 4 indicated a significant increase in the proinflammatory marker NF- κ B p65 in the testes of mice exposed to WPS. Nootkatone treatment alone showed a slight increase in NF- κ B when compared with that from the untreated controls. Concomitant administration of nootkatone to mice exposed to WPS significantly reduced the levels of NF- κ B p65 compared to those expressed in the testes exposed to WPS alone ($P < 0.0001$).

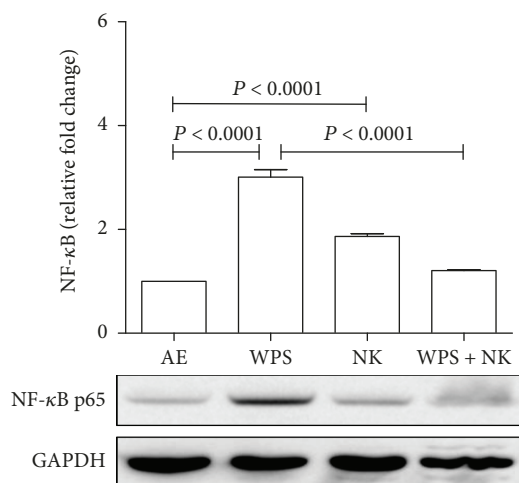


FIGURE 4: Representative Western blots indicated that proinflammatory NF- κ B was increased in the mouse testes as a result of WPS exposure and nootkatone reduced its effect. Densitometry quantification of two independent blots using Image Lab software showed that the NF- κ B in the testes of mice exposed to WPS was significantly increased compared to that of the control and/or nootkatone-treated mice. Nootkatone caused a slight increase in NF- κ B. However, its use along with WPS exposure caused a significant reduction in mice treated with nootkatone and exposed to WPS. The error bars represent the standard error of the mean of two independent experimental replicates. P less than 0.05 was considered significant.

3.7. DNA Oxidative Damage in Testicular Tissue. As shown in Figure 5, the DNA oxidative damage in the immunofluorescent-stained testis sections was measured by quantifying the nuclear staining of 8-Oxo-2'-deoxyguanosine (8-Oxo-dG) represented by the green fluorescence in the nucleus. The latter overlapped with the nuclear stain DAPI in the testes of mice exposed to WPS but was not detected in controls, mice treated with nootkatone alone, or mice treated with nootkatone plus WPS exposure.

Control (AE) and nootkatone-treated mice showed considerably less oxidative damage than that seen in WPS-exposed mice. WPS markedly increased the DNA oxidative damage, represented by the increase in the intensity of 8-Oxo-dG (fluorescent green stain), evident in the nucleus of spermatocytes of WPS-treated mice. WPS-exposed mice treated with nootkatone had substantially less oxidative damage than WPS-exposed mice.

3.8. Histopathology. Figure 6 illustrates the histopathological examination of mouse testes in the 4 studied groups. In the control group, there was a complete spermatogenesis in 31% of the seminiferous tubules (score 10) (Table 2). In other areas of the control group, many spermatozoa were present but there was disorganized spermatogenesis in 38% of the seminiferous tubules (score 9) (Table 2). Moreover, only a few spermatozoa were present in 19% of the seminiferous tubules (score 8) (Table 2). The spermatogenesis was affected in some of the seminiferous tubules in which 12% of the tubules showed no spermatozoa and where there was a block differentiation at the

spermatid level (Table 2). The overall MTBS score of the control group is 8.8.

In the WPS group, there was a complete spermatogenesis in 14% of the seminiferous tubules (score 10) (Table 2). In other areas of the WPS group, many spermatozoa were present but there was disorganized spermatogenesis in 31% of the seminiferous tubules (score 9) (Table 2). Also, only a few spermatozoa were present in 35% of the seminiferous tubules (score 8) (Table 2). The spermatogenesis was affected in some of the seminiferous tubules in which 20% of the tubules showed no spermatozoa and where there was a block differentiation at the spermatid level (Table 2). The overall MTBS score of the WPS group is 8.31.

In the NK group, there was a complete spermatogenesis in 33% of the seminiferous tubules (score 10) (Table 2). In other areas of the NK group, many spermatozoa were present but there was disorganized spermatogenesis in 33% of the seminiferous tubules (score 9) (Table 2). Furthermore, only a few spermatozoa were present in 19% of the seminiferous tubules (score 8) (Table 2). The spermatogenesis was affected in some of the seminiferous tubules in which 15% of the tubules showed no spermatozoa and where there was a block differentiation at the spermatid level (Table 2). The overall MTBS score of the NK group is 8.79.

In the WPS + NK group, there was a complete spermatogenesis in 30% of the seminiferous tubules (score 10) (Table 2). In other areas of the WPS + NK group, many spermatozoa were present but there was disorganized spermatogenesis in 28% of the seminiferous tubules (score 9) (Table 2). Furthermore, only a few spermatozoa were present in 26% of the seminiferous tubules (score 8) (Table 2). The spermatogenesis was affected in some of the seminiferous tubules in which 16% of the tubules showed no spermatozoa and where there was a block differentiation at the spermatid level (Table 2). The overall MTBS score of the WPS + NK group is 8.66.

4. Discussion

In this work, 30 min daily exposure of mice for one month to WPS significantly decreased the plasma concentrations of testosterone, estradiol, and androgen-binding protein and increased that of inhibin B and uric acid and LDH activity. These results confirm and extend the previously reported deleterious effects of WPS on male reproduction in mice [12, 13]. As far as we are aware, there are no data on the effect of WPS on human reproduction. The previous research in humans have shown that the information about the effect of cigarette smoking on male and female sex hormones is at variance (reviewed by [16]). In view of the current wide use of WPS in many regions of the world, the effect of active and passive WPS exposure on various aspects of human reproduction is warranted, especially in countries where pregnant women are commonly exposed to passive smoking or use cigarettes and/or WPS [17].

Uric acid was measured in the plasma in this work because it is known to cause endothelial dysfunction, which is an important feature for erectile dysfunction [18]. The

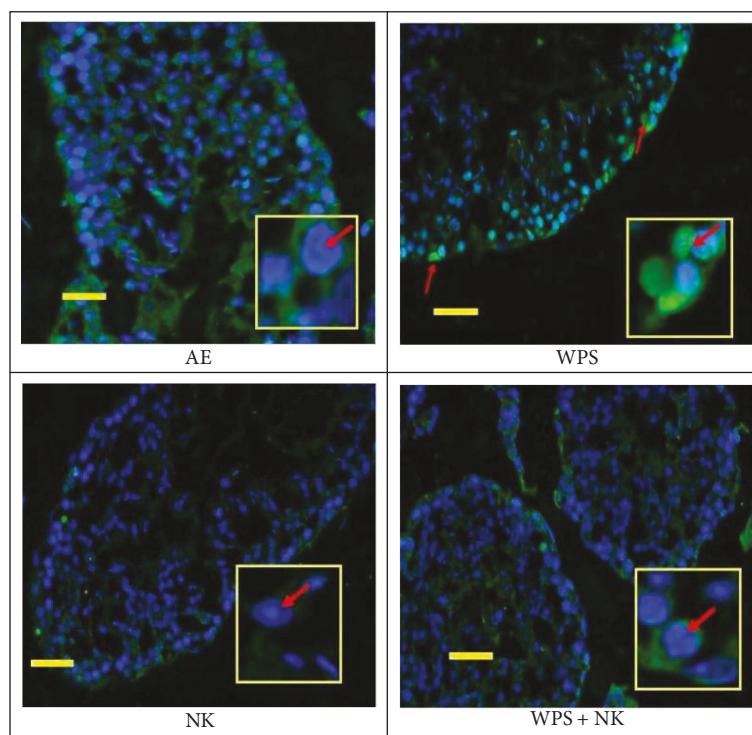


FIGURE 5: DNA oxidation damage was observed in mouse testes as a result of WPS use in mice. 8-Oxo-2'-deoxyguanosine/DAPI staining for mouse testes showed no nuclear disposition in control mice (a); an increase in the DNA oxidation represented by the increase in the intensity of 8-Oxo-dG (fluorescent green stain) in the nucleus of spermatocytes of the water pipe smoke- (WPS-) treated mice (b). The use of nootkatone in mice exposed to air (c) and the use of nootkatone for the mice exposed to WPS reduced the oxidation damage, and there was no nuclear disposition of 8-Oxo-dG (d).

latter occurs via decreased NO production. Our results showed that testicular NO concentration is decreased in WPS-exposed mice. This is a direct evidence for the implication of both NO and uric acid in the deleterious effects of WPS on male reproduction in mice. It has been suggested that addiction to cigarette smoking (CS) involves inhaled NO from CS, in addition to endogenous NO released from nervous tissue following stimulation of nicotinic acetylcholine receptors by nicotine, and that CS causes dysfunction in the endothelial nitric oxide synthase [19]. The same possible mechanism may occur with WPS.

Previously we found a significant increase in LDH activity in bronchoalveolar lavage (BAL) fluid of mice exposed to WPS, suggesting cytolysis, and proteins in BAL fluid, reflecting increased epithelial permeability [20]. In the present study, WPS exposure significantly increased the LDH activity in plasma, an action that was ameliorated by nootkatone. Such effect has never been reported before. LDH activity in plasma and testes has long been known to positively correlate with exposure to toxicants. In humans, CS has been shown to increase LDH activity in serum and saliva, suggesting that it can be used as an indicator of tissue damage in the oral cavity [21]. However, no such action has been reported in humans exposed to WPS.

In this work, we found that WPS exposure significantly increases the oxidative and nitrosative free radicals and increased lipid peroxidation, as assessed by malondialdehyde measurement. Oxidative and nitrosative stresses are known

to be associated with deleterious effects on male reproduction, as they disrupt the integrity of sperm DNA and diminish the fertilizing potential of the reproductive cells due to collateral damage inflicted upon proteins and lipids in the sperm plasma membrane [22]. Excess free radical load due to increased reactive oxygen species and nitric oxide generation may cause severe testicular oxidative damage by causing peroxidation of lipids and formation of carbonyls [23].

We evaluated DNA damage in the testicular homogenates by measuring 8-OHdG levels. 8-OHdG is one of the prominent forms of free radical-induced oxidative lesions in DNA and has therefore been widely used as a biomarker of nucleic damage owing to oxidative damage [24]. It has also been used as a reliable biomarker for measuring oxidative damage, detecting male infertility, and investigating sperm DNA fragmentation [25].

Cytochrome C plays a principal role in the electron transport chain in mitochondria. It has been shown that exposure of mice to cigarette smoke [26] or WPS [27] induces oxidative stress causing a rise in the expression or release of cytochrome C in cardiac cells, suggesting mitochondrial damage. Here, we have shown that cytochrome C concentration is also elevated in testicular homogenates of mice exposed to WPS, an action that was significantly reversed by nootkatone.

The NF- κ B p65 level was also found to be increased by WPS exposure. This protein complex controls transcription of DNA, cytokine production, and cell survival and plays

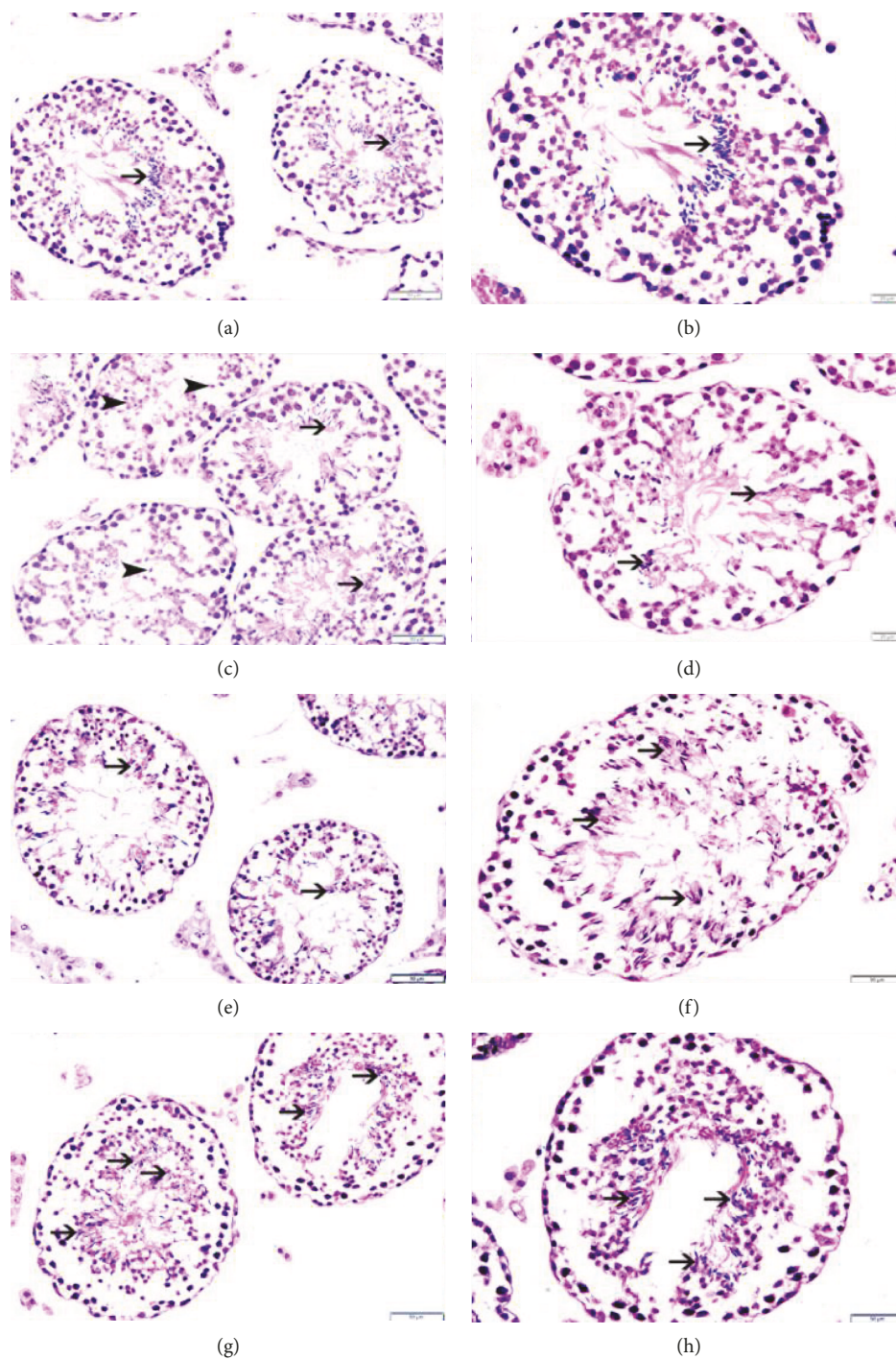


FIGURE 6: Histopathological examination of mouse testes in the air (control), water pipe smoke (WPS), nootkatone (NK), and WPS + NK groups: (a, b) representative sections from testes of the control group showing well-maintained spermatogenesis with spermatozoa (thin arrow) in seminiferous tubules; (c, d) representative sections from testes of the WPS group showing well-maintained spermatogenesis with spermatozoa (thin arrow) in seminiferous tubules, while some of the tubules show no spermatozoa but spermatids in seminiferous tubules (arrowhead); (e, f) representative sections from testes of the NK group showing well-maintained spermatogenesis with spermatozoa (thin arrow) in seminiferous tubules; (g, h) representative sections from testes of the WP + NK group showing a well-maintained spermatogenesis with spermatozoa (thin arrow) in seminiferous tubules.

an important role in several pathophysiological processes such as immune reaction, inflammation, and apoptosis [28]. It is possible that an inflammatory response is triggered due to an oxidative stress in the tissues (including testes) in

response to WPS (as indicated in this work by the significant elevation of $IL-1\beta$ in plasma). This confirms the role of redox-sensitive transcription factors in the pathway of signaling the proinflammatory mediators such as $NF-\kappa B$ [29]. We

TABLE 2: Frequency of Johnsen's mean testicular biopsy score in experimental groups.

Score	Johnsen's score									
	10	9	8	7	6	5	4	3	2	1
AE	31%	38%	19%	9%	2%	1%	0%	0%	0%	0%
WPS	14%	31%	35%	16%	2%	2%	0%	0%	0%	0%
NK	33%	33%	19%	11%	2%	2%	0%	0%	0%	0%
WPS + NK	30%	28%	26%	11%	4%	1%	0%	0%	0%	0%

The data are expressed in % of the seminiferous tubules which achieved a particular Johnsen's score in the air exposure (AE), water pipe smoke (WPS), nootkatone (NK), and WPS + NK groups ($n = 5-6$). Nootkatone (90 mg/kg/day) was given to the mice by oral gavage for 30 days, 1 h before WPS or air exposure.

have recently shown that WPS increases the expression of NF- κ B in lung tissues and exercise training inhibits the signaling pathways that lead to activation of NF- κ B [28]. The inhibitory action of nootkatone on signaling pathways that lead to activation of NF- κ B has been reported before in isolated HaCaT cells [30].

Our work revealed a significant increase in testicular 8-OHdG after WPS exposure, an action that was significantly reversed by concomitant treatment with nootkatone. It has recently been confirmed that the use of WPS in healthy humans significantly increases this DNA damage marker [31]. Moreover, the histological examination of testes revealed that WPS induces alteration of spermatogenesis and that nootkatone treatment ameliorated this effect. Such finding has never been reported before.

In the present study, we did not measure nicotine concentration in our experimental animals due to several technical challenges. Instead, we measured the urinary cotinine concentrations in all of these mice. Cotinine is the main tobacco-specific metabolite of nicotine and is considered an established marker of tobacco exposure, whereby subjects with higher levels of cotinine are considered to be more exposed to nicotine [32].

We conclude that nootkatone ameliorated the WPS-induced testicular inflammation and oxidative stress and hormonal and spermatogenesis alterations. Our study provides experimental evidence that the use of nootkatone, pending further pharmacological and toxicological studies, can be considered a useful agent and could have the potential to alleviate the testicular toxicity induced by WPS.

Data Availability

The data that support the findings of this study are available from Professors Badreldin H. Ali and Abderrahim Nemmar upon reasonable request.

Conflicts of Interest

The authors declare that they have no conflicts of interest.

Acknowledgments

This research was funded by a joint grant from the United Arab Emirates University (UAEU), Sultan Qaboos University (CL/SQU-UAEU/18/01), and College of Medicine and Health Sciences, United Arab Emirates University.

References

- [1] GBD 2015 Tobacco Collaborators, "Smoking prevalence and attributable disease burden in 195 countries and territories, 1990–2015: a systematic analysis from the Global Burden of Disease Study 2015," *The Lancet*, vol. 389, no. 10082, pp. 1885–1906, 2017.
- [2] K. Szyfter, M. Napierala, E. Florek et al., "Molecular and health effects in the upper respiratory tract associated with tobacco smoking other than cigarettes," *International Journal of Cancer*, vol. 144, no. 11, pp. 2635–2643, 2019.
- [3] N. H. Al-Rawi, A. S. Alnuaimi, and A. T. Uthman, "Shisha smoking habit among dental school students in the United Arab Emirates: enabling factors and barriers," *International Journal of Dentistry*, vol. 2018, Article ID 2805103, 11 pages, 2018.
- [4] M. Ataeiasl, P. Sarbakhsh, H. Dadashzadeh, C. Augner, M. Anbarlouei, and A. Mohammadpoorasl, "Relationship between happiness and tobacco smoking among high school students," *Epidemiology and Health*, vol. 40, article e2018009, 2018.
- [5] T. E. Barnett, T. Smith, Y. He et al., "Evidence of emerging hookah use among university students: a cross-sectional comparison between hookah and cigarette use," *BMC Public Health*, vol. 13, no. 1, p. 302, 2013.
- [6] M. Jawad, A. Wilson, J. T. Lee, S. Jawad, F. L. Hamilton, and C. Millett, "Prevalence and predictors of water pipe and cigarette smoking among secondary school students in London," *Nicotine & Tobacco Research*, vol. 15, no. 12, pp. 2069–2075, 2013.
- [7] M. H. Boskabady, L. Farhang, M. Mahmodinia, M. Boskabady, and G. R. Heydari, "Comparison of pulmonary function and respiratory symptoms in water pipe and cigarette smokers," *Respirology*, vol. 17, no. 6, pp. 950–956, 2012.
- [8] Centers for Disease Control and Prevention, "Smoking and tobacco use. Data and statistics. Fast facts and fact sheets. Hookahs. Source: National Center for Chronic Disease Prevention and Health Promotion," 2018, https://www.cdc.gov/tobacco/data_statistics/fact_sheets/tobacco_industry/hookahs/index.htm.
- [9] O. F. Khabour, E. S. Alsatari, M. Azab, K. H. Alzoubi, and M. F. Sadiq, "Assessment of genotoxicity of waterpipe and cigarette smoking in lymphocytes using the sister-chromatid exchange assay: a comparative study," *Environmental and Molecular Mutagenesis*, vol. 52, no. 3, pp. 224–228, 2011.
- [10] A. Nemmar, S. Al-Salam, S. Beegam, P. Yuvaraju, and B. H. Ali, "Thrombosis and systemic and cardiac oxidative stress and DNA damage induced by pulmonary exposure to diesel exhaust particles and the effect of nootkatone thereon," *American Journal of Physiology-Heart and Circulatory Physiology*, vol. 314, no. 5, pp. H917–H927, 2018.
- [11] A. Nemmar, S. Al-Salam, S. Beegam, P. Yuvaraju, N. Hamadi, and B. Ali, "In vivo protective effects of nootkatone against particles-induced lung injury caused by diesel exhaust is

- mediated via the NF- κ B pathway,” *Nutrients*, vol. 10, no. 3, p. 263, 2018.
- [12] B. H. Ali, S. A. Adham, K. A. al Balushi et al., “Reproductive toxicity to male mice of nose only exposure to water- pipe smoke,” *Cellular Physiology and Biochemistry*, vol. 35, no. 1, pp. 29–37, 2015.
- [13] B. H. Ali, K. A. al Balushi, M. Ashique et al., “Chronic water-pipe smoke exposure induces injurious effects to reproductive system in male mice,” *Frontiers in Physiology*, vol. 8, p. 158, 2017.
- [14] A. Nemmar, S. Al-Salam, P. Yuvaraju, S. Beegam, J. Yasin, and B. H. Ali, “Chronic exposure to water-pipe smoke induces cardiovascular dysfunction in mice,” *American Journal of Physiology-Heart and Circulatory Physiology*, vol. 312, no. 2, pp. H329–H339, 2017.
- [15] S. G. Johnsen, “Testicular biopsy score count – a method for registration of spermatogenesis in human testes: normal values and results in 335 hypogonadal males,” *Hormone Research in Paediatrics*, vol. 1, no. 1, pp. 2–25, 1970.
- [16] H. Jandíková, M. Dušková, and L. Stárka, “The influence of smoking and cessation on the human reproductive hormonal balance,” *Physiological Research*, vol. 66, Supplement 3, pp. S323–S331, 2017.
- [17] P. Salameh, Rachidi, A. al-Hajje et al., “Risky substance exposure during pregnancy: a pilot study from Lebanese mothers,” *Drug, Healthcare and Patient Safety*, vol. 5, pp. 123–131, 2013.
- [18] A. Barassi, M. M. Corsi Romanelli, R. Pezzilli et al., “Levels of uric acid in erectile dysfunction of different aetiology,” *The Aging Male*, vol. 21, no. 3, pp. 200–205, 2018.
- [19] T. M. Abdelghany, R. S. Ismail, F. A. Mansoor, J. R. Zweier, F. Lowe, and J. L. Zweier, “Cigarette smoke constituents cause endothelial nitric oxide synthase dysfunction and uncoupling due to depletion of tetrahydrobiopterin with degradation of GTP cyclohydrolase,” *Nitric Oxide*, vol. 76, pp. 113–121, 2018.
- [20] A. Nemmar, A. A. Hemeiri, N. A. Hammadi et al., “Early pulmonary events of nose-only water pipe (shisha) smoking exposure in mice,” *Physiological Reports*, vol. 3, no. 3, article e12258, 2015.
- [21] K. Rao, S. G. Babu, U. A. Shetty, R. L. Castelino, and S. R. Shetty, “Serum and salivary lactate dehydrogenase levels as biomarkers of tissue damage among cigarette smokers. A biochemical study,” *Stomatologija*, vol. 19, no. 3, pp. 91–96, 2017.
- [22] R. J. Aitken, T. B. Smith, M. S. Jobling, M. A. Baker, and G. N. De Iulii, “Oxidative stress and male reproductive health,” *Asian Journal of Andrology*, vol. 16, no. 1, pp. 31–38, 2014.
- [23] S. Shahin, S. P. Singh, and C. M. Chaturvedi, “2.45 GHz microwave radiation induced oxidative and nitrosative stress mediated testicular apoptosis: involvement of a p53 dependent bax-caspase-3 mediated pathway,” *Environmental Toxicology*, vol. 33, no. 9, pp. 931–945, 2018.
- [24] A. Valavanidis, T. Vlachogianni, and C. Fiotakis, “8-hydroxy-2’ -deoxyguanosine (8-OHdG): a critical biomarker of oxidative stress and carcinogenesis,” *Journal of Environmental Science and Health, Part C*, vol. 27, no. 2, pp. 120–139, 2009.
- [25] M. Muratori, L. Tamburrino, S. Marchiani et al., “Investigation on the origin of sperm DNA fragmentation: role of apoptosis, immaturity and oxidative stress,” *Molecular Medicine*, vol. 21, no. 1, pp. 109–122, 2015.
- [26] N. Hu, X. Han, E. K. Lane, F. Gao, Y. Zhang, and J. Ren, “Cardiac-specific overexpression of metallothionein rescues against cigarette smoking exposure-induced myocardial contractile and mitochondrial damage,” *PLoS One*, vol. 8, no. 2, article e57151, 2013.
- [27] A. Nemmar, S. Al-Salam, S. Beegam, P. Yuvaraju, A. Oulhaj, and B. H. Ali, “Water-pipe smoke exposure-induced circulatory disturbances in mice, and the influence of betaine supplementation thereon,” *Cellular Physiology and Biochemistry*, vol. 41, no. 3, pp. 1098–1112, 2017.
- [28] A. Nemmar, S. Al-Salam, P. Yuvaraju, S. Beegam, and B. H. Ali, “Exercise training mitigates water pipe smoke exposure-induced pulmonary impairment via inhibiting NF- κ B and activating Nrf2 Signalling pathways,” *Oxidative Medicine and Cellular Longevity*, vol. 2018, Article ID 7459612, 10 pages, 2018.
- [29] M. J. Morgan and Z. G. Liu, “Crosstalk of reactive oxygen species and NF- κ B signaling,” *Cell Research*, vol. 21, no. 1, pp. 103–115, 2011.
- [30] H. J. Choi, J. H. Lee, and Y. S. Jung, “(+)-Nootkatone inhibits tumor necrosis factor α /interferon γ -induced production of chemokines in HaCaT cells,” *Biochemical and Biophysical Research Communications*, vol. 447, no. 2, pp. 278–284, 2014.
- [31] A. M. Alsaad, M. N. al-Arifi, Z. H. Maayah et al., “Genotoxic impact of long-term cigarette and waterpipe smoking on DNA damage and oxidative stress in healthy subjects,” *Toxicology Mechanisms and Methods*, vol. 29, no. 2, pp. 119–127, 2018.
- [32] S. Torres, C. Merino, B. Paton, X. Correig, and N. Ramírez, “Biomarkers of exposure to secondhand and thirdhand tobacco smoke: recent advances and future perspectives,” *International Journal of Environmental Research and Public Health*, vol. 15, no. 12, p. 2693, 2018.